

# Contents

## INTRODUCTION TO MICROWAVES

1—10

1.1 History	3
1.2 Microwave Region and Band Designations	4
1.3 <u>Advantages of Microwaves</u>	7
1.4 <u>Applications of Microwaves</u>	9
Review Questions	10

## 2. REVIEW OF ELECTROMAGNETICS

11—25

2.1 Introduction	12
2.2 <u>Maxwell's Equations</u>	18
2.2.1 Ampere's Law	18
2.2.2 Faraday's Law	19
2.2.3 Gauss's Law	19
2.3 Wave Equations	20
2.4 TEM/TE/TM/HE Wave Definitions	22
Review Questions	25

## 3. TRANSMISSION LINES

27—60

3.1 Introduction	28
3.2 Two Wire Parallel Transmission Lines	28
3.3 Voltage and Current Relationships on a Transmission Line	32
3.4 Characteristic Impedance	35
3.5 Reflection Coefficient ( $\rho$ )	36

3.6	Input Impedance	39
3.7	Standing Waves	41
3.7.1	Voltage Standing Wave Ratio (VSWR)	42
3.7.2	Impedance at a Voltage Minimum and at a Voltage Maximum	43
3.7.3	Losses due to mismatch in Transmission Lines	44
3.7.4	Impedance Matching	45
3.7.5	Stub Matching	47
3.7.6	Travelling Waves on a Lossless Transmission Line	51
3.8	Solved Examples	53
		59

*Review Questions*

61–168

**4. MICROWAVE TRANSMISSION LINES**

4.1	Introduction	62
4.2	Multiconductor Transmission Lines	63
4.2.1	Coaxial Lines	63
4.2.2	Breakdown Power of a Coaxial Cable	65
4.2.3	Strip Lines	66
4.2.4	Microstrip Line	68
4.2.5	Types of Microstrip Lines	72
4.2.6	Microwave Components using Strip Lines	74
4.3	Waveguides (Single Lines)	91
4.3.1	Comparison of Waveguides with 2-wire Transmission Lines Similarities	91
4.3.2	Types of Waveguides	92
4.3.3	Propagation of Waves in Rectangular Waveguides	94
4.3.4	Propagation of TEM waves	97
4.3.5	TE and TM Modes	97
4.3.6	Propagation of TM Waves in Rectangular Waveguide	98
4.3.7	TM Modes in Rectangular Waveguides	103
4.3.8	Guide Wavelength, Group and Phase Velocity	105
4.3.9	Propagation of TE Waves in a Rectangular Waveguide	113
4.3.10	TE Modes in Rectangular Waveguides	118
4.3.11	Wave Impedance ( $Z_g$ ) in TM and TE Waves	119
4.3.12	Power Transmission Rectangular Waveguide	121
4.3.13	Power Losses in a Waveguide	122
4.3.14	Dominant Mode and Degenerate Modes in Rectangular Waveguides	123
4.3.15	Breakdown Power in Rectangular Waveguides	125
4.3.16	Power Handling Capacity of Rectangular Waveguides	125
4.3.17	Standard Dimensions of Rectangular Waveguides	125
4.3.18	Circular Waveguides	126
4.3.19	Propagation of TE Waves in Circular Waveguide	126
4.3.20	Propagation of TM in Circular Waveguide	131
4.3.21	Cutoff Wavelength in Circular Waveguide	132
4.3.22	Phase Velocity, Group Velocity, Guide Wavelength and Wave Impedance	132
4.3.23	TEM Wave in Circular Waveguide	135

Referred  
 Books  
 1. *Antennas and  
Wave Propagation*  
 2. *Electromagnetic  
Waves and  
Waves*

4.3.24 Advantages, Disadvantage and Applications of Circular Waveguides	135
4.3.25 Standard Dimension of Circular Waveguides	135
4.3.26 Power Landing Capacity of Circular Waveguides	137
4.4 Open Boundary Structures (Open Electromagnetic waveguides)	137
4.5 Microwave Integrated Circuits	139
4.5.1 Introduction	139
4.5.2 Materials used for MMIC's Fabrication	140
4.5.3 Thin Film Devices	141
4.5.4 Planar Transmission Lines	143
4.5.5 Hybrid Integrated Circuit : Fabrication	143
4.5.6 Use of Gallium Arsenide for Building Microwave Integrated Circuits	144
4.5.7 GaAs Fabrication Technology	144
4.5.8 Applications	146
4.5.9 Disadvantages of MIC's	148
4.6 Solved Examples	148
Review Questions	166

## 5. CAVITY RESONATORS

169—197

5.1 Introduction	170
5.2 Expression for $f_o$ in a Rectangular Cavity Resonator	171
5.3 Expression for $f_o$ in a Circular Cavity Resonator	172
5.4 Application of Cavity Resonators	173
5.5 Field Expressions for $TM_{mnp}$ and $TE_{mnp}$ Modes in a Rectangular Cavity Resonator	173
5.6 Field Expressions for $TM_{nmp}$ and $TE_{nmp}$ Modes in a Rectangular Cavity Resonator	182
5.7 Solved Examples	185
5.8 Field Patterns	187
5.9 Quality Factor (Q) of Cavity Resonators	189
5.9.1 Q of a Rectangular Cavity Resonator	191
5.9.2 Q of a Circular Cavity Resonator	192
5.10 Reentrant Cavities	194
5.11 Coupling to Cavities	195
Review Questions	196

## 6. MICROWAVE COMPONENTS

199—260

6.1 Introduction	200
6.2 Waveguide Microwave Junctions	200
6.2.1 Scattering or (S) Parameters	201
6.3 Microwave T-Junctions	204
6.3.1 H-Plane Tee Junction	204
6.3.2 E-Plane Tee	208

6.3.3	E-H Plane (Hybrid or Magic) Tee	22
6.3.4	Applications of Magic Tee	22
6.3.5	Rat Race Junction	22
<b>6.4</b>	<b>Directional Couplers</b>	
6.4.1	Two-hole Directional Coupler	22
6.4.2	Bethe or Single-hole Coupler	22
6.4.3	Scattering Matrix of a Directional Coupler	22
<i>def. dr.</i>	Waveguide Joints	22
6.6	Waveguide Bends, Corners, Transitions and Twists	22
6.7	Waveguide Irises	22
6.8	Posts and Tuning Screws	22
6.9	Coupling Probes and Coupling Loops	22
6.10	Waveguide Terminations	22
<b>6.11</b>	<b>Ferrite Devices</b>	
6.11.1	Faraday Rotation in Ferrites	22
6.11.2	Microwave Devices which make use of Faraday rotation	22
6.12	Microwave Filters	22
6.12.1	YIG Filter Resonators	22
6.13	Surface Acoustic Wave (SAW) Devices	24
6.14	Phase Shifters	24
6.15	Microwave Attenuators	24
6.16	Solved Examples	24

### *Review Questions*

## **7. MICROWAVE MEASUREMENTS**

261—296

<b>7.1</b>	<b>Introduction</b>	262
<b>7.2</b>	<b>Microwave Bench-General Measurement Set-Up</b>	262
<b>7.3</b>	<b>Measurement Devices and Instrumentation</b>	262
7.3.1	Slotted Line	263
7.3.2	Tunable Detector	263
7.3.3	VSWR Meter	265
7.3.4	Power Meter	265
7.3.5	Wave Meter	268
7.3.6	Spectrum Analyser	269
7.3.7	Network Analyser	270
7.3.8	Test Set-up for Reflection-Transmission Measurement	272
7.3.9	Test Set-up for S-Parameter Measurement	274
<b>7.4</b>	<b>Frequency Measurement</b>	275
7.4.1	Electronic Techniques	276
<b>7.5</b>	<b>Measurement of Power</b>	276
<b>7.6</b>	<b>Attenuation Measurement</b>	276
7.6.1	Power Ratio Method	281
7.6.2	RF Substitution Method	281
<b>7.7</b>	<b>Measurement of Phase Shift</b>	282
		283

7.8	Measurement of Voltage Standing Wave Ratio (VSWR)	284
7.8.1	Measurement of Low VSWR's ( $S < 10$ )	285
7.8.2	Measurement of High VSWR ( $S > 10$ )	285
7.9	<u>Measurement of Impedance</u>	
7.9.1	Measurement of Impedance Using Slotted Line	286
7.9.2	Measurement of Impedance Using Reflectometer	286
7.10	Measurement of Insertion Loss	288
7.11	Measurement of Dielectric Constant	288
7.12	Measurement of Noise Factor	291
7.13	Measurement of Q of A Cavity Resonator	292
7.14	Solved Examples	293
	Review Questions	295

297—368

## 8. MICROWAVE TUBES AND CIRCUITS

8.1	Introduction	298
8.2	High Frequency Limitations of Conventional Tubes	298
8.2.1	Inter Electrode Capacitance (IEC) Effect	299
8.2.2	Lead Inductance (LI) Effect	300
8.2.3	Transit Time Effect	300
8.2.4	Combined Effect of LI, IEC and Transit Time	304
8.2.5	Gain Bandwidth Limitation	305
8.2.6	Effect Due to RF Losses	305
8.2.7	Radiation Losses	306
8.3	Special Tubes at UHF (300-3000 MHz)	308
8.3.1	ACORN Tube	308
8.3.2	Disk Seal Tube or Light House Tube	308
8.3.3	Pencil Triodes	309
8.4	Microwave Tubes	317
8.5	Klystrons	318
8.5.1	Two Cavity Klystron Amplifier	319
8.5.2	Multicavity Klystron	330
8.5.3	Two Cavity Klystron Oscillator	331
8.5.4	Reflex Klystron	332
8.6	Travelling Wave Tube (TWT)	339
8.6.1	Constructional Features of TWT	339
8.6.2	Operation	341
8.7	Backward Wave Oscillator	341
8.7.1	Operation	353
8.8	Magnetrons	367
8.8.1	Cavity Magnetron	
8.9	Solved Examples	
	Review Questions	

## 9. SOLID STATE MICROWAVE DEVICES

369—436

<u>9.1</u>	Introduction	370
<u>9.2</u>	Microwave Transistors	370
<u>9.3</u>	MESFETs (Metal Semi Conductor Field Effect Transistors)	375
<u>9.4</u>	Classification of Solid State Microwave Devices	378
<u>9.5</u>	Varactor Diodes	379
9.5.1	Construction of Varactor Diode	381
9.5.2	Equivalent Circuit	382
9.5.3	Figure of Merit	383
<u>9.6</u>	Parametric Amplifiers	384
9.6.1	Manley-Rowe Relations	386
9.6.2	Amplification Mechanism of a Par amp	388
<u>9.6.3</u>	Parametric Up Converter (PUC)	389
<u>9.6.4</u>	Parametric Down Converter (PDC)	390
9.6.5	Negative Resistance Par amp	390
9.6.6	Degenerate Par amp (or Oscillator)	391
9.6.7	Broadband Par-amps	392
9.6.8	Cooled Par amps	392
<u>9.7</u>	Pin Diode	393
9.7.1	Operation of PIN Diode	395
9.7.2	Applications of PIN Diode	395
<u>9.8</u>	Schottky Barrier Diode (SBD)	398
9.8.1	Construction	398
9.8.2	Operation	399
9.8.3	Applications	399
<u>9.9</u>	Tunnel Diode (ESAKI Diode)	399
9.9.1	Volt-amp Characteristics of a Tunnel Diode	400
9.9.2	Tunnel Diode Equivalent Circuit of Oscillator	402
9.9.3	Negative Resistance Amplifier Theory (As Applied to Tunnel Diode)	403
9.9.4	Tunnel Diode Amplifier with Circulator	405
9.9.5	Tunnel Diode Oscillator Using Cavity	406
9.9.6	Performance Characteristics and Applications	406
<u>9.10</u>	Transferred Electron Devices (Ted's)	407
9.10.1	Gunn Effect Devices	407
9.10.2	Domain Formation	410
9.10.3	Transit Time Domain Mode ( $fL = 107 \text{ cm/sec}$ )	413
9.10.4	Delayed Domain Mode ( $106 \text{ cms/sec} < fL < 107 \text{ cm/sec}$ )	413
9.10.5	Quenched Domain Mode ( $fL > 2 \times 107 \text{ cm/sec}$ )	413
9.10.6	Limited Space Charge Accumulation Mode ( $fL > 2 \times 107 \text{ cm/sec}$ )	415
9.10.7	Construction Gunn Diode	415
9.10.8	Typical Characteristics	416
9.10.9	Gunn Diode Amplifier	416
9.10.10	Gunn Oscillator	417
9.10.11	Applications of Gunn Diode	417

9.11	<u>Avalanche transit time devices</u>	419
9.11.1	<u>IMPATT Diode</u>	419
9.11.2	<u>TRAPATT Diode</u>	423
9.11.3	<u>BARITT Diodes</u>	426
9.12	Stimulated Emission (Quantum Electronic Devices)	428
9.13	Solved Examples	430
	<i>Review Questions</i>	435

Gsum

## 10. MICROWAVE COMMUNICATION SYS

437—511

10.1	Introduction	438
10.2	Propagation Modes	439
10.3	Microwave Communication Systems	443
10.4	<u>Analog Microwave Communication</u>	443
10.4.1	<u>LOS Microwave Systems</u>	444
10.4.2	<u>OTH Microwave Systems</u>	449
10.4.3	Transmission Interference and Signal Damping	451
10.4.4	Derivation for LOS Communication Range	452
10.4.5	Derivation for Field Strength of a Tropospheric Wave	457
10.4.6	Duct Propagation	460
10.4.7	Fading in Troposphere and its Effect on Troposcatter Propagation	462
10.5	Satellite Communications	463
10.5.1	Satellite Orbits	464
10.5.2	Satellite Frequencies	467
10.5.3	Satellite Attitude/Station Keeping	468
10.5.4	Transmission Path	469
10.5.5	Link Calculations	470
10.5.6	Noise Considerations	472
10.5.7	Factors Affecting Satellite Communication	474
10.6	Digital Microwave Communication	475
10.6.1	Digital Hierarchies	476
10.6.2	Why Digital	480
10.6.3	Digital Microwave System	481
10.6.4	Bandwidth Efficiency	484
10.6.5	Bandwidth Efficient Digital Radio Systems	488
10.6.6	Hybrid Microwave Systems	490
10.7	Microwave Antennas	490
10.7.1	Horn Antenna	494
10.7.2	Parabolic Reflectors or Paraboloids or Microwave Dish Antenna	500
10.7.3	Lens Antenna	502
10.7.4	Slot Antennas	503
10.7.5	Microstrip Antennas	504
10.8	Solved Problems	509
	<i>Review Questions</i>	

11.1	Introduction	514
11.2	Block Diagram of a Simple Radar	515
11.3	Classification	517
11.4	Free Space Radar Range Equation	519
11.4.1	Factors Affecting Range of a Radar	521
11.5	Maximum Unambiguous Range ( $R_{\text{unamb}}$ )	524
11.6	Pulsed Radar System	527
11.7	Radar Receivers-General Principles/Salient Features	530
11.8	Modulators	535
11.8.1	Line-Pulse Modulator	535
11.8.2	Active-Switch Modulator	537
11.9	Radar Displays	537
11.9.1	A-Scope Display	537
11.9.2	B-Scope, E-Scope and F-Scope Displays	538
11.9.3	Plan-Position Indicator (PPI)	540
11.10	Target Detection	541
11.11	Scanning and Tracking with Radars	545
11.11.1	Scanning	545
11.11.2	Tracking	546
11.12	Doppler Effect	554
11.13	CW Doppler Radar	556
11.14	Moving Target Indicator (MTI) Radar	557
11.14.1	Blind Speeds	560
11.15	Frequency Modulated CW Radar	561
11.16	Radio Navigational Aids	562
11.16.1	Radio Direction Finding System	562
11.16.2	Direction Findings Using Loop Antenna	562
11.16.3	Direction Finding Using Adcock Antenna	565
11.16.4	Long Range Navigational Aid (LORAN)	566
11.17	Radar Antennas	567

# 2

## Review of Electromagnetics

### 2.1 INTRODUCTION

Electromagnetic waves are oscillations that propagate through free space (space that does not interfere with the normal radiation and propagation of electromagnetic waves, no magnetic or fractional fields, no solid bodies and no ionised particles) with a velocity of light ( $c = 3 \times 10^8$  m/sec). Strictly speaking the velocity of light in vacuum is 299,792,462 meters/sec (and for all practical purposes in air as well). In fact, it was James Clerk Maxwell, a Scottish physicist (1831–1879) who predicted that all electromagnetic waves travel in free space with a velocity.

$$v = \frac{1}{\sqrt{\mu_0 \epsilon_0}} \approx 3 \times 10^8 \text{ m/sec}$$

where permeability of free space is  $\mu_0 = 4\pi \times 10^{-7}$  N/m and the permittivity of free space is  $\epsilon_0 = 8.854 \times 10^{-12}$  F/m. These values are simply the distributed values of  $L$  and  $C$  of free space.

Electromagnetic waves are similar to propagation or outward travel of water waves on a pond after a stone has been thrown into it with the only difference that water waves are longitudinal (oscillations in the direction of propagation) and electromagnetic waves are transverse (oscillations perpendicular to the direction of propagation). Also that direction of propagation of the electric field and the magnetic field are mutually perpendicular in electromagnetic waves. These electric and magnetic fields vary with time and are governed by certain physical laws given by a set of equations known as MAXWELL'S equations. Further if the wave is travelling through a medium other than free space, it can be shown that the velocity will decrease. [It is known that the absolute permittivity of a medium is  $\epsilon = \epsilon_r \epsilon_0$ , where  $\epsilon_r$  is the relative permittivity (dielectric constant) which may vary between 1 to 10 for most microwave elements and  $\epsilon_0$  is the permittivity of free space i.e.,  $\epsilon_r = \epsilon/\epsilon_0$ . Similarly absolute permeability of a medium is  $\mu_r = \mu/\mu_0$ .  $\mu_r = 1$  for vacuum and most non-magnetic metals]. As the new medium is virtually always non-magnetic ( $\mu = 1$ ), the new velocity is given by

$$V_r = \frac{c}{\sqrt{\epsilon_r}}$$

where,  $V_r$  = relativity velocity in the new medium

$c$  = velocity of light ( $3 \times 10^8$  m/s)

$\epsilon_r$  = dielectric constant

The frequency of an electromagnetic source signal is the number of cycles per second the signal contains which is measured in Hertz (Hz). It remains constant, once set even if the medium through which the signal travels may vary. However, this is not true for velocity or wavelength (to be defined later) of the signal. The period of the signal is the time of one complete cycle and is inversely proportional to frequency, i.e.,

$$T = 1/f$$

where,  $T$  = period in secs of one cycle

$f$  = frequency in Hz.

The wavelength ( $\lambda$ ) of an electromagnetic wave is the physical distance the wave travels in one cycle  $\lambda = cT$  (similar to basic distance formula  $S = Vt$ , where  $S$  = distance,  $V$  = velocity,  $t$  = time travelled to find the distance a wave travels in a given time). The wavelength  $\lambda = ct$ , where  $c$  = velocity of light and  $T$  = the time taken by the wave to travel through one cycle (or from one crest to the next or from one trough to the next).

Since

$$\begin{aligned} f &= 1/t \\ \lambda &= c/f \end{aligned}$$

where,  $\lambda$  = wavelength, mtrs

$c = 3 \times 10^8$  m/s

$f$  = frequency, Hz

When the medium changes, wavelength also changes. The wavelength of an electromagnetic wave in a dielectric medium is shorter than in free space given by

$$\lambda = \frac{c}{f\sqrt{\epsilon_r}}$$

where  $\epsilon_r$  is the dielectric constant of the medium. Wavelength can be expressed in radians, metres or wavelengths depending upon a phase scale, physical length scale or electrical wavelength scale, as shown in Fig. 2.1.

The concepts of electric and magnetic fields are very necessary in dealing with propagation of waves at microwaves. In addition, the properties of the medium in which the waves travel such as conductivity, permeability and permittivity are to be known.

Knowledge of plane wave propagation is very essential to study the propagation of microwaves. A changing electric field produces a magnetic field and a changing magnetic field induces a changing electric field in the surrounding region. The changing electric field in turn produces further changing magnetic field in a still more distant field and the cycle repeats as shown in Fig. 2.2a.

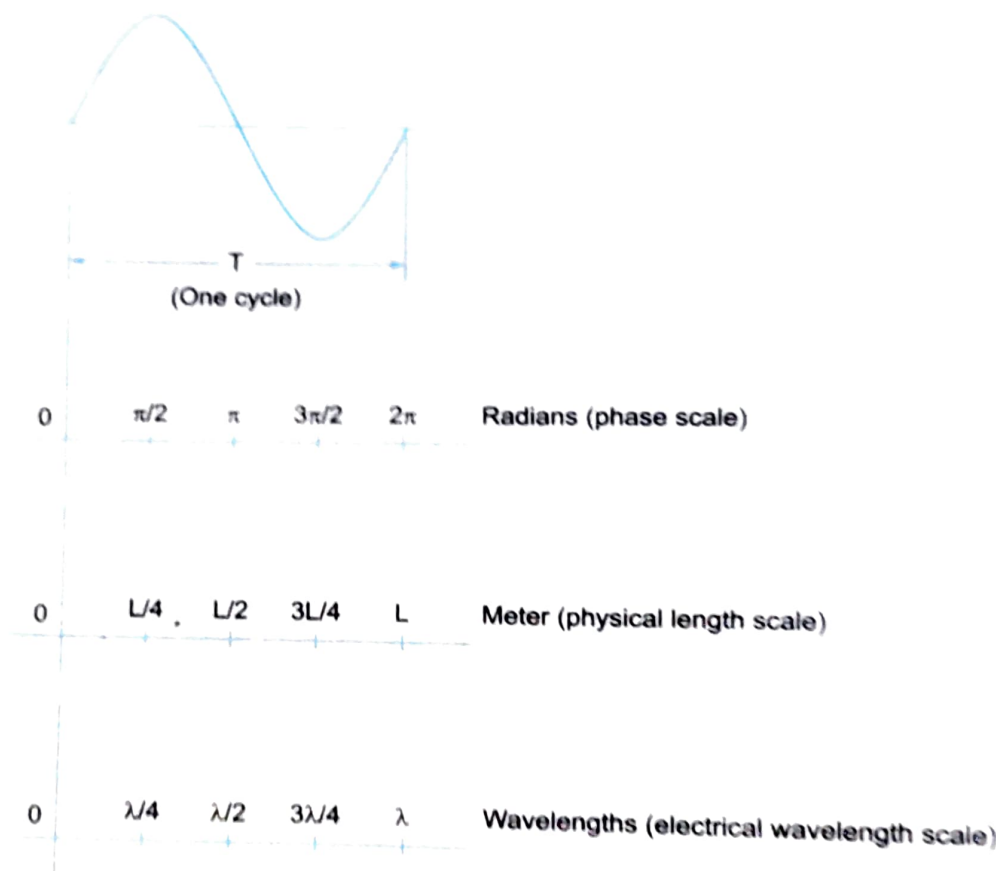


Fig. 2.1

A plane transverse electromagnetic (TEM) wave is defined as a wave in which both the electric ( $E$ ) and magnetic ( $H$ ) vectors are at right angles to the direction of propagation. At any instant of time, both vectors have the same magnitude and direction at all points in the transverse plane which contains them. This is clearly shown in Fig. 2.2.

It is easily seen that a conductor at low frequencies, the electric field ( $E$ ) and the magnetic field ( $H$ ) follow normal Ohm's law principles and as the frequency is raised higher and higher, the same conductor behaves like a transmission line and follows Maxwell's equations. A transmission line terminated by a radiating component (called an antenna) sees the  $E/H$  mutual fields radiate into space. The fields are at right angles to each other and also to the direction of propagation, i.e., the direction of propagation, causing a curved wavefront in the near field and a flat wavefront in the far field. Such a wave is nothing but the TEM wave which occurs only in free space and on a wire transmission line.

If the field,  $E$  of an EM wave is in the vertical direction, then the EM wave is said to be vertically polarized. If it is in the horizontal direction, the wave is said to be horizontally polarized. The orientations of the electric field are also known as linear polarization. It is necessary that the transmitting and receiving antennas must be mutually oriented with respect to the type of polarization used for maximum transfer of power. For example, a car antenna is oriented in

vertical direction since AM (amplitude modulated) signals transmitted are vertically polarized, whereas roof top TV antenna are oriented horizontally since conventional TV signals are transmitted with horizontal polarization.

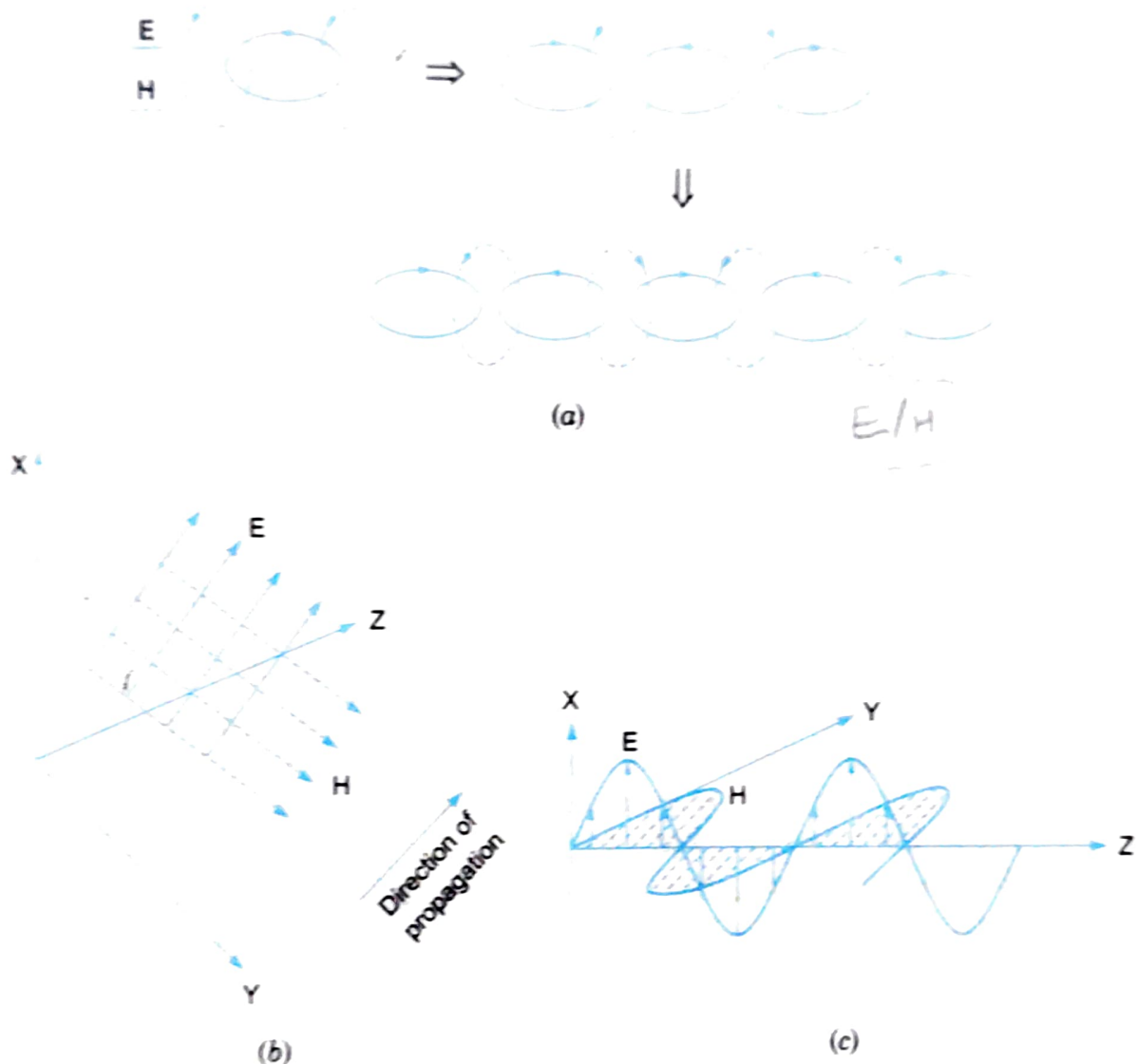


Fig. 2.2

Many a times, as in the case of a DBS (Direct Broadcast Satellite) service, the signal is circularly polarized. In fact, a satellite down links a signal with simultaneous vertical and horizontal polarized waves. A circularly polarized wave is the resultant sum of two equal amplitudes E field vectors in phase quadrature (one vector at  $90^\circ$  out of phase with the other), i.e., A circularly polarized wave contains all polarizations and all information of a linearly polarized wave although at reduced amplitude. The advantage of this polarization is that the antenna alignment will not be critical and also the attenuation due to rain is reduced if circular polarization is used. The different polarizations are shown in Fig. 2.3.

16

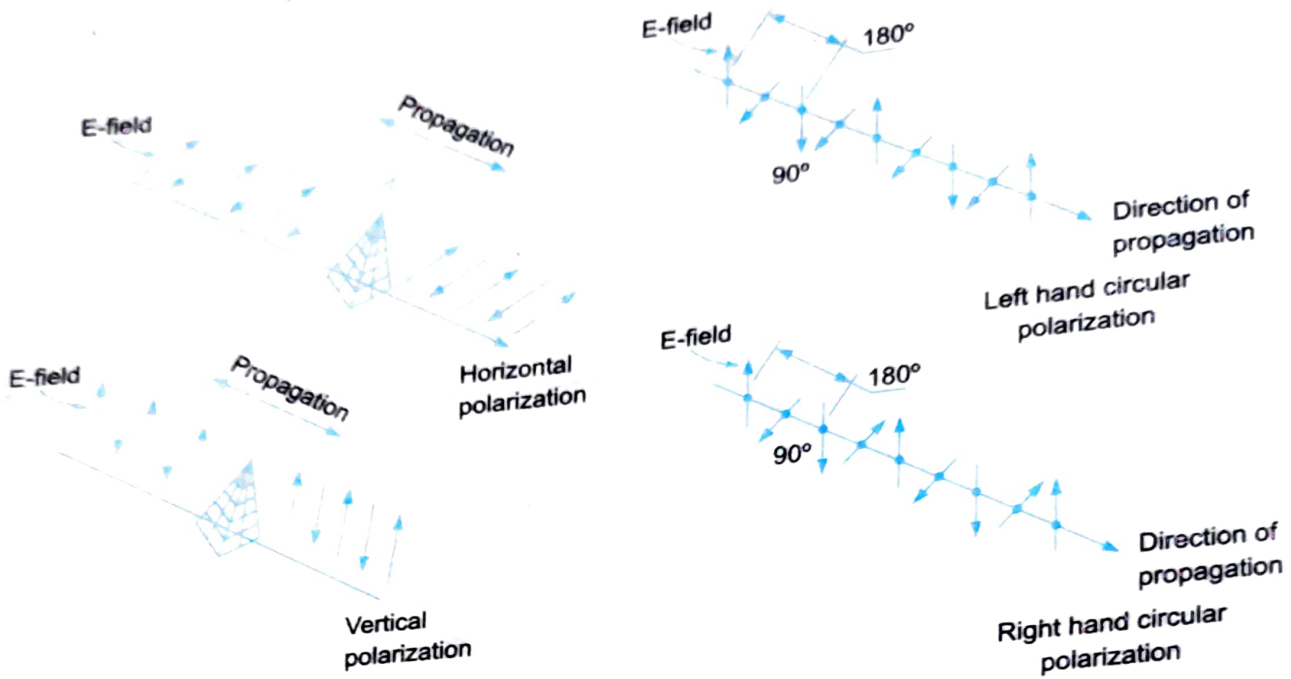


Fig. 2.3

The TEM waves are propagated equally in all directions if the source is a point source, called an isotropic source. From this point a sphere forms similar to a balloon being blown up equally expanding in all directions. At a far away distance from the point source the wavefront would appear as a flat plane. The spherical TEM wave is known as a plane wave since the wavefront appears to be a 2-D (two-dimensional) shape. The energy contained in the wavefront at a distance, say  $r$ , from the source would distribute itself equally in all directions over the sphere. The area of this sphere is determined by the formula  $A = 4\pi r^2$ . The power density ( $P_d$ ) at any point in free space as a function of the total power radiated ( $P_t$ ) divided by the area ( $A$ ) over which it is distributed is given by

$$P_d = \frac{P_t}{A} = \frac{P_t}{4\pi r^2}$$

where  $P_d$  = power density at any point in free space watt/m<sup>2</sup>

$P_t$  = total power radiated, watts

$A$  = area =  $4\pi r^2$ , m<sup>2</sup>

As the power spreads out, the sphere continues to expand. It is also seen that the power density is inversely proportional to the distance ( $r$ ) squared, i.e., if the distance doubles, the power density is reduced by 1/4th (inverse square law).

Assuming no losses, the energy carried by an EM wave is contained in both its electric (E) and magnetic (H) fields and each cubic metre of space contains the total energy. The energy  $W$  is given by

$$W = \frac{1}{2} (D\mathbf{E} + B\mathbf{H}) J/m^3$$

$$= \frac{1}{2} (\epsilon_0 \mathbf{E}^2 + \mu_0 \mathbf{H}^2) J/m^3.$$

It can also be written as

$$\boxed{W = \frac{1}{2} (\epsilon_0 \mathbf{E}_z^2 + \mu_0 \mathbf{H}_z^2) J/m^3} \quad \dots(2.1)$$

where,  $D$  = Electric flux density =  $\epsilon_0 \epsilon_r \mathbf{E}$

$B$  = Magnetic flux density =  $\mu_0 \mu_r \mathbf{H}$

$\epsilon_0$  is the permittivity of free space

$$= 8.854 \times 10^{-12} \text{ or } 10^{-9}/36\pi \text{ farads/metre}$$

and  $\mu_0$  is the permeability of free space

$$= 4\pi \times 10^{-7} \text{ Henry/metre}$$

and  $\mathbf{E}_z$  and  $\mathbf{H}_z$  are the rms values of the electric and magnetic field strength vectors along the  $z$  direction respectively.

Under no loss conditions

$$\boxed{\frac{1}{2} \epsilon_0 \mathbf{E}_z^2 = \frac{1}{2} \mu_0 \mathbf{H}_z^2}$$

and the ratio of ( $\mathbf{E}$  and  $\mathbf{H}$  always oscillate in phase and their ratio is always constant)

$$\boxed{\frac{\mathbf{E}}{\mathbf{H}} = \sqrt{\frac{\mu_0}{\epsilon_0}}} \\ = 120\pi = 377\Omega$$

This ratio has the characteristic of an impedance and has designated as the intrinsic impedance of free space.

If we assume that the wave travels through space with the velocity of light  $c$ , the energy,  $S$ , passing through each square metre of the plane perpendicular to the direction of propagation in each second is given by

$$\boxed{S = c \times W = \frac{c}{2} [\epsilon_0 \mathbf{E}_z^2 + \mu_0 \mathbf{H}_z^2] \text{ w/m}^2} \quad (\text{using Eq. 2.1})$$

$$= \frac{c}{2} \times 2\epsilon_0 \mathbf{E}_z^2 \quad (\because \epsilon_0 \mathbf{E}_z^2 = \mu_0 \mathbf{H}_z^2)$$

$$= \frac{\epsilon_0 \mathbf{E}_z^2}{\sqrt{\epsilon_0 \mu_0}} \quad \left( \because c = \frac{1}{\sqrt{\epsilon_0 \mu_0}} \text{ m/sec} \right)$$

$$S = \frac{\mathbf{E}_z^2}{\sqrt{\mu_0/\epsilon_0}}$$

$$= \frac{\mathbf{E}_z^2}{120\pi} = \frac{\mathbf{H}_z^2}{120\pi} \quad \dots(2.2)$$

## 2.2 MAXWELL'S EQUATIONS

These equations combine the fundamental laws of electricity and magnetism and are of profound importance in the analysis of most electromagnetic wave problems. The Ampere's Faraday's Law and Gauss's Law lead to Maxwell equations.

### 2.2.1 Ampere's Law

In its basic form, it is given by

$$\int \mathbf{H} \cdot d\mathbf{l} = I \quad \dots(2)$$

where  $d\mathbf{l}$  is the incremental length of the closed loop,  $\mathbf{H}$  is the magnetic field vector, and  $I$  is the current enclosed by the loop.

The current  $I$  can be replaced by the surface integral of the conduction current density  $\mathbf{J}_T$  over the area bounded by the path of integration. The total current density is given by

$$\mathbf{J}_T = \mathbf{J} + \frac{\partial \mathbf{D}}{\partial t} \quad \dots(1)$$

where,  $\mathbf{J} = \sigma \mathbf{E}$  is the conduction current density and

$\frac{\partial \mathbf{D}}{\partial t}$  is the displacement current density.

Displacement current is similar to the current flowing in pure capacitor dielectric to which ac voltage is applied, current does not flow through the dielectric but the external effect is though it did and so we imagine a current there which we will call as displacement current in dielectric.

$$\int \mathbf{H} \cdot d\mathbf{l} = \iint_s \left( \mathbf{J} + \frac{\partial \mathbf{D}}{\partial t} \right) \cdot d\mathbf{s} \quad \dots(2.5)$$

where  $s$  stands for surface integration. Equation 2.5 is the integral form of Maxwell's 1st equation.

By applying Stokes theorem

$$\int \mathbf{H} \cdot d\mathbf{l} = \iint_s (\nabla \times \mathbf{H}) \cdot d\mathbf{s}$$

$$\iint_s (\nabla \times \mathbf{H}) \cdot d\mathbf{s} = \iint_s \left( \mathbf{J} + \frac{\partial \mathbf{D}}{\partial t} \right) \cdot d\mathbf{s}$$

The equation derived above is the differential form of Maxwell's 1st equation.

$$\nabla \times \mathbf{H} = \mathbf{J} + \frac{\partial \mathbf{D}}{\partial t}$$

2.2.2 Faraday's Law

In its basic form it is given by

$$V = - \frac{d\phi}{dt} \quad \dots(2.7)$$

Since

$$\phi = \int_s \mathbf{B} \cdot d\mathbf{s} \quad \text{and} \quad \int_s \mathbf{E} \cdot d\mathbf{l}$$

$$\therefore \int_s \mathbf{E} \cdot d\mathbf{l} = - \frac{\partial}{\partial t} \int_s \mathbf{B} \cdot d\mathbf{s} \quad \dots(2.8)$$

Equation 2.8 is the integral form of Maxwell's 2nd equation.

Applying Stokes theorem we get the differential form of Maxwell's 2nd equation

$$\nabla \times \mathbf{E} = - \frac{\partial \mathbf{B}}{\partial t} \quad \dots(2.9)$$

2.2.3 Gauss's Law

In its basic form it is given by

$$\int_s \mathbf{D} \cdot d\mathbf{s} = \int_V \rho dV \quad \dots(2.10)$$

where,  $s$  = surface of integration,

$V$  = volume enclosed by it,

$\rho$  = charge density

$$\lim_{dv \rightarrow 0} \int_s \frac{\mathbf{D} \cdot d\mathbf{s}}{dv} = \nabla \cdot \mathbf{D} \quad [\text{Divergence of } \mathbf{D}]$$

The 3rd Maxwell's equation is therefore given by

$$\nabla \cdot \mathbf{D} = \rho \quad \dots(2.11)$$

In the case of magnetic fields the surface integral of ' $\mathbf{B}$ ' over a closed surface is zero. This is because a magnetic field has neither a source nor a sink.

The 4th Maxwell's equation is given by

$$\nabla \cdot \mathbf{B} = 0 \quad \dots(2.12)$$

### Summarizing

$$1. \quad \nabla \times \mathbf{H} = \mathbf{J} + \frac{\partial \mathbf{D}}{\partial t}$$

$$2. \quad \nabla \times \mathbf{E} = - \frac{\partial \mathbf{B}}{\partial t}$$

$$3. \quad \nabla \cdot \mathbf{D} = \rho$$

$$4. \quad \nabla \cdot \mathbf{B} = 0$$

where the symbols have their usual meanings.

### 2.3 WAVE EQUATIONS

If we assume that all field vectors vary with respect to time 't' in a sinusoidal manner.

$$\mathbf{E} = E_0 e^{j\omega t} \quad \dots(2.13)$$

where,  $E_0$  = maximum value of electric field intensity.

$\omega = 2\pi f$ , where  $f$  is the frequency of sinusoidal variations.

Differentiating Eq. 2.13 partially with respect to 't' we get

$$\begin{aligned} \frac{\partial \mathbf{E}}{\partial t} &= E_0 \cdot e^{j\omega t} \cdot j\omega \\ &= \mathbf{E} \cdot j\omega = j\omega \mathbf{E} \end{aligned} \quad \dots(2.14)$$

We can define an operator

$$\frac{\partial}{\partial t} = j\omega \quad \dots(2.15)$$

Differentiating Eq. 2.14 again partially w.r.t. 't' we get

$$\frac{\partial^2 \mathbf{E}}{\partial t^2} = j\omega E_0 \cdot e^{j\omega t} \cdot j\omega \quad \dots(2.16)$$

$$\frac{\partial^2 \mathbf{E}}{\partial t^2} = -\omega^2 E_0 \cdot e^{j\omega t} = -\omega^2 \times \mathbf{E} \quad \dots(2.17)$$

We can define another operator

$$\frac{\partial^2}{\partial t^2} = -\omega^2 \quad \dots(2.18)$$

Now consider a medium which does not contain any free charges and is also non-conducting, for example air or free space. Then we have  $\rho = 0$ ,  $\sigma = 0$ .

From Maxwell's 1st equation (Eq. 2.6), we know,

$$\nabla \times \mathbf{H} = \mathbf{J} + \frac{\partial \mathbf{D}}{\partial t} = \sigma \mathbf{E} + \frac{\partial}{\partial t} (\epsilon \mathbf{E})$$

$$\nabla \times \mathbf{H} = 0 + \epsilon \frac{\partial \mathbf{E}}{\partial t} = \epsilon \cdot j\omega \mathbf{E} = j\omega \epsilon \mathbf{E}$$

i.e.,

$$\nabla \times \mathbf{H} = j\omega \epsilon \mathbf{E} \quad \dots(2.19)$$

From Maxwell's 2nd equation (Eq. 2.9)

$$\nabla \times \mathbf{E} = -\frac{\partial \mathbf{B}}{\partial t} = -\frac{\partial(\mu \mathbf{H})}{\partial t} = -j\omega \mu \mathbf{H}$$

i.e.,

$$\nabla \times \mathbf{E} = -j\omega \mu \mathbf{H} \quad \dots(2.20)$$

Taking curl of  $\nabla \times \mathbf{E}$ , we get (using Eqns. 2.19 and 2.20)

$$\nabla \times \nabla \times \mathbf{E} = \nabla \times (-j\omega \mu \mathbf{H}) = -j\omega \mu (\nabla \times \mathbf{H}) = -j\omega \mu (j\omega \epsilon \mathbf{E})$$

$$\nabla \times \nabla \times \mathbf{E} = \omega^2 \mu \epsilon \mathbf{E}$$

We know from vector analysis, that  $\nabla \times \nabla \times \mathbf{E} = \nabla (\nabla \cdot \mathbf{E}) - \nabla^2 \mathbf{E}$

$$\nabla(\nabla \cdot \mathbf{E}) - \nabla^2 \mathbf{E} = \omega^2 \mu \epsilon \mathbf{E}$$

We know from Maxwell's 3rd equation (Eq. 2.11),

$$\nabla \cdot \mathbf{D} = \rho = 0$$

$$\epsilon(\nabla \cdot \mathbf{E}) = 0$$

$$\epsilon \neq 0, \therefore \nabla \cdot \mathbf{E} = 0$$

or  
Eq. 2.21 becomes

$$-\nabla^2 \mathbf{E} = +\omega^2 \mu \epsilon \mathbf{E}$$

$$\nabla^2 \mathbf{E} = -\omega^2 \mu \epsilon \mathbf{E}$$

Resolving  $\mathbf{E}$  into 3 mutually perpendicular directions, we get

$$\nabla^2 (i\mathbf{E}_x + j\mathbf{E}_y + k\mathbf{E}_z) = -\omega^2 \mu \epsilon [i\mathbf{E}_x + j\mathbf{E}_y + k\mathbf{E}_z]$$

where  $i, j, k$  are unit vectors along  $x, y$  and  $z$  directions respectively.

Equating coefficients of  $i, j$  and  $k$  on both sides, we get

$$\nabla^2 \mathbf{E}_x = -\omega^2 \mu \epsilon \mathbf{E}_x$$

$$\nabla^2 \mathbf{E}_y = -\omega^2 \mu \epsilon \mathbf{E}_y$$

$$\nabla^2 \mathbf{E}_z = -\omega^2 \mu \epsilon \mathbf{E}_z$$

The solutions of these equations are similar but their boundary conditions will be different.

Similarly

$$\nabla^2 \mathbf{H} = -\omega^2 \mu \epsilon \mathbf{H}$$

and

$$\nabla^2 \mathbf{H}_x = -\omega^2 \mu \epsilon \mathbf{H}_x$$

$$\nabla^2 \mathbf{H}_y = -\omega^2 \mu \epsilon \mathbf{H}_y$$

$$\nabla^2 \mathbf{H}_z = -\omega^2 \mu \epsilon \mathbf{H}_z$$

Again solutions for these equations will be same but their boundary conditions will be different.

In general, wave equations can be written as

$$\nabla^2 \mathbf{E} = -\omega^2 \mu \epsilon \mathbf{E}$$

and

$$\nabla^2 \mathbf{H} = -\omega^2 \mu \epsilon \mathbf{H}$$

Replacing  $-\omega^2$  by  $\frac{\partial^2}{\partial t^2}$  as per Eq. 2.18 in the above equations, we get

$$\nabla^2 \mathbf{E} = \mu \epsilon \frac{\partial^2 \mathbf{E}}{\partial t^2} \text{ and } \nabla^2 \mathbf{H} = \mu \epsilon \frac{\partial^2 \mathbf{H}}{\partial t^2}$$

$$\mu \epsilon = \mu_0 \mu_r \cdot \epsilon_0 \epsilon_r = \mu_0 \epsilon_0$$

$$\mu_0 = 4\pi \times 10^{-7} \text{ H/m}$$

and

$$\epsilon_0 = (1/36\pi) 10^{-9} \text{ F/m}$$

$$\mu \epsilon = 4\pi \times 10^{-7} \times \frac{10^{-9}}{36\pi}$$

$$= \frac{1}{9 \times 10^{16}} = \frac{1}{(3 \times 10^8)^2} = \frac{1}{c^2}$$

$$(\because c = 3 \times 10^8 \text{ m/sec})$$

where  $c$  is the velocity of light.

22

$$\nabla^2 \mathbf{E} = \frac{1}{c^2} \frac{\partial^2 \mathbf{E}}{\partial t^2}$$

...(2.25)

$$\nabla^2 \mathbf{H} = \frac{1}{c^2} \frac{\partial^2 \mathbf{H}}{\partial t^2}$$

...(2.26)

and

These two equations represent waves propagating through free space with a velocity equal to that of light and are also known as Helmholtz's wave equations.

## 2.4 TEM/TE/TM/HE WAVE DEFINITIONS

After learning about wave equations in the preceding section we now define TEM, TE, TM, HE waves. The direction of electric and magnetic field components along three mutually perpendicular directions  $x, y, z$  are shown in Fig. 2.4.

### 1. TEM (Transverse electromagnetic wave)

Here both electric and magnetic fields are purely transverse to the direction of propagation and consequently have no ' $z$ ' directed components.

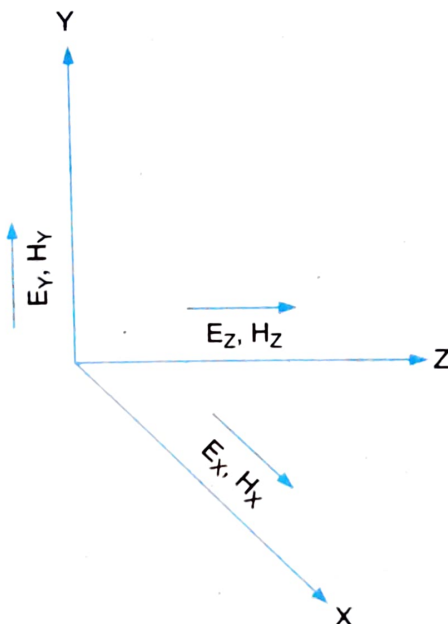


Fig. 2.4

i.e.,

$$\mathbf{E}_z = 0 \quad \text{and} \quad \mathbf{H}_z = 0$$

### 2. TE [Transverse electric] wave

Having looked at the definition of

### 3. TM [Transverse magnetic] wave

Here only the magnetic field is transverse to the direction of propagation and the electric field is not purely transverse.

$$\mathbf{E}_z \neq 0, \quad \mathbf{H}_z = 0$$

i.e.,

### 4. HE (Hybrid) wave

Here neither electric nor magnetic fields are purely transverse to the direction of propagation.

$$\mathbf{E}_z \neq 0, \quad \mathbf{H}_z \neq 0$$

i.e.,

Now we define a few more relations.

(a)  $\nabla^2 \mathbf{E}$  in *rectangular co-ordinate system* as shown in Fig. 2.5 is given by

$$\nabla^2 \mathbf{E} = \frac{\partial^2 \mathbf{E}}{\partial x^2} + \frac{\partial^2 \mathbf{E}}{\partial y^2} + \frac{\partial^2 \mathbf{E}}{\partial z^2} \quad \dots(2.27)$$

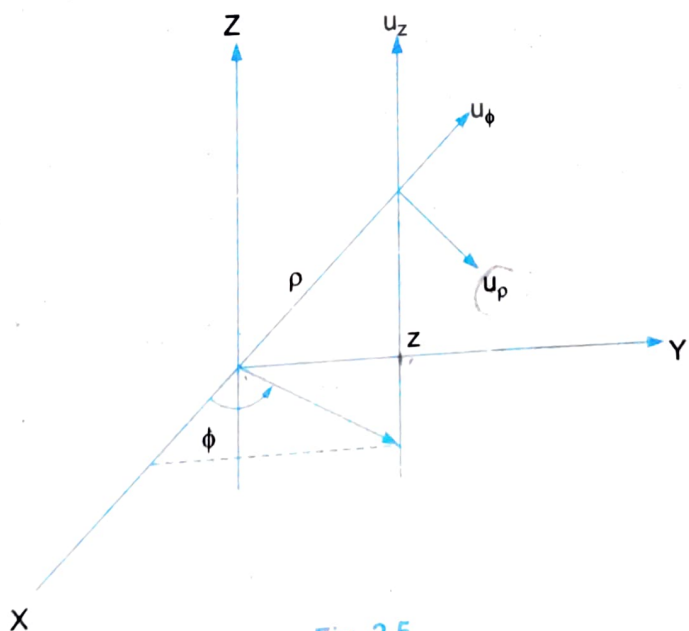


Fig. 2.5

(b)  $\nabla^2 \mathbf{E}$  in *cylindrical co-ordinate system* : Fig. 2.6 shows such a system.



Fig. 2.6

In this case, the wave equation takes the form

$$\nabla^2 \mathbf{E} = \frac{\partial^2 \mathbf{E}}{\partial \rho^2} + \frac{1}{\rho} \frac{\partial \mathbf{E}}{\partial \rho} + \frac{1}{\rho^2} \frac{\partial^2 \mathbf{E}}{\partial \phi^2} + \frac{\partial^2 \mathbf{E}}{\partial z^2} \quad \dots(2.28)$$

where.  $\rho$  = radius vector that varies from 0 to  $a$ ,

$\phi$  = angle vector that varies from 0 to  $2\pi$ ,

$z$  = propagation vector that varies along the length of the cylinder.

(c)  $\nabla \times \mathbf{H}$  in cylindrical co-ordinates is given by

$$\nabla \times \mathbf{H} = \begin{vmatrix} \frac{1}{\rho} \hat{u}_\rho & \hat{u}_\phi & \frac{1}{\rho} \hat{u}_z \\ \frac{\partial}{\partial \rho} & \frac{\partial}{\partial \phi} & \frac{\partial}{\partial z} \\ \mathbf{H}_\rho & \rho \mathbf{H}_\phi & \mathbf{H}_z \end{vmatrix} \quad \dots(2.29)$$

where  $\hat{u}_\rho$ ,  $\hat{u}_\phi$  and  $\hat{u}_z$  are unit vectors along  $\rho$ ,  $\phi$  and  $z$  directions.

(d)  $\nabla \times \mathbf{H}$  in rectangular co-ordinates is given by

$$\nabla \times \mathbf{H} = \begin{vmatrix} \hat{i} & \hat{j} & \hat{k} \\ \frac{\partial}{\partial x} & \frac{\partial}{\partial y} & \frac{\partial}{\partial z} \\ \mathbf{H}_x & \mathbf{H}_y & \mathbf{H}_z \end{vmatrix} \quad \dots(2.30)$$

where  $\hat{i}, \hat{j}, \hat{k}$  are unit vectors along  $x, y$ , and  $z$  directions.

(e) If we consider a wave travelling along positive 'z' directions then the wave equations take the form.

$$\nabla^2 \mathbf{E}_z = -\omega^2 \mu \epsilon \mathbf{E}_z \quad \text{for TM wave} \quad \dots(2.31)$$

$$\text{and} \quad \nabla^2 \mathbf{H}_z = -\omega^2 \mu \epsilon \mathbf{H}_z \quad \text{for TE wave} \quad \dots(2.32)$$

$$\text{Then} \quad \mathbf{E}_z = E_{oz} \cdot e^{-\gamma z} \quad \dots(2.33)$$

where,  $E_{oz}$  = Maximum value of electric field along  $z$  direction, and

$$\gamma = \alpha + j\beta$$

where,  $\gamma$  = propagation constant

$\alpha$  = attenuation constant

$\beta$  = phase constant =  $2\pi/\lambda$

The condition for wave propagation is that  $\gamma$  must be imaginary. Differentiating Eq. 2.33 w.r.t 'z', we get

$$\frac{\partial \mathbf{E}_z}{\partial z} = E_{oz} \cdot e^{-\gamma z} (-\gamma) \quad \dots(2.34)$$

but

$$E_{oz} \cdot e^{-\gamma z} = \mathbf{E}_z,$$

$$\frac{\partial \mathbf{E}_z}{\partial z} = -\mathbf{E}_z \gamma = -\gamma \mathbf{E}_z$$

Hence we can define an operator

$$\frac{\partial}{\partial z} = -\gamma \quad \dots(2.35)$$

Differentiating Eq. 2.34 again w.r.t. 'z',

$$\begin{aligned} \frac{\partial^2 \mathbf{E}_z}{\partial z^2} &= E_{oz} \cdot e^{-\gamma z} (-\gamma) (-\gamma), \\ &= \gamma^2 \mathbf{E}_z \end{aligned} \quad \dots(2.36)$$

Another operator  $\frac{\partial^2}{\partial z^2} = \gamma^2$  can be defined

These operators defined by Eqs. 2.15, 2.18, 2.35 and 2.36 will be useful while developing the wave equations for wave propagation in waveguides. (Chapter 4).

## REVIEW QUESTIONS

- 2.1 What are electromagnetic waves? Obtain an expression for the total energy carried by such a wave.
- 2.2 Define polarization of an EM wave. Briefly explain vertical, horizontal, left hand and right hand circular polarizations.
- 2.3 Define velocity, frequency and wavelengths of an EM wave.
- 2.4 State Maxwell's equations in integral and differential forms.
- 2.5 Starting from Maxwell's equations derive the wave equations. Show that these represent wave propagating in free space with velocity of light.
- 2.6 Define TEM, TE, TM, HE waves. Write down the wave equations for a TE and a TM wave.



# 3

# Transmission Lines

## 3.1 INTRODUCTION

In this chapter we shall study the transmission lines that are limited to high frequency applications i.e., when the length of the transmission line is of atleast the same order of magnitude as the wavelengths of the signal. Generally, the study of transmission lines includes investigation of properties of a system of conductors carrying electromagnetic waves right from low frequency to microwave frequencies. The theory of transmission lines is important for communication engineers. It gives them a means for making the most efficient use of power and equipment, i.e., ensure maximum transfer of power from the feeder line to the antenna, while transmitting or ensure that a receiving antenna matches correctly to the line that connects it to the receiver (so that no power is wasted).

The theory of transmission lines is strictly applicable to only those system of conductors that have a go and return path i.e., those which can support a TEM wave. Although hollow waveguides used in microwave region are not considered to be belonging to this category, the concepts of transmission lines can be applied. Hence, we need to study the basic transmission line theory.

Transmission lines can also be used as circuit elements such as inductors, capacitors, resonant circuits, filters, transformers, as measuring devices at high frequencies etc. in addition to transmitting energy from one point to another. Basically, there are four types of transmission lines, the two wire parallel transmission lines, coaxial lines, strip type substrate transmission lines and waveguides.

## 3.2 TWO WIRE PARALLEL TRANSMISSION LINES

The two wire parallel transmission line is the most common transmission line with a pair of uniform size wires and used for transmission of electrical energy (Fig. 3.1). Such lines are used for power transmission, telephone lines and television signals. Usually these are balanced

transmission lines normally limited to frequencies below 500 MHz due to radiation losses. The possibility of radiation can be prevented by keeping the separation between the two wires as low as one tenth of a wavelength. The electric current flowing through the wires creates a magnetic field around the line. Since these magnetic field lines link the two wires, an inductance is said to be present, uniformly distributed along the entire length of the transmission line. The two wires are made of a conducting material with resistance uniformly distributed over the entire length of the line which will be in series with the inductance. The conductor wire being separated by air dielectric will result in a capacitance between the two wires. A conductance is also said to be present since a conduction current flows between the wires due to non-perfect dielectric. The capacitance and conductance are also uniformly distributed throughout the length of the two wire transmission lines. Considering a portion  $\Delta x$  of this transmission line, the approximate equivalent electric circuit for the two wire transmission line can be shown as in Fig. 3.2. Figure 3.3 shows the electromagnetic field existing in the 2-wire transmission lines.

The dominant mode for the two wire transmission line is the TEM mode.

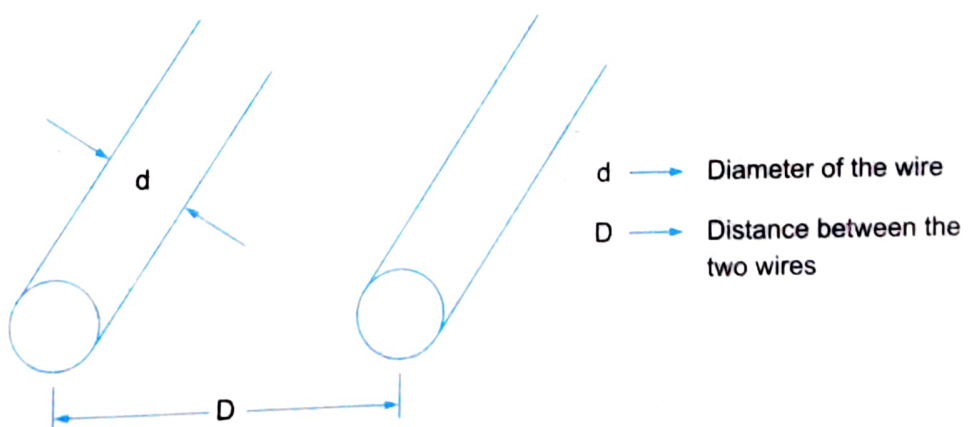


Fig. 3.1 Geometry of parallel transmission line.

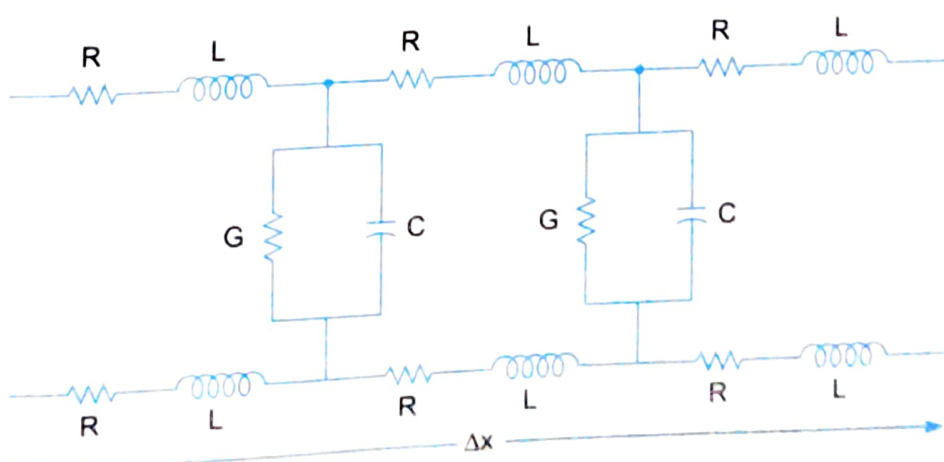
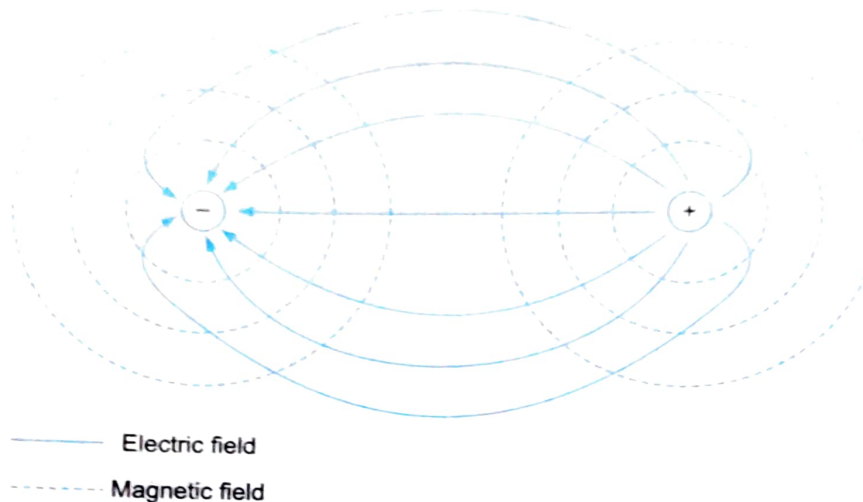


Fig. 3.2 Equivalent electric current (approx.) of a two wire transmission line



**Fig. 3.3** Electromagnetic field of a two wire transmission line.

The impedance per unit length is given by  $Z = R + j\omega L$  and the shunt admittance per unit length by  $\gamma = G + j\omega C$ , where  $R$ ,  $L$ ,  $G$  and  $C$  are the resistance, inductance, conductance and capacitance per unit length.

The inductance per unit length is given by

$$L = \frac{\mu}{\pi} \ln \frac{2D}{d} \text{ H/m} \quad \dots(3.1)$$

where  $\mu$  is the permeability (refers to the basic magnetic property of any arbitrary material and is a measure of the flux density produced by a magnetizing current, given by  $\mu = \mu_r \mu_0$ , where  $\mu_r$  is the relative permeability,  $\mu_0$  is the free space permeability when  $\mu_r = 1$ ) in H/m.

i.e.,

$$L = \frac{\mu_r \mu_0}{\pi} \ln \frac{2D}{d} \text{ H/m} \quad \dots(3.2)$$

Since  $\mu_r = 1$  for non-magnetic materials and since the permeability of free space is  $\mu_0 = 4\pi \times 10^{-7}$  H/m Eq. 3.2 reduces to

$$L = 4 \times 10^{-7} \ln \frac{2D}{d} \text{ H/m} \quad \dots(3.3)$$

The capacitance per unit length is given by

$$C = \frac{\pi \epsilon}{\ln \frac{2D}{d}} \text{ F/m} \quad \dots(3.4)$$

where  $\epsilon$  is the permittivity (refers to the basic property of a dielectric medium as the permittivity of a material increases the volume of electric charge produced by a fixed configuration and as fixed voltage increases) given by  $\epsilon = \epsilon_r \epsilon_0$ , where  $\epsilon_r$  is the relative permittivity or dielectric constant.  $\epsilon_0$  is the free space permittivity when  $\epsilon_r = 1$  in F/m.

Since  $\epsilon = \epsilon_0$  in free space  $= 8.854 \times 10^{-12} \text{ F/m}$ .

Eq. 3.4 reduces to

$$C = 27.78 \times 10^{-12} \frac{\epsilon_r}{\ln \frac{2D}{d}} \text{ F/m} \quad \dots(3.5)$$

Characteristic Impedance. This is one of the most important parameters used in describing a transmission line defined as

$$Z_0 = \frac{\text{Voltage wave value}}{\text{Current wave value}}$$

Any uniform transmission line will have particular value of characteristic impedance associated with it. It may be a complex number or a real number. It is always a real number whenever the transmission line is lossless (i.e., when both series resistance  $R$  and shunt conductance  $G$  are assumed to be zero). In this case  $Z_0 = R_0$ .

In general,

$$Z_0 = \frac{R + j\omega L}{G + j\omega C}$$

$$\text{For a lossless line, } R_0 = \sqrt{\frac{L}{C}} \quad \dots(3.6)$$

where  $L$  and  $C$  are the inductance and capacitance per unit lengths.

For two wire parallel transmission lines  $R_0$  varies from  $300 \Omega$  to  $600 \Omega$ .

Substituting for  $L$  and  $C$  in Eq. 3.6, from Eq. 3.3 and Eq. 3.5, we get the characteristic impedance of two wire parallel transmission line as

$$R_0 = \frac{1}{\pi} \sqrt{\frac{\mu}{\epsilon}} \ln \frac{2D}{d} \Omega \quad \dots(3.7)$$

Since  $\mu_r = 1$  for non-magnetic materials, we obtain after substituting the values of  $\epsilon_0$  and  $\mu_0$  into Eq. 3.7.

$$R_0 = \frac{120}{\sqrt{\epsilon_r}} \cdot \ln \frac{2D}{d} \Omega \quad \dots(3.8)$$

The velocity of propagation on any transmission line is given by

$$v = \frac{1}{\sqrt{LC}}$$

Substituting for  $L$  and  $C$  again, we get the velocity of propagation for a two wire parallel transmission line as

$$v = \frac{1}{\sqrt{\epsilon \mu}} = \frac{1}{\sqrt{\epsilon_r \epsilon_0 \cdot \mu_r \mu_0}} = \frac{C}{\sqrt{\epsilon_r}}$$

i.e.,

$$v = \frac{3 \times 10^8}{\sqrt{\epsilon_r}} = \text{m/s} \quad \dots(3.9)$$

where,  $C = \frac{1}{\sqrt{\epsilon_0 \mu_0}} = 3 \times 10^8 \text{ m/s}$

For most applications of parallel lines, the medium surrounding the conductors is air in which  $\epsilon_r = 1$  is assumed. Therefore, the velocity of propagation is the speed of light.

### 3.3 VOLTAGE AND CURRENT RELATIONSHIPS ON A TRANSMISSION LINE

As already stated, a transmission line consists of continuous conductors with a cross-sectional configuration that is uniform along the whole length of the line. A small length of the line (say  $\delta z$ ) can be represented by an equivalent circuit as shown in Fig. 3.4 with constant parameters  $R$ ,  $L$ ,  $G$  and  $C$  per unit length.  $R$  (the resistance per unit length) takes into account the ohmic losses in the conductor,  $L$  (the inductance/unit length) takes into account the magnetic energy storage of the conductor and  $G$  (the conductance/unit length) takes into account the dielectric loss between the conductors and  $C$  (capacitance/unit length) represents the storage of electric energy. A voltage is placed across the line at the sending end and it is necessary to be able to determine how it changes with distance so that its value at the load (or at some other point of interest) can be found. Similarly the knowledge of the current may also be required.

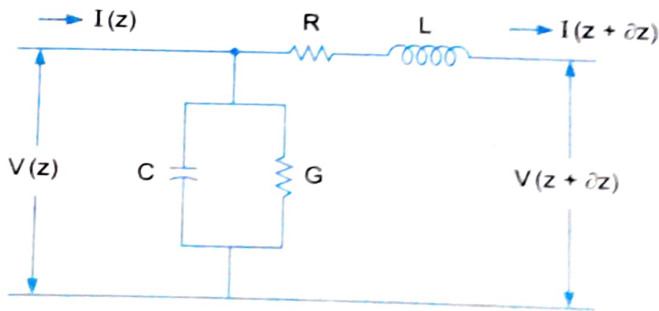


Fig. 3.4 Equivalent circuit for element of length  $\delta z$ .

The current through the shunt circuit is

$$I(z) - (I(z + \delta z)) = G\delta z V(z) + C\delta z \frac{\partial}{\partial t} V(z) \quad \dots(3.10)$$

and the voltage drop in the series circuit is

$$V(z) - V(z + \delta z) = R\delta z I(z + \delta z) + L\delta z \frac{\partial}{\partial t} I(z + \delta z) \quad \dots(3.11)$$

For small  $\delta z$ ,

$$I(z + \delta z) \approx I(z) + \frac{i}{\partial t} (z) \delta z$$

Then Eq. 3.10 becomes

$$\frac{\partial I}{\partial z}(z) = - \left( G + C \frac{\partial}{\partial t} \right) V(z) \quad \dots(3.12)$$

Eq. 3.11 becomes

$$\frac{\partial V(z)}{\partial z} = - \left( R + L \frac{\partial}{\partial t} \right) I(z + \partial z)$$

$$\frac{\partial V(z)}{\partial z} = - \left( R + L \frac{\partial}{\partial t} \right) \left[ I(z) + \frac{\partial I(z)}{\partial z} (z) \partial z \right]$$

i.e., Since  $\frac{\partial I(z)}{\partial z} (z) \partial z$  is very small compared to other terms, we can write

$$\frac{\partial V(z)}{\partial z} = - \left( R + L \frac{\partial}{\partial t} \right) I(z) \quad \dots(3.13)$$

Assuming the signal on the line as sinusoidal, we can write the time dependent terms by  $e^{j\omega t}$ ,

and  $\frac{\partial}{\partial t}$  by  $j\omega$ , in Eqs. 3.12 and 3.13, we get

$$\frac{dI}{dz} = - (G + j\omega C) V \quad \dots(3.14)$$

$$\frac{dV}{dz} = - (R + j\omega L) I \quad \dots(3.15)$$

where the partial derivatives have been replaced by total differentials and  $V$  and  $I$  are implicitly assumed to be functions of both  $z$  and  $t$ .

Differentiating, Eq. 3.15

$$\frac{d^2V}{dz^2} = (R + j\omega L) \frac{dI}{dz}$$

Substituting from Eq. 3.14 for  $\frac{dI}{dz}$ , we get

$$\frac{d^2V}{dz^2} = + (R + j\omega L) (G + j\omega C) V \quad \dots(3.16)$$

Eq. 3.16 can conveniently be expressed as

$$\frac{d^2V}{dz^2} = \gamma^2 V \quad \dots(3.17)$$

where  $\gamma^2 = (R + j\omega L) (G + j\omega C) = ZY$

where  $Z = R + j\omega L$ , the series impedance,  $Z = G + j\omega C$ , the shunt admittance/unit length of the line.

Also

$$\gamma^2 = \alpha + j\beta$$

$\gamma$  is known as the propagation constant, ' $\alpha$ ' the attenuation constant and ' $\beta$ ' the phase constant.

$$\gamma = \sqrt{(R + j\omega L)(G + j\omega C)}$$

The total voltage on the line is given by the solution of Eq. 3.18 given by

$$V = V_1 e^{-\gamma z} + V_2 e^{+\gamma z} \quad \dots(3.19)$$

where  $V_1$  and  $V_2$  are determined by the applied voltage and condition of the line.

$$(Similarly, I = I_1 e^{-\gamma z} + I_2 e^{+\gamma z})$$

Eq. 3.19 can be written as

$$V = V_1 e^{-(\alpha + j\beta)z} + V_2 e^{(\alpha + j\beta)z}$$

$$V = V_1 e^{-\alpha z} e^{-j\beta z} + V_2 e^{\alpha z} e^{j\beta z}$$

i.e.,

Thus the voltage at any point  $z$  from the sending end is the sum of the two components

$$(i) V_1 e^{-\alpha z} e^{-j\beta z}, \text{ and}$$

$$(ii) V_2 e^{\alpha z} e^{j\beta z}$$

In the first component, the initial voltage  $V_1$  at  $z = 0$  is attenuated as it travels down the line (i.e., amplitude decreases with  $z$  as  $e^{-\alpha z}$ ). The term  $e^{-j\beta z}$  is the phase term and does not influence the amplitude of the voltage. This component is called the *forward or incident wave*. In the second component, the amplitude term  $V_2 e^{\alpha z}$  increases with necessary with increasing  $z$ , i.e.,  $z$  must decrease because the voltage must be attenuated as it travels along the line. This component is called the *backward or reflected wave* that is produced by a mismatch between the transmission line and the load.

Hence, we can say that the voltage at a point on the line at a distance  $z$  from the sending end is the sum of the voltages of the forward and reflected waves at that point.

The attenuation constant ( $\alpha$ ), phase constant ( $\beta$ ) and propagation constant ( $\gamma$ ) are called the *line parameters*.

Both the forward and reflected waves are attenuated exponentially at a rate  $\alpha$  with distance travelled,  $\alpha$  the real part of Eq. 3.18 is a function of all the line parameters  $R$ ,  $L$ ,  $G$  and  $C$  expressed in nepers/m or dB/m.

The phase constant  $\beta$  is the imaginary part of Eq. 3.18 which shows the phase dependence with  $z$  of both forward and backward waves. If  $z$  changes from  $z_1$  by a wavelength  $\lambda$  to  $z_1 + \lambda$ , the phase of the wave must change by  $2\pi$ .

$$\therefore \beta(z_1 + \lambda) - \beta(z_1) = 2\pi$$

or

$$\beta = \frac{2\pi}{\lambda} \quad \dots(3.20)$$

The propagation constant  $\gamma$  is the complex sum of attenuation constant  $\alpha$  and phase constant  $\beta$ , called so since it determines how the voltage on the line change with  $z$ .

In general, the voltage and current at any point  $z$ , on the transmission line can be written as

$$V(z) = V_s e^{-\gamma z} + V_r e^{+\gamma z} \quad \dots(3.21)$$

and

$$I(z) = I_s e^{-\gamma z} + I_r e^{+\gamma z} \quad \dots(3.22)$$

where  $V_s$  is the sending voltage amplitude

$I_s$  is the sending current amplitude

$V_r$  is the reflected voltage amplitude

$I_r$  is the reflected current amplitude.

### 3.4 CHARACTERISTIC IMPEDANCE

Characteristic impedance  $z_0$  of a transmission line is also defined as the impedance measured at the input of the transmission line when its length is infinite.

We know from Eq. 3.15

$$\frac{dV}{dz} = -(R + j\omega L) I$$

$$I = \frac{1}{(R + j\omega L)} \frac{dV}{dz}$$

From Eq. 3.18

$$V = V_1 e^{-\gamma z} + V_2 e^{+\gamma z}$$

Differentiating w.r.t.  $z$ , we have

$$\frac{dV}{dz} = \gamma [V_2 e^{\gamma z} - V_1 e^{-\gamma z}]$$

Substituting this in the relation for  $I$  above, we have

$$\begin{aligned} I &= \frac{\gamma}{R + j\omega L} [V_1 e^{-\gamma z} - V_2 e^{\gamma z}] \\ &= \frac{\sqrt{(R + j\omega L)(G + j\omega C)}}{R + j\omega L} [V_1 e^{-\gamma z} - V_2 e^{\gamma z}] \end{aligned}$$

i.e.,

$$I = \sqrt{\frac{G + j\omega C}{R + j\omega L}} [V_1 e^{-\gamma z} - V_2 e^{\gamma z}]$$

This equation is of the form current =  $K \times$  voltage and by analogy with Ohm's law  $\left[ \frac{R + j\omega L}{G + j\omega C} \right]^{1/2}$  is an impedance. Its value at any particular frequency is determined entirely by the line parameters  $R, L, G$  and  $C$  and hence called the characteristic impedance of the line,  $Z_0$  where

$$Z_0 = \sqrt{\frac{R + j\omega L}{G + j\omega C}} \quad \dots(3.23)$$

When the reflected wave in the line is zero, the ratio of  $V(z)/I(z)$  (Eqs. 3.21 and 3.22) is called the characteristic impedance of the line, given by Eq. 3.23.

$Z_0$ , the characteristic impedance can be thought of as

- (i) the value which the load impedance must have to match the load to the line.
- (ii) the impedance seen from the sending end of an infinitely long line.
- (iii) the impedance seen looking towards the load at any point on a matched line-moving along the line produces no change in impedance towards the load.

For low loss lines and at microwave frequencies,  $\omega L \gg R$  and  $\omega C \gg G$ . Hence,

$$Z_0 = \sqrt{\frac{\omega L}{\omega C}} = \sqrt{\frac{L}{C}} = R_0 \quad \dots(3.24)$$

Also

$$\gamma = \sqrt{(R + j\omega L)(G + j\omega C)} = \sqrt{j\omega L \cdot j\omega C}$$

i.e.,

$$\gamma = j\omega \sqrt{LC} = j\beta \quad \dots(3.25)$$

$$\alpha = 0$$

and

$$\beta = \omega \sqrt{LC} \quad \dots(3.26)$$

and

$$\frac{\omega}{\beta} = \frac{1}{\sqrt{LC}} \quad \dots(3.27)$$

The ratio  $\frac{\omega}{\beta}$  is known as the phase velocity of the wave.

### 3.5 REFLECTION COEFFICIENT ( $\rho$ )

We know that a line is matched if it is terminated in a load equal to its characteristic impedance ( $Z_0$ ) which means that the forward wave is totally absorbed by the load and the reflected wave is zero (i.e.,  $V_r = 0$ ). But, the load in normal circumstances will be different from  $Z_0$ , say  $Z_L$  and some of the incident wave will be reflected back down the line. The size of the reflected wave will depend on the difference between  $Z_0$  and  $Z_L$ . The amount of reflection caused by the load is expressed in terms of the voltage reflection coefficient,  $\rho$ . It is defined as the ratio of the reflected voltage to the incident voltage at the load terminals. Let the load be at the position  $z = l$  as shown in Fig. 3.5.

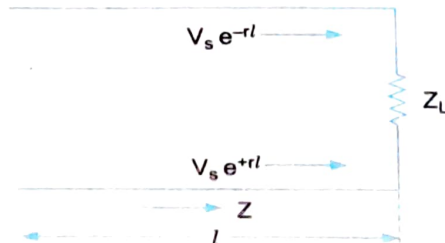


Fig. 3.5

The voltage at  $z = l$  is given by (from Eq. 3.20)

$$V_L = V_s e^{-rl} + V_r e^{rl} \quad \dots(3.28)$$

$$\rho = \frac{V_r}{V_s} = \frac{V_r e^{rl}}{V_s e^{-rl}} = \left( \frac{V_r}{V_s} \right) e^{2rl} \quad \dots(3.29)$$

Usually  $\rho$  will be a complex quantity and can be expressed in polar form as

$$\rho = | \rho | e^{j\psi} \quad \dots(3.30)$$

where  $\psi$  is the angle of reflection coefficient. The current at the load is given by (from Eqs. 3.22 and 3.23, with  $V_1$  replaced by  $V_s$  and  $V_2$  replaced by  $V_r$ ).

$$I_L = \frac{V_s e^{-\gamma l}}{Z_0} - \frac{V_r e^{\gamma l}}{Z_0} \quad \dots(3.31)$$

and

$$Z_L = \frac{V_L}{I_L}$$

Substituting for  $V_L$  and  $I_L$  from Eqs. 3.28 and 3.31, where,

$$Z_L = \frac{\frac{V_s e^{-\gamma l}}{Z_0} V_r e^{\gamma l}}{\frac{V_s}{Z_0} e^{\gamma l} - \frac{V_r}{Z_0} e^{\gamma l}}$$

Dividing by  $V_s e^{-\gamma l}$  throughout,

$$Z_L = Z_0 \left[ \frac{1 + \frac{V_r}{V_s} e^{2\gamma l}}{1 - \frac{V_r}{V_s} e^{2\gamma l}} \right]$$

Using Eq. 3.29, we have

i.e.,

$$Z_L = Z_0 \left( \frac{1 + \rho}{1 - \rho} \right) \quad \therefore \quad \frac{Z_L - Z_0}{Z_L + Z_0} = \dots(3.22)$$

or

$$\rho = \frac{Z_L - Z_0}{Z_L + Z_0} \quad \dots(3.23)$$

Following three cases (with  $Z_L = 0$ ,  $Z_L = \infty$  and  $Z_L = R_L + jX_L$ ) can be considered.

1.  $Z_L = 0$ : This is the case of short circuit load. Here  $\rho = -1$ . From Eq. 3.30  $|\rho| = 1$  and  $\psi = \pi$ .

2.  $Z_L = \infty$ : This is the case of open circuit load. Here  $\rho = 1$ , so that  $|\rho| = 1$  and  $\psi = 0$ .

3.  $Z_L = R_L + jX_L$ : Let  $R_L = 150 \Omega$ ,  $X_L = 100 \Omega$  and  $Z_0 = 50 \Omega$ . Then  $\rho = \frac{100 + j 100}{200 + j 100}$

$$\therefore \rho = 0.6 + j 0.2$$

i.e.,  $|\rho| = 0.63$  and  $\psi = 18.43^\circ$ .

The three cases are shown in Fig. 3.6.

Similar to voltage reflection coefficient, current reflection coefficient  $\rho_I$  can also be defined, given by

$$\rho_I = \frac{Z_0 - Z_L}{Z_0 + Z_L}, \quad \rho_I = |\rho_I| e^{j\psi_I}$$

For a short circuit load,  $\rho_L = 1$  ( $|\rho_L| = 1, \psi = 0$ ), i.e., there is no change of phase between incident and reflected waves.

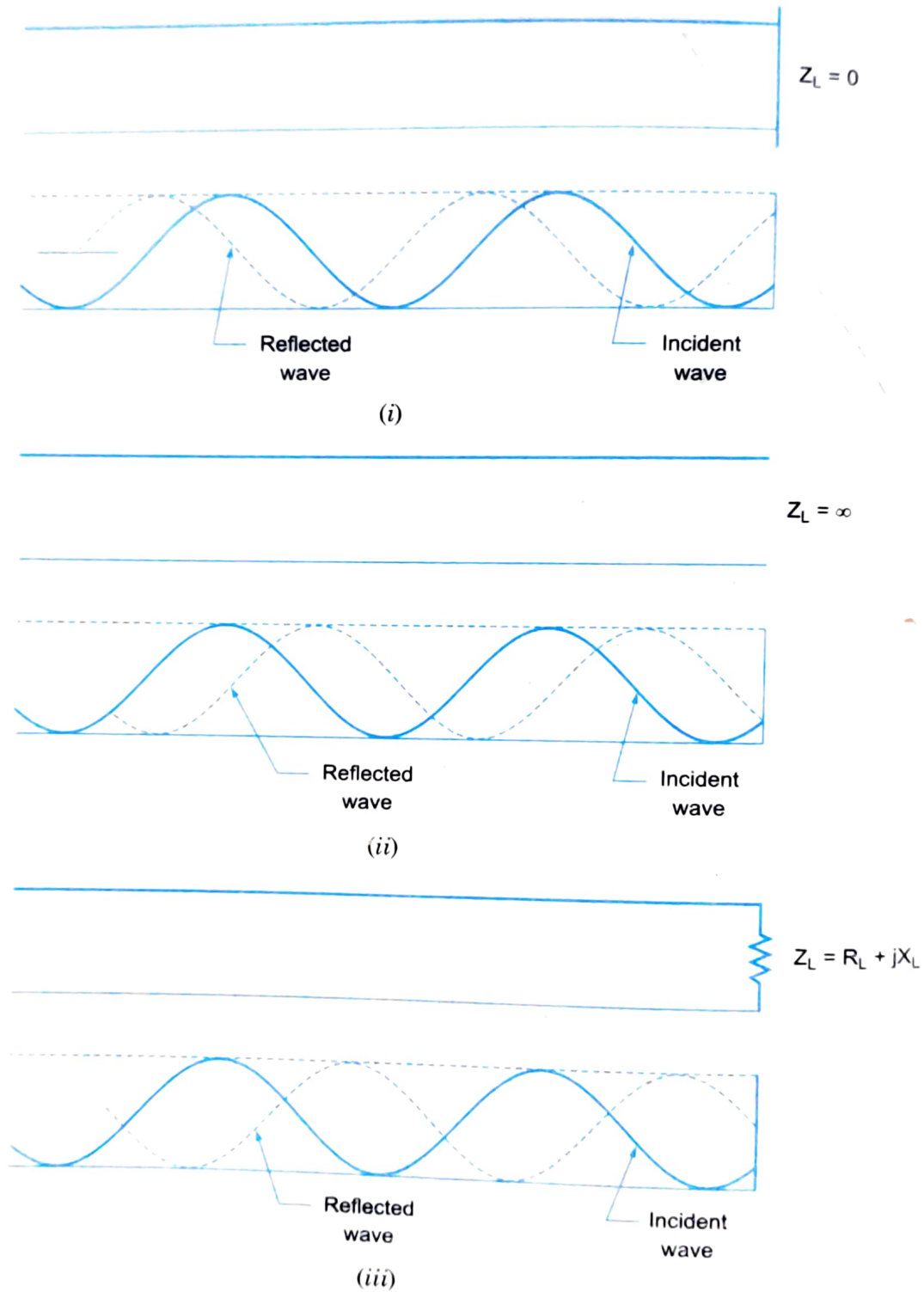


**Fig. 3.6** (i) Short circuit load  $|\rho| = 1, \psi = \pi$  (ii) Open circuit load,  $|\rho| = 1, \psi = 0$   
 (iii) Regular load  $Z_L = R_L + jX_L, |\rho| = R_L + jX_L, \psi = \text{some value}$

It is clear that the phase of the reflected wave relative to the incident wave is determined by  $Z_L$  and  $Z_0$ . If there are no reflected waves,  $V_r = I_r = 0$ , then

$$Z_0 = \frac{V_s e^{-\gamma z}}{I_s e^{-\gamma z}} = \frac{V_s}{I_s} = \text{Real}$$

i.e.,  $Z_0$  is real and hence  $V_s$  and  $I_s$  will be in phase.

### 3.6 INPUT IMPEDANCE

The transmission line and the connected load present some impedance to the source. The degree of mismatch between the source and the line can be determined. The impedance looking into the line from the source (or generator) is called input impedance or sending end impedance. It can be obtained in terms of  $Z_0$ ,  $Z_L$  and  $l$  (the length of the line).

Consider a line, as in Fig. 3.7 with some point  $P$  at a distance  $z$  from the generator. Then

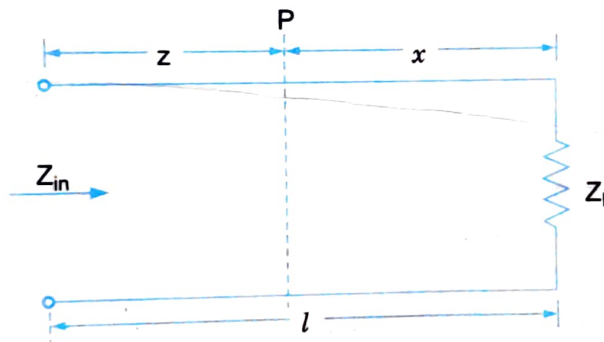


Fig. 3.7

$$Z_P = \frac{V_P}{I_P} = Z_0 \left[ \frac{V_s e^{-\gamma z} + V_r e^{+\gamma z}}{V_s e^{-\gamma z} - V_r e^{+\gamma z}} \right]$$

Substituting for  $\frac{V_r}{V_s}$  from Eq. 3.29, we have

$$Z_P = Z_0 \left[ \frac{e^{\gamma(l-z)} + \rho e^{-\gamma(l-z)}}{e^{\gamma(l-z)} + \rho e^{-\gamma(l-z)}} \right]$$

From Fig. 3.7,  $x = l - z$ , substituting in  $Z_P$  above,

$$Z_P = Z_0 \left[ \frac{e^{\gamma x} + \rho e^{-\gamma x}}{e^{\gamma x} - \rho e^{-\gamma x}} \right]$$

Substituting for  $\rho$  from Eq. 3.23,

$$\begin{aligned} Z_P &= Z_0 \left[ \frac{(Z_L + Z_0) e^{\gamma x} + (Z_L - Z_0) e^{-\gamma x}}{(Z_L + Z_0) e^{\gamma x} - (Z_L - Z_0) e^{-\gamma x}} \right] \\ &= Z_0 \left[ \frac{Z_L (e^{\gamma x} + e^{-\gamma x}) + Z_0 (e^{\gamma x} - e^{-\gamma x})}{Z_L (e^{\gamma x} - e^{-\gamma x}) + Z_0 (e^{\gamma x} + e^{-\gamma x})} \right] \end{aligned}$$

$$= Z_0 \left[ \frac{Z_L \cosh \gamma x + Z_0 \sinh \gamma x}{Z_L \sinh \gamma x + Z_0 \cosh \gamma x} \right]$$

i.e.,  $Z_P = Z_0 \left[ \frac{Z_L + Z_0 \tanh \gamma x}{Z_L \tanh \gamma x + Z_0} \right] \quad \dots(3.24)$

Putting  $x = l$  in Eq. 3.24, we get  $Z_P = Z_{in}$

$$\therefore Z_{in} = Z_0 \left[ \frac{Z_L + Z_0 \tanh \gamma l}{Z_L \tanh \gamma l + Z_0} \right] \quad \dots(3.25)$$

Normalising  $Z_{in}$  and  $Z_L$  with the characteristic impedance of the line,

$$Z_{in} = \frac{Z_{in}}{Z_0} \text{ and } Z_L = \frac{Z_L}{Z_0}$$

$$\therefore Z_{in} = \frac{Z_{in}}{Z_0} = \left[ \frac{\frac{Z_L}{Z_0} + \tanh \gamma l}{1 + \frac{Z_L}{Z_0} \tanh \gamma l} \right]$$

i.e.,  $Z_{in} = \frac{Z_L + \tanh \gamma l}{1 + Z_L \tanh \gamma l} \quad \dots(3.26)$

We can again consider three cases :

(i) If  $Z_L = 0$ ,  $V_L = 0$  (short circuited line). Then

$$Z_{in}(SC) = \tanh \gamma l \quad \dots(3.27)$$

(ii) If  $Z_L = \infty$ ,  $I_L = 0$  (open circuited line). Then

$$Z_{in} = Z_0 \left[ \frac{Z_L + Z_0 \tanh \gamma l}{Z_L \tanh \gamma l + Z_0} \right] = Z_0 \cosh \gamma l \quad \dots(3.28)$$

(iii)  $\alpha = 0$ ,  $\gamma = j\beta$  (lossless line). Then

$$Z_{in} = Z_0 \left[ \frac{Z_L + jZ_0 \tan \beta l}{Z_0 + jZ_L \tan \beta l} \right] \quad \dots(3.29)$$

$$\because \tanh j\beta l = j \tan \beta l$$

$$Z_{in} = \left[ \frac{Z_L + j \tan \beta l}{1 + Z_L \tan \beta l} \right] \quad \dots(3.30)$$

$$Z_{in}(SC) = jZ_0 \tan \beta l \quad \dots(3.31)$$

$$Z_{in}(OC) = -jZ_0 \cot \beta l \quad \dots(3.32)$$

For quarter wave transformer ( $l = \pi/4$ ) than,  $\tan \beta l = \tan \pi/2 = \infty$ . Then

$$Z_{in} = \left[ \frac{\frac{Z_L}{\tan \beta l} + jZ_0}{\frac{Z_0}{\tan \beta l} + jZ_L} \right] = \frac{Z_0^2}{Z_L} \quad \text{or} \quad Z_{in} Z_L = Z_0^2 \quad \dots(3.33)$$

Therefore, for matching a known load to known input (line) impedance a quarter wave section of lossless line (with a characteristic impedance calculated from Eq. 3.33) can be placed between them. The only problem is the frequency sensitivity of this quarter wave transformer since  $\tan \theta$  varies rapidly about  $0 = \pi/2$ .

### 3.7 STANDING WAVES

The total voltage on a lossless line at some point  $z$  from the sending end is given by

$$V = V_s e^{-j\beta z} + V_r e^{j\beta z} \quad (\text{from Eq. 3.20})$$

If the wave is time dependent

$$\begin{aligned} V &= (V_s e^{-j\beta z} + V_r e^{j\beta z}) e^{j\omega t} \\ V &= V_s e^{j\omega t} e^{-j\beta l} [e^{j\beta x} + \rho e^{-j\beta x}] \end{aligned} \quad \dots(3.34)$$

*D 5561*  
*621.384 kvl*

$$\left( \text{Using } \frac{V_s}{V_r} = \rho e^{-2\gamma l} \text{ and } l - z = x \right)$$

This equation represents a *voltage standing wave*, i.e., a stationary wave consisting of the *incident forward wave* and the *reflected backward wave*. The shape of the standing wave depends on the value of reflection coefficient  $\rho$  (which may be complex).

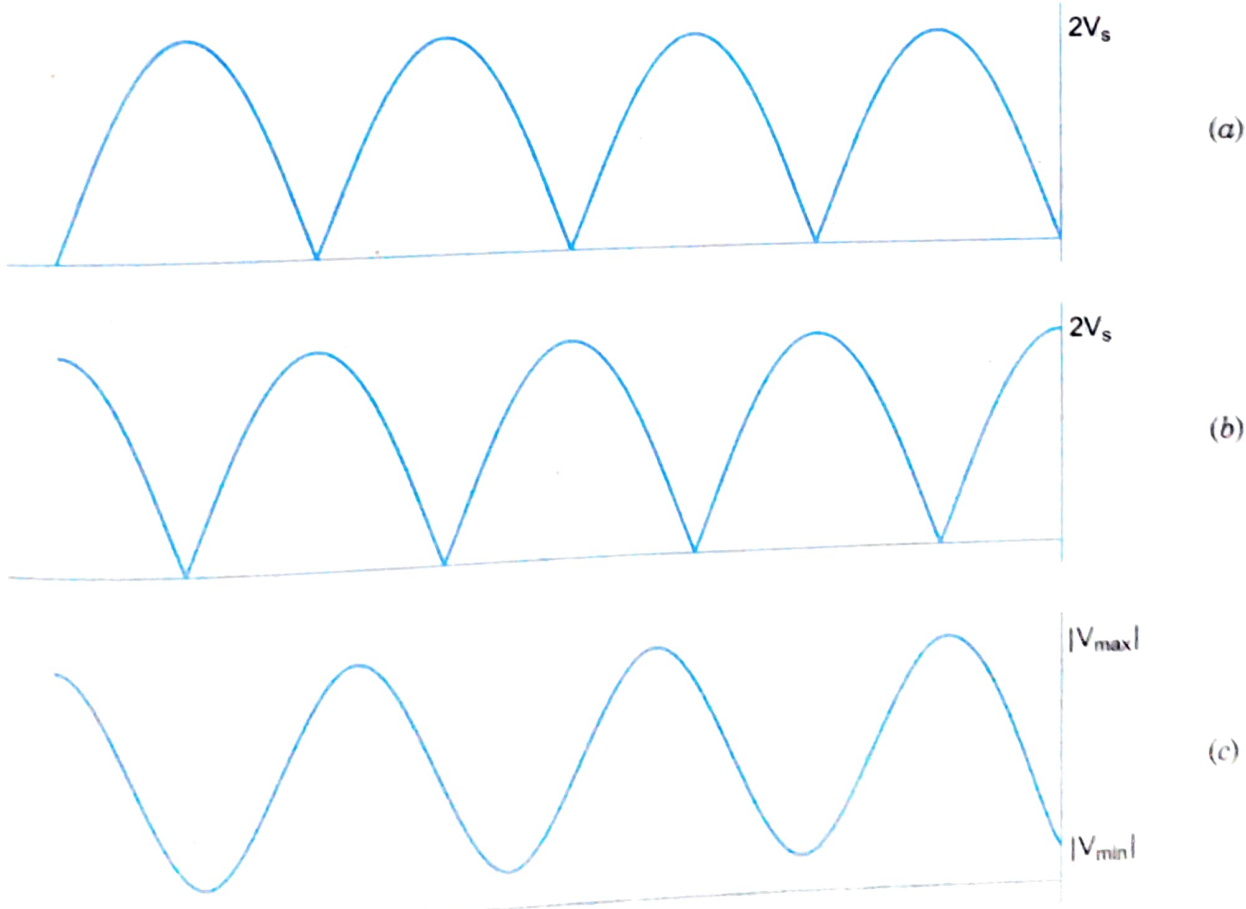


Fig. 3.8 Standing wave (a) due to short circuit (b) due to open circuit  
(c) due to complex load  $z_L = R_L + jX_L$

When the load is a short or open circuit,  $\rho$  has values of  $-1$  or  $+1$  respectively. For a short circuited load ( $\rho = -1$ ), Eq. 3.34 becomes.

$$V = V_s e^{-j\omega t} [e^{j\beta x} - e^{-j\beta x}]$$

Without taking the time dependence,

$$V = V_s e^{-j\beta l} e^{j\beta x} [e^{-j\beta x} - e^{-j\beta x}]$$

i.e.,

$$V = j2V_s e^{-j\beta l} \sin \beta x \quad \dots(3.3)$$

A standing wave detector can be used to measure this standing wave that can display the real part of  $|V|$  in Eq. 3.35.

i.e.,  $|V| = \text{Re} [2V_s e^{-j\beta l} |\sin \beta x|] \quad \dots(3.3)$

The same is shown in Fig. 3.8(a).

In Eq. 3.36, the minimas of  $|V|$  occur when  $\beta x = (n - 1) \pi$  where  $n$  is any positive integer. Adjacent minimas will be separated by  $\pi/\beta$ , i.e., by  $\lambda/2$  ( $\because \beta = 2\pi/\lambda$ ). The first voltage minimum will be at the load terminal.

For an open circuit load, the detected voltage is given by

$$|V| = \text{Re} [2V_s e^{-j\beta l} |\cos \beta x|]$$

Here also the minimas are separated by  $\lambda/2$  with a maximum at the load terminal as shown in Fig. 3.8(b).

For complex load (where  $\rho$  is complex), the minimas do not fall to zero and the maximas do not rise to  $2V_s$ . But still, adjacent minimas are  $\lambda/2$  apart whatever be the value of  $\rho$ .

Similar to voltage standing waves, current standing waves also exist. However, the current maximas will correspond to voltage minimas and vice versa, i.e., voltage standing wave and current standing wave are  $90^\circ$  out of phase along the line.

### 3.7.1 Voltage Standing Wave Ratio (VSWR)

The magnitude of the standing waves can be measured in terms of standing wave ratios. Referring to Fig. 3.8 (c), a moving detector along the line can indicate the voltage maximas ( $V_{\max}$ ) and minimas ( $V_{\min}$ ). The ratio of these two is called the *voltage standing wave ratio* or VSWR denoted by  $S$ .

i.e.,

$$S = \frac{|V_{\max}|}{|V_{\min}|}$$

which allows  $S$  to take values in the range  $1 \leq S \leq \infty$ . The value of  $s$  can be measured experimentally by using a slotted line (discussed in later chapters). Its value depends on the degree of mismatch at the load, i.e., on the reflection coefficient, as can be seen if the complex form of  $\rho$ , ( $\rho = |\rho| e^{j\psi}$ ) is substituted in Eq. 3.34.

i.e.,

$$V = V_s e^{-j\beta l} [e^{j\beta x} + |\rho| e^{j\psi} e^{-j\beta x}]$$

$$= V_s e^{-j\beta(l-x)} [1 + |\rho| e^{j(\psi - 2\beta x)}]$$

when  $\psi - 2\beta x = 2(m-1)\pi$ ,  $m = 1, 2, 3, \dots$

... (3.3)

... (3.38)

and

when  $(\psi - 2\beta x) = 2(m - 1)\pi, m = 1, 2, 3, \dots$ Now VSWR  $s$  is given by (using Eqs. 3.37 and 3.38),

$$S = \frac{|V_{\max}|}{|V_{\min}|} = \frac{1 + |\rho|}{1 - |\rho|} \quad \dots(3.39)$$

$$|\rho| = \frac{S - 1}{S + 1} \quad \dots(3.40)$$

or

Hence  $-1 \leq \rho \leq +1$ .For a short circuit load,  $\rho = -1$  and  $S = \infty$ For an open circuit load,  $\rho = +1$  and  $S = \infty$ For a matched load ( $Z_L = Z_0$ ),  $\rho = 0$  and  $S = 1$ . Hence the ideal values of  $\rho$  and  $S$  are 0 and 1 respectively. If the load is complex ( $+jX$ ),  $\rho = e^{j2\tan^{-1}(X/Z_0)}$  and  $S = \infty$ .For a matched load ( $Z_L = Z_0$ ),  $\rho = 0$  and  $S = 1$ . Hence the ideal values of  $\rho$  and  $S$  are 0 and 1 respectively. If the load is complex ( $+jX$ ),  $\rho = e^{j2\tan^{-1}(X/Z_0)}$  and  $S = \infty$ .For a capacitor load ( $-jx$ ),  $\rho = e^{-j2\tan^{-1}(x/z_0)}$  and  $S = \infty$ .For a resistive load in a lossless line, we know that  $\rho = \frac{R_L - R_0}{R_L + R_0}$  and hence

$$\begin{aligned} S &= \frac{1 + |\rho|}{1 - |\rho|} = \frac{1 + \frac{R_L - R_0}{R_L + R_0}}{1 - \frac{R_L - R_0}{R_L + R_0}} \\ &= \frac{R_L + R_0 + R_L - R_0}{R_L + R_0 - R_L - R_0} \\ &= \frac{R_L}{R_0} \geq 1, \text{ for } R_L \geq R_0 \end{aligned} \quad \dots(3.41)$$

$$= \frac{R_0}{R_L} \geq 1, \text{ for } R_L \leq R_0 \quad \dots(3.42)$$

### 3.7.2 Impedance at a Voltage Minimum and at a Voltage Maximum

It is possible to show that for a lossless line with real characteristic impedance  $Z_0$ , the impedances at a voltage minimum and at a voltage maximum are pure real.

At a voltage minimum (or current maximum),

$$Z_{in} = Z_{min} = \frac{V_{min}}{I_{max}} = Z_0 \left[ \frac{1 - |\rho|}{1 + |\rho|} \right] = \frac{Z_0}{S} \quad \dots(3.43)$$

At a voltage maximum (or voltage minimum),

$$Z_{in} = Z_{max} = \frac{V_{max}}{I_{min}} = Z_0 \left[ \frac{1 + |\rho|}{1 - |\rho|} \right] = Z_0 S \quad \dots(3.44)$$

### 3.7.3 Losses due to mismatch in Transmission Lines

If a transmission line is not terminated in a matched load, there is bound to be a mismatch between the input and output termination of a lossy transmission line. There are various losses encountered like attenuation loss, reflection loss, transmission loss, return loss and insertion loss due to mismatch. We shall discuss these very briefly.

(i) **Attenuation loss** is a measure of the power loss due to absorption of the signal in the transmission line given by

$$\text{Attenuation loss (dB)} = 10 \log_{10} \left( \frac{E_i - E_r}{E_t} \right)$$

where  $E_i$  is the input energy

$E_r$  is the reflected energy from load to the input

and  $E_t$  is the transmitted energy to the load, i.e.,

$$L_a = 10 \log_{10} \frac{|V_s|^2 - |V_r|^2}{[|V_s|^2 - |V_r|^2] e^{-2\alpha l}} \quad \dots(3.45)$$

$$L_a = 8.686 \alpha l$$

where  $l$  is the length of transmission line and  $\alpha$  is the attenuation constant.

(ii) **Reflection loss** is a measure of the power loss due to reflection of the signal due to impedance mismatch of the transmission line, given by

$$\text{Reflection loss (dB)} = 10 \log_{10} \left( \frac{E_r}{E_i - E_r} \right)$$

where  $E_i$  is the input energy

and  $E_r$  is the reflected energy

$$\text{i.e., } L_r = 10 \log_{10} \left( \frac{1}{1 - |\rho|^2} \right) = 10 \log_{10} \frac{(S + 1)^2}{4S} \quad \dots(3.46)$$

(iii) **Transmission loss** is a measure of the power loss due to transmission through the transmission line, given by

$$\text{Transmission loss (dB)} = 10 \log_{10} \frac{E_i}{E_t}$$

$$\text{i.e., } L_t = 10 \log_{10} \frac{|V_s|^2}{|V_s|^2 - |V_r|^2 e^{-2\alpha l}}$$

$$= 10 \log_{10} \frac{e^{2\alpha l}}{1 + |\rho|^2}$$

$$= 8.686 \alpha l + 10 \log_{10} \frac{1}{1 + |\rho|^2}$$

$$L_t = L_a (\text{dB}) + (L_r)_{\text{dB}}$$

... (3.47)

(iv) **Return loss** is a measure of the power reflected by the transmission line given by

$$\text{Return loss (dB)} = 10 \log_{10} \frac{E_i}{E_r} = 10 \log_{10} \frac{|V_s|^2}{|V_r|^2}$$

i.e.,

$$L_{\text{RET}} = 10 \log_{10} \frac{1}{|\rho|^2} = -20 \log_{10} |\rho| \quad \dots(3.48)$$

(v) **Insertion loss** is a measure of the energy loss through a transmission line as compared to direct transmission of energy without the transmission line, given by

$$\text{Insertion loss (dB)} = 10 \log_{10} \frac{E_1}{E_2} \quad \dots(3.49)$$

where  $E_1$  is the energy received by the load when connected directly to the source without the transmission line, and  $E_2$  is the energy received by the load when the transmission line is inserted between the source and the load, keeping the input energy constant.

The insertion loss is due to mismatch losses at the input and output plus the attenuation loss in the transmission line.

### 3.7.4 Impedance Matching

For maximum power transfer from the source to the load, the resistance of the load should be equal to that of the source. The reactance of the load should be equal to that of the source but opposite in sign, i.e.,  $R_L = R_s$  and  $+jx = -jx$  meaning if the source is inductive, the load should be capacitive and vice versa. When this condition is satisfied, we say impedance matching has been achieved. There are several methods to achieve impedance matching. Components used are referred to as impedance matching devices or in transmission lines impedance matching lines.

Generally, signal sources have fixed impedances and impedance matching therefore, reduced to choosing a proper load impedance by some means. If the load impedance is also a fixed value, then it needs to be transferred to the required matched value by means of a matching network. In transmission line system too, this matching becomes important as it is required to achieve unity SWR, to avoid danger of flash at large value of power, to ensure transmission of a given power with a smaller peak voltage and for obtaining greater transmission efficiencies without reflections. Moreover, a properly terminated transmission line with its characteristic impedance  $Z_0$  will be non-resonant, i.e., its input impedance remains at the value of  $Z_0$  even when the frequency is varied and it will not load the source.

Transmission lines having a length of  $\lambda/4$  (quarter wave line) or  $\lambda/2$  (half wave line) have special properties that can be employed for impedance matching purposes.

For a quarter wave line (or an odd multiple of  $\lambda/4$ ), the impedance of the source ( $Z_s$ ) looking towards load is given by

$$Z_s = \frac{Z_0^2}{Z_L}$$

For example, a dipole antenna with a resistive input impedances,  $R_s$  can be matched to the main transmission line (having characteristic impedance,  $Z_0$ ) by means of a quarter wave line (quarter wave transformer) having a characteristic impedance  $Z_0' = \sqrt{Z_0 \cdot R_s}$  shown in Fig. 3.9.

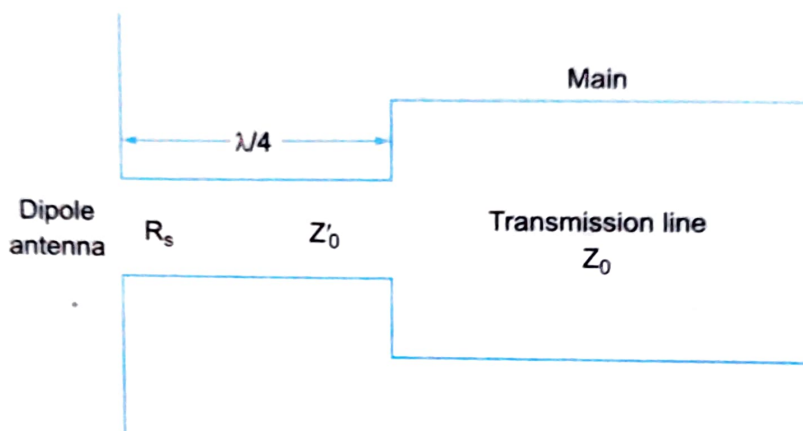


Fig. 3.9

The simple quarter wave transformer however suffers from the disadvantage of being sensitive to change in frequency, since at a new wavelength the quarter wave section will be no longer  $\lambda/4$  length. In such cases, two or more stages of  $\lambda/4$  line stages may be required for increased range of frequencies (broadband impedance matching).

A  $\lambda/2$  long transmission line (half wave line) can also be used for impedance matching. If the load is placed at the far end of a half wave line, the input source impedance will be equal to the load impedance. This property of half wave line is applicable to low loss lines. It however has the disadvantage of frequency dependence and is independent of characteristic impedance. This property can often be helpful when we need to short circuit a line at a point which is not physically accessible. This is achieved by placing a short circuit on the line at a point which is half wavelength away from the desired point. However, this is true only for a particular frequency for which the length is exactly  $\lambda/2$ .

The above properties of  $\lambda/4$  and  $\lambda/2$  transmission lines can act in the same manner as their LC counterparts as shown in Fig. 3.10.

A  $\lambda/4$  transmission line shorted at the far end looks like an open circuit at the other end and behaves like a parallel tuned circuit.

A  $\lambda/4$  open circuited at the far end looks like a series resonant circuit. A short circuited transmission line  $< \lambda/4$  long will act as a pure inductor and an open circuited transmission line  $< \lambda/4$  long will act as a pure capacitor. Similarly a transmission line  $> \lambda/4$  long short circuited at the far end acts like a pure capacitance and that open circuited acts like a pure inductance.

Similarly a  $\lambda/2$  line open circuited at the far end looks like an open circuit at the other end too.

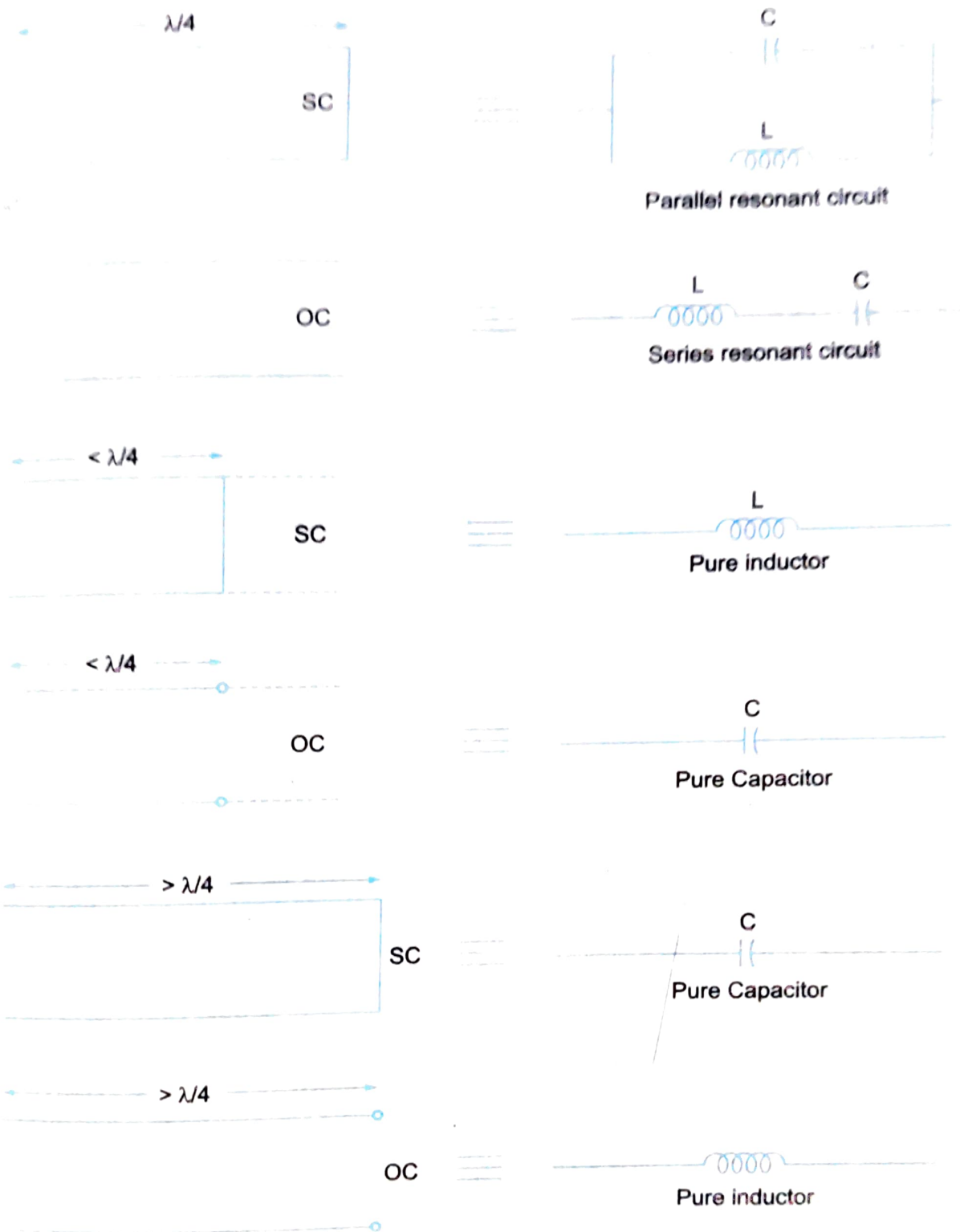


Fig. 3.10

### 3.7.5 Stub Matching

We have seen that a section of transmission line can be used as a matching section by inserting them between the source and the load. It is also possible to connect sections of open or short circuited lines called *stubs in shunt* with the main line at some point or points to effect impedance matching. This method of achieving matching is also called *stub matching*.

At lower RF frequencies, matching can be done by tuning out the complex load reactance (by an inductor or capacitor) and then transforming the resistive component of the load impedance to a value equal to the characteristic impedance of the line. However, at higher microwave frequencies this method may not be useful and transmission line techniques like stub matching is employed.

There are basically two stub matching techniques.

- (i) Single stub matching.
- (ii) Double stub matching.

(i) **Single Stub Matching:** In this technique, a short circuited stub of length  $l'$  is placed at a distance  $l$  from the receiving end impedance  $Z_L \neq Z_0$  as shown in Fig. 3.11.

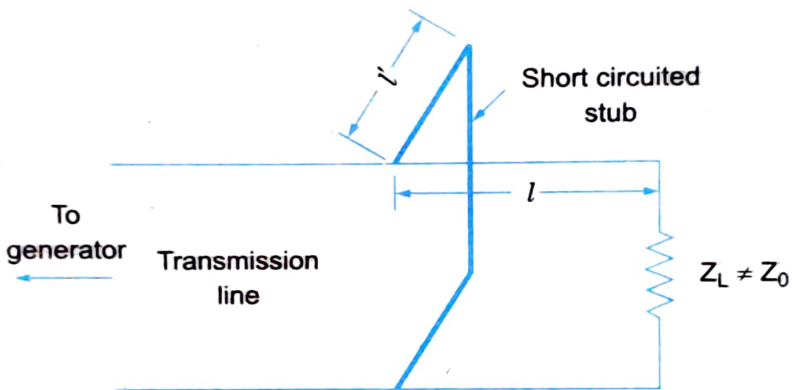


Fig. 3.11 Single stub matching

At microwave frequencies,  $Z_0 = R_0$ , a pure resistance and at a length  $l$  from the load, the input impedance  $R_1 + jX_1$  is such that  $R_1 = R_0$ . Now, the length ( $l'$ ) and the position ( $l$ ) of the stub required for matching are to be found. We know that the input impedance at any point of the transmission line is given by

$$Z_{in} = Z_0 \frac{Z_L + Z_0 \tanh \gamma l}{Z_0 + Z_L \tanh \gamma l}$$

Converting impedance into admittance, we get

$$Y_{in} = Y_0 \frac{Y_L + Y_0 \tanh \gamma l}{Y_0 + Y_L \tanh \gamma l}$$

For a high frequency line,  $\alpha = 0$  so that  $\gamma = j\beta$ . Also changing admittance into normalised admittance in the above equation, we have

$$y_{in} = \frac{y_L + j \tan \beta l}{1 + j y_L \tan \beta l} \quad \dots(3.5)$$

where  $y_{in} = \frac{Y_{in}}{Y_0}$  and  $y_L = \frac{Y_L}{Y_0}$

Eq. 3.50 can be rationalised to get

$$\begin{aligned} y_{in} &= \frac{y_l + j \tan \beta l}{1 + j y_l \tan \beta l} \times \frac{1 - j y_l \tan \beta l}{1 - j y_l \tan \beta l} \\ y_{in} &= g' + j b' = \frac{y_l (1 + \tan^2 \beta l) + j (1 - y_l^2) \tan \beta l}{1 + y_l^2 \tan^2 \beta l} \end{aligned} \quad \dots(3.51)$$

If there are no reflections from load end,  $Y_{in} = Y_0$  or  $\frac{Y_{in}}{Y_0} = 1$ , i.e.,  $y_{in} = 1$ .

Thus the stub has to be located at a point where the real part of  $y_{in}$  (given by Eq. 3.51) is unity.

$$\text{i.e., } \frac{y_l (1 + \tan^2 \beta l)}{1 + y_l^2 (\tan^2 \beta l)} = 1$$

$$\text{or } \tan^2 \beta l (y_l - y_l^2) = 1 - y_l$$

$$\text{or } \tan \beta l = \frac{1}{\sqrt{y_l}} = \sqrt{\frac{Y_0}{Y_l}} = \sqrt{\frac{Z_l}{Z_0}}$$

$$\text{i.e., } \beta l = \tan^{-1} \sqrt{\frac{Z_l}{Z_0}}$$

$$\text{i.e., } \frac{2\pi}{\lambda} l = \tan^{-1} \sqrt{\frac{Z_l}{Z_0}}$$

$$\text{or } l = \frac{\lambda}{2\pi} \tan^{-1} \sqrt{\frac{Z_l}{Z_0}} \quad \dots(3.52)$$

Eq. 3.52 gives the location of stub  $l$  from the load end.

For getting the length of the stub, we equate imaginary part of Eq. 3.51.

$$\begin{aligned} \text{i.e., } \frac{b'}{Y_0} &= \frac{(1 - Y_l^2) \tan \beta l}{(1 + Y_l^2) \tan^2 \beta l} \\ &= \frac{\left(1 - \frac{Y_l^2}{Y_0^2}\right) \sqrt{Y_0 / Y_L}}{1 + \frac{Y_l^2}{Y_0^2} \frac{Y_0}{Y_L}} \quad \therefore \tan \beta l = \sqrt{\frac{Y_0}{Y_L}} \\ &= \left(1 - \frac{Y_L}{Y_0}\right) \sqrt{\frac{Y_0}{Y_L}} \\ b' &= (Y_0 - Y_L) \sqrt{\frac{Y_0}{Y_L}} \quad \dots(3.53) \end{aligned}$$

i.e., the susceptance that should be added at this point by the stub should be  $b'$ , which can be obtained either by an open circuited or short circuited stub. The desired length of the stub ( $l'$ ) to yield the susceptance  $b'$  can be easily computed. Normally short circuited stub will be employed since it radiates less power and also its effective length can be varied by use of a shorting bar (like a shorting plug).

The susceptance of a lossless short circuited (S.C.) stub is  $-Y_0 \cos \beta l'$ , where  $l'$  is the length of the S.C. stubs.

$$(Y_0 - Y_L) \sqrt{\frac{Y_0}{Y_L}} = +Y_0 \cot \beta l'$$

or  $\cot \beta l' = (Y_0 - Y_L) \sqrt{\frac{1}{Y_0 Y_L}}$

or  $\beta l' = \tan^{-1} \frac{\sqrt{Z_l Z_0}}{(Z_L - Z_0)}$

or  $l' = \frac{\lambda}{2\pi} \tan^{-1} \left( \frac{\sqrt{Z_l Z_0}}{(Z_L - Z_0)} \right)$  ... (3.54)

$l$  and  $l'$  from Eq. 3.52 and Eq. 3.54 give the position and length of the S.C. stubs for matching the line.

However, there are certain disadvantages of single stub matching. It is useful only for a fixed frequency since any frequency change requires the location of the stub to be changed (Narrowband system). Also the matching is achieved by final adjustment of the stub by moving along the line slightly. This may be suitable for open wire lines but in coaxial lines it could be inaccurate.

To overcome the disadvantages of single stub matching, double stub matching is employed.

(ii) **Double Stub Matching:** Here two S.C. stubs whose lengths are adjustable independent but whose position are fixed, may be used as shown in Fig. 3.12.

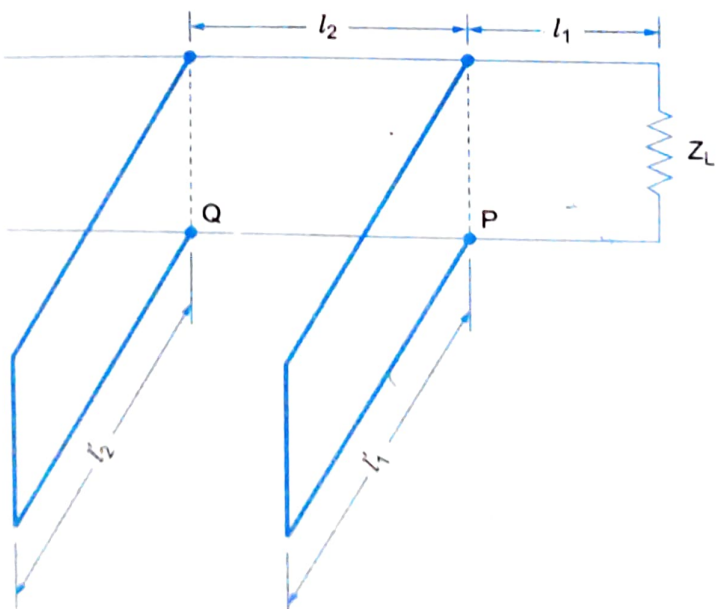


Fig. 3.12 Double stub matching

Let the first S.C. stub whose length is  $l_1'$ , be located at point  $P$  at a distance of  $l_1$  from the load end. The normalized input admittance at that point is given by

$$\begin{aligned}
 y_P &= \frac{Y_P}{Y_0} = \frac{y_l + j \tan \beta l_1}{1 + j y_l \tan \beta l_1} \\
 &= \frac{y_l + j \tan \beta l_1}{1 + j y_l \tan \beta l_1} \times \frac{1 - j y_l \tan \beta l_1}{1 - j y_l \tan \beta l_1} \\
 &= \frac{y_l (1 + \tan^2 \beta l_1) + j (1 - y_l^2) \tan \beta l_1}{1 + y_l^2 \tan^2 \beta l_1} \\
 &= \frac{y_l \sec^2 \beta l_1 + j (1 - y_l^2) \tan \beta l_1}{1 + y_l^2 \tan^2 \beta l_1} \\
 &= g_P + b_P
 \end{aligned} \tag{3.56}$$

where  $g_P = \frac{y_l \sec^2 \beta l_1}{1 + y_l^2 \tan^2 \beta l_1}$  and  $b_P = \frac{(1 - y_l^2) \tan \beta l_1}{1 + y_l^2 \tan^2 \beta l_1}$

When a stub having a susceptance  $b_1$  is added at this point the new admittance will be

$$Y'_P = g_P + j b_P$$

The conductance part remains the same as only the susceptance rate gets affected due to addition of the stub.  $Y'_P$  must be of such value that the admittance  $Y_Q$  equals  $1 + j b_P$ . The stub length at  $Q$  is so adjusted that the new value of  $Y_Q$  is 1 to provide proper matching. The distance  $l_2$  is always kept  $< \lambda/2$ . Generally it is chosen as either  $\lambda/4$  or  $3\lambda/8$ . There is a similar a restriction on length  $l_1$  also. The total distance  $l_1 + l_2$  should be kept as small as possible to avoid reflection loss occurring to the right of  $Q$  (since matching is obtained between point  $Q$  and the generator) or atleast be kept at its minimumm. For this reason, the first stub itself should be placed at the load. In practice, however  $l_1$  is generally  $0.1\lambda$  to  $0.15\lambda$ .

### 3.7.6 Travelling Waves on a Lossless Transmission Line

Considering the forward and backward waves along a transmission line taking into account a time varying input signal we have (from Eq. 3.12 and Eq. 3.13).

$$\frac{\partial I}{\partial z} = - \left( G + C \frac{\partial}{\partial z} \right) V \tag{3.57}$$

and

$$\frac{\partial V}{\partial z} = - \left( R + L \frac{\partial}{\partial z} \right) I \tag{3.58}$$

Differentiating Eq. 3.57 w.r.t.  $t$  and Eq. 3.58 w.r.t.  $z$ ,

$$\frac{\partial^2 I}{\partial t \partial z} = - \left( G + C \frac{\partial}{\partial z} \right) \frac{\partial V}{\partial t} \tag{3.59}$$

and

$$\frac{\partial^2 V}{\partial z^2} = - \left( R + L \frac{\partial}{\partial z} \right) \frac{\partial I}{\partial z} \tag{3.60}$$

For a lossless line,  $R$  and  $G$  can be ignored.

$$\therefore \frac{\partial^2 I}{\partial t \partial z} = -C \frac{\partial^2 V}{\partial t^2} \text{ and } \frac{\partial^2 V}{\partial z^2} = -L \frac{\partial^2 I}{\partial t \partial z}$$

Substituting for  $\frac{\partial^2 I}{\partial t \partial z}$  in  $\frac{\partial^2 V}{\partial z^2}$  relation, we have

$$\frac{\partial^2 V}{\partial z^2} = LC \frac{\partial^2 V}{\partial t^2} \quad \dots(3.61)$$

This is the usual form of what is known as the wave equation. It is satisfied by any function of the form  $f(t - z/v)$  so that if  $V = V_s f(t - z/v)$ , then,

$$\frac{\partial^2 V}{\partial z^2} = \frac{V_s}{v^2} \text{ and } \frac{\partial^2 V}{\partial t^2} = V_s$$

Eq. 3.61 then will be satisfied if  $\frac{1}{v^2} = LC$  with a similar argument, the same condition on the function  $f(t + z/v)$  is also a solution of Eq. 3.61. Hence the total voltage on the line is given by

$$V = V_s f\left(t - \frac{z}{v}\right) + V_r f\left(t + \frac{z}{v}\right) \quad \dots(3.62)$$

The function  $f(t - z/v)$  represents a travelling wave if it is assumed that in order to retain a position of constant phase on the line, it is necessary that  $(t - z/v)$  is a constant.

$$\text{i.e.,} \quad t - \frac{z}{v} = t + \partial t - \frac{z + \partial z}{v}$$

where  $\partial z$  indicates a movement in the  $z$ -direction

$\partial t$  is the time it takes to make the movement.

$$\text{i.e.,} \quad \partial t = \frac{\partial z}{v} \text{ or } v = \frac{\partial z}{\partial t}$$

This  $v$  is the velocity of the wave given by  $v = 1/\sqrt{LC}$  referred to as the phase velocity of the wave.

If a sinusoidal signal is applied to the transmission line, the function  $f[t \pm z/v]$  are written as  $e^{j\omega(t \pm \beta z)}$  for a lossless line. Then

$$V = V_s e^{j\omega(t - \beta z)} + V_r e^{j\omega(t + \beta z)} \quad \dots(3.63)$$

Comparing Eqs. 3.62 and 3.63,

$$\frac{\beta}{\omega} = \frac{1}{v_p} \text{ i.e., } v_p = \frac{\omega}{\beta} \quad \dots(3.64)$$

We know that  $v_p = 1/\sqrt{LC}$ . Hence,

$$\beta = \omega \sqrt{LC} \quad \dots(3.65)$$

In the microwave region, transmission lines are low loss or lossless lines and hence all the above relations are valid which can be summarized as below

$$Z_0 = \sqrt{\frac{L}{C}}$$

$$\gamma = \alpha + j\beta = j\omega \sqrt{LC} \quad (\because \alpha = 0)$$

$$\beta = \omega \sqrt{LC}$$

$$v_P = \frac{\omega}{\beta} = \frac{1}{\sqrt{LC}}$$

# 4

# Microwave Transmission Lines

## 4.1 INTRODUCTION

Microwaves propagate through various microwave circuits, components and devices that act as section of microwave transmission lines that are broadly called *waveguides*. These microwave signals travel as electromagnetic waves and many of the concepts developed in the previous chapter on transmission lines are applicable. These waves can either be radiated into surface via an antenna or can be transmitted over a transmission line. The conventional open wire transmission lines are not suitable for microwave transmission. The reason being, high radiation losses that are associated when the wavelength becomes smaller than the physical lengths of the conventional lines at high frequency. At microwave frequencies, the following transmission lines will be employed.

### (i) Multiconductor lines

- Coaxial lines
- Microstrip lines
- Coplanar lines etc.
- Strip lines
- Slot lines

### (ii) Single conductor lines (waveguides)

- Rectangular waveguides
- Ridge waveguides etc.
- Circular waveguides

### (iii) Open-boundary structures

- Dielectric rods
- Open waveguides etc.

Multiconductor lines normally support TEM or quasi TEM mode of propagation. The single conductor lines (waveguides) support TE or TM waves while open conductor guides can support a combination of TE and TM modes (the hybrid HE modes as they are called).

## 4.2 MULTICONDUCTOR TRANSMISSION LINES

### 4.2.1 Coaxial Lines

The coaxial transmission line is the most widely used transmission line for high frequency applications. A cross-sectional view of a typical coaxial cable is shown in Fig. 4.1a and the TEM mode field supported by it is shown in Fig. 4.1b

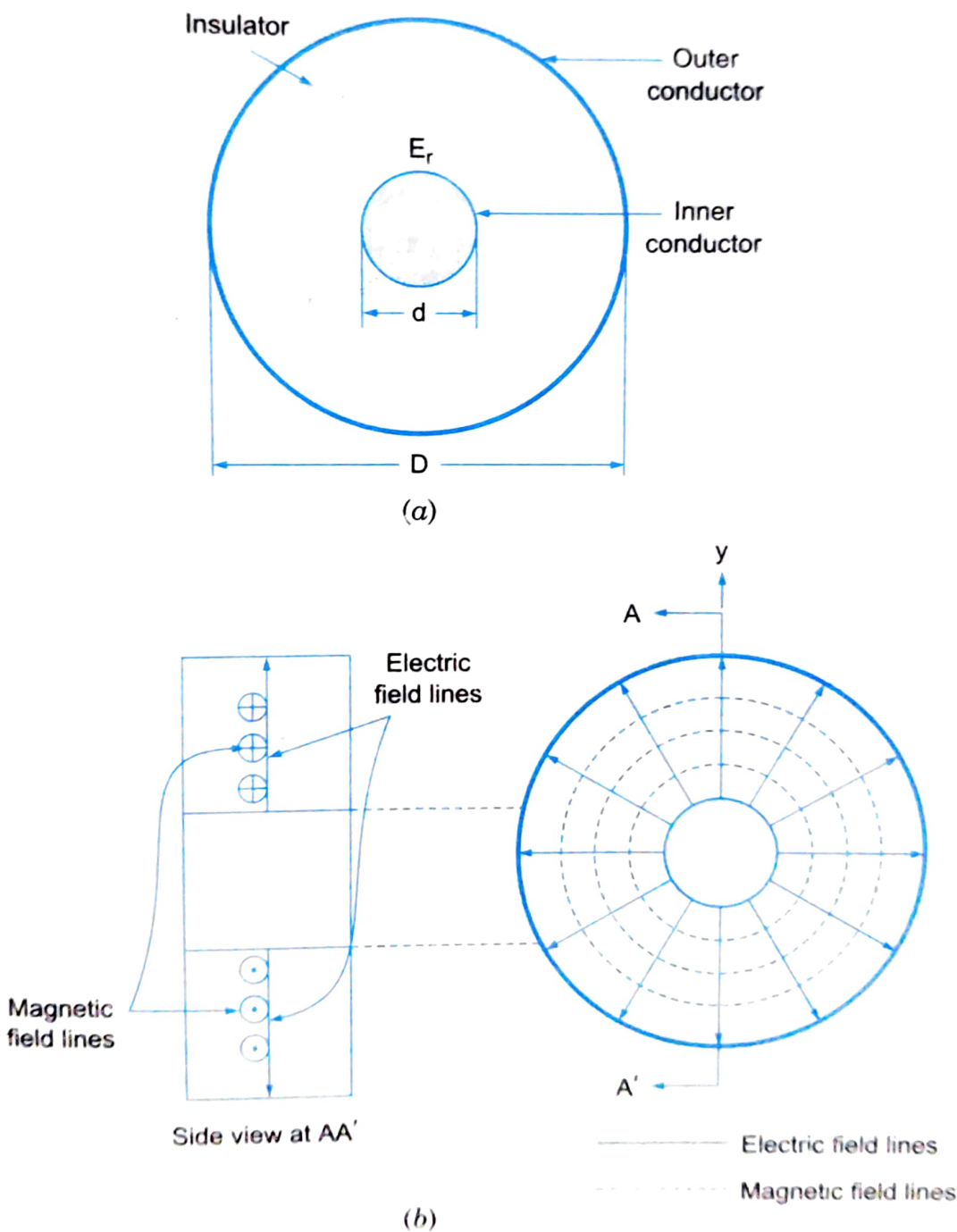


Fig. 4.1 (a) Cross-sectional view (b) TEM wave in coaxial line

A coaxial line consists of an inner conductor with diameter  $d$  which is surrounded by a concentric cylinder of an insulating material with a dielectric constant of  $\epsilon_r$ . The outer conductor is a concentric cylinder with inner diameter  $D$ . The coaxial cable is an unbalanced transmission line since the outer conductor is normally at ground potential. The dominant mode in a coaxial line is the TEM

mode although higher modes do exist (Fig. 4.1b) at high frequencies. The lowest order high order-modes in coaxial cables are  $\text{TE}_{11}$  and  $\text{TM}_{01}$ . The cutoff wavelengths of these modes are  $(\text{TE}_{11}) \approx \pi(D + d)$  and  $\lambda_c (\text{TM}_{01}) \approx 2(D - d)$ . Hence the average circumference of the inner and outer conductors in the propagating cross-section of the coaxial line should be less than the operating wavelengths to prevent higher order mode interference.

As shown in the mode patterns, coaxial lines are non-radiating since the e.m. fields are confined in the insulator between the inner and outer conductors. Coaxial lines can operate well upto 40 GHz due to development of precision connectors for smaller diameter coaxial cables.

The inductance and capacitance per unit length of a coaxial cable are given by

$$L = \frac{\mu}{2\pi} \ln \frac{D}{d} \text{ H/m} ; C = \frac{2\pi \epsilon}{\ln(D/d)} \text{ F/m}$$

Since  $\mu_r = 1$  and  $\mu_0 = 4\pi \times 10^{-7} \text{ H/m}$  and  $\epsilon = \epsilon_r \epsilon_0$  and  $\epsilon_0 = 8.854 \times 10^{-12} \text{ F/m}$

$$L = 2 \times 10^{-7} \ln \frac{D}{d} \text{ H/m} \text{ and } C = 55.56 \times 10^{-12} \frac{\epsilon_r}{\ln(D/d)} \text{ F/m} \quad \dots(4.1)$$

Hence the characteristic impedance of coaxial lines will be,

$$R_0 = \frac{1}{\sqrt{2\pi}} \sqrt{\frac{\mu}{\epsilon}} \ln \left( \frac{D}{d} \right) \Omega$$

Since  $\mu_r = 1$  for nonmagnetic materials, substituting for  $\epsilon_0$  and  $\mu_0$ , we get

$$R_0 = \frac{60}{\sqrt{\epsilon_r}} \ln \left( \frac{D}{d} \right) \Omega \quad \dots(4.2)$$

The velocity of propagation for the coaxial cable is given by

$$v = \frac{1}{\sqrt{\mu \epsilon}} = \frac{c}{\sqrt{\mu_r \epsilon_r}} \text{ m/s}$$

Since  $c = \frac{1}{\sqrt{\mu_0 \epsilon_0}}$  and  $\mu_r = 1$  for coaxial cables,

$$v = \frac{1}{\sqrt{\epsilon_r}} \text{ m/s} \quad \dots(4.3)$$

Also since TEM mode does not have a cutoff frequency, a coaxial cable/line is a broad device. The electric and magnetic field for a wave propagating in the  $z$  direction are given by

$$E = E_t = E_0(\rho, \phi) e^{-j\beta z} = \frac{V_0}{\ln(D/d)} \frac{\hat{\rho}}{\rho} e^{-j\beta z} \quad \dots(4.4)$$

and

$$H = H_t = \pm \frac{\hat{z} \times E_0(\rho, \phi)}{\eta} e^{-j\beta z} = \frac{V_0}{\eta \ln(D/d)} \frac{\hat{\theta}}{\rho} e^{-j\beta z} \quad \dots(4.5)$$

where  $\beta = w \sqrt{\mu \epsilon}$  and  $\eta = \sqrt{\frac{\mu}{\epsilon}}$ , the wave impedance of the TEM wave.

The current density on the outer surface of the inner core is given by

$$J_s = \hat{n} \times H = \hat{\rho} \times H_t = \frac{V_0 e^{-\beta z}}{\eta d \ln(D/d)} \quad \dots(4.6)$$

The power flow through the coaxial line is given by

$$P = \frac{1}{2} \operatorname{Re} \int_d^D \int_0^{2\pi} E \times H \, ds = \frac{\pi V_0^2}{\eta \ln(D/d)} \quad \dots(4.7)$$

where  $ds = \rho d\rho d\phi$

The power loss in the coaxial cable is due to finite conductivity ( $\sigma$ ) of the conductor and the dielectric loss in the insulator between the inner and outer conductors.

For low loss lines,  $\alpha = \frac{1}{2} \left( R \sqrt{\frac{C}{L}} + G \sqrt{\frac{L}{C}} \right) \quad \dots(4.8)$

where

$$R = \frac{R_s}{2\pi} \left( \frac{1}{d} + \frac{1}{D} \right)$$

$$G = \frac{w \epsilon'' C}{\epsilon'}$$

and  $L$  and  $C$  are given by Eq. 4.1 with  $G \rightarrow 0$ , the attenuation ' $\alpha$ ' is minimum for  $D/d = 3.6$ . With an air dielectric ( $\epsilon_r = 1$ ) and  $D/d = 3.6$  gives a characteristic impedance ( $Z_0$ ) of  $76.86 \Omega$ . With solid polyethylene dielectric ( $\epsilon_r = 2.3$ ) and  $D/d = 3.6$  gives  $Z_0$  of  $50.67 \Omega$ . Generally  $50 \Omega$  coaxial lines are preferred for minimum attenuation. For low power transmission, coaxial cables can operate upto 40 GHz whereas for high power transmission they can be employed only upto 34 GHz.

#### 4.2.2 Breakdown Power of a Coaxial Cable

The breakdown of a coaxial cable is determined by the dielectric breakdown. The maximum breakdown field strength is given by

$$E_{bd} = \frac{V_{peak}}{2a} \sqrt{\ln \frac{b}{a}}$$

where  $V_{peak}$  is the peak voltage at breakdown. The breakdown power for a matched coaxial line

$$P_{bd} = \left( \frac{V_{peak}}{\sqrt{2}} \right)^2 / Z_0$$

$$= 4a^2 (E_{bd})^2 \ln \frac{b}{a}$$

For the TEM mode and an air-filled coaxial line at  $E_{bd} = 30 \text{ kV/cm}$ , the breakdown power is given by

$$P_{bd} = 3600a^2 \ln \left( \frac{b}{a} \right) \text{kW}$$

where  $a$  and  $b$  are in cm.

Compared to dominant waveguides operating at the same frequency, coaxial lines have a low breakdown power due to reduced separation distance between the inner and outer conductors.

### 4.2.3 Strip Lines

Strip lines are essentially modifications of the two wire lines and coaxial lines. These are basic planar transmission lines that are widely used at frequencies from 100 MHz to 100 GHz. Fig. 4.2 shows a cross-sectional view of the strip line structure.

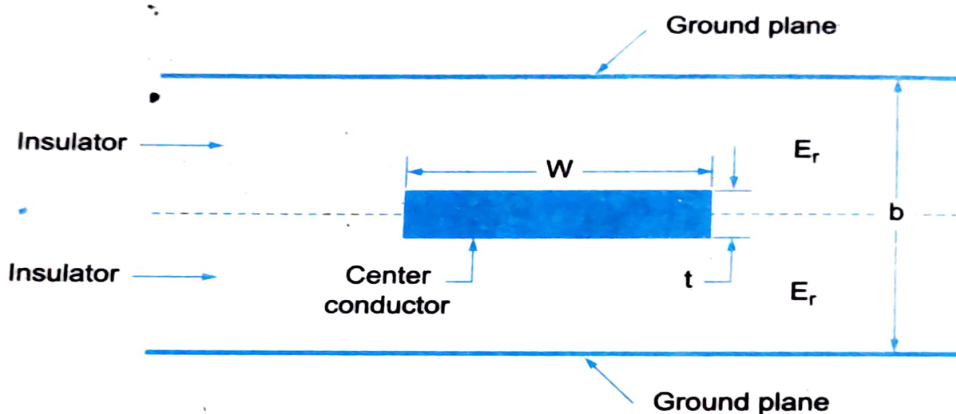


Fig. 4.2 Strip line transmission line.

As seen in Fig. 4.2, a strip line consists of a central thin conducting strip of width  $w$  which is greater than its thickness  $t$ , placed inside the low loss dielectric ( $\epsilon_r$ ) substrate of thickness  $b$  between two wide ground plates. Usually the thicknesses of the metallic central conductor and metallic ground planes are the same. The dominant mode for the strip line is a TEM mode shown in Fig. 4.3, and the fields are confined within the transmission line with no radiation losses. The width of the ground planes is at least five times greater than the spacing between the plates to avoid any vertical side walls at the two transverse ends. There are practically no fringe fields after a certain distance from the edges of the centre conductor. For  $b < \lambda/2$ , there will be propagation in the transverse direction.

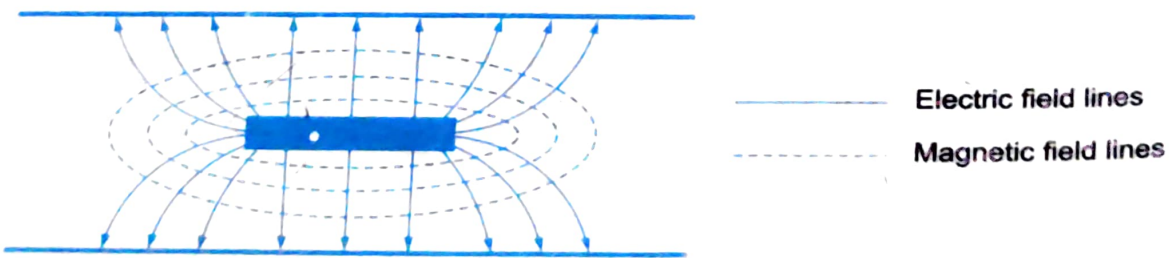


Fig. 4.3 TEM mode of strip line

However, there are certain disadvantages of strip lines in that the circuit is not accessible during development for adjustment and tuning and also it is difficult to mount discrete and active components (like transistors, diodes, circulators, chip resistors, chip capacitors etc.).

The characteristic impedance of strip line has been analysed by a combination of analytical and empirical techniques by H. The design equations are divided into high-impedance region and low-impedance region determined by the ratio of  $w$  to  $(b-t)$ . The impedance of a strip line is inversely proportional to the ratio of the width  $w$  of the inner conductor to the distance  $b$  between the ground planes.

## High Impedance Region:

$$\frac{w}{b-t} \leq 0.35 \text{ and } \frac{t}{b} \leq 0.25$$

The characteristic impedance of a strip line in the high impedance region is given by

$$z_0 = \frac{60}{\sqrt{\epsilon_r}} \ln\left(\frac{4b}{\pi d}\right) \Omega \quad \dots(4.9)$$

where  $d$  is the diameter of a circular conductor equivalent to the rectangular conductor of the strip line with width  $w$  and thickness  $t$

$$d = \frac{w}{2} \left\{ 1 + \frac{t \left[ 1 + \ln\left(\frac{4\pi W}{t}\right) + 0.51\pi \left(\frac{t}{w}\right)^2 \right]}{\pi W} \right\} \quad \dots(4.10)$$

## Low Impedance Region:

$$\frac{w}{b-t} > 0.35$$

Here

$$z_0 = \frac{94.15}{\sqrt{\epsilon_r} \left( \frac{W}{bA} + B \right)} \Omega \quad \dots(4.11)$$

where  $A = 1 - \frac{t}{b}$  and

$$B = \frac{1}{\pi} \left[ \frac{2}{A} \ln\left(1 + \frac{1}{A}\right) - \left(\frac{1}{A} - 1\right) \ln\left(\frac{1}{A^2} - 1\right) \right]$$

The velocity of propagation for the strip line transmission line is given by

$$v = \frac{c}{\sqrt{\epsilon_r}} \text{ m/s} \quad \dots(4.12)$$

and the wavelength of the electromagnetic signal on the strip line transmission line is given by

$$\lambda = \frac{v}{f} = \frac{c}{\sqrt{\epsilon_r} f} \text{ m} \quad \dots(4.13)$$

A graph of characteristic impedance ( $Z_0$ ) vs strip width ratio ( $w/b$ ) is used as a design aid for determining the width of the conductor for a strip line (as a function of  $Z_0$ ,  $\epsilon_r$ ,  $t/b$ ). Nowadays, computer aided design tools are available for designing strip line circuits and transmission lines.

#### 4.2.4 Microstrip Line

Microstrip line is an unsymmetrical strip line that is nothing but a parallel plate transmission line having dielectric substrate, the one face of which is metallised ground and the other (top) face has a thin conducting strip of certain width ' $w$ ' and thickness ' $t$ '. This is shown in Fig. 4.4. The top ground plane is not present in a microstrip as compared to a strip line. Sometimes a cover plate is used for shielding purposes but it is kept much farther away than the ground plane so as not to affect the microstrip field lines as shown in Fig. 4.5.

There are certain advantages of microstrip lines over strip lines, coaxial lines, and waveguides.

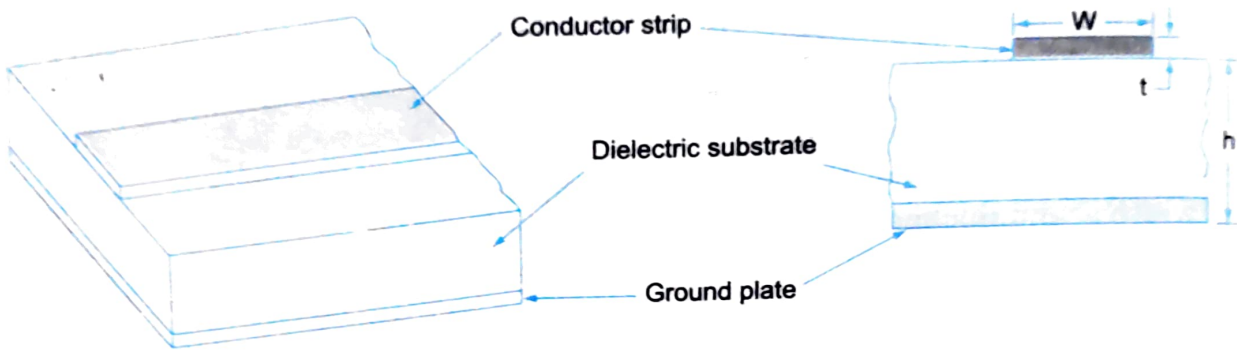


Fig. 4.4 Microstrip line.

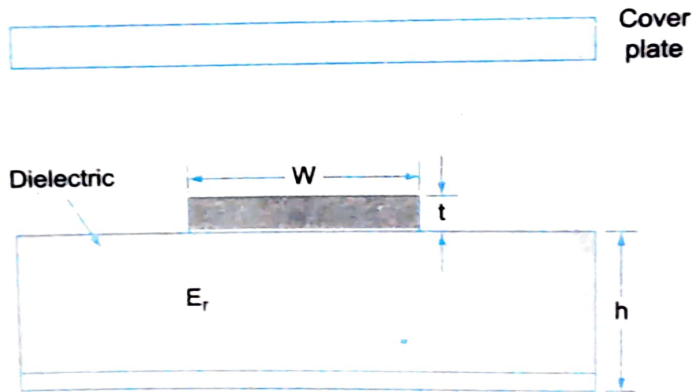


Fig. 4.5 Microstrip line with a cover plate

1. Complete conductor pattern may be deposited and processed on a single dielectric substrate which is supported by a single metal ground plane. Thus fabrication costs would be substantially lower than strip line, coaxial or waveguide circuits.
2. Due to the planar nature of the microstrip structure, both packaged and unpackaged semiconductor chips can be conveniently attached to the microstrip element.
3. Also there is an easy access to the top surface making it easy to mount passive or active discrete devices and also for making minor adjustments after the circuit has been fabricated. This also allows access for probing and measurement purposes.

However, microstrips have some limitations too.

1. Due to the openness of the microstrip structure, they have higher radiation losses or interference due to nearby conductors. These can be reduced by choosing thin substrates with high dielectric constants.
2. Because of the proximity of the air-dielectric air interface with the microstrip conductor at the interface, a discontinuity in the electric and magnetic fields is generated. This results in a microstrip configuration that becomes a mixed dielectric transmission structure with unpure TEM modes propagating. This makes the analysis complicated.

The approximate distribution of electric and magnetic field is shown in Fig. 4.6.

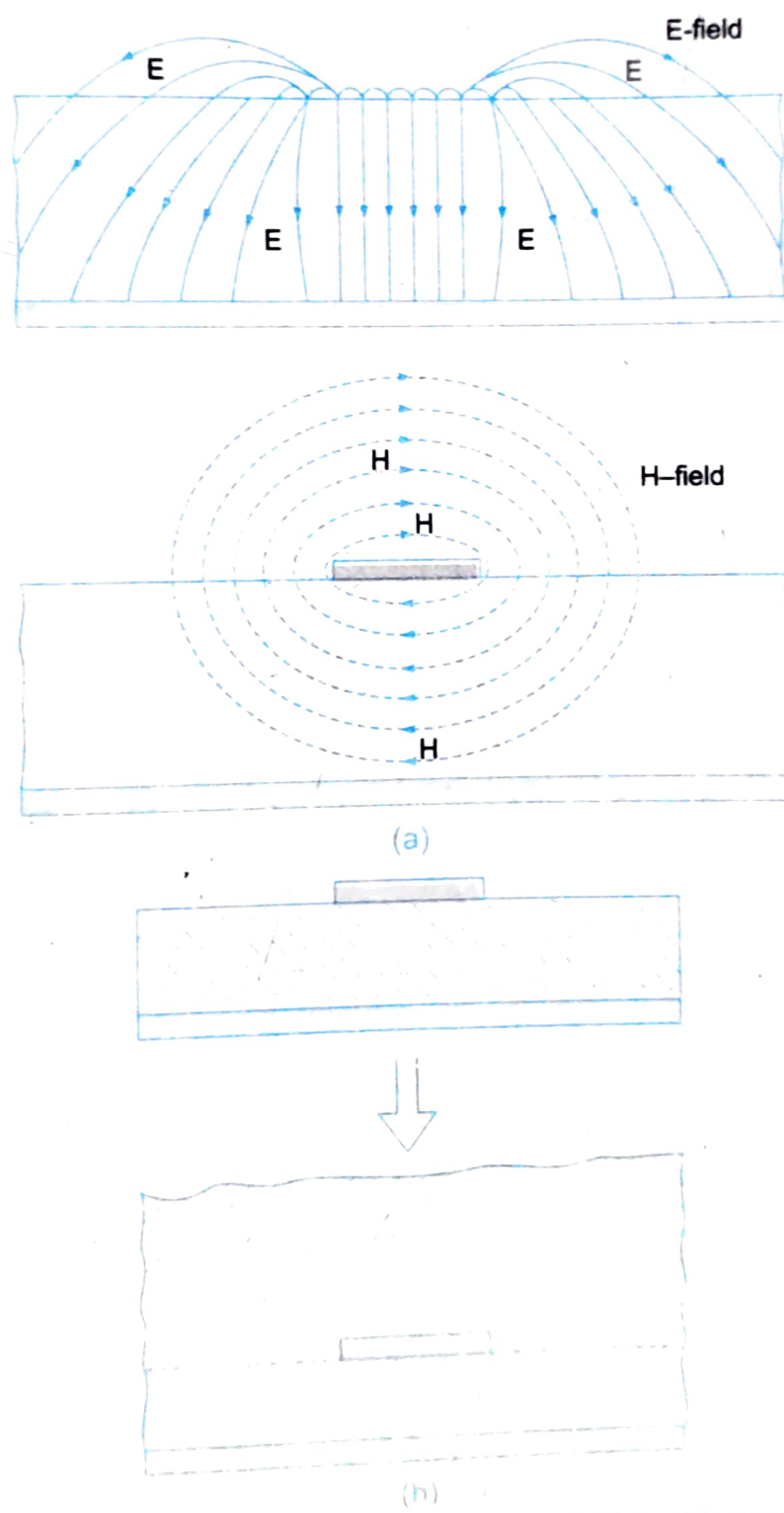


Fig. 4.6 Approximate electric and magnetic field in a microstrip line

We can see that there is a concentration of fields below the microstrip element. The electric field crossing the air dielectric boundary is small and although a pure TEM mode cannot exist, a small deviation from TEM mode does exist which can be neglected.

The characteristic impedance of a microstrip is a function of the strip line width ( $w$ ), thickness ( $t$ ) and the distance between the line and the ground plane ( $h$ ). In fact, the variation of characteristic impedance in terms of  $w/h$  ratio is shown in Fig. 4.7.

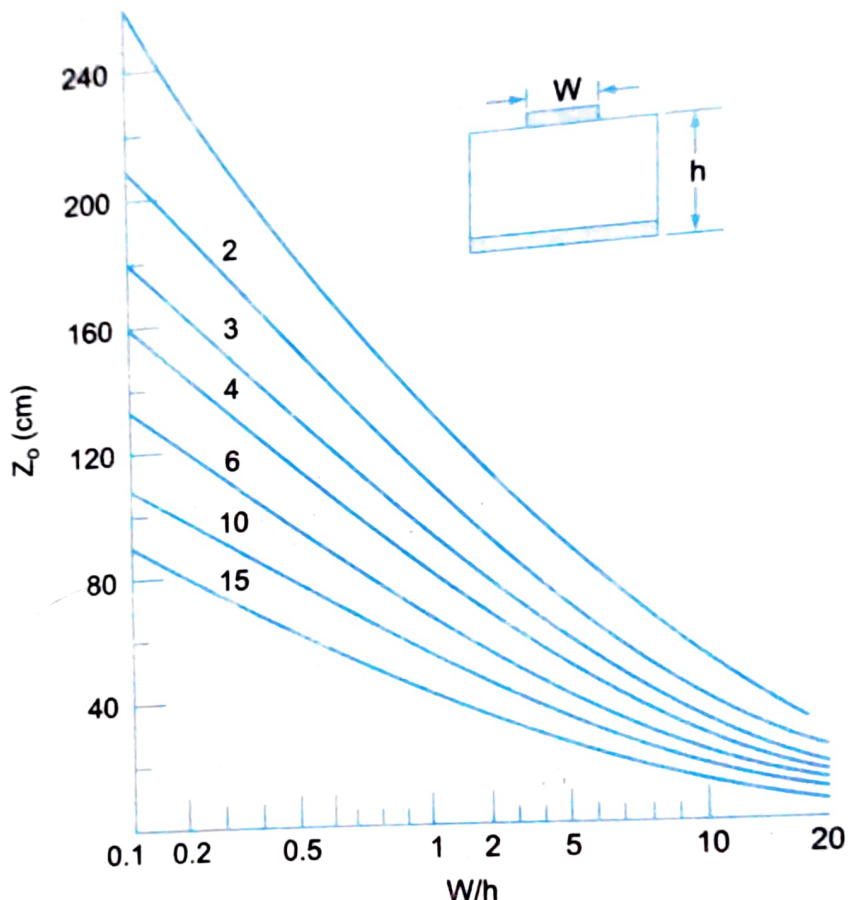


Fig. 4.7  $Z_0$  vs  $w/h$  ratios.

Empirical relation for  $Z_0$  for a microstrip line is given by

$$Z_0 = \frac{60}{\sqrt{\epsilon_r}} \ln \left( \frac{4h}{d} \right) \text{ for } h \gg d$$

where,  $\epsilon_r$  = dielectric constant of the dielectric medium

$h$  = distance between the microstrip line and the ground plane

$d$  = diameter of the wire (wire over ground transmission line).

Effective dielectric constant, ( $\epsilon_{re}$ ) also has an empirical relation given by (due to Digia)

$$\epsilon_{re} = 0.475 \epsilon_r + 0.67$$

where,  $\epsilon_r$  = relative dielectric constant of the board material.

$\epsilon_{re}$  = effective relative dielectric constant for a microstrip line.

Since the cross-section of microstrip line is rectangular, diameter ( $d$ ) also has an empirical relation given by (due to Springfield),

$$d = 0.67 w \left( 0.8 + \frac{t}{w} \right) \quad \dots(4.16)$$

where symbols have their usual significance.

The phase velocity of a microstrip line is given by

$$V_p = V_c / \sqrt{\epsilon_{re}} \quad \dots(4.17)$$

where,  $V_c$  = velocity of electromagnetic waves.

$\epsilon_{re}$  is given by an impartial relation (due to Schmeiter)

$$\epsilon_{re} = \frac{\epsilon_r + 1}{2} + \frac{\epsilon_r - 1}{2} \left( 1 + \frac{10h}{w} \right)^{-1/2} \quad \dots(4.18)$$

Hence design of microstrip is quite complex as it has to take care of so many factors discussed above like  $w$ ,  $h$ ,  $\epsilon_r$ ,  $\epsilon_{re}$ ,  $\epsilon_{eff}$  etc.

Taking into account the relationships for  $\epsilon_{re}$  and  $d$  (from Eqs. 4.15 and 4.16),  $Z_o$  can be written as,

$$Z_o = \frac{87}{\sqrt{\epsilon_r + 1.41}} \ln \left[ \frac{5.98h}{0.8w + t} \right] \text{ for } h < 0.8w \quad \dots(4.19)$$

If  $w \gg h$ , i.e., for a wide microstrip line,  $Z_o$  is given by (as per Assadourian)

$$Z_o = \frac{377}{\sqrt{\epsilon_r}} \cdot \frac{h}{w} \quad \dots(4.20)$$

The microstrip lines have a power handling capacity of a few watts which is quite adequate for most microwave circuits. Microstrip lines offer advantage of miniaturization but for long transmission lengths, they suffer from excessive attenuation per unit length. The attenuation of a microstrip depends upon the electric properties of the substrate and the conductors and also on the frequency. The attenuation constant  $\alpha$ , is given by

$$\alpha = \alpha_d + \alpha_c \quad \dots(4.21)$$

where,  $\alpha_d$  = dielectric attenuation constant (due to dielectric in substrate)

$\alpha_c$  = ohmic attenuation constant (due to ohmic skin losses in conductor and the ground plane)

Radiation loss of a microstrip line depends on the substrate thickness and dielectric constant as well as its geometry.

The quality factor  $Q$  of a microstrip line is very high which may be the requirement for high quality resonant MICs. It is however limited by the radiation losses of the substrate and with low dielectric constant. The  $Q$  of a microstrip line is given by

$$Q_d = \frac{1}{\tan \theta} \quad \dots(4.22)$$

where,  $\theta$  = dielectric loss tangent.

#### 4.2.5 Types of Microstrip Lines

There are many varieties of microstrip lines that have been used in practice such as embedded microstrip, standard inverted microstrip, suspended microstrip and slotted transmission line. The cross-sectional views of these are shown in Fig. 4.8. In addition to all these lines, some other TE<sub>01</sub> lines such as parallel strip lines, coplanar strip lines also have been used for MIC's.

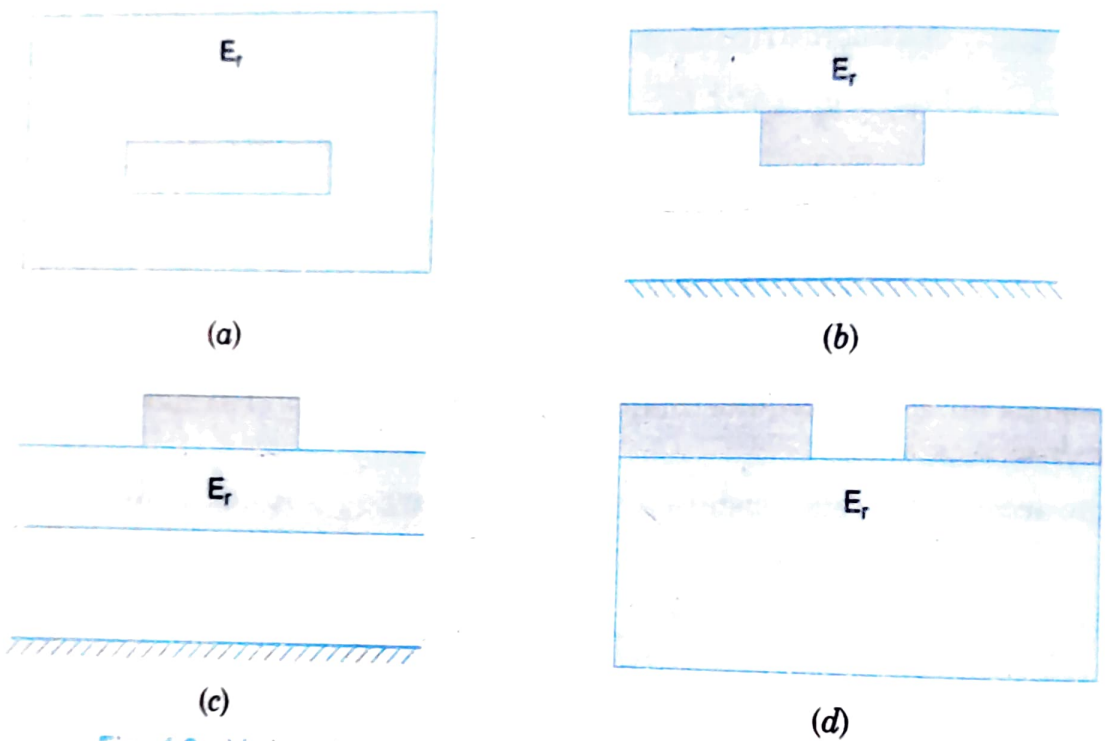


Fig. 4.8 Various types of microstrip lines (a) embedded microstrip, (b) inverted Microstrip (c) suspended microstrip, and (d) slotted microstrip.

#### Parallel Strip Lines

A parallel strip line consists of two perfect dielectric slabs of uniform thickness, as shown in Fig. 4.9.

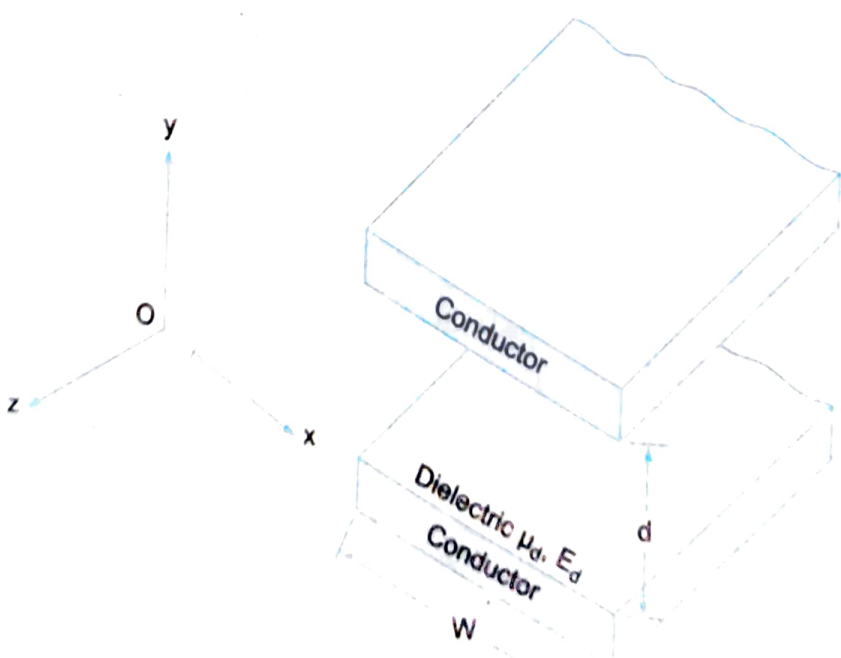


Fig. 4.9 Parallel strip line

The parallel strip line is similar to a two conductor transmission line, with the result it can support a quasi TEM mode.

### Coplanar Strip Lines

A coplanar strip line consists of two conducting strips on one substrate surface with one strip grounded as shown in Fig. 4.10.

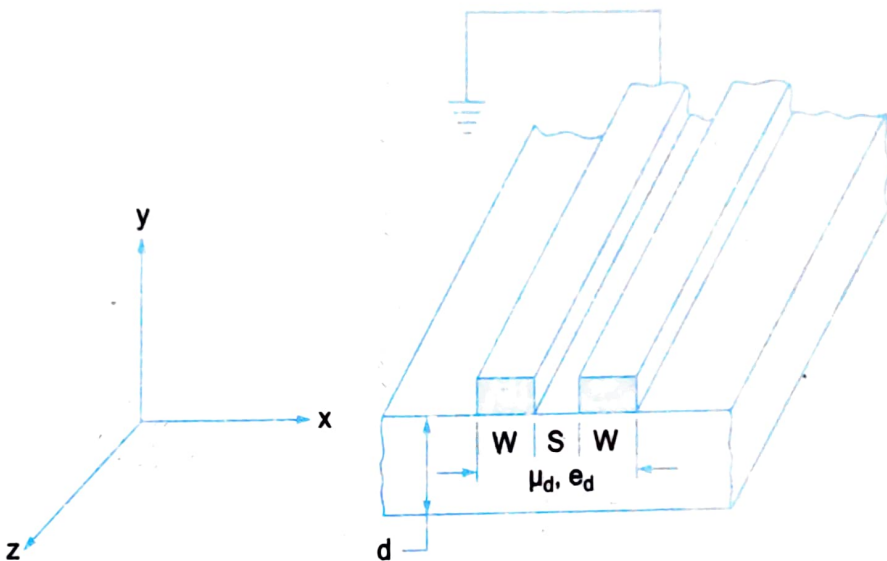


Fig. 4.10 Coplanar strip line.

The coplanar strip line has advantages over the conventional parallel strip line because its two strips are on the same substrate surface for convenient connections.

### Slot Line and Coplanar Waveguide

Two other types of transmission lines are used in MICs. These are known as slot line and coplanar waveguide.

As shown in Fig. 4.11a, a slot line consists of a slot or gap in a conducting coating on a dielectric substrate. The fabrication process is identical to that of microstrip lines.

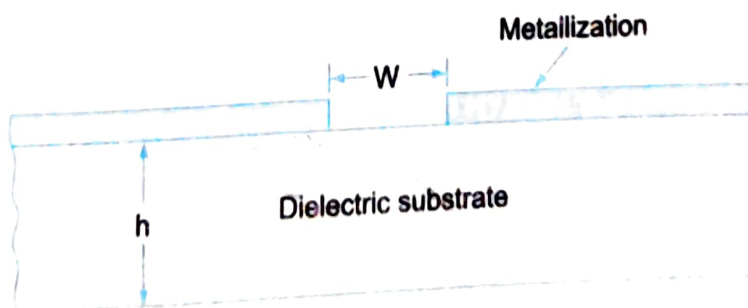


Fig. 4.11 (a) Slot line

As shown in Fig. 4.11b a coplanar wave guide consists of a strip of thin metallic film deposited on the surface of a dielectric slab with two ground electrodes running adjacent and parallel to the strip on the same surface.

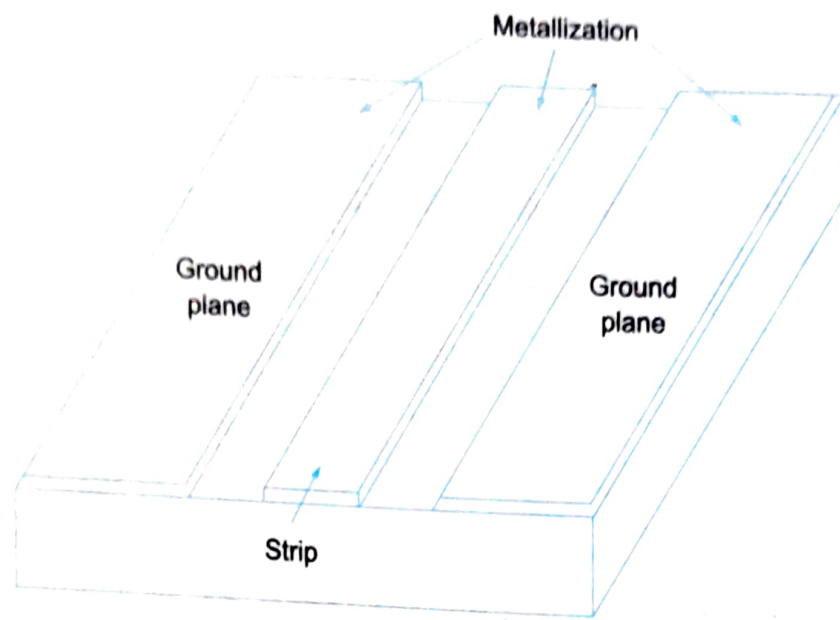


Fig. 4.11 (b) Coplanar waveguide.

#### 4.2.6 Microwave Components using Strip Lines

It is possible to design/construct most of the microwave components using strip lines as the strip line particularly lends itself to satisfactory fabrication processes. The dielectrics used in the development of components include polystyrene and laminated phenolic plastics. Fibrous materials impregnated with a thermosetting resin have had their use limited to guide wavelength studies only due to their excessive attenuation. The products are available commercially in strip form with either or both sides coated with copper and have been used with the mechanical stripping, photo engraving and etching processes. In case of polystyrene, cementing of metal conductors to the surface gives good performance without introducing appreciable dissipation. Preformed shapes of line conductor can thus be cemented on place to form a particular configuration. Sandwich type construction is readily accomplished by cementing under pressure such as 1 GHz, 5 GHz and 10 GHz. Some of them include

1. **Transitions:** Strip to coaxial transition equivalent to coaxial to waveguide transmission with VSWR's as low as 1.2 at 5 GHz.
  - Waveguide to strip line or crossbar feed waveguide to coaxial transitions.
2. **Crystal Modulators:** A coaxial transition with the crystal holder as an integral part of the coaxial with VSWR's less than 1.5 in the 4.4 to 5 GHz band.
3. **Magic Tees:** With extremely low VSWR's balanced crystal response and negligible radiation loss.
4. **Attenuator Pads and Loads:** Microstrip line coated with a lossy dielectric or graphite paint of appropriate characteristics. The lossy dielectric can be tapered to get proper matching.

- Attenuators with a range of 0 to 15 dB similar to flap attenuator. Variation of attenuation is obtained by rotation of the flap which adjusts the length of the dielectric run with respect to the strip line.
- 5. Directional couplers, filter elements and antennas can also be fabricated.
- 6. Microwave receivers with noise figures better than 16 dB and very little conversion losses can be fabricated in one piece.

## Microstrip Lines Advantages and Disadvantages

The microstrip lines can be used at microwaves particularly in those applications where it is more bulky and expensive to manufacture conventional plumbing is at a disadvantage.

However there are a number of limitations to microstrips.

1. Open structure of microstrip leads to a somewhat greater coupling between side-by-side configurations as compared to waveguide or coaxial system. The absolute value of coupling is however small.
2. Higher attenuation compared to waveguide structures. Hence cannot be used in systems where extremely low loss is the requirement. For example, in microwave receivers where line length are smaller, the insertion loss can be made negligible compared to other losses.
3. Low resonant impedance is inherent in microstrip structures which limit the magnitude of the obtainable  $Q$ .

A practical compromise between the extremes of maximum in electrical performance and optimum physical realisation can be made.

## Design Considerations of a Microstrip Line

The design parameters are

1. Characteristic impedance

$$Z = Z_o / \sqrt{\epsilon_{eff}}$$

2. Guide wavelength

$$\lambda = \lambda_o / \sqrt{\epsilon_{eff}}$$

3. Effective dielectric component is a function of  $w/h$ ,  $\epsilon_r$  and frequency. (Refer Fig. 4.12).

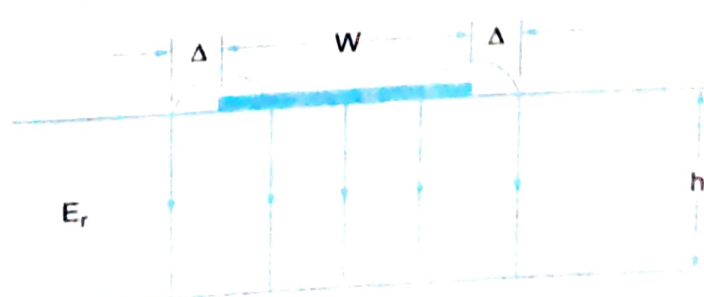


Fig. 4.12 Designing microstrip line

Hence  $Z$  and  $\lambda$  are functions of  $w/h$ ,  $\epsilon_r$ , and frequency  $f$ .

Design of microstrip involves choosing

1. suitable substrate ( $\epsilon_r$ ).
2. thickness of the substrate ( $h$ ) and calculating  $w$  to get desired impedance ( $Z$ ).

While selecting  $\epsilon_r$ ,  $h$  and  $w$ , it is to be ensured that only dominant mode is propagated.

However there could be certain limitations while designing microstrip lines. Some of them discussed earlier can be summarised as below.

1. Since most of the field is concentrated in the dielectric substrate, a slight change in  $\epsilon_r$ , due to temperature change and batch to batch variation, will change the impedance and guide wavelength considerably.
2. Thinner substrates permit high frequency operation, but at the expense of  $Q$ -factor (10).
3. Circuit dimensions at millimeter wave frequency are very small which results in fabrication problems.
4. Integration with other planer transmission lines are not very good; especially at mm-wave frequency.
5. Useful frequency range of microstrip is 0–50 GHz.

## Microstrip Antennas

Microstrip antennas are the promising candidates for microwave and millimeter wave applications where low cost, low profile, confirmability and ease of manufacture are found to outweigh the electrical disadvantages such as narrow bandwidth and low power capability. In arrays, they allow easy integration with active and passive circuits for beam control and signal processing.

Use of printed circuit technology has brought about rapid growth in the development of antennas having patches of conducting materials etched on one side of a dielectric substrate, the other side of the board being a metal ground plane. Such antennas are commonly referred to as Microstrip patch antennas. As the resulting printed circuit board is very thin, (about 1 mm thick), these are also known as paper thin antennas.

The simplest configuration of a microstrip antenna is shown in Fig. 4.13.

The popularity of such antennas arises from the fact that the structure is planar in configuration and enjoys all the advantages of printed circuit technology. The feed lines and matching networks are fabricated simultaneously with the antenna structure. The solid state components can also be added directly on the microstrip antenna board and hence such antennas are compatible with modular designs. These antennas meet the prime requirements i.e., small size, low weight and hence it is easy to manufacture on mass scale with low manufacturing cost. Also these can be applied directly to metallic surface on an aircraft or missile and not disturb aerodynamic flow and thus have better aerodynamic properties. Accordingly these antennas are replacing old and bulky antennas on aerospace vehicles i.e., on satellite, missile, rocket or aircraft etc.

The other advantages of microstrip antennas are that linear and circular polarisations are possible with simple change in feed position and dual frequency antennas can be made possible.

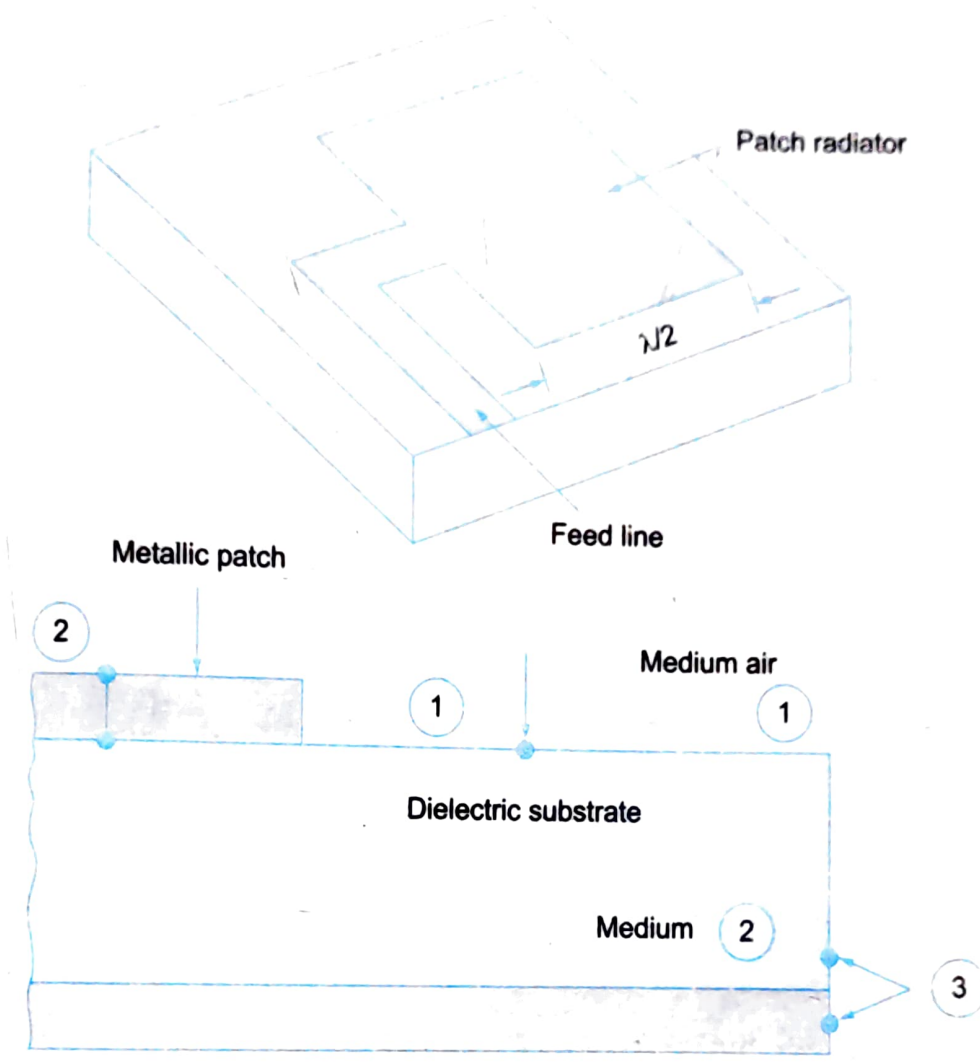


Fig. 4.13 Microstrip patch antenna.

The main limitations however are

1. Narrow bandwidth (a few percent)
2. Practical limitations on maximum gain ( $\sim 20$  db)
3. Radiate into a half plane
4. Poor endfire radiation performance
5. Low power handling capability
6. Possibility of excitation of surface waves.

Various shapes of patches used in practice are shown in Fig. 4.14 with microstrip fed patches.

The choice depends on the required type of the radiated field viz. linear, circular or elliptical polarization.

### Principle of Operation

Microstrip antennas are essentially suitably shaped discontinuities that are designed to radiate. The discontinuities represent abrupt changes in the microstrip line geometry e.g., a step change in width, an open end or a microstrip bend. Discontinuities alter the electric and magnetic field distributions. These result in energy storage and sometimes radiation at the discontinuity. As long as the physical dimensions and relative dielectric constant of the line remain constant, virtually no radiation occurs. However, the discontinuity introduced by the rapid change in line width at the

junction between the feed line and patch radiates. The other end of the patch where the metallization abruptly ends also radiates. When the fields on a microstrip line encounter an abrupt change in width at the input to the patch, electric fields spread out. It creates fringing fields at this edge indicated. After this transition the patch looks like another microstrip line. The fields propagate down this transmission line until the other edge is reached. Here the abrupt ending of the patch again creates fringing fields as for the open end discontinuity. The fringing fields store energy. The edges appear as capacitors to ground since the changes in the electric field are greater than that of the magnetic field. Because the patch is much wider than a typical microstrip line, the fringing fields also radiate, which is represented by a conductance in shunt with the edge capacitors, which accounts for power lost due to radiation as shown in Fig. 4.15.

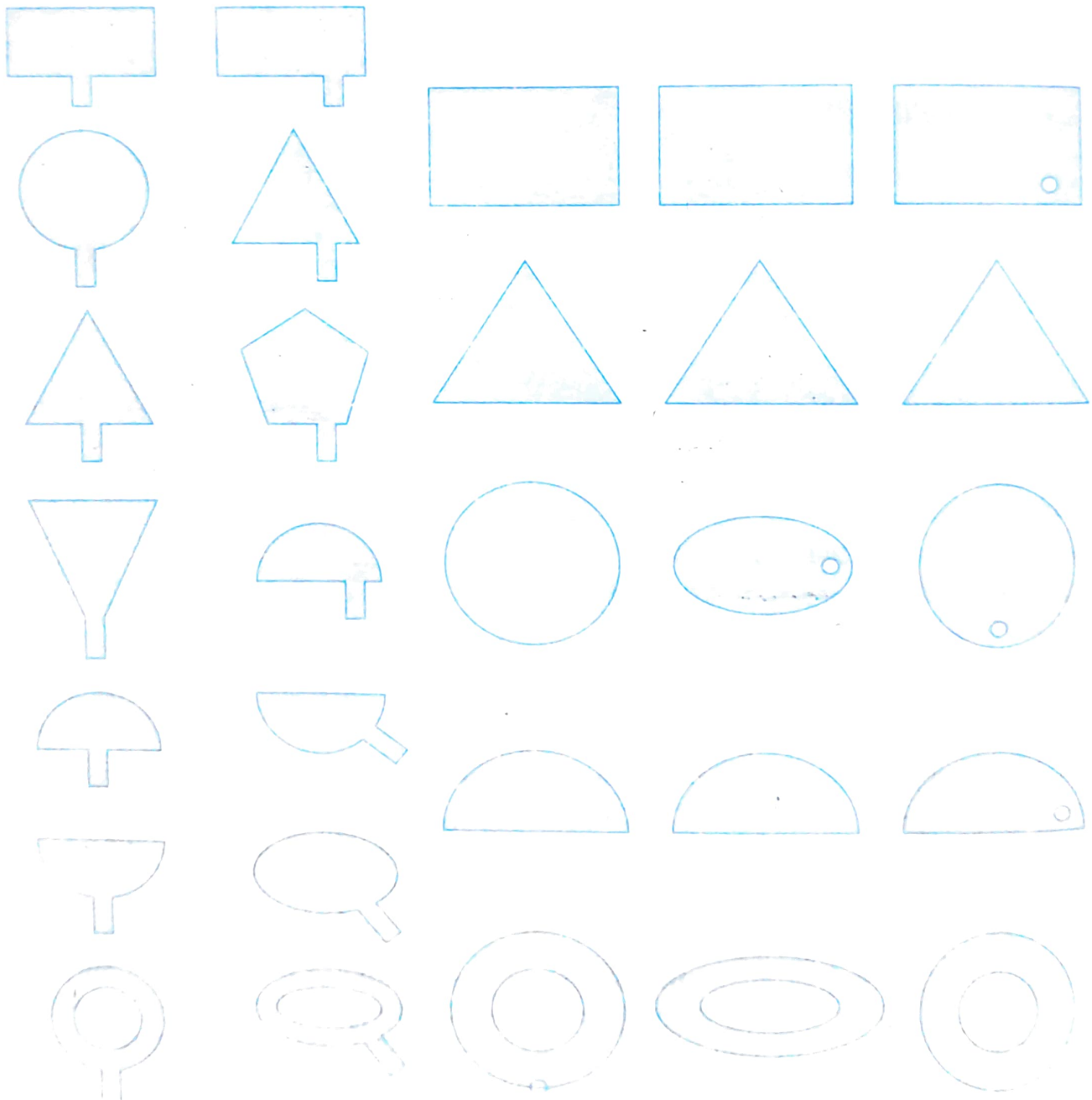
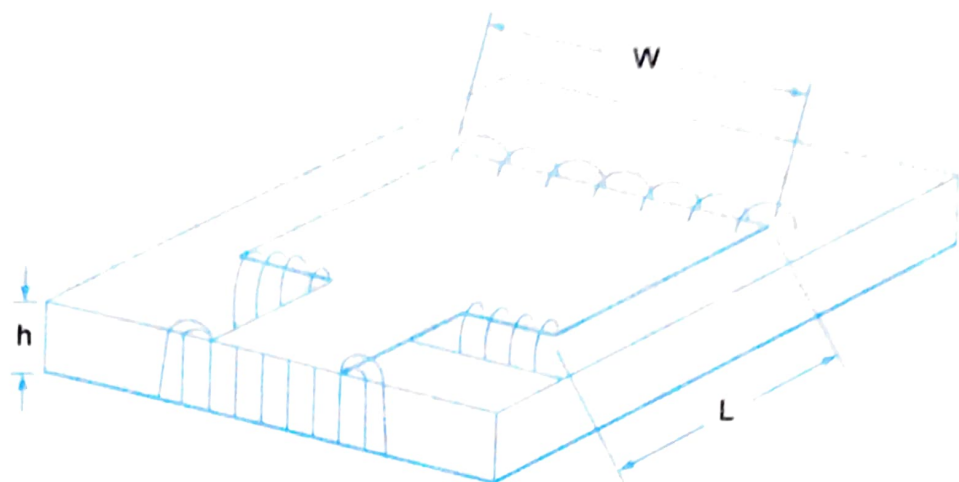
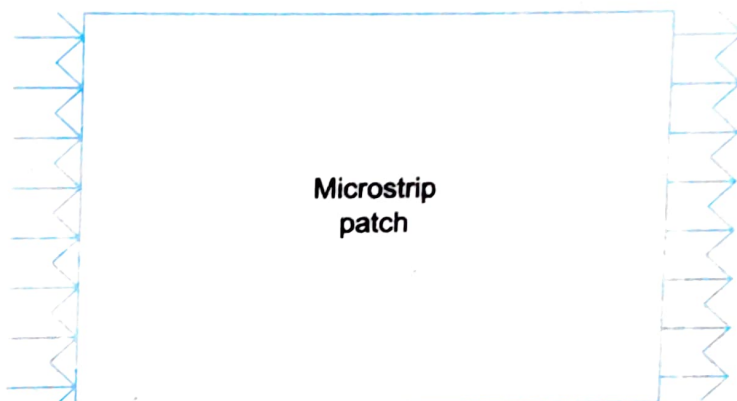


Fig. 4.14 Microstrip line fed patches

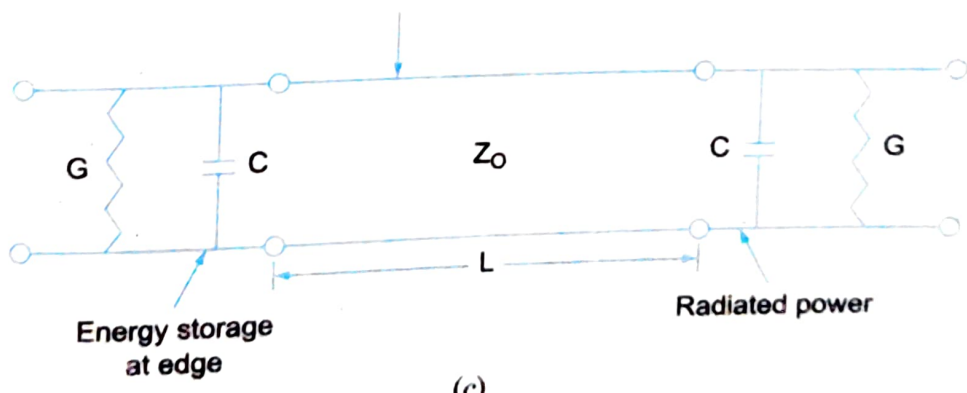


(a)



(b)

Transmission line formed by  
microstrip patch



(c)

Fig. 4.15 Microstrip antenna (a) Radiation mechanism (b) Fringing fields (c) Equivalent circuit

When the patch is  $0.5 \lambda$  wavelength long, the fringing fields of the output edge are out of phase with respect to those at the input edge. If we assume the input-edge fields are positive i.e., they point upward from the ground plane to the patch. The output edge fields will then point downwards towards the ground plane. When looking directly down on the patch, the fringing fields point in the same direction. The radiation from these fields add up to produce a far-field pattern with a maximum broadside to the patch.

The microstrip antenna when operating in the transmitting mode is driven with a voltage source between the feed probe and the ground plane as shown in Fig. 4.16a. The electric field components parallel to ground plane are small as the dielectric substrate is electrically very thin. As the length of the patch is near  $\lambda/2$ , there are large currents and field amplitudes at resonance. The resulting radiation may be interpreted as follows in two ways from field equivalence principle.

1. The antenna is viewed as a cavity with slot type radiators at  $x=0$  and  $x=L$  with equivalent magnetic currents  $\mathbf{M} = \mathbf{E} \times \mathbf{n}$  radiations in the presence of the ground plane.

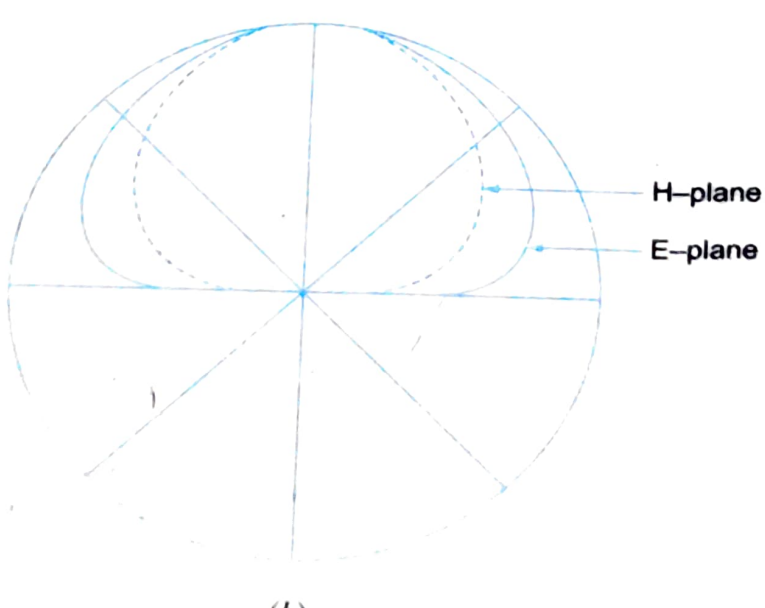
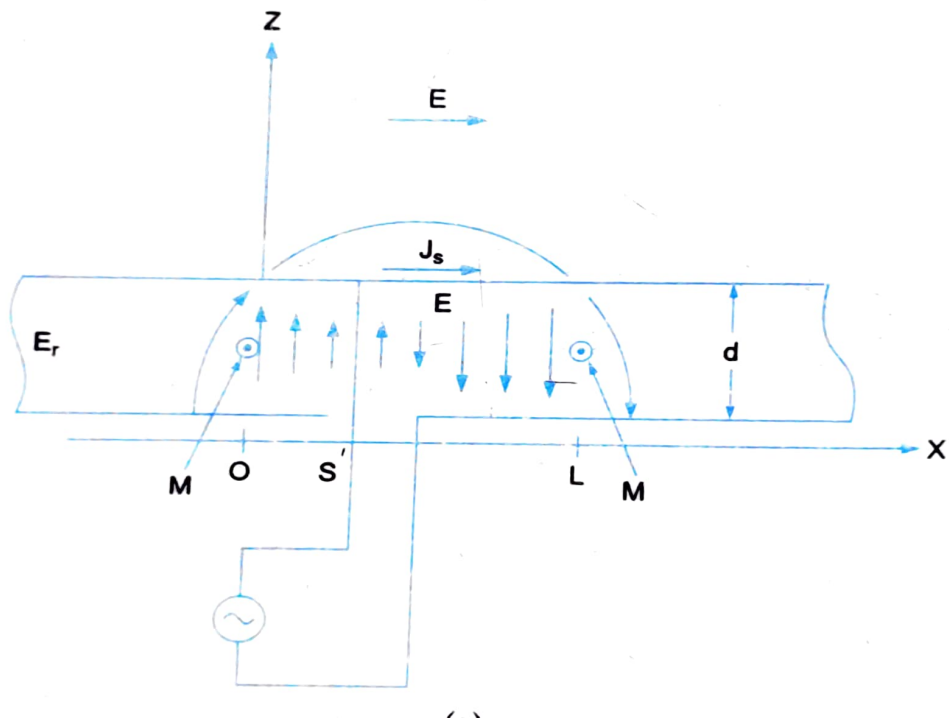


Fig. 4.16 (a) Microstrip antenna in transmitting mode (b) E and H-plane patterns

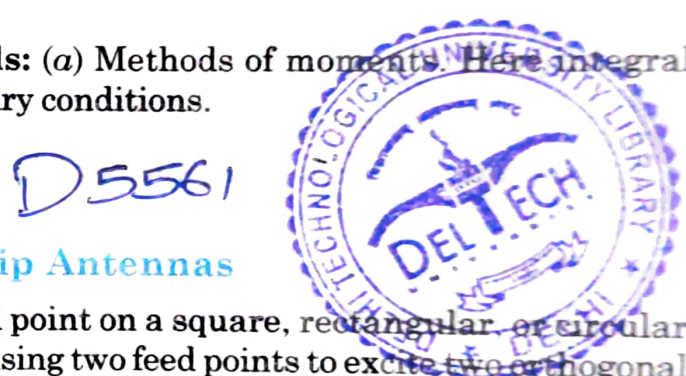
2. Radiation is due to induced surface current density  $\mathbf{J}_s = \mathbf{n} \times \mathbf{H}$  on the patch conductor in the presence of the ground dielectric surface.

The antenna radiates a relatively broad beam broadside to the plane of the substrate with poor end fire radiation i.e., the maximum radiation is normal to the plane of the strip. Typical  $E$  and  $H$  plane patterns are shown in Fig. 4.16b.

## Methods of Analysis of Microstrip Antennas

Although microstrip antennas are relatively simple structures, their analysis is quite complicated. The primary complicating factor is the presence of the dielectric substrate with the backing conducting ground plane. The various models available are as follows.

1. **Transmission line model:** Two opposite sides of a rectangular patch are joined together by a low impedance strip line.
2. **Cavity model:** Field between patch and ground plane is expanded in terms of a series of cavity resonant modes.
3. **Integral and differential equation models:** (a) Methods of moments. Here integral equation is formulated by imposing the boundary conditions.  
 (b) Finite element method  
 (c) Finite difference method etc.



## Polarisation (Linear/circular) in Microstrip Antennas

Linear polarization can be achieved using single feed point on a square, rectangular or circular element. The circular polarizations could be achieved using two feed points to excite two orthogonal modes with  $90^\circ$  phase difference as below.

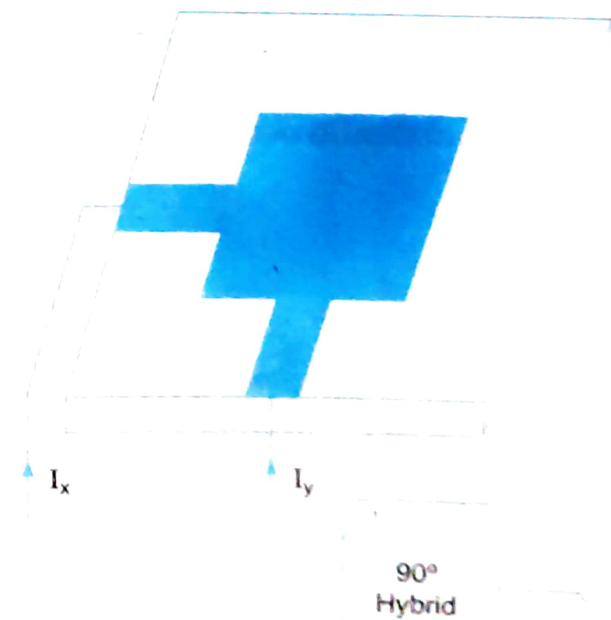
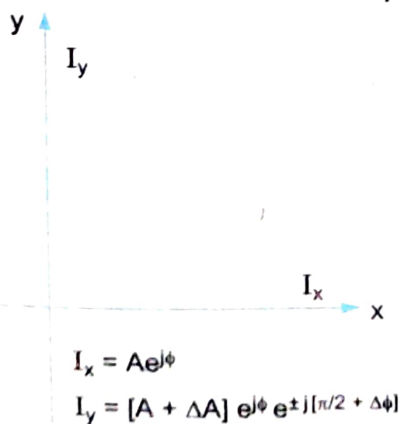


Fig. 4.17 (a)

(b) Orthogonal current is radiating circular polarisation (d) Circular polarised microstrip antenna using a square

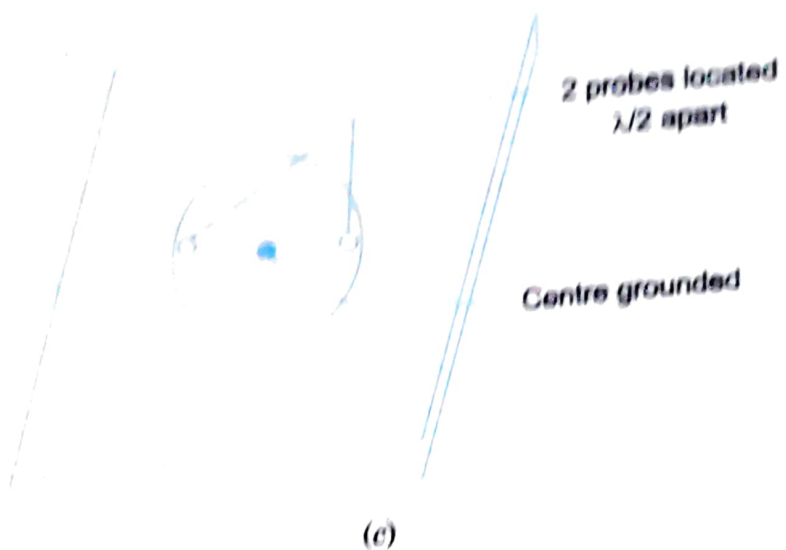


Fig. 4.17 (c) Circular polarised microstrip antenna

- With a square element driven from adjacent sides through a  $90^\circ$  hybrid. The common method is to use two orthogonal linear polarized elements and feed them with equal amplitude signals phased  $90^\circ$  apart as shown in Fig. 4.17a. However a circular polarisation can also be obtained by using a single square patch which is capable of dual linear polarisation with orthogonal feed points.
- With a circular element (entire grounded) and driven by two probes located  $\lambda_0/4$  apart as shown in Fig. 4.17b, exciting two orthogonal modes on this patch with a  $90^\circ$  phase difference as shown in Fig. 4.17c.

### Dual-frequency Microstrip Antennas

These are made by feeding from adjacent sides of a rectangular patch antenna or by stacking two conductor elements as shown in Fig. 4.18. The resonant frequencies should be separated by more than 10% and should not be harmonically related.

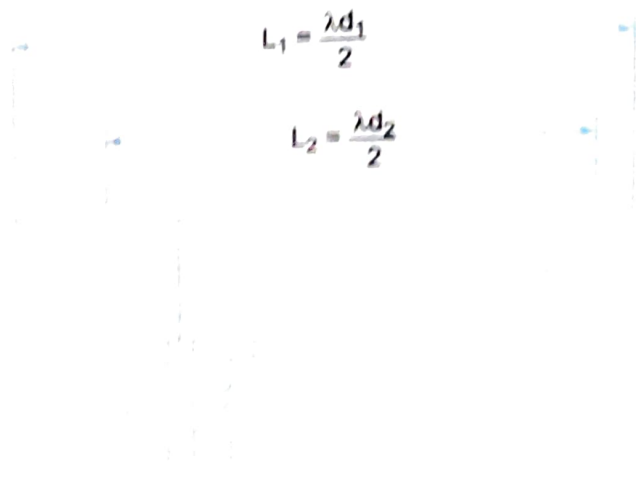


Fig. 4.18 Dual-frequency microstrip antenna

## Microstrip Arrays

The greatest advantage of microstrip antennas is the ease with which microstrip arrays can be made which are required for high gain (narrow beamwidth) to provide increased range, rejection against interference, beam scanning or steering and for some specific radiation pattern. The feed network and the radiating elements are monolithically etched from one side of a printed circuit board simultaneously.

Such arrays are very reliable because the entire array is one continuous piece of copper. However they are limited in that they tend to radiate effectively only over a narrow band of frequencies and they can not operate at high power levels of waveguide, coaxial line or even strip line. The total field from a 2-element array having antennas positioned on  $x$ -axis, separated by a distance  $d$  and excited with equal amplitudes and in phase as shown in Fig. 4.19 is given by

$$E(\theta) = E_1(\theta)e^{-jkr/r} + E_2(\theta)e^{-jkr_1/r_1}$$

where,  $E_1(\theta)$  and  $E_2(\theta)$  are the far field patterns of each antenna

$$k = 2\pi/\lambda_0$$

$r$  and  $r_1$  are the distances from antenna to the point in the far field.

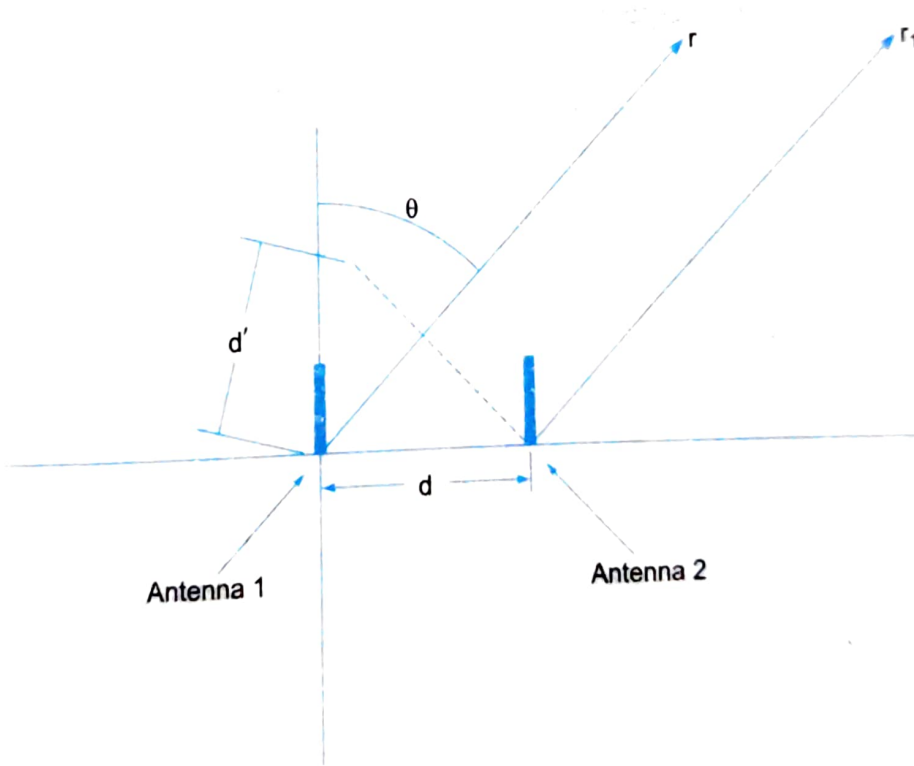


Fig. 4.19 A two element array with associated geometry

When the point is located at a sufficient distance away,  $r$  and  $r_1$  are essentially parallel to each other as shown in Fig. 4.19 when antennas are identical and mutual coupling small, the patterns are identical and  $E_1(\theta) \approx E_2(\theta)$ .

$$E(\theta) = E_1(\theta) e^{-jkr/r} [1 + e^{jkd \sin \theta}]$$

84

An array with all elements equally excited is called a uniform array. It produces the narrowest possible beamwidth alongwith the highest side lobe level. The side lobe level is reduced by introducing a taper in the amplitudes of the elements.

Microstrip arrays are built various types of feeds viz. series fed or parallel fed etc. as shown in Fig. 4.20.

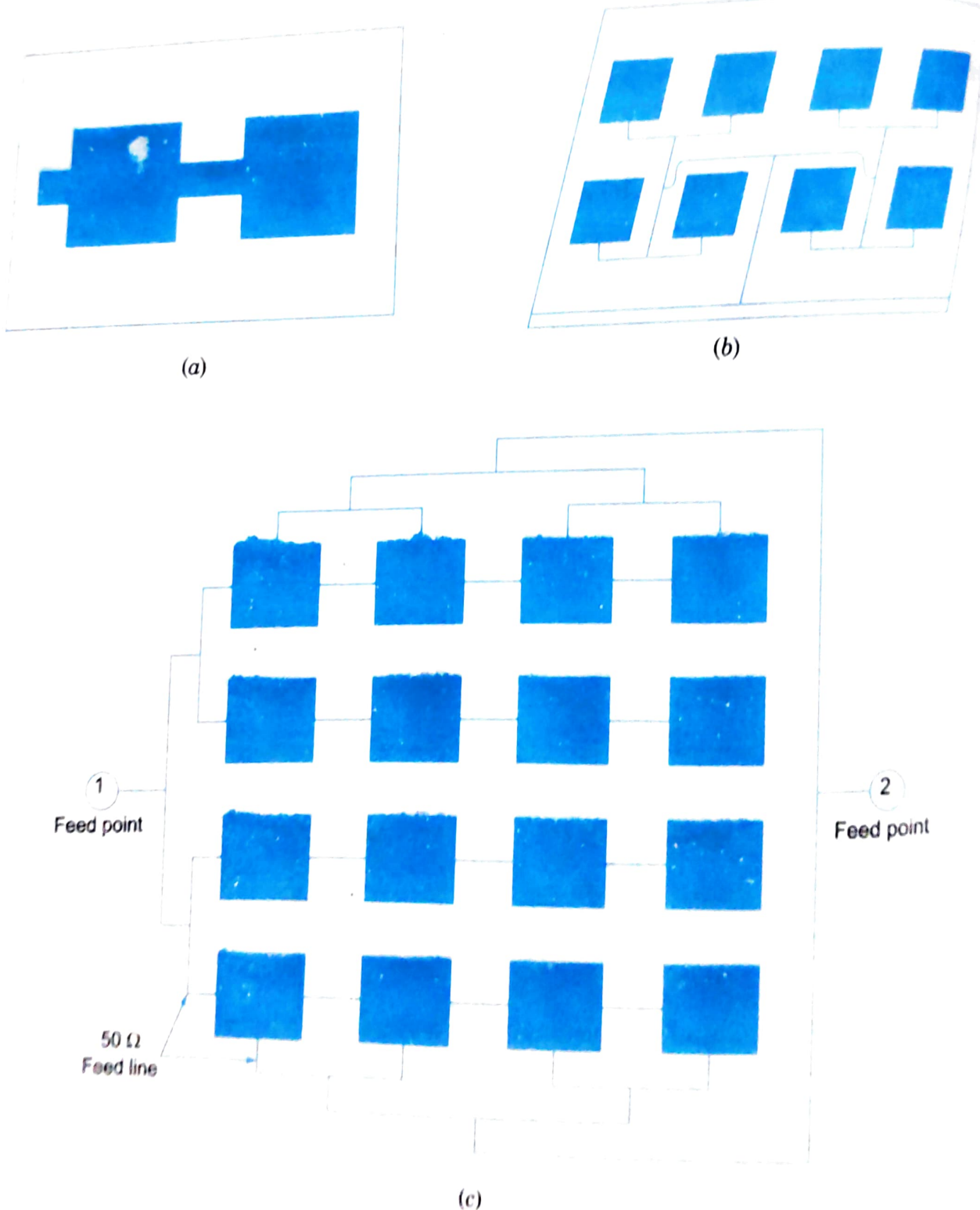


Fig. 4.20 Microstrip arrays

In two-dimensional arrays, the elements are arranged in a rectangular grid defined by a pair of axes and the pattern is now effected in both  $\theta$  and  $\phi$  directions.

In series fed linear arrays, the patches are connected with microstrip feed lines in series or shunt as shown in Fig. 4.20. For series mounted patches, the amplitude of the element excitation is controlled by varying the patch width while in shunt mounted elements, the width of microstrip line from the main feed line to patch controls the amplitude.

*Centre feeding* also shown in Fig. 4.20, is more efficient and is used in broadside beams because it has maximum symmetry.

Two-dimensional end-fed array is shown in Fig. 4.21.

In *hybrid feed*, combinations of corporate (parallel) and series feed are used.

In *parallel feed* (corporate) arrays, pairs of patches are connected with power splitter. Connected pairs are in turn connected with another power splitter as shown in Fig. 4.22.

In *two dimensional arrays*, the patches are fed in phase with equal amplitudes. The array is composed of 4 subarrays each having 4 elements as shown in Fig. 4.23.

## Design and Development of Microstrip Antenna

**Selection of Substrate:** The major electrical properties taken into consideration are relative dielectric constant,  $\epsilon_r$  and loss tangent,  $\tan \delta$ .

1. A high dielectric constant results in smaller patch which reduces bandwidth as well as it results in tighter fabrication tolerances. Generally, it is desirable to select a substrate with low possible constant consistent with the space available for the antenna.
2. A high loss tangent reduces antenna efficiency and increases feed losses.
3. Substrate thickness is chosen as large as possible to maximize bandwidth and efficiency but not so large as to risk surface wave excitation. Hence

$$h \leq \frac{0.3 c}{2\pi f_u \sqrt{\epsilon_r}}$$

where,  $c$  is the velocity of light.

$\epsilon_r$  is the relative dielectric constant.

$f_u$  is the maximum operating frequency

4. Other factors taken into consideration are dielectric constant stability, operating temperature range, dimensional changes with temperature, thermal conductivity, machinability and flexibility etc. Substrates used in hybrid MICs are shown in Table 4.1.

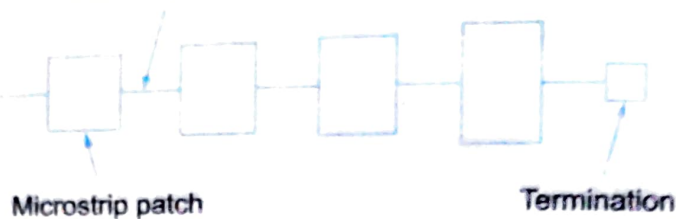
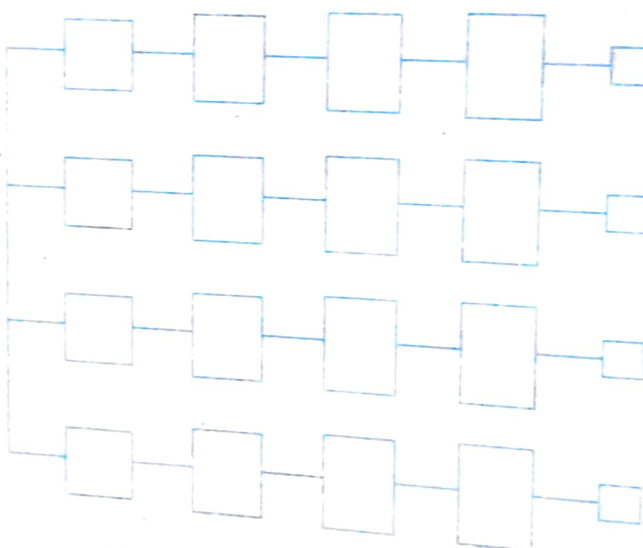
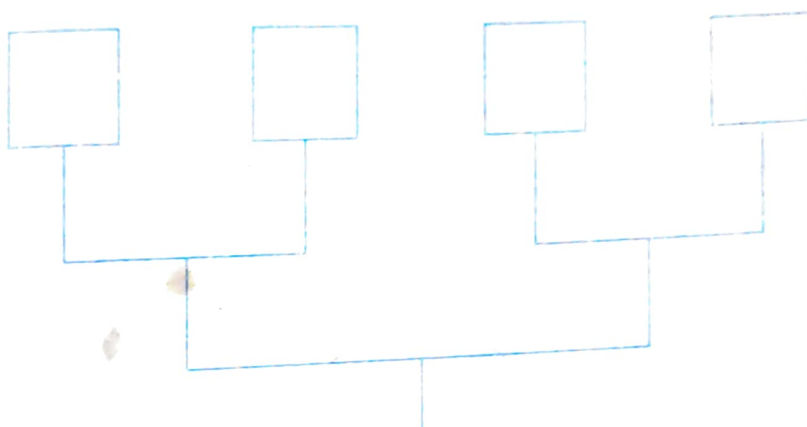
*Microstrip feed line**Series-connected patches**Series array with center fed**End fed two-dimensional array**Hybrid-fed array*

Fig. 4.24 Microstrip antenna

Microstrip patch



Shunt connected patches



Corporate fed linear array

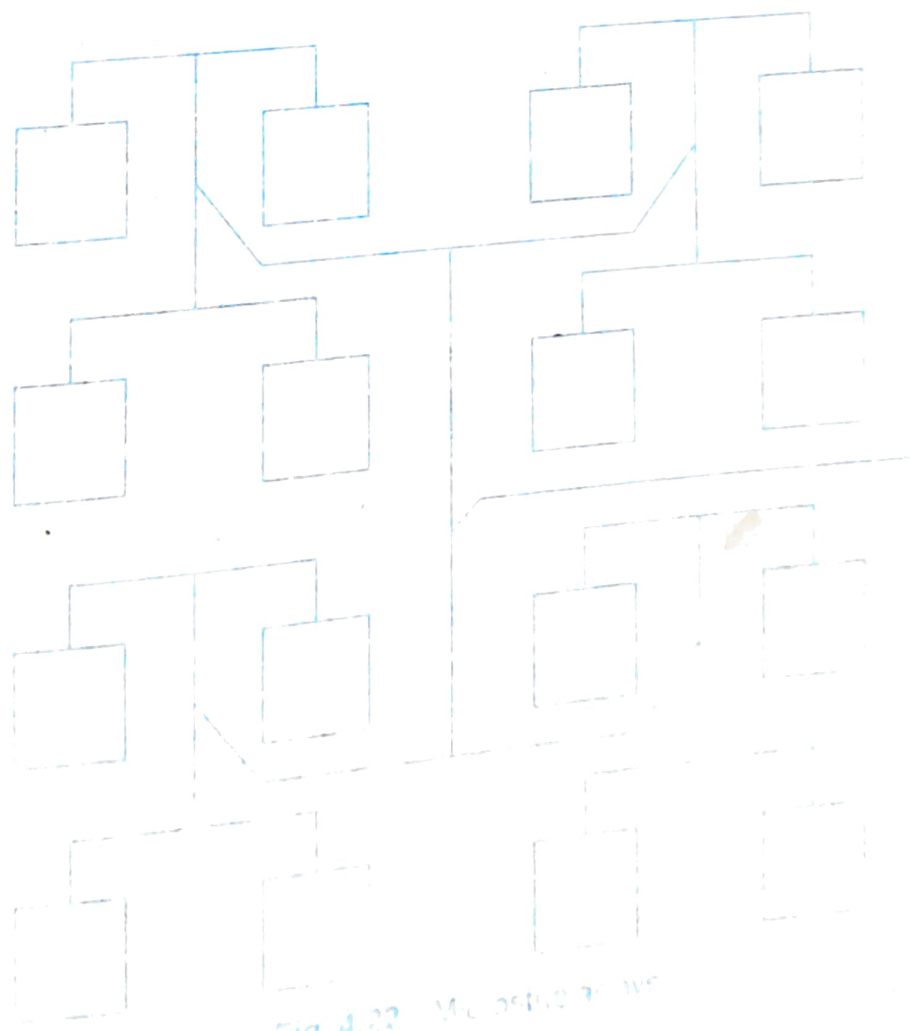


Fig. 4.22 Microstrip patch

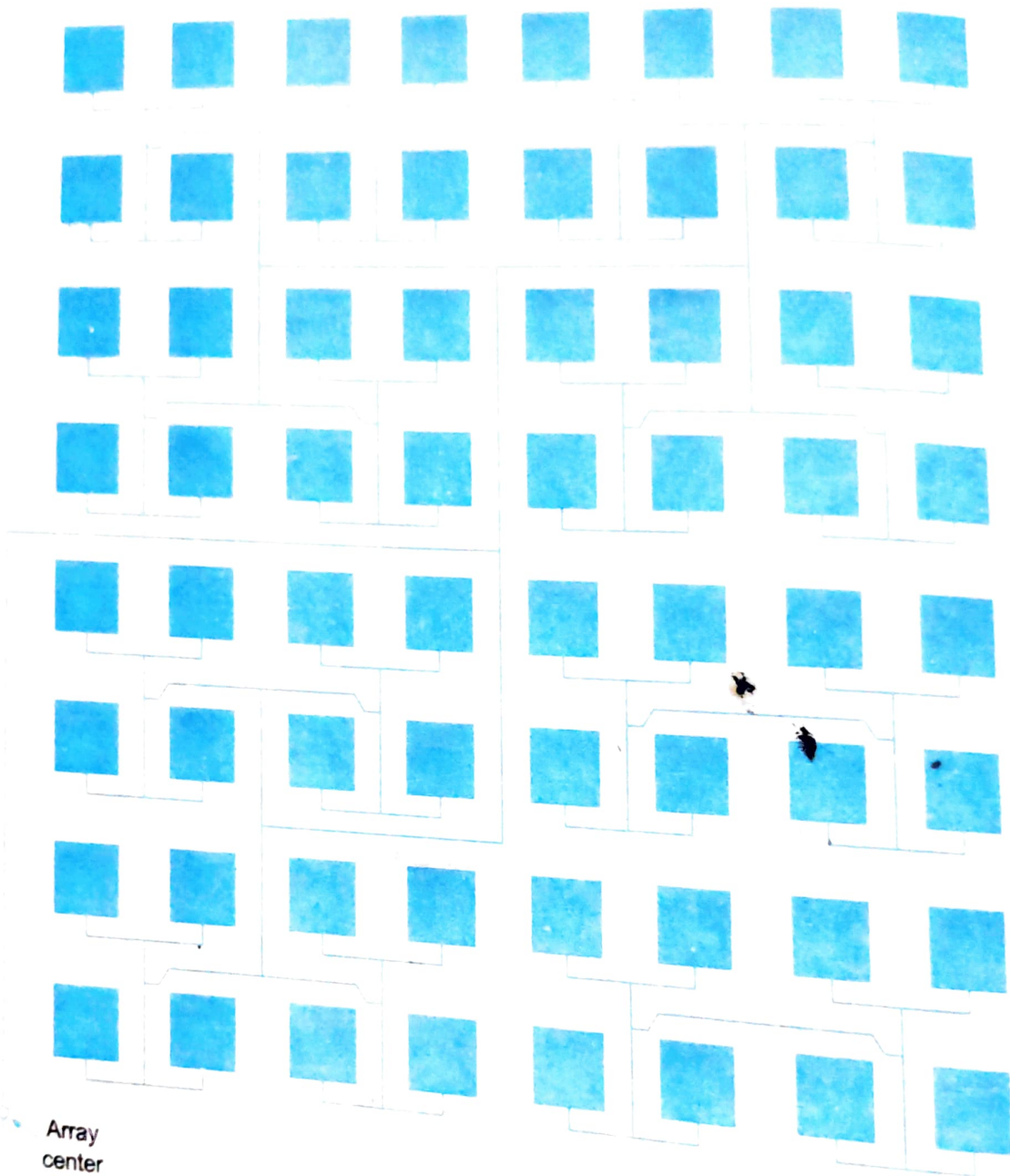


Fig. 4.23 Layout of 1/4 of the array

Table 4.1

Material	$\epsilon_r$	$\tan \delta \times 10^4$ at 10 GHz	rms surface roughness $\mu m$ ,	thermal conductivity $k$ ( $W/cm^2/C$ )
RT Duroid 5880	2.16-2.24	5-15	75-1	0.0026
Epsilam 10	10-13	20	-	
Alumina	9.6-10.4	0.5-3	0.05-0.25	0.0037
Fused Quartz	3.75	1	0.006-0.025	0.37
Beryllia	6.6	1	0.05-1.25	0.01
Ferrite	13.16	2	0.25	2.5
Sapphire	-	0.4-0.7	0.005	0.03
				0.4

## Selection of a Feed

### Direct-contacting feeds

1. **Microstrip line feed:** As shown in Fig. 4.24a, the patch is notched to provide an inset feed point. The equivalent circuit is also shown where series inductor represents inductance of feed and parallel RLC network represents resonator patch.

2. **Coaxial feed:** These antennas are fed by a coaxial connector soldered to the back of a ground plane. The central feed pin of the coaxial connector is soldered properly to microstrip patch as shown in Fig. 4.24b.

### Non-contacting feeds

1. **Proximity feed:** Here a two layer substrate is used with patch on upper substrate and feeding microstrip line on the lower substrate terminating in an open stub below the patch. The two are capacitively coupled as shown in Fig. 4.24c. The patch exists on a relatively thick substrate to improve bandwidth while feed line sees a thinner substrate to reduce spurious radiation of coupling. Bandwidth of about 13% are realised using this method.

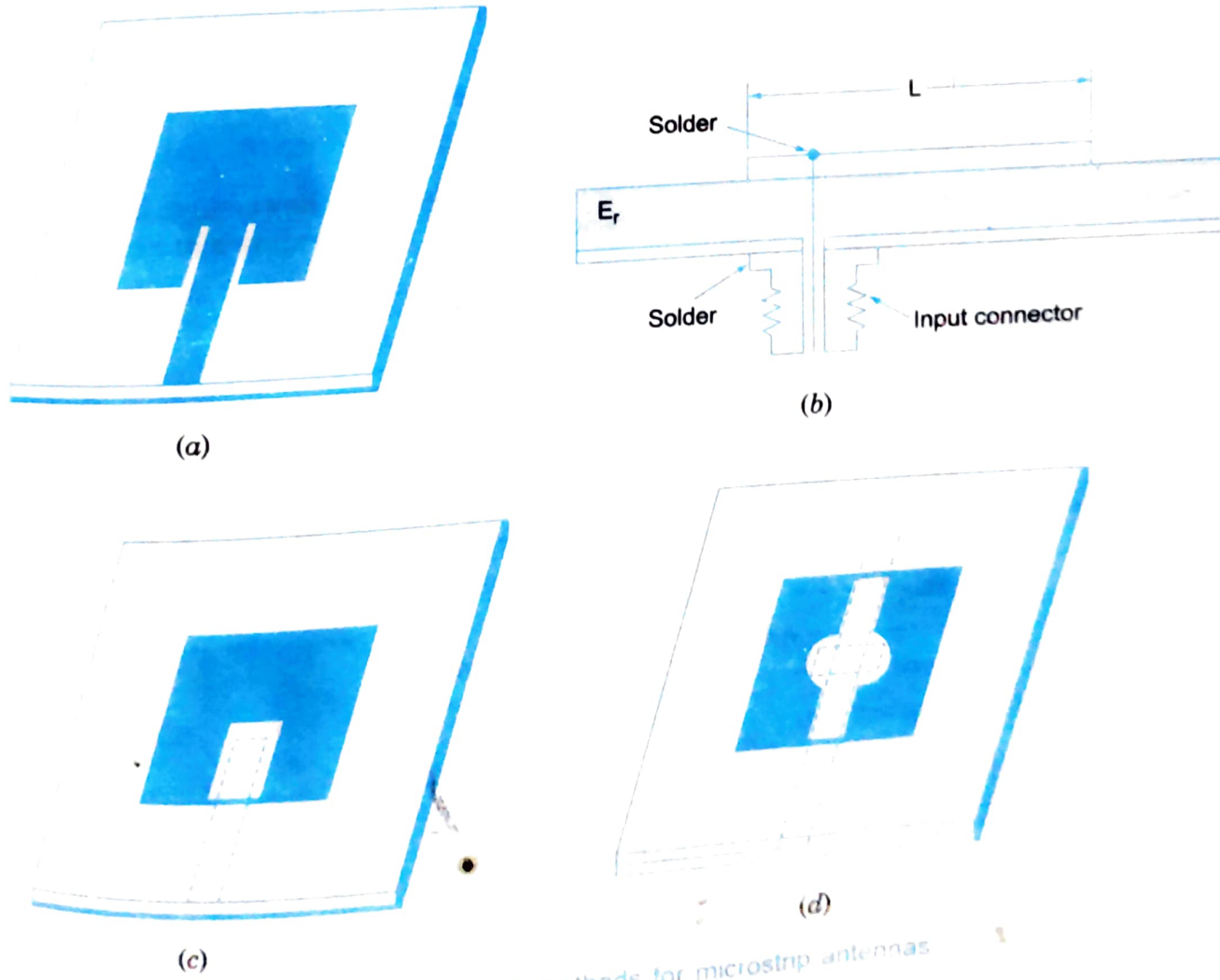


Fig. 4.24 Feeding methods for microstrip antennas

**2. Aperture coupled feed:** It uses two parallel substrates separated by a ground plane shown in Fig. 4.24d. The patch is on the top which is coupled through a small aperture in ground plane to a microstrip feed line on the bottom substrate. It enables to use a thin dielectric constant substrate for feed and a thick low dielectric constant substrate for antenna as to optimise both the feed and radiation.

### Determining the Patch Length

The patch length is determined by the condition for resonance. This occurs when the input impedance is purely real. The patch is about 0.48 to 0.49 of the wavelength in the dielectric.

The resonant frequency of the antenna is given by

$$f_{or} = \frac{c}{2(L + 2\Delta l)\sqrt{\epsilon_{eff}}}$$

where effective dielectric constant is given as

$$\epsilon_{eff} = \frac{\epsilon_r + 1}{2} + \frac{\epsilon_r - 1}{2} \sqrt{1 + 12(h/w)} \quad w/lh \gg 1$$

and correction to open end is given as

$$\Delta l = 0.412 h \frac{\epsilon_{eff} + 0.3}{\epsilon_{eff} - 0.258} \frac{w/h + 0.264}{w/h + 0.8}$$

This correction is due to the fringe capacitances at both ends which has been transformed an equivalent length of transmission line. The various dimensions are shown in Fig. 4.25. where,  $w$  = width of the patch

$\epsilon_r$  = relative permittivity of substrate

$h$  = thickness of substrate

$\lambda_0$  = free space wavelength =  $c/f$

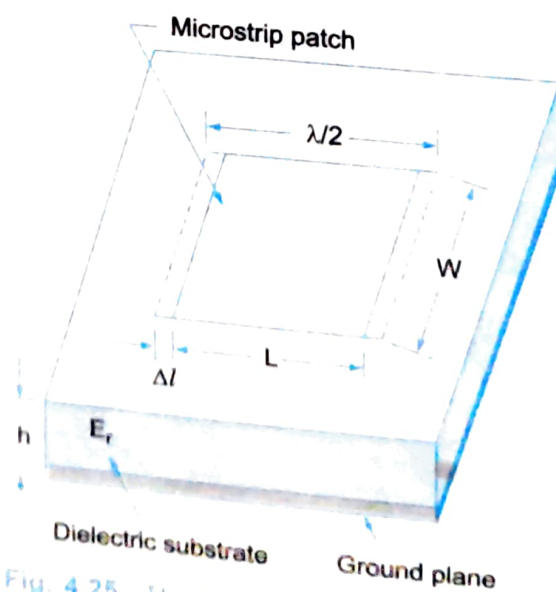


Fig. 4.25 Rectangular microstrip antenna

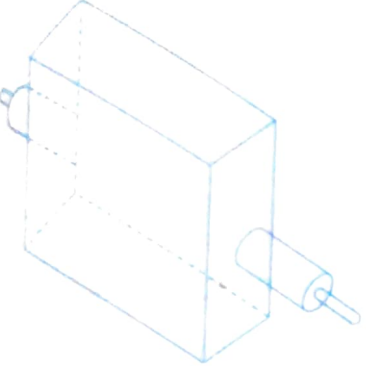
## Deciding Patch Width

The patch width generally lies between 0.5 to 2.0 times the length. It can be used to vary the input impedance with wide patches having lower impedances. Too small width ( $w$ ) of the patch results in low antenna efficiency and too large width in higher order modes, the optimum width is found as

$$w = \frac{\lambda_0}{2\sqrt{(\epsilon_r + 1)/2}}$$

## Applications and Future Scenario of Microstrip Antennas

Microstrip antennas find their use in airborne and spacecraft systems mainly due to their low profile, conformal nature and easy integration with MICs. This trend is likely to continue with possibility of latest materials like high temperature superconductors. Conducting polymers, electric or magnetic anisotropic materials as patch conductors for improving the electrical performance of these antennas. Ferrite materials could also be used for frequency and polarization agility etc.



# 5

## CAVITY RESONATORS

### CHAPTER OUTLINES

- 5.1 Introduction
- 5.2 Expression for  $f_0$  in a Rectangular Cavity Resonator
- 5.3 Expression for  $f_0$  in a Circular Cavity Resonator
- 5.4 Application of Cavity Resonators
- 5.5 Field Expressions for  $TM_{mnp}$  and  $TE_{mnp}$  Modes in a Rectangular Cavity Resonator
- 5.6 Field Expressions for  $TM_{nmp}$  and  $TE_{nmp}$  Modes in a Rectangular Cavity Resonator
- 5.7 Solved Examples
- 5.8 Field Patterns
- 5.9 Quality Factor (Q) of Cavity Resonators
  - 5.9.1 Q of a Rectangular Cavity Resonator
  - 5.9.2 Q of a Circular Cavity Resonator
- 5.10 Reentrant Cavities
- 5.11 Coupling to Cavities
- Review Questions

# 5

## Cavity Resonators

### 5.1 INTRODUCTION

When one end of the waveguide is terminated in a shorting plate there will be reflections and hence standing waves as shown in Fig. 5.1. When another shorting plate is kept at a distance of a "multiple of  $\lambda_g/2$ " then the hollow space so formed can support a signal which bounces back and forth between the two shorting plates. This results in resonance and hence the hollow space is called cavity and the resonator as the cavity resonator.

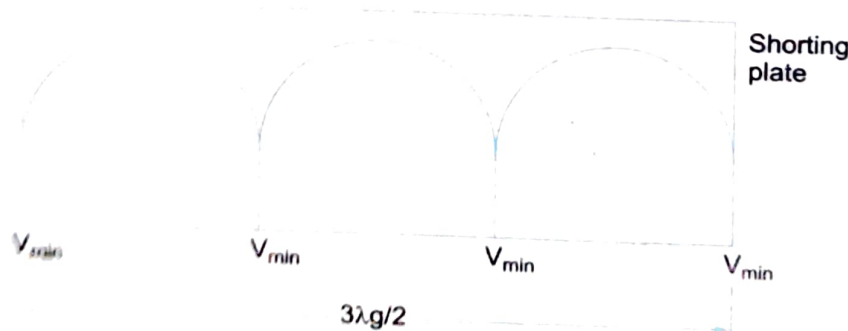


Fig. 5.1

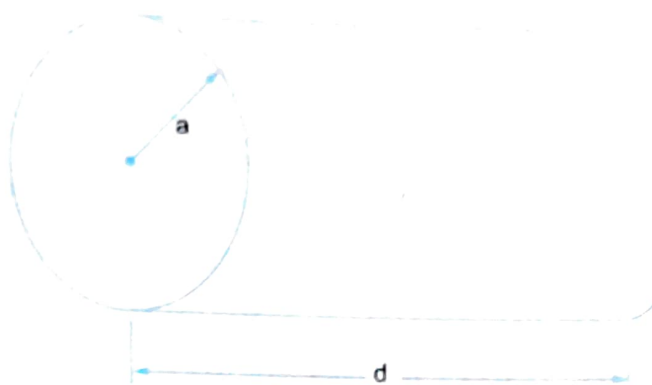


Fig. 5.3 Circular cavity resonator

The waveguide section can be rectangular or circular as shown in Fig. 5.2 and 5.3. The microwave cavity resonator is akin to a tuned circuit at low frequencies having a resonant frequency

$$f_o = \frac{1}{2\pi\sqrt{LC}} \quad \dots(5.1)$$

The cavity resonator can resonate at only one particular frequency just as a parallel resonant circuit shown in Fig. 5.4.

From Fig. 5.1,  $d = 3\lambda_g/2$

For a given resonator and mode  $a$ ,  $b$ ,  $m$  and  $n$  are constants. Therefore  $\lambda_c$  is also fixed and  $\lambda_o$  will also have a fixed value. But  $\lambda_o = c/f_o$  and  $f$  will also have a constant value, equal to  $f_o$ , which is the resonant frequency of the cavity resonator.

Fig. 5.4

## 5.2 EXPRESSION FOR $f_o$ IN A RECTANGULAR CAVITY RESONATOR

We know that for a rectangular waveguide

$$h^2 = \gamma^2 + \omega^2 \mu \epsilon = A^2 + B^2 = \left(\frac{m\pi}{a}\right)^2 + \left(\frac{n\pi}{b}\right)^2$$

$$\omega^2 \mu \epsilon = \left(\frac{m\pi}{a}\right)^2 + \left(\frac{n\pi}{b}\right)^2 - \gamma^2$$

or

$$\omega^2 \mu \epsilon = \left(\frac{m\pi}{a}\right)^2 + \left(\frac{n\pi}{b}\right)^2 - \gamma^2$$

For wave propagation  
or

$$\gamma = j\beta$$

$$\gamma^2 = j^2 \beta^2 = -\beta^2$$

$$\omega^2 \mu \epsilon = \left(\frac{m\pi}{a}\right)^2 + \left(\frac{n\pi}{b}\right)^2 + \beta^2 \quad \dots(5.2)$$

If a wave has to exist in a cavity resonator there must be a phase change corresponding to a given guide wavelength ( $\beta = 2\pi/\lambda_g$ ). The condition for the resonator to resonate is

$$\beta = p\pi/d$$

where,  $p$  = a constant = 1, 2, 3, ...  $\infty$ , that indicates half wave variation of either electric or magnetic field along the  $z$  direction.

$d$  = length of the resonator.

When

$$\beta = \frac{p\pi}{d}, f = f_o, \omega = 2\pi f_o = \omega_o$$

Substituting for  $\beta$  in Eq. 5.2, we get

$$\omega_o^2 \mu \epsilon = \left( \frac{m\pi}{a} \right)^2 + \left( \frac{n\pi}{b} \right)^2 + \left( \frac{p\pi}{d} \right)^2$$

or

$$f_o = \frac{1}{2\pi\sqrt{\mu\epsilon}} \left[ \left( \frac{m\pi}{a} \right)^2 + \left( \frac{n\pi}{b} \right)^2 + \left( \frac{p\pi}{d} \right)^2 \right]^{1/2}$$

or

$$f_o = \frac{c}{2} \left[ \left( \frac{m}{a} \right)^2 + \left( \frac{n}{b} \right)^2 + \left( \frac{p}{d} \right)^2 \right]^{1/2} \quad \dots(5.3)$$

General mode of propagation in a cavity resonator is TE<sub>mnp</sub> or TM<sub>mnp</sub>. For both TE and TM the resonant frequency is the same in a rectangular cavity resonator.

### 5.3 EXPRESSION FOR $f_o$ IN A CIRCULAR CAVITY RESONATOR

Here circular end plates are used to short both ends.

$a$  = radius of the waveguide and

$d$  = length or height of the cylindrical waveguide.

The condition for resonance is  $\beta = \frac{p\pi}{d}$

For a circular waveguide section, we know that,

$$h^2 = \gamma^2 + \omega^2 \mu \epsilon = h_{nm}^2 = \left( \frac{P_{nm}}{a} \right)^2$$

$$\therefore \omega^2 \mu \epsilon = \left( \frac{P_{nm}}{a} \right)^2 - \gamma^2 \quad \dots(5.4)$$

For wave propagation  $\gamma = j\beta$  and for resonance  $\beta = \frac{p\pi}{d}$  and  $\omega = \omega_o$   
Therefore Eq. 5.4 becomes,

$$\omega_o^2 \mu = \left( \frac{P_{nm}}{a} \right)^2 + \left( \frac{p\pi}{d} \right)^2$$

$$f_o = \frac{1}{2\pi\sqrt{\mu\epsilon}} \left[ \left( \frac{P_{nm}}{a} \right)^2 + \left( \frac{p\pi}{d} \right)^2 \right]^{1/2}$$

$$f_o = \frac{c}{2\pi} \left[ \left( \frac{P'_{nm}}{a} \right)^2 + \left( \frac{p\pi}{d} \right)^2 \right]^{1/2} \quad \dots(5.5)$$

or

This is for  $\text{TM}_{nmp}$  mode.Similarly for  $\text{TE}_{nmp}$  mode.

$$f_o = \frac{c}{2\pi} \left[ \left( \frac{P'_{nm}}{a} \right)^2 + \left( \frac{p\pi}{d} \right)^2 \right]^{1/2} \quad \dots(5.6)$$

## 5.4 APPLICATION OF CAVITY RESONATORS

They can be used

as tuned circuits,

in UHF tubes, Klystron amplifier/oscillators, cavity magnetron,

in duplexers of radars,

cavity wavemeters in measurement of frequency etc.

## 5.5 FIELD EXPRESSIONS FOR $\text{TM}_{nmp}$ AND $\text{TE}_{nmp}$ MODES IN A RECTANGULAR CAVITY RESONATOR

**Case 1. TM waves :** The field expressions can be obtained by considering a rectangular cavity resonator as shown in Fig. 5.5.



Fig 5.5

For a TM wave

$$H_z = 0 \text{ and } E_z \neq 0$$

The wave equation is given by

$$\frac{\partial^2 E_z}{\partial x^2} + \frac{\partial^2 E_z}{\partial y^2} + \gamma^2 E_z = -\omega^2 \mu \epsilon E_z$$

$$\frac{\partial^2 E_z}{\partial x^2} + \frac{\partial^2 E_z}{\partial y^2} + E_z [\gamma^2 + \omega^2 \mu \epsilon] = 0 \quad \dots(5.7)$$

Let  $\gamma^2 + \omega^2 \mu \epsilon = h^2$

Equation 5.7 becomes

$$\frac{\partial^2 E_z}{\partial x^2} + \frac{\partial^2 E_z}{\partial y^2} + h^2 E_z = 0$$

This is a partial differential equation of 2nd order. The solution can be obtained by separation of variables method

Let  $E_z = XY$  be the required solution ...(5.8)

$$\frac{\partial^2 XY}{\partial x^2} + \frac{\partial^2 XY}{\partial y^2} + h^2 XY = 0$$

where,  $X$  is a function of  $x$  only.

$Y$  is a function of  $y$  only.

$$Y \frac{d^2 X}{dx^2} + X \frac{d^2 Y}{dy^2} + h^2 XY = 0 \quad \dots(5.9)$$

Dividing throughout by  $XY$ , we get

$$\frac{1}{X} \frac{d^2 X}{dx^2} + \frac{1}{Y} \frac{d^2 Y}{dy^2} + h^2 = 0 \quad \dots(5.10)$$

Let

$$\frac{1}{X} \frac{d^2 X}{dx^2} = -B^2 \quad \text{and} \quad \frac{1}{Y} \frac{d^2 Y}{dy^2} = -A^2 \quad \dots(5.11)$$

∴ Equation 5.10 becomes

$$-A^2 - B^2 + h^2 = 0$$

or

$$h^2 = A^2 + B^2$$

The solution for Eqs in 5.11 are given by

$$\left. \begin{array}{l} X = C_1 \cos Bx + C_2 \sin Bx \\ Y = C_3 \cos Ay + C_4 \sin Ay \end{array} \right\} \quad \dots(5.12)$$

The constants  $C_1, C_2, C_3, C_4$  can be determined by the application of boundary conditions.

From Eq. 5.8 the required solution is

$$E_z = XY$$

Substituting for  $X$  and  $Y$  from Eq. 5.12

$$E_z = (C_1 \cos Bx + C_2 \sin Bx) (C_3 \cos Ay + C_4 \sin Ay) \quad \dots(5.13)$$

We shall now apply Boundary conditions to determine the constants  $C_1, C_2, C_3$  and  $C_4$ .

### Applying 1st Boundary condition (Bottom wall)

$E_z = 0$ , for  $y = 0$  and all values of  $x$  varying from 0 to  $a$ .

Substituting these values in Eq. 5.13, we get

$$\begin{aligned} 0 &= (C_1 \cos Bx + C_2 \sin Bx) (C_3 \cos 0 + C_4 \sin 0) \\ 0 &= (C_1 \cos Bx + C_2 \sin Bx) C_3 \end{aligned}$$

For all values of  $x$  varying from 0 to  $a$

$$\cos Bx \neq 0, \text{ and } \sin Bx \neq 0$$

∴ Only  $C_3 = 0$

Substituting  $C_3 = 0$  in Eq. 5.13

$$E_z = (C_1 \cos Bx + C_2 \sin Bx) (C_4 \sin Ay) \quad \dots(5.14)$$

is the intermediate solution.

### Applying 2nd boundary condition (Left side wall)

$E_z = 0$  for  $x = 0$  and all values of  $y$  varying from 0 to  $b$ .

Substituting these in Eq. 5.14, we get

$$0 = (C_1 \cos 0 + C_2 \sin 0) (C_4 \sin Ay)$$

$$0 = C_1 C_4 \sin Ay$$

Since  $\sin Ay \neq 0$  for all values of  $y$  varying from 0 to  $b$ , only  $C_1 = 0$ . With  $C_1 = 0$ , Eq. 5.14 becomes

$$E_z = C_2 \sin Bx C_4 \sin Ay.$$

This is the intermediate solution.

### Applying 3rd boundary condition

$E_z = 0$  for  $y = b$  and for all values of  $x$  varying from 0 to  $a$ .

Putting these values in Eq. 5.15.

$$0 = C_2 \sin Bx C_4 \sin Ab.$$

$\sin Bx \neq 0$  since  $x$  varies from 0 to  $a$ .

$C_2$  and  $C_4 \neq 0$ , therefore only  $\sin Ab = 0$

$Ab = \text{multiple of } \pi \text{ radian}$

$Ab = n\pi$  where  $n = 0, 1, 2, 3, \dots$

... (5.16)

$$A = \frac{n\pi}{b}$$

where,  $b$  = height of the waveguide.

## Applying 4th boundary condition

i.e.,

$$E_z = 0 \text{ at } x = a \text{ and } y \text{ varies from } 0 \text{ to } b.$$

Putting these values in Eq. 5.15

$$0 = C_2 C_4 \sin Ba \sin Ay$$

$$C_2 \neq 0 \text{ and } C_4 \neq 0 \text{ and also } \sin Ay \neq 0$$

therefore only

$$\sin Ba = 0$$

$$Ba = m\pi \quad \text{where } m = 0, 1, 2, 3, \dots$$

$$B = \frac{m\pi}{a}$$

... (5.17)

where,  $a$  = the width of the waveguide.

Substituting the values of  $A$  and  $B$  from Eqs. 5.16 and 5.17 in Eq. 5.15, we get

$$E_z = C_2 C_4 \sin\left(\frac{m\pi}{a}\right) x \sin\left(\frac{n\pi}{b}\right) y \cdot e^{j\omega t} \cdot e^{-\gamma z} \quad \dots (5.18)$$

for the wave propagating along the positive  $z$  direction.

Similarly,

$$E_z = C_2 C_4 \sin\left(\frac{m\pi}{a}\right) x \sin\left(\frac{n\pi}{b}\right) y \cdot e^{j\omega t} \cdot e^{\gamma z} \quad \dots (5.19)$$

for the wave propagating in the negative  $z$  direction.

We also know when the wave propagates,  $\gamma = j\beta$ . Adding the fields of two travelling waves i.e., one in positive ' $z$ ' direction and the other in the negative ' $z$ ' direction, we obtain

$$E_z = C_2 C_4 \sin\left(\frac{m\pi}{a}\right) x \sin\left(\frac{n\pi}{b}\right) y e^{j(\omega t \pm \beta z)} \quad \dots (5.20)$$

Let  $A^+$  be the amplitude constant for the wave propagating in the positive  $z$  direction and  $A^-$  be the amplitude constant for the wave propagating in the negative direction

Then,

$$E_z = [A^+ e^{-j\beta z} + A^- e^{j\beta z}] \quad \dots (5.21)$$

To make  $E_z$  vanish at  $z = 0$  we must choose  $A^- = A^+$ , so that the Eq. 5.21 reduces to

$$E_z = [A^+ e^{-j\beta z}] C_2 C_4 \sin\left(\frac{m\pi}{a}\right) x \sin\left(\frac{n\pi}{b}\right) y e^{j\omega t} \quad \dots (5.22)$$

In order that  $E_z$  vanishes at  $z = 0$  and  $z = d$ , choose

$$A^+ = A^- = A$$

Then Eq. 5.22 reduces to

$$E_z = C_2 C_4 A [e^{-j\beta d} + e^{j\beta d}] \sin\left(\frac{m\pi}{a}\right) x \sin\left(\frac{n\pi}{b}\right) y e^{j\omega t} \quad \dots (5.23)$$

But

$$e^{-j\theta} + e^{+j\theta} = 2 \cos \theta$$

$$e^{-j\beta d} + e^{+j\beta d} = 2 \cos \beta d$$

With these values, the Eq. 5.23 becomes

$$E_z = C_2 C_4 2A \cos \beta d \sin\left(\frac{m\pi}{a}\right) x \sin\left(\frac{n\pi}{b}\right) y \cdot e^{j\omega t} \quad \dots (5.24)$$

$E_z = 0$  all along the surface of the resonator. Eq. 5.24 becomes,

$$0 = C_2 C_4 2A \cos \beta d \sin\left(\frac{m\pi}{a}\right)x \sin\left(\frac{n\pi}{b}\right)y \cdot e^{j\omega t}$$

Since  $C_2 C_4$ ,

$$\sin\left(\frac{m\pi}{a}\right)x \text{ and } \sin\left(\frac{n\pi}{b}\right)y \neq 0 \text{ and } A \neq 0 \text{ only } \cos \beta d = 0$$

$$\beta = \frac{p\pi}{d}$$

Now, Eq. 5.24 becomes (with this value of  $\beta$ )

$$E_z = C \sin\left(\frac{m\pi}{a}\right)x \sin\left(\frac{n\pi}{b}\right)y \cos\left(\frac{p\pi}{d}\right)ze^{-j\omega t - \gamma z}$$

where  $C = 2C_2 C_4 A$

$$E_z = C \sin\left(\frac{m\pi}{a}\right)x \sin\left(\frac{n\pi}{b}\right)y \cos\left(\frac{p\pi}{d}\right)ze^{j\omega t - \gamma z}$$

$$E_z(\text{TM}_{mnp}) = C \sin\left(\frac{m\pi}{a}\right)x \sin\left(\frac{n\pi}{b}\right)y \cos\left(\frac{p\pi}{d}\right)ze^{j\omega t - \gamma z} \quad \dots(5.26)$$

where

$m = 0, 1, 2, 3, \dots$  represents the number of half wave variations in the  $x$  direction

$n = 0, 1, 2, 3, \dots$  represents the number of half wave variations in the  $y$  direction

$p = 1, 2, 3, \dots$  represents the number of half wave variations in the  $z$  direction

**Case 2. For TE Waves:** TM<sub>mnp</sub> mode of propagation in a rectangular waveguide is shown with components in Fig. 5.6.

For TE<sub>m,n</sub> wave to propagate  $E_z = 0$  and  $H_z \neq 0$ . We know from Maxwell's equation,

$$\nabla^2 H_z = -\omega^2 \mu \epsilon H_z$$

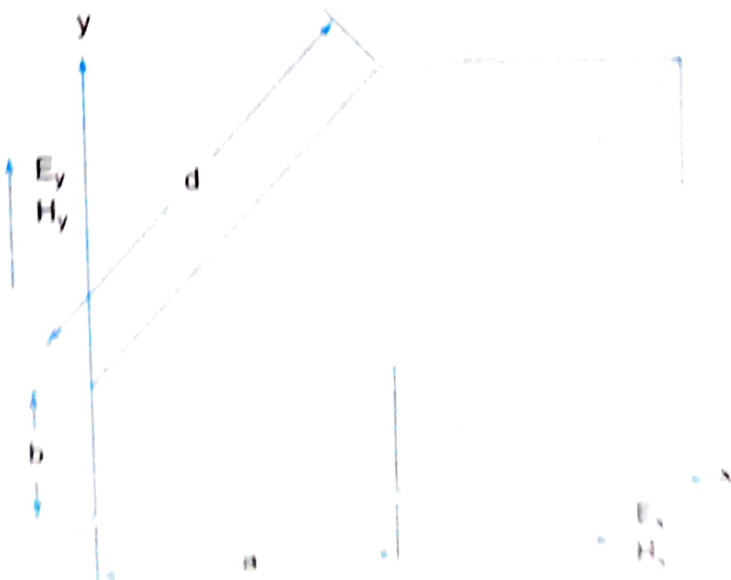


Fig. 5.6

$$\frac{\partial^2 H_z}{\partial x^2} + \frac{\partial^2 H_z}{\partial y^2} + \frac{\partial^2 H_z}{\partial z^2} = -\omega^2 \mu \epsilon H_z \quad \dots(5.27)$$

But  $\frac{\partial^2}{\partial z^2} = \gamma^2$  an operator.

$$\therefore \frac{\partial^2 H_z}{\partial x^2} + \frac{\partial^2 H_z}{\partial y^2} + \gamma^2 H_z + \omega^2 \mu \epsilon H_z = 0$$

$$\text{or } \frac{\partial^2 H_z}{\partial x^2} + \frac{\partial^2 H_z}{\partial y^2} + H_z [\gamma^2 + \omega^2 \mu \epsilon] = 0 \quad \dots(5.28)$$

$$\text{Let } \gamma^2 + \omega^2 \mu \epsilon = h^2$$

Now Eq. 5.28 becomes

$$\therefore \frac{\partial^2 H_z}{\partial x^2} + \frac{\partial^2 H_z}{\partial y^2} + h^2 H_z = 0$$

This is a partial differential equation of 2nd order.

$$\text{Let } H_z = XY \quad \dots(5.29)$$

where  $X$  is a function of  $x$  alone,  $Y$  is a function of  $y$  alone.

$$Y \frac{d^2 X}{dx^2} + X \frac{d^2 Y}{dy^2} + h^2 XY = 0$$

Dividing by  $XY$  throughout,

$$\frac{1}{X} \frac{d^2 X}{dx^2} + \frac{1}{Y} \frac{d^2 Y}{dy^2} + h^2 = 0$$

$$\text{Let } \frac{1}{X} \frac{d^2 X}{dx^2} = -A^2 \quad \dots(5.30a)$$

$$\frac{1}{Y} \frac{d^2 Y}{dy^2} = -B^2 \quad \dots(5.30b)$$

where  $A^2$  and  $B^2$  are constants.

$$\therefore -A^2 - B^2 = -h^2$$

$$\text{or } h^2 = A^2 + B^2$$

The solutions for above Eqs. 5.30a, b are

$$\begin{aligned} X &= C_1 \cos Bx + C_2 \sin Bx \\ Y &= C_3 \cos Ay + C_4 \sin Ay \end{aligned} \quad \dots(5.31)$$

The constants  $C_1, C_2, C_3$  and  $C_4$  are Determined by applying Boundary Conditions.

### 1st Boundary Condition (Bottom Wall)

$E_x = 0$  for  $y = 0$  and all values of  $x$  varying from 0 to  $a$ . We know,

$$E_x = \frac{-\gamma}{h^2} \frac{\partial E_z}{\partial x} - \frac{j\omega \mu}{h^2} \frac{\partial H_z}{\partial y}$$

But  $E_z = 0$  for a TE wave

$$\therefore E_x = \frac{-j\omega\mu}{h^2} \frac{\partial H_z}{\partial y}$$

But  $H_z = XY$  from Eq. 5.29.

Using Eq. 5.31,  $H_z$  reduces to

$$H_z = (C_1 \cos Bx + C_2 \sin Bx) (C_3 \cos Ay + C_4 \sin Ay) \quad \dots(5.32)$$

$$E_x = \frac{-j\omega\mu}{h^2} \frac{\partial}{\partial y} (C_1 \cos Bx + C_2 \sin Bx) (C_3 \cos Ay + C_4 \sin Ay) \quad \dots(5.33)$$

But  $E_x = 0$  for  $y = 0$  and all values of  $x$  varying from 0 to  $a$ .

Substituting these values in Eq. 5.33 after differentiating with respect to  $y$ , Eq. 5.33 becomes

$$0 = \frac{-j\omega\mu}{h^2} [(C_1 \cos Bx + C_2 \sin Bx) (-AC_3 \sin Ay + AC_4 \cos Ay)] \quad \dots(5.34)$$

$$C_1 = \text{and } C_2 \neq 0$$

Since  $x$  takes a values from 0 to  $a$ ,

$$\cos Bx \text{ and } \sin Bx \neq 0 \text{ and } y = 0$$

With these values Eq. 5.34 becomes

$$0 = \frac{-j\omega\mu}{h^2} [(C_1 \cos Bx + C_2 \sin Bx) AC_4]$$

Therefore only condition is that  $C_4 = 0$  since  $x$  has a value 0 to  $a$

Therefore, the intermediate solution is

$$H_z = (C_1 \cos Bx + C_2 \sin Bx) (C_3 \cos Ay) \quad \dots(5.35)$$

## 2nd Boundary Condition (Left Side Wall)

$E_y = 0$  for  $x = 0$  and  $y$  varying from 0 to  $b$ .

We know that,

$$E_y = \frac{-\gamma}{h^2} \frac{\partial E_z}{\partial y} + \frac{j\omega\mu}{h^2} \frac{\partial H_z}{\partial x}$$

But  $E_z = 0$  for a TE wave, and substituting for  $H_z$  from Eq. 5.35, we get

$$E_y = \frac{j\omega\mu}{h^2} \frac{\partial}{\partial x} [(C_1 \cos Bx + C_2 \sin Bx) C_3 \cos Ay] \quad \dots(5.36)$$

$$\text{i.e., } E_y = \frac{j\omega\mu}{h^2} [(-C_1 \sin Bx + BC_2 \cos Bx) C_3 \cos Ay]$$

Substituting the Boundary condition,

$E_y = 0$  for  $x = 0$  and  $y$  varying from 0 to  $b$ , Eq. 5.36 becomes,

$$0 = \frac{j\omega\mu}{h^2} [(0 + BC_2) C_3 \cos Ay]$$

Now,  $\cos Ay$  and  $C_3 \neq 0$

Therefore only solution is  $C_2 = 0$

With this, the intermediate solution Eq. 5.35 becomes

$$H_z = (C_1 \cos Bx C_3 \cos Ay) \quad \dots(5.37)$$

### 3rd Boundary Condition (Top Wall)

$E_x = 0$  for  $y = b$  and  $x$  varies from 0 to  $a$ .

We know that,

$$E_x = \frac{-\gamma}{h^2} \frac{\partial E_z}{\partial x} - \frac{j\omega\mu}{h^2} \frac{\partial H_z}{\partial y}$$

But,  $E_z = 0$  for TE wave

$$E_x = \frac{-j\omega\mu}{h^2} \frac{\partial H_z}{\partial y}$$

From Eq. 5.37,

$$H_z = C_1 \cos Bx C_3 \cos Ay$$

$$\therefore E_x = -\frac{j\omega\mu}{h^2} \frac{\partial}{\partial y} [C_1 \cos Bx C_3 \cos Ay] \quad \dots(5.38)$$

Substituting the boundary condition,

$E_x = 0$  for  $y = b$  and  $x$  varies from 0 to  $a$  in Eq. 5.8, we get

$$0 = \frac{j\omega\mu}{h^2} [-C_1 C_3 A \cos Bx \sin Ay]$$

Here,  $\cos Bx \neq 0$  and  $C_1 C_3 \neq 0$

Therefore, only  $\sin Ay = 0$

But  $y = b$ . Putting  $y = b$ , we get

$$\sin Ab = 0 \text{ or } Ab = n\pi \text{ where } n = 0, 1, 2, 3, \dots$$

or

$$A = \frac{n\pi}{b}$$

### 4th Boundary Condition (Right Side Wall)

$E_y = 0$  for  $x = a$  and  $y$  varying from 0 to  $a$ .

$$E_y = \frac{-\gamma}{h^2} \frac{\partial E_z}{\partial y} + \frac{j\omega\mu}{h^2} \frac{\partial H_z}{\partial x}$$

Since,  $E_z = 0$  for TE wave, and  $H_z = C_1 \cos Bx C_3 \cos Ay$ , we have

$$E_y = \frac{j\omega\mu}{h^2} \frac{\partial}{\partial x} [C_1 \cos Bx C_3 \cos Ay]$$

i.e.,

$$E_y = \frac{j\omega\mu}{h^2} [-C_1 B \sin Bx \cdot C_3 \cos Ay]$$

Substituting Boundary Condition,

$E_y = 0$  for  $x = a$  and  $y$  varying from 0 to  $b$ , we get

$$0 = [-C_1 B \sin Ba C_3 \cos Ay]$$

Here,  $C_1 \neq 0$ ;  $C_3 \neq 0$  and also  $\cos A_y \neq 0$ .

Therefore only  $\sin Ba = 0$

$$Ba = m\pi \quad \text{where } m = 0, 1, 2 \dots$$

or

$$B = \frac{m\pi}{a}$$

Therefore, the solution for  $H_z$  is given by Eq. 5.37. The values of  $A$  and  $B$  are substituted to give,

$$H_z = C_1 C_3 \cos\left(\frac{m\pi}{a}x\right) \cos\left(\frac{n\pi}{b}y\right) e^{j(\omega t - \gamma z)} \quad \dots(5.39)$$

Since  $\gamma = j\beta$  for a wave propagating along the positive  $z$  direction

$$H_z = C \cos\left(\frac{m\pi}{a}x\right) \cos\left(\frac{n\pi}{b}y\right) e^{j(\omega t - \beta z)} \quad \dots(5.40)$$

where,  $C = C_1 C_3$

and for the wave propagating along the negative  $z$  direction,

$$H_z = C \cos\left(\frac{m\pi}{a}x\right) \cos\left(\frac{n\pi}{b}y\right) e^{j(\omega t + \beta z)} \quad \dots(5.41)$$

The amplitude constant along the positive ' $z$ ' direction is represented by  $A^+$ , and that along the negative ' $z$ ' direction by  $A^-$ . Adding the two travelling waves to obtain the fields of standing wave we have from Eqs. 5.40 and Eq. 5.41.

$$H_z = (A^+ e^{-j\beta z} + A^- e^{+j\beta z}) \cos\left(\frac{m\pi}{a}x\right) \cos\left(\frac{n\pi}{b}y\right) e^{j\omega t} \quad \dots(5.42)$$

To make  $E_y$  vanish at  $z=0$  and  $z=d$  we must make  $A^+ = -A^-$  or  $A^- = -A^+$  and also we know that

$$E_y = -\frac{\gamma}{h^2} \frac{\partial E_z}{\partial y} + \frac{j\omega\mu}{h^2} \frac{\partial H_z}{\partial x}$$

For TE waves,  $E_z = 0$ ,

$$E_y = \frac{j\omega\mu}{h^2} \frac{\partial H_z}{\partial x}$$

$$E_y = \frac{j\omega\mu}{h^2} \left[ \frac{\partial}{\partial x} (A^+ e^{-j\beta z} + A^- e^{+j\beta z}) \cos\left(\frac{m\pi}{a}x\right) \cos\left(\frac{n\pi}{b}y\right) \right] e^{j\omega t}$$

Since  $E_y$  vanishes at  $z=0$  and  $z=d$ , we have

$$0 = \left[ (A^+ e^{-j\beta z} + A^- e^{+j\beta z}) - \left(\frac{m\pi}{a}\right) \sin\left(\frac{m\pi}{a}x\right) \cos\left(\frac{n\pi}{b}y\right) \right] e^{j\omega t} \quad \dots(5.43)$$

But

$$\sin\left(\frac{m\pi}{a}x\right) \text{ and } \cos\left(\frac{n\pi}{b}y\right) \neq 0$$

Therefore only  $A^+ e^{-j\beta z} + A^- e^{+j\beta z} = 0$

To make  $E_y = 0$  choose  $A^- = -A^+$ . Putting these in Eq. 5.43, we get

182

$$0 = (A^+ e^{-j\beta z} - A^+ e^{j\beta z}) = A^+ [e^{-j\beta z} - e^{+j\beta z}]$$

We know that  $(e^{-i\theta} - e^{+i\theta}) = -2i \sin \theta$

$$0 = -2jA^+ \sin \beta z$$

$\therefore$  since  $A^+ \neq 0$  only  $\sin \beta d = 0$  with  $z = d$

or  $\beta = \frac{\pi}{d}$

or  $\beta = \frac{p\pi}{d}$  where  $p = 1, 2, 3, \dots$

$$H_z = -2jA^+ \cos\left(\frac{m\pi}{a}\right)x \cos\left(\frac{n\pi}{b}\right)y \sin\left(\frac{p\pi}{d}\right)ze^{j(\omega t - \gamma z)}$$

Putting  $-2jA^+ = C$ , another constant,

$$H_z = C \cos\left(\frac{m\pi}{a}\right)x \cos\left(\frac{n\pi}{b}\right)y \sin\left(\frac{p\pi}{d}\right)ze^{j(\omega t - \gamma z)}$$

For TE<sub>mnp</sub> mode,

$$H_z = C \cos\left(\frac{m\pi}{a}\right)x \cos\left(\frac{n\pi}{b}\right)y \sin\left(\frac{p\pi}{d}\right)ze^{j(\omega t - \gamma z)} \quad \dots(5.44)$$

## 5.6 FIELD EXPRESSION FOR TE<sub>nmp</sub> AND TM<sub>nmp</sub> MODES IN A CIRCULAR CAVITY RESONATOR

### Case I : For a TE Wave

Consider a TE mode to be propagating in a circular cavity resonator by placing shorting plates at each end. Hence a cylindrical cavity is a section of circular waveguide of length 'd' and radius 'a' as shown in Fig. 5.7.

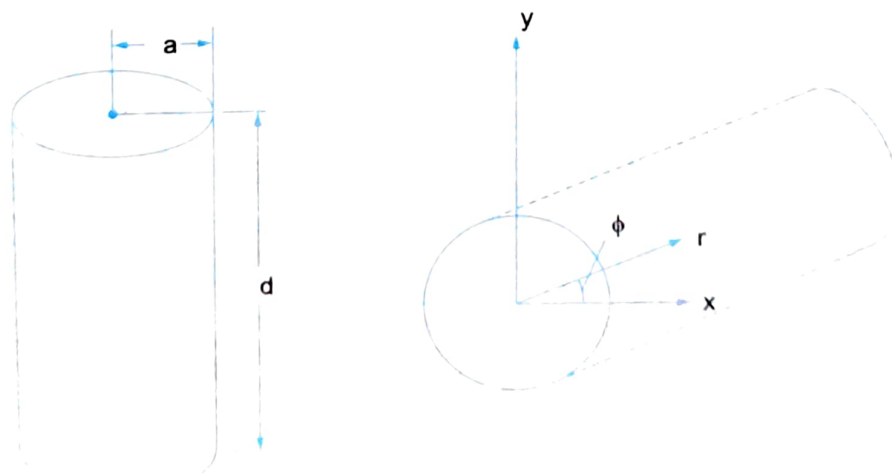


Fig. 5.7

In Chapter 4, we have shown that for a circular waveguide, for TE mode of propagation,

$$H_z = A' J_n (\rho h) \cos(n\phi') e^{j(\omega t - \gamma z)}$$

where  $A' = \sqrt{(A'_n)^2 + (B'_n)^2}$

and  $n\phi' = n\phi - \tan^{-1} \frac{B'_n}{A'_n}$

Now, the wave travelling in positive 'z' direction is given by

$$H_z = A' J_n (\rho h) \cos(n\phi') e^{j(\omega t - \beta z)} \quad \dots(5.45)$$

and in the negative 'z' direction by

$$H_z = A' J_n (\rho h) \cos(n\phi') e^{j(\omega t + \beta z)} \quad \dots(5.46)$$

Let  $A^+$  be the amplitude component of the wave in positive 'z' direction and  $A^-$  be the amplitude component in negative 'z' direction

$$[A^+ e^{-\beta z} + A^- e^{\beta z}] \cos(n\phi') = H_z \quad \dots(5.47)$$

Since  $H_z$  cannot be made equal to zero only  $E_\phi$  and  $E_\rho$  can be made equal to zero, therefore to make  $E_\phi$  and  $E_\rho$  vanish at  $z = 0$  and  $d$  we choose  $A^- = A^+$ .

- (i) Then the factor  $A^+ e^{-\beta d} + A^- e^{\beta d}$  becomes equal to  $-2jA^+ \sin \beta d$
- (ii) To make  $\sin \beta z$  vanish,

$$\beta d = p\pi \text{ where } p = 1, 2, 3, \dots \text{ etc.}$$

$$\beta = \frac{p\pi}{d}$$

Therefore, Eq. 5.46 reduces to,

$$H_z = -2jA J_n (\rho h) \cos(n\phi') \sin\left(\frac{p\pi}{d}\right) z e^{j(\omega t - \gamma z)}$$

i.e.,

$$H_z = C J_n (\rho h) \cos(n\phi') \left(\sin \frac{p\pi}{d}\right) z e^{j(\omega t - \beta z)}$$

where  $C = -2jA$

i.e.,

$$H_z = C J_n (\rho h) \cos(n\phi') [A^+ e^{-j\beta z} + A^- e^{+j\beta z}] \quad \dots(5.48)$$

### Take II: For a TM Wave

We can show (similar to a TE wave), that

$$E_z = C J'_n (\rho h) [A'_n \cos n\phi + B'_n \sin n\phi]$$

where  $A' = \sqrt{(A'_n)^2 + (B'_n)^2}$

$$n\phi' = n\phi - \tan^{-1} \frac{B'_n}{A'_n}$$

$$E_z = A' J'_n (\rho h) \cos(n\phi') \quad \dots(5.49)$$

The wave travelling in positive 'z' direction is given by

$$E_z = A' J'_n (\rho h) \cos(n\phi') e^{j(\omega t - \beta z)} \quad \dots(5.50)$$

Since  $\gamma = j\beta$ , the wave travelling in negative 'z' direction is given by

$$\begin{aligned} E_z &= A' J'_n (\rho h) \cos(n\phi') e^{j(\omega t + \beta z)} \\ E_z &= J'_n (\rho h) [A^+ e^{-\beta z} + A^- e^{\beta z}] \cos(n\phi') \end{aligned} \quad \dots(5.51)$$

To make  
choose

$$E_z = 0 \text{ at } z = 0 \text{ and } z = d$$

$$A^+ = -A^- \text{ or } A^- = -A^+$$

$$0 = J'_n (\rho h) A^+ [e^{-\beta z} - e^{\beta z}] \cos(n\phi')$$

But  $e^{-\beta z} - e^{\beta z} = -2j \sin \beta z$

But at  $z = 0$ ;  $E_z = 0 \text{ and } z = d$

$$0 = J'_n (\rho h) A^+ (-2j \sin \beta d) \cos(n\phi')$$

$$A^+ \neq 0 \text{ and } \cos(n\phi') = 0$$

only  $\sin \beta d = 0$   
or  $\beta d = p\pi$

$$\beta = \frac{p\pi}{d} \text{ where } p = 1, 2, 3, \dots$$

$$\therefore J'_n (\rho h) \cos(n\phi') \sin\left(\frac{p\pi}{d}\right) z e^{j(\omega t - \beta z)} \quad \dots(5.52)$$

along positive 'z' direction and

$$J'_n (\rho h) \cos(n\phi') \sin\left(\frac{p\pi}{d}\right) z e^{j(\omega t + \beta z)} \quad \dots(5.53)$$

along negative 'z' direction

Thus summarizing,

For Rectangular cavity resonator field equations are given by

$$H_z = C \cos\left(\frac{m\pi}{a}\right) x \cdot \cos\left(\frac{n\pi}{b}\right) y \sin\left(\frac{p\pi}{d}\right) z e^{j(\omega t - \gamma z)} \quad (\mathbf{TM}_{mnp})$$

where,  $m = 0, 1, 2, 3$ , representing the number of half wave periodicity in the 'x' direction.

$n = 0, 1, 2, 3$ , representing the number of half wave periodicity in the 'y' direction.

$p = 1, 2, 3, 4$  representing the number of half wave periodicity in the 'z' direction  
and

$$E_z = C \sin\left(\frac{m\pi}{a}\right) x \sin\left(\frac{n\pi}{b}\right) y \cos\left(\frac{p\pi}{d}\right) z e^{j(\omega t - \gamma z)} \quad (\mathbf{TM}_{mnp})$$

where  $m, n, p$  have usual notations.

The resonant frequency is given by

$$f_0 = \frac{c}{2} \left[ \left(\frac{m}{a}\right)^2 + \left(\frac{n}{b}\right)^2 + \left(\frac{p}{d}\right)^2 \right]^{1/2} \quad (\mathbf{TE}_{mnp} \mathbf{TM}_{mnp})$$

dominant mode is  $\mathbf{TE}_{101}$  for  $a, b$  and  $d$ .

For circular cavity resonator, field equations are given by

$$H_z = CJ_n(\rho h) \cos(n\phi') \sin\left(\frac{p\pi}{d}\right) z e^{j(\omega t - \gamma z)} (\text{TE}_{nmp})$$

where

$n = 0, 1, 2, 3, \dots$  is the number of full cycle variations in the  $\phi$  direction.

$m = 1, 2, 3, 4, \dots$  is the number of full cycle variations radial ( $\gamma$ ) direction.

$p = 1, 2, 3, 4, \dots$  is the number of half cycle variations axial ( $z$ ) direction.

and

$$E_z = J'_n(\rho h) \cos(n\phi') \sin\left(\frac{p\pi}{d}\right) z e^{j(\omega t - \gamma z)} (\text{TM}_{nmp})$$

where  $n, m$  and  $p$  have usual rotations.

The resonant frequency is given by

$$f_o = \frac{c}{2\pi} \left[ \left( \frac{P_{nm}}{a} \right)^2 + \left( \frac{p\pi}{d} \right)^2 \right]^{1/2} (\text{TM}_{nmp})$$

$$f_o = \frac{c}{2\pi} \left[ \left( \frac{P'_{nm}}{a} \right)^2 + \left( \frac{p\pi}{d} \right)^2 \right]^{1/2} (\text{TM}_{nmp})$$

Dominant modes are

$\text{TM}_{110}$  for  $2a > d$  and  $\text{TE}_{111}$  for  $d \geq 2a$ .

## 5.8 FIELD PATTERNS

From the discussion on resonant frequency of cavity resonators, it is clear that an electromagnetic field can exist in the lossless cavity only when the excitation frequency is exactly equal to the resonant frequency,  $f_o$ . Since,  $m$ ,  $n$  and  $p$  in Eqs. 5.3 and 5.5 can take on all integer values, the cavity has an infinite number of resonant modes each with its own resonant frequency. We define the primary mode as the one that has the lowest resonant frequency. For rectangular cavity,  $TE_{101}$  is the primary mode.

For  $TE_{mnp}$  modes the field components  $E_x$ ,  $E_y$ ,  $H_x$  and  $H_y$  can be obtained from the  $H_z$  expression given in Eq. 5.44 and the same can be used to sketch the field patterns of the various cavity modes. The subscripts  $m$ ,  $n$  and  $p$  actually represent the half wave periodicity of the field in the  $x$ ,  $y$  and  $z$  directions respectively.

For a  $TE_{101}$  primary or dominant mode, the electric and magnetic fields are shown in Fig. 5.8 for four different instant  $t = 0, T/4, T/2$  and  $3T/4$ . We can easily see that the field components have no variations in the  $y$  directions and one half wave variation in the  $x$  and  $y$  directions. Since  $n = 0$ ,  $m = p = 1$ . It is also clear that electric and magnetic fields are  $90^\circ$  out of phase i.e., when magnetic field is maximum, the electric field is zero and vice versa. This shows that no real power flow occurs and that the cavity just stores the energy associated with the field similar to stored energy exchanges every half cycle in  $L-C$  resonant circuits.

Field patterns for  $TE_{101}$  and  $TE_{111}$  are shown in Fig. 5.9.

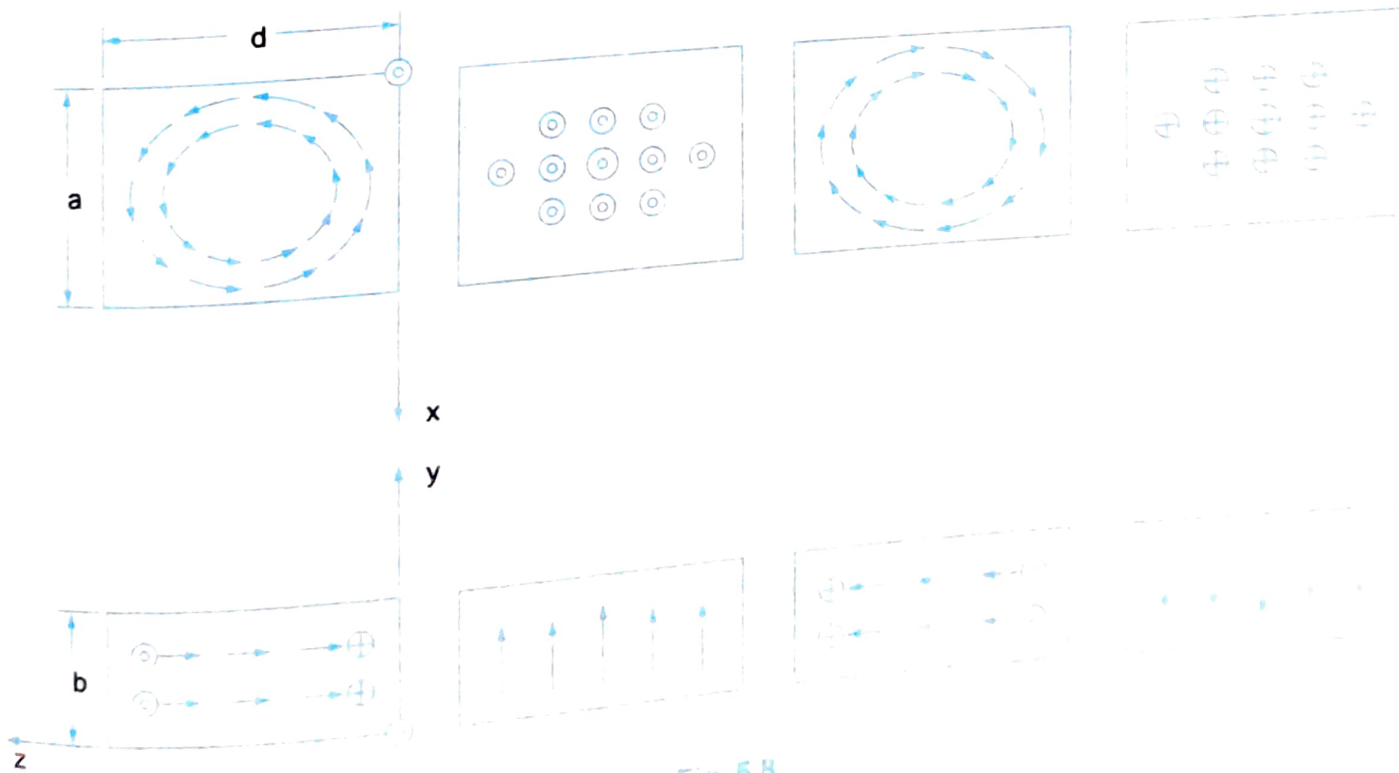
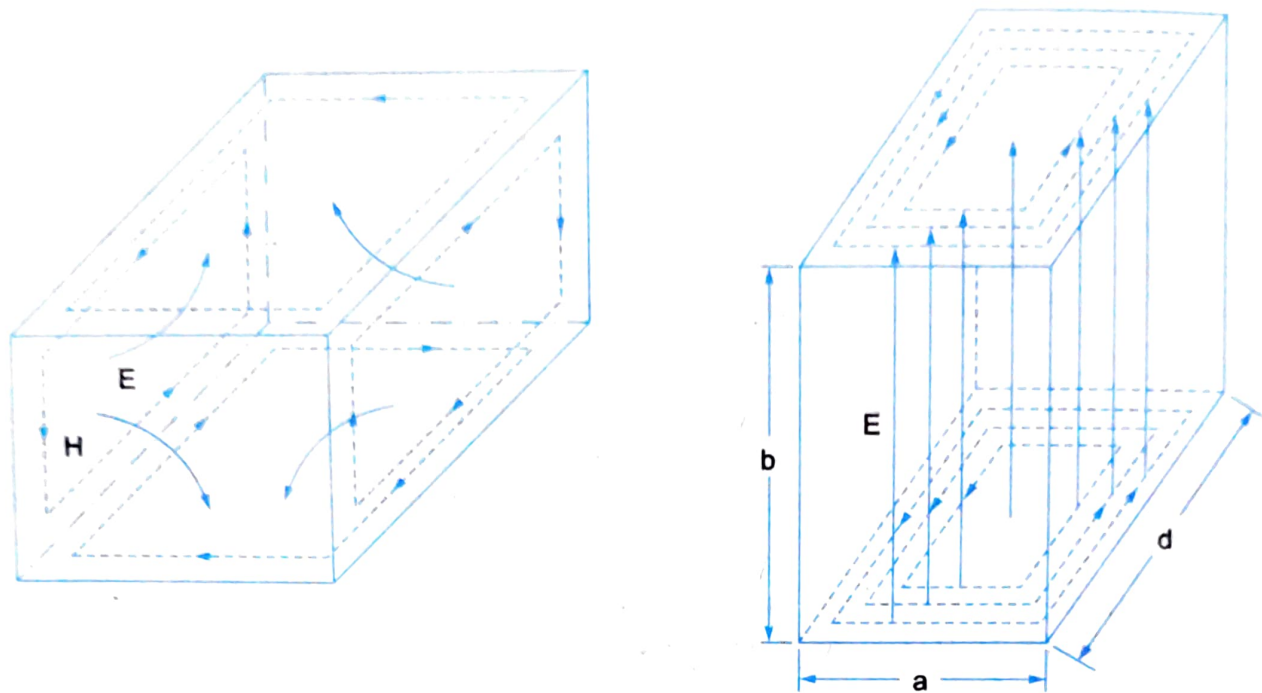
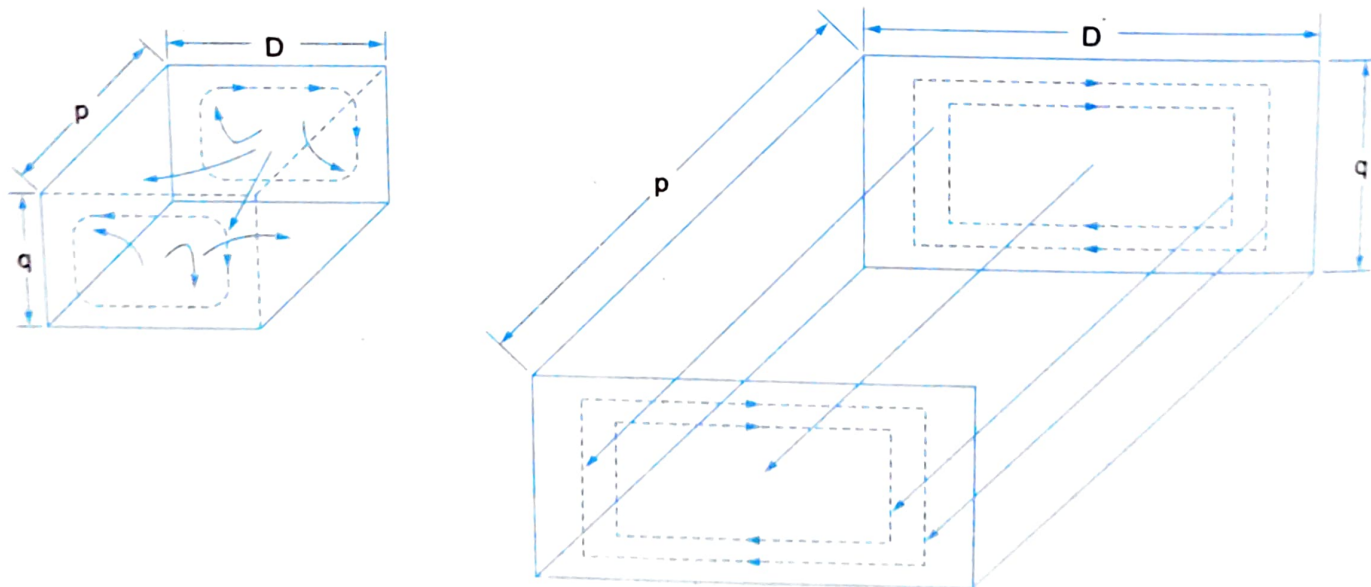


Fig. 5.8



**Fig. 5.9** Field pattern in  $TE_{101}/TE_{111}$  mode of a rectangular cavity.

The field patterns for  $TM_{101}$  and  $TM_{111}$  modes are shown in Fig. 5.10. It must be noted that  $TM_{111}$  mode is the dominant mode.



**Fig. 5.10** Field pattern for  $TM_{101}/TM_{111}$  modes of a rectangular cavity resonator.

In circular cavity resonators, the general mode is given by  $TE_{nmp}$  or  $TM_{nmp}$  where  $n$ ,  $m$  and  $p$  have usual notations. The field patterns for  $TE_{111}$  and  $TM_{011}$  which are the dominant modes are shown in Fig. 5.11.

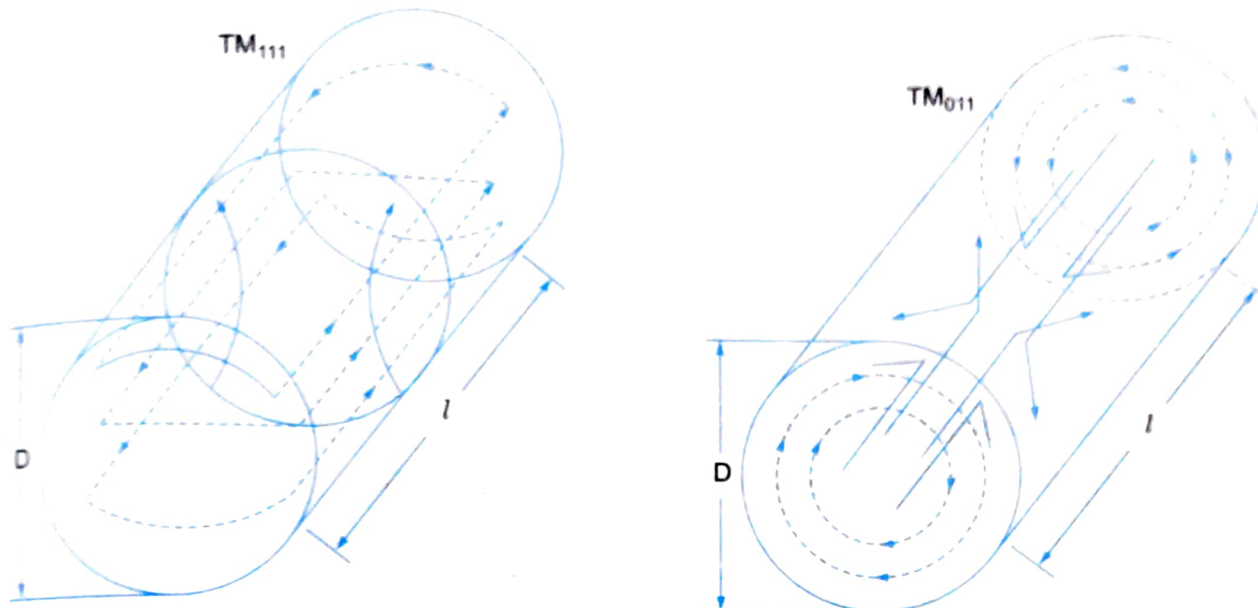


Fig. 5.11 Field pattern for  $TE_{111}/TM_{011}$  modes in a cylindrical cavity resonator

## 5.9 QUALITY FACTOR (Q) OF CAVITY RESONATORS

The quality factor ( $Q$ ) of any resonant or anti-resonant circuit is a measure of frequency selectivity and is defined by the equation

$$Q = \frac{\omega_0 W}{P} \quad \dots(5.54)$$

where,  $W$  = maximum energy stored

$P$  = average power loss (or dissipated power) and

$\omega_0$  = resonant frequency.

i.e., 
$$Q = 2\pi \cdot \frac{\text{Maximum energy stored per cycle}}{\text{Energy dissipated for cycle}}$$

The  $Q$  of a perfect or ideal cavity resonator is infinite since in a perfect conductor forming the cavity,  $P$  would be zero and also once energised it would resonate for ever. Equation 5.56 is true for a cavity resonator that is resonant at one frequency only. If there is more than one resonant frequency, there will be different values of  $Q$  for the various values of frequencies. Normally coupling loops are used to couple the energy in and out of a cavity resonator. This coupling has the effect of an imperfectly reflecting wall and so is the finite termination or load of the cavity. This would also change the value of  $Q$ . This  $Q$  that takes into account the coupling between the cavity and coupling paths is known as the loaded  $Q_L$ . So,  $Q_L$  can be given by

$$\frac{1}{Q_L} = \frac{1}{Q_0} + \frac{1}{Q_{ext}} \quad \dots(5.55)$$

where,  $Q_0$  =  $Q$  of an unloaded cavity

$Q_{ext}$  =  $Q$  due to external ohmic losses.

There are three types of couplings, resulting in critically coupled, under coupled and over coupled cases. An unloaded resonator can be represented by a series or parallel resonant circuit. The unloaded  $Q$  is then given by

$$Q_o = \frac{\omega_o L}{R} \quad \dots(5.56)$$

The  $Q_{ext}$  can be written as,

$$Q_{ext} = \frac{Q_o}{k} = \frac{\omega_o L}{kR} \quad \dots(5.57)$$

which,  $k$  = coupling coefficient of the cavity.

For critical coupled cavity (resonator matched to the generator),  $k = 1$  and hence loaded  $Q$  ( $Q_L$ ) is given by

$$Q_L = \frac{1}{2} Q_{ext} = \frac{1}{2} Q_o \quad \dots(5.58)$$

For under coupled cavity,  $k = 1$ , the cavity terminals are at a voltage minimum and the input impedance is the reciprocal of standing wave ratio

i.e.,  $k = \frac{1}{\rho}$

Therefore  $Q_L = \frac{\rho}{1 + \rho} Q_o \quad \dots(5.59)$

For over coupled cavity,  $k > 1$ , cavity terminals are at a voltage maximum and the impedance is standing wave ratio

i.e.,  $k = \rho$

Therefore  $Q_L = \frac{Q_o}{1 + \rho} \quad \dots(5.60)$

*Unloaded Quality factor* ( $Q_o$ ) of a cavity can also be defined by taking into consideration the volume of cavity that stores the energy and the value of the metal that determines the energy dissipated. Volume of the metal in which currents are flowing is equal to the surface area of the cavity multiplied by the skin depth ( $\delta$ ). Hence,  $Q_o$  is also given by

$$Q_o = \frac{\text{Volume of cavity}}{\delta \times \text{surface area of cavity}} \quad \dots(5.61)$$

$$Q_o \cong \frac{\text{Cross-section area of cavity}}{\delta \times \text{periphery of cavity}} \quad \dots(5.62)$$

Thus  $Q$  factor of a cavity can be increased by increasing the size of cavity or conductivity of the walls or by decreasing the coupling into the cavity.  $Q$  also increases with an increase in frequency as skin depth decreases with frequency.

### 5.0.1 Q of a Rectangular Cavity Resonator

We know that in a resonant circuit the electric and magnetic energy are in time quadrature, that is, while one is maximum, the other is zero. The stored energy in a resonator is obtained by integrating over the volume of the resonator, the power loss by integrating the power density over the surface of the resonator.

$$U_{\text{stored}} = \frac{1}{2} \int_{\text{vol}} E^2 dv = \frac{1}{2} \int_{\text{vol}} \mu H^2 dv \quad \dots(5.63)$$

$$U_{\text{lost}} = \frac{R_s}{2} \int_{\text{Sur}} H_t^2 dA \quad \dots(5.64)$$

where,  $E, H, H_t$  = peak values,

$R_s$  = surface resistance of the resonator wall.

$$Q = \omega \cdot \frac{U_{\text{stored}}}{U_{\text{lost}}} = \frac{\frac{\omega \mu}{2} \int_{\text{vol}} H^2 dv}{\frac{R_s}{2} \int_{\text{Sur}} |H_t|^2 dA} = \frac{\omega \mu \int_{\text{vol}} H^2 dv}{R_s \int_{\text{Sur}} |H_t|^2 dA}$$

Also,

$$H^2 = H_t^2 + H_n^2$$

$H_t^2$  is approximately twice of  $H^2$  over the volume of the resonator

$$\therefore Q = \frac{\omega \mu (\text{vol})}{2 R_s (\text{sur})} \quad \dots(5.65)$$

Stored energy ' $E_{\text{stored}}$ ' is given by

$$E_{\text{stored}} = \frac{1}{2} \cdot \iiint_{0 \ 0 \ 0}^{a \ b \ c} |E|^2 dx dy dz \quad \dots(5.66)$$

For TE<sub>011</sub> mode, we will have only  $E_x$  component and all the remaining components ( $E_y, E_z, H_x, H_y$  and  $H_z$ ) will be zero.

$$\therefore E_{\text{stored}} = \frac{1}{2} \cdot \int_{\text{vol}} E_o^2 \cdot \sin^2 \frac{\pi}{b} y \cdot \sin^2 \frac{\pi}{c} z dx dy dz \quad \dots(5.67)$$

We know that

$$\sin^2 X = \frac{1}{2}(1 - \cos 2X)$$

Using this in Eq. 5.67. We will be left with only the constant term as the cosine terms vanish over a cycle.

$$\therefore E_{\text{stored}} = \frac{1}{8} \cdot E_o^2 abc = U_{\text{stored}} \quad \dots(5.68)$$

The energy dissipated is evaluated for each of  $xy, yz$  and  $xz$  planes and added.

$$E_{\text{lost}} = U_{\text{lost}} = \frac{1}{2} R_s E_o^2 \frac{\pi^2}{\omega^2 \mu^2} \left[ \frac{ac}{b^2} + \frac{ab}{c^2} + \frac{bc}{2} \left( \frac{1}{b^2} + \frac{1}{c^2} \right) \right] \quad \dots(5.69)$$

$$Q = \frac{U_{\text{stored}}}{U_{\text{lost}}} = \frac{\frac{1}{8} \cdot E_o^2 abc}{\frac{1}{2} R_s E_o^2 \frac{\pi^2}{\omega^2 \mu^2} \left[ \frac{ac}{b^2} + \frac{ab}{c^2} + \frac{bc}{2} \left( \frac{1}{b^2} + \frac{1}{c^2} \right) \right]} \quad \dots(5.70)$$

For a cubic resonator  $a = b = c$ ,

$$Q = \frac{1}{6} \frac{1}{R_s} \frac{1}{\pi^2} \omega^2 \mu^2 a^3 \quad \dots(5.71)$$

We see that  $Q$  is proportional to  $\omega^2$ .  $Q$  of the resonator will be very large at microwave frequencies.  $Q$ 's of the order of 10,000 to 40,000 are easily achievable.

## 5.8.2 Q of a Circular Cavity Resonator

As already stated a circular cavity resonator will be formed by closing the ends of a circular waveguide the length being a multiple of  $\lambda/2$ . Circular resonators have higher selectivity and  $Q$ 's. The electric vector ( $E$ ) is a maximum at the centre and dies off to zero at conducting walls while the magnetic field ( $H$ ) surrounds the electric vector circumstantially. Neither  $E$  nor  $H$  varies in axial or circumferential directions. The  $TM_{01}$  mode whose attenuation decreases with frequency is considered for the derivation of  $Q$  of a circular cavity resonator.

$$\begin{aligned} U_{\text{stored}} &= \frac{1}{2} \epsilon \int_{\text{vol}} E^2 \cdot \rho \cdot d\rho \cdot d\phi \cdot dl \\ &= \frac{1}{2} \epsilon \int_0^a \left[ \frac{\beta}{k_c^2} E_o J'_o(k_c r) \right]^2 r dr \cdot \int_0^{2\pi} d\phi \int_0^c dl \end{aligned}$$

where

$$k_c = \omega_c \sqrt{\mu} = \frac{x}{a}$$

where  $x$  = value of argument

$a$  = radius

Also

$$\rho = r$$

$$\begin{aligned} U_{\text{stored}} &= \frac{1}{2} \epsilon \frac{c \beta^2}{k_c^4} \cdot E_o^2 \left[ J'_o(k_c r) \right]^2 \int_0^a r \cdot dr \\ &= \frac{1}{2} \pi \epsilon \cdot c \cdot a^2 \cdot \frac{\beta^2}{k_c^4} [J'_o(k_c r)]^2 \cdot E_o^2 \end{aligned} \quad \dots(5.72)$$

Power dissipated is along the wall length ( $c$ ) and end plates.

$$\begin{aligned} \text{Cylindrical Walls} &= \frac{1}{2} R_s H^2 \cdot 2\pi a(c) \\ &= \pi R_s ac \cdot \frac{\omega^2}{k_c^4} E_o^2 [J'_o(k_c r)]^2 \end{aligned} \quad \dots(5.73)$$

$$\begin{aligned}
 \text{Two end walls} &= 2 \cdot \frac{1}{2} R_s \int_0^a \int_0^{2\pi} H^2 r \cdot dr \cdot d\phi \\
 &= \pi R_s \frac{\omega^2 \mu^2}{k_c^4} E_o^2 [J'_o(k_c r)]^2
 \end{aligned} \quad \dots(5.74)$$

Total power dissipated is the sum of Eqs. 5.73 and 5.74

$$\text{i.e., } U_{\text{lost}} = \pi R_s \cdot \frac{\omega^2 \mu^2}{k_c^4} E_o^2 [J'_o(k_c r)]^2 a(a+c) \quad \dots(5.75)$$

$$\begin{aligned}
 Q &= \frac{\omega U_{\text{stored}}}{U_{\text{lost}}} \\
 &= \frac{\frac{1}{2} \cdot \omega E_o^2 \pi \cdot c \cdot a^2 \cdot \frac{\beta^2}{k_c^4} [J'_o(k_c r)]^2}{\pi R_s \cdot \frac{\omega^2 \mu^2}{k_c^4} E_o^2 [J'_o(k_c r)]^2 a(a+c)} \\
 &= \omega \cdot \frac{1}{2} \cdot \frac{1}{R_s} \frac{\beta^2}{\omega^2} \left( \frac{ac}{a+c} \right)
 \end{aligned}$$

Bessel function value for first crossing of zero being 2.405 for TM<sub>01</sub> mode and putting  $r = a$  in  $k_c r$

$$\begin{aligned}
 k_c \cdot a &= 2.405 \\
 k_c^2 &= \omega_c^2 \mu \\
 f_c &= \frac{1}{2\pi} \frac{k}{\sqrt{\mu}} = \frac{0.382 v_c}{a},
 \end{aligned}$$

where  $v_c$  = velocity of light,

$$\begin{aligned}
 \text{Q for TM}_{01} &= \frac{1}{2} \frac{1}{R_s} \cdot \beta^2 \frac{1}{2\pi} \frac{\lambda}{v_c} \left( \frac{ac}{a+c} \right) \\
 \text{i.e., } Q &= \frac{2.6178}{4\pi R_s} a \frac{\beta^2}{v_c} \frac{1}{\left[ \frac{ac}{a+c} \right]} \quad \dots(5.76)
 \end{aligned}$$

Eq. 5.76 indicates that Q for a circular cavity resonator is a function of

$$a \cdot \frac{ac}{a+c} = \frac{a}{\frac{1}{a} + \frac{1}{c}}$$

It means that for larger values of  $a$ ,  $Q$  is large. Also, resonance frequency,  $f_c$  is an inverse function of ' $a$ ', that is, at higher frequencies, radius ' $a$ ' is smaller. Hence a trade off for  $Q$  is to be made at higher frequencies for a circular cavity resonator.

## 5.10 REENTRANT CAVITIES

For a cavity resonator at microwave frequency, it is necessary that the inductance and capacitance have to be considerably reduced so that it maintains resonance at the operating frequency. Such a cavity resonator where the metallic boundaries will extend into the interior of the cavity are called *re-entrant cavities* as in the case of a coaxial cavity shown in Fig. 5.12.

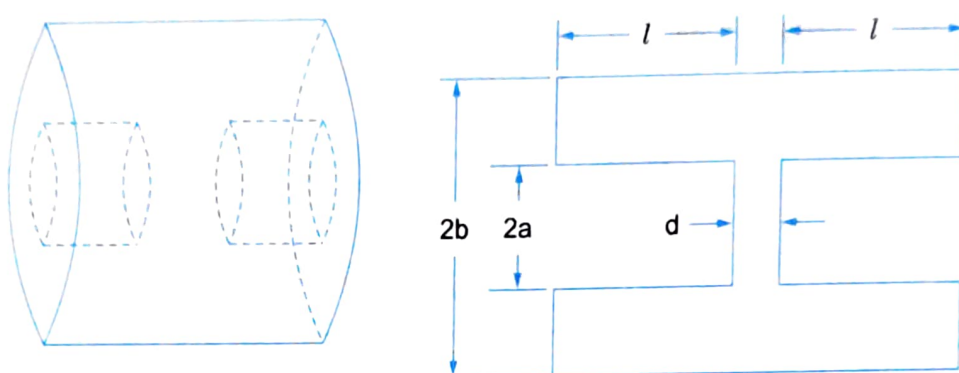


Fig. 5.12 Coaxial cavity.

Reentrant cavity similar to a coaxial line shorted at two ends and joined the centre by a capacitor. Such a reentrant cavity can support an infinite number of resonant frequencies. Hence it is useful for making klystron devices to be discussed in Chapter 8. Another example of a reentrant cavity is the radial reentrant cavity shown in Fig. 5.13.

In a reentrant cavity the inductance and resistance are reduced because of the hollow scoops within. The coaxial cavity may be considered as a coaxial line shorted at two ends  $RQ$ ,  $RS$  and joined at the neck by a capacitor as shown in Fig. 5.14.

Applying transmission line theory.

$$Z_o = \frac{1}{2\pi} \sqrt{\frac{\mu}{\epsilon}} \ln\left(\frac{b}{a}\right) \text{ ohms.}$$

The input impedance of the shorted line is

$$Z_{in} = j Z_o \tan(\beta l)$$

where,  $l$  = length of coaxial line

$$Z_{in} = j \frac{1}{2\pi} \sqrt{\frac{\mu}{\epsilon}} \ln\left(\frac{b}{a}\right) \tan(\beta l).$$

The inductance ' $L$ ' of the cavity is given by

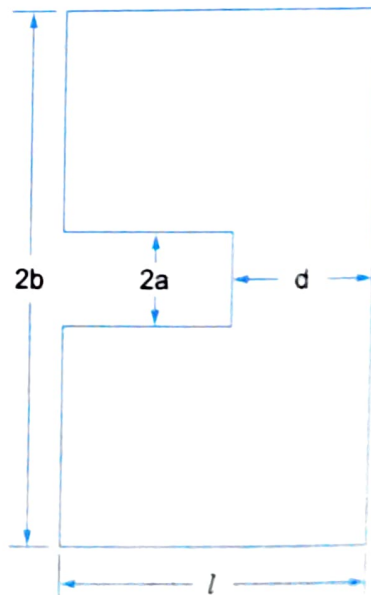


Fig. 5.13 Radial reentrant cavity.



Fig. 5.14

$$L = \frac{2Z_0}{\omega} = \frac{1}{\pi\epsilon} \sqrt{\frac{\mu}{\epsilon}} \ln\left(\frac{b}{a}\right) \tan(\beta l) \quad \dots(5.77)$$

The capacitance of the gap 'C<sub>g</sub>' is given by

$$C_g = \epsilon \frac{\pi a^2}{t}$$

At resonance

$$\omega L = \frac{1}{\omega C_g}$$

$$\frac{1}{\pi} \sqrt{\frac{\mu}{\epsilon}} \ln\left(\frac{b}{a}\right) \tan(\beta l) = \frac{t}{\omega \epsilon \pi a^2}$$

or

$$\tan(\beta l) = \frac{t}{\omega a^2} \sqrt{\frac{1}{\mu \epsilon} \times \frac{1}{\ln(b/a)}} \quad \dots(5.78)$$

A tangent function has infinite number of solutions and therefore, there will be infinite number of resonant frequencies or modes. The solution of Eq. 5.78 gives the resonant frequency of the coaxial cavity.

## 5.11 COUPLING TO CAVITIES

Fields inside a cavity cannot exist inside completely enclosed resonators unless the energy is supplied by some means of coupling into the resonator from the outside. There are several ways of coupling like,

- Loop Coupling :** By introducing a conducting loop with plane normal to the magnetic field lines as shown in Fig. 5.15.
- Iris/Aperture Coupling :** By coupling through a hole in the cavity, called iris coupling as shown in Fig. 5.16. For a reflection cavity and in Fig. 5.17 for a transmission cavity. Figure 5.17 shows a means of aperture coupling through waveguide feeds.



Fig. 5.15

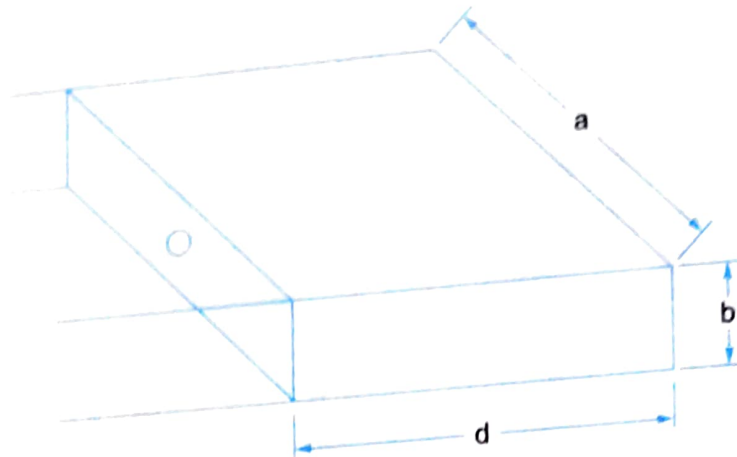


Fig. 5.16

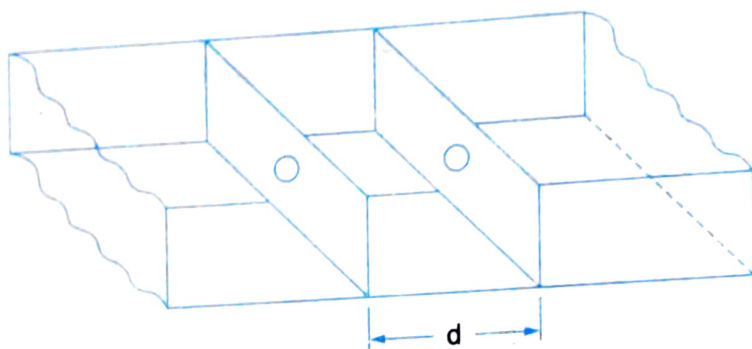


Fig. 5.17

It is also possible to excite a resonator by introduction of a modulated electron beam passing through a small gap in the resonator in the direction of electric field lines as we do it in case of microwave tubes.

## REVIEW QUESTIONS

- 5.1 What are cavity Resonators ? Derive the equations for resonant frequencies for a rectangular and circular cavity resonator.
- 5.2 Derive the field expressions for a rectangular cavity resonator. Plot the field patterns for the dominant mode of propagation in such a resonator for TE and TM modes.
- 5.3 Derive the field expression for a circular cavity resonator. Plot the field pattern for TE and TM modes assuming dominant modes.
- 5.4 What do you understand by Quality factor of a cavity resonator ? Discuss the term unloaded  $Q_{\text{loaded}}$ ,  $Q_{\text{critical}}$ , coupled  $Q$ , under coupled  $Q$  and over coupled  $Q$  with reference to a cavity resonator.
- 5.5 Define a reentrant cavity and give at least two examples. Where are these used ?
- 5.6 A rectangular cavity resonator has dimensions  $a = 4 \text{ cms}$ ,  $b = 2 \text{ cm}$  and  $d = 6 \text{ cms}$ . Determine the primary mode resonant frequency of the cavity.
- 5.7 An air-filled circular waveguide has a radius of 5 cm and is used as a resonator for  $\text{TE}_{111}$  mode at 8 GHz by placing two perfectly conducting plates at its two ends. Determine the minimum distance between the two end plates.

# 6

# Microwave Components

## 6.1 INTRODUCTION

Microwave systems normally consist of several microwave components including the source and the load being connected to each other by waveguide or co-axial or transmission line system. All these components must be built with low standing wave ratios, lower attenuation, lower insertion losses and other desirable characteristics to achieve the desired transmission of microwave signal.

The rectangular and circular waveguides, cavity resonators etc. that were discussed in previous chapters are also microwave components. In this chapter we study other components like waveguide junctions, joints, corners, drives, posts and screws, directional couplers, ferrite devices phase shifters, filters etc.

## 6.2 WAVEGUIDE MICROWAVE JUNCTIONS

At a certain position in a waveguide system, many a times it becomes necessary to split all or part of the microwave energy into particular directions. This is achieved by waveguides or in general by microwave junctions. These are combined to form coupler units that direct the energy as required. Alternately the same junction may be used to combine two or more signals. In general, a microwave junction is an interconnection of two or more microwave components as shown in Fig. 6.1.

This junction has four ports similar to low frequency two-port networks. Fig. 6.2 shows a microwave source at port ① and microwave loads at ports ②, ③ and ④.

The microwave junction is analogous to a traffic junction where a number of roads meet on which vehicles enter and leave the traffic junction. In a similar manner, when input from microwave source is applied at port ① a part of it comes out of port ② another part out of port ③ some part out

### Cavity Resonators

of port ② and the remaining part may come out of port ① itself due to mismatch between port ① and microwave junction.

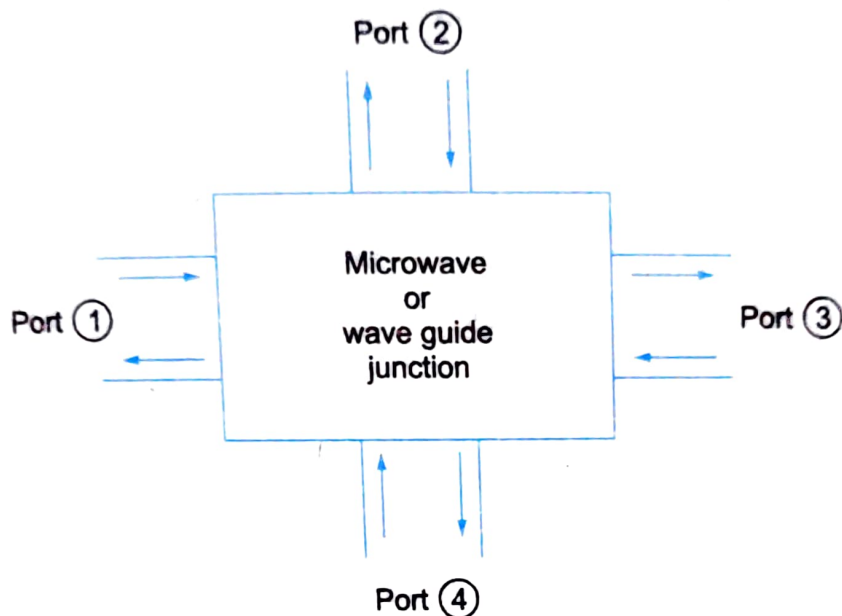


Fig. 6.1

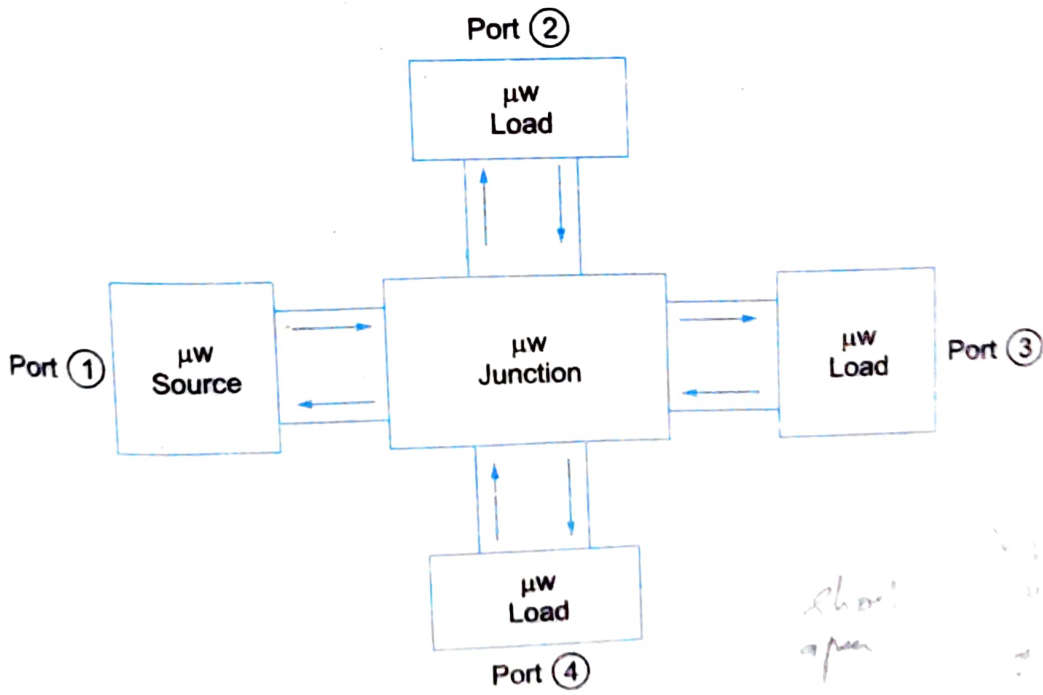


Fig. 6.2

6.2.1

### Scattering or (S) Parameters

Low frequency circuits can be described by two port networks and their parameters such as  $Z$ ,  $Y$ ,  $H$ ,  $ABCD$  etc. as per network theory. Here network parameters relate the total voltages and total currents as shown in Fig. 6.3.

In a similar way at microwave frequencies, we talk of travelling waves with associated powers instead of voltages and currents and the microwave junction can be defined by what are called as S-parameters or scattering parameters (similar to H, Y, Z parameters). Referring to Fig. 6.2, it can be seen that for an input at one port, we have four outputs as discussed earlier. Similarly if we apply inputs to all the ports, we will have 16 combinations, which are represented in a matrix form and that matrix is called as a *Scattering Matrix*. It is a square matrix which gives all the combinations of power relationships between the various input and output ports of a microwave junction. The elements of this matrix are called *scattering coefficients or scattering (S) parameters*.

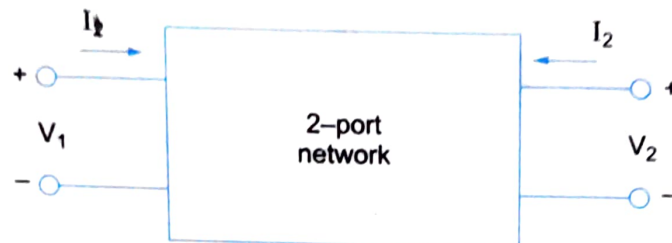


Fig. 6.3

To obtain the relationship between the scattering matrix and the input/output powers at different ports, consider a junction of 'n' number of transmission lines wherein the  $i^{\text{th}}$  line ( $i$  can be any line from 1 to  $n$ ) is terminated in a source as shown in Fig. 6.4.

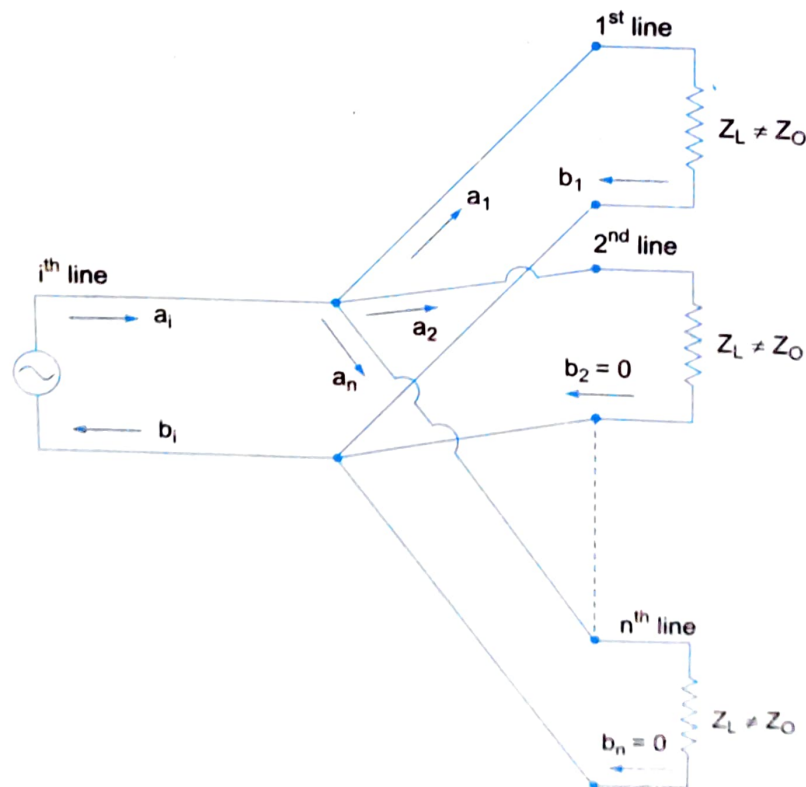


Fig. 6.4

**Case 1** Let the first line be terminated in an impedance other than the characteristic impedance (i.e.  $Z_L \neq Z_0$ ) and all the remaining lines (from 2nd to  $n^{\text{th}}$  line) in an impedance equal to  $Z_0$  (i.e.  $Z_L = Z_0$ ).

If  $a_i$  be the incident wave at the junction due to a source at the  $i$ th line, then it divides itself among  $(n - 1)$  number of lines as  $a_1, a_2, \dots, a_n$  as shown in Fig. 6.4. There will be no reflections from 2nd to  $n$ th line and the incident waves are absorbed since their impedances are equal to characteristic impedance ( $Z_o$ ). But, there is a mismatch at the 1st line and hence there will be a reflected wave  $b_1$  going back into the junction.

$b_1$  is related to  $a_1$  by.

$$b_1 = (\text{reflection coefficient}) a_1 = S_{i1} \cdot a_1$$

where,  $S_{i1}$  = reflection coefficient of 1st line.

$i$  = reflection from 1st line and

$i$  = source connected at  $i$ th line.

Hence, the contribution to the outward travelling wave in the  $i$ th line is given by

$$b_i = S_{i1} \cdot a_1 \quad [ \because b_2 = b_3 = \dots = b_n = 0 ]$$

**Case 2:** Let all the  $(n - 1)$  lines be terminated in an impedance other than  $Z_o$ . (i.e.  $Z_L \neq Z_o$  for all the lines)

Then, there will be reflections into the junction from every line and hence the total contribution to the outward travelling wave in the  $i$ th line is given by

$$b_i = S_{i1} \cdot a_1 + S_{i2} \cdot a_2 + S_{i3} \cdot a_3 + \dots + S_{in} \cdot a_n \quad \dots(6.1)$$

$i = 1$  to  $n$  since  $i$  can be any line from 1 to  $n$

Therefore, we have,

$$b_1 = S_{11} a_1 + S_{12} a_2 + S_{13} a_3 + \dots + S_{1n} a_n$$

$$b_2 = S_{21} a_1 + S_{22} a_2 + S_{23} a_3 + \dots + S_{2n} a_n$$

:

:

:

$$b_n = S_{n1} a_1 + S_{n2} a_2 + S_{n3} a_3 + \dots + S_{nn} a_n$$

In matrix form,

$$\begin{bmatrix} b_1 \\ b_2 \\ \vdots \\ b_n \end{bmatrix} = \begin{bmatrix} S_{11} & S_{12} & \dots & S_{1n} \\ S_{21} & S_{22} & \dots & S_{2n} \\ \vdots & \vdots & & \vdots \\ \vdots & \vdots & & \vdots \\ \vdots & \vdots & & \vdots \\ S_{n1} & S_{n2} & \dots & S_{nn} \end{bmatrix} \begin{bmatrix} a_1 \\ a_2 \\ \vdots \\ a_n \end{bmatrix} \quad \dots(6.2)$$

Column Matrix  $[b]$   
corresponding to  
Reflected waves  
or Output

Scattering Column  
Matrix  $[S]$   
of order  $n \times n$

Matrix  $[a]$   
Corresponding to  
Incident Waves  
or Input

$$[b] = [S] [a]$$

...(6.3)

When a junction of n number of waveguides is considered,

a's represent inputs to particular ports.

b's represent outputs out of various ports.

$S_{ij}$  corresponds to scattering coefficients resulting due to input at ith port and output taken out of jth port.

$S_{ii}$  denotes how much of power is reflected back from the junction into the ith port when input power is applied at the ith port itself.

## Properties of (S) Matrix

1. [S] is always a square matrix of order ( $n \times n$ )

2. [S] is a symmetric matrix.

$$\text{i.e., } S_{ij} = S_{ji}$$

3. [S] is a unitary matrix

$$\text{i.e., } [S][S]^* = [I]$$

where, [S] = complex, conjugate of [S]

[I] = unit matrix or Identity matrix of the same order as that of [S].

4. The sum of the products of each term of any row (or column) multiplied by the complex conjugate of the corresponding terms of any other row (or column) is zero.

$$\text{i.e., } \sum_{i=1}^n S_{ik} S_{ij}^* = 0 \quad k \neq j \quad \left( \begin{array}{l} k = 1, 2, 3, \dots, n \\ j = 1, 2, 3, \dots, n \end{array} \right)$$

5. If any of the terminal or reference planes (say the  $k$ th port) are moved away from the junction by an electric distance  $\beta_k l_k$ , each of the coefficients  $S_{ij}$  involving  $k$  will be multiplied by the factor  $e^{-j\beta_k l_k}$ .

## 6.3 MICROWAVE T-JUNCTIONS

A T-junction is an intersection of three waveguides in the form of English alphabet 'T'. There are several types of Tee junctions. The following Tee junctions will be discussed.

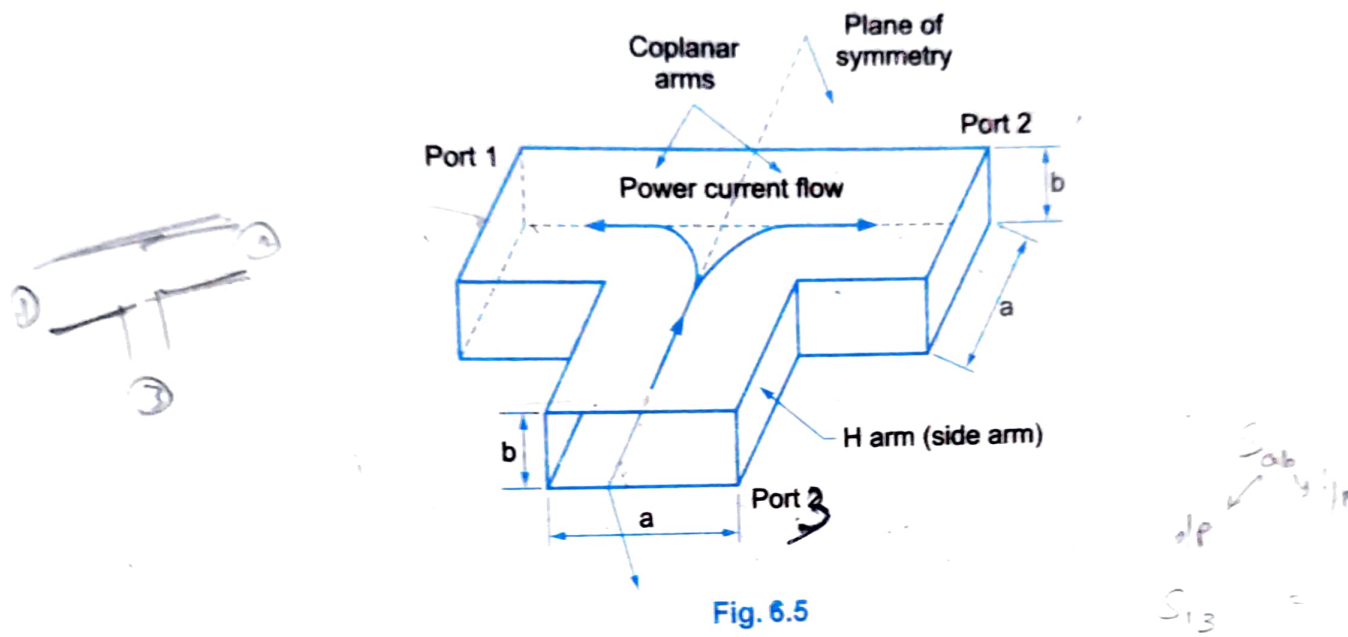
1. H-plane Tee junction
2. E-plane Tee junction
3. E-H plane Tee junction (Hybrid T junction)
4. Magic-T junction
5. Rat race junction

### 6.3.1 H-plane Tee Junction

A H-plane Tee junction is formed by cutting a rectangular slot along the width of a main waveguide and attaching another waveguide — the side arm — called the H-arm as shown in Fig. 6.5. The port ① and port ② of the main waveguide are called collinear ports and port ③ is the H-arm or side arm.

H-plane Tee is so called because the axis of the side arm is parallel to the planes of the main transmission line. As all three arms of H-plane Tee lie in the plane of magnetic field, the magnetic field divides itself into the arms. Therefore this is also called a current junction.

The properties of a H-plane Tee can be completely defined by its [S] matrix. The order of scattering matrix is  $3 \times 3$  since there are three possible inputs and 3 possible outputs.



$$[S] = \begin{bmatrix} S_{11} & S_{12} & S_{13} \\ S_{21} & S_{22} & S_{23} \\ S_{31} & S_{32} & S_{33} \end{bmatrix} \quad \dots(6.4)$$

Now we determine the S-parameters  $S_{ij}$ ,  $i \rightarrow 1, 2, 3, j \rightarrow 1, 2, 3$  by applying the properties of [S].

- Because of plane of symmetry of the junction scattering coefficients  $S_{13}$  and  $S_{23}$  must be equal.

$$S_{13} = S_{23}$$

- From the symmetric property,  $S_{ij} = S_{ji}$

$$S_{12} = S_{21}, S_{23} = S_{32} = S_{13},$$

$$S_{13} = S_{31}$$

- Since port is perfectly matched to the junction

$$S_{33} = 0$$

With these properties [S] matrix of Eq. 6.4 becomes,

$$[S] = \begin{bmatrix} S_{11} & S_{12} & S_{13} \\ S_{12} & S_{22} & S_{13} \\ S_{13} & S_{13} & 0 \end{bmatrix} \quad \dots(6.5)$$

i.e., We have four unknowns.

#### 4. From the unitary property

$$[S] [S]^* = [I]$$

i.e.,

$$\begin{bmatrix} S_{11} & S_{12} & S_{13} \\ S_{12} & S_{22} & S_{13} \\ S_{13} & S_{13} & 0 \end{bmatrix} \begin{bmatrix} S_{11}^* & S_{12}^* & S_{13}^* \\ S_{12}^* & S_{22}^* & S_{13}^* \\ S_{13}^* & S_{13}^* & 0 \end{bmatrix} = \begin{bmatrix} 1 & 0 & 0 \\ 0 & 1 & 0 \\ 0 & 0 & 1 \end{bmatrix}$$

Multiplying we get,

$$R_1 C_1: \quad S_{11} S_{11}^* + S_{12} S_{12}^* + S_{13} S_{13}^* = 1 \quad (R_1 C_1 = \text{row 1, column 1})$$

$$\text{or} \quad |S_{11}|^2 + |S_{12}|^2 + |S_{13}|^2 = 1 \quad \dots(6.6)$$

$$\text{Similarly } R_2 C_2: \quad |S_{12}|^2 + |S_{22}|^2 + |S_{13}|^2 = 1 \quad \dots(6.7)$$

$$R_3 C_3: \quad |S_{13}|^2 + |S_{13}|^2 = 1 \quad \dots(6.8)$$

$$R_3 C_1: \quad S_{13} S_{11}^* + S_{13} S_{12}^* = 0 \quad \dots(6.9)$$

From Eq. 6.8

$$2 |S_{13}|^2 = 1 \quad \text{or} \quad S_{13} = \frac{1}{\sqrt{2}} \quad \dots(6.10)$$

Comparing Eqs. 6.6 and 6.7, we get

$$|S_{11}|^2 = |S_{22}|^2 \quad \dots(6.11)$$

$$\therefore S_{11} = S_{22} \quad \dots(6.11)$$

$$\text{From Eq. 6.9,} \quad S_{13} \neq 0, (S_{11}^* + S_{12}^* = 0, \quad \text{or} \quad S_{11}^* = -S_{12}^*)$$

$$\text{or} \quad S_{11} = -S_{12} \quad \text{or} \quad S_{12} = -S_{11} \quad \dots(6.12)$$

Using these in Eq. 6.6.

$$|S_{11}|^2 + |S_{11}|^2 + \frac{1}{2} = 1 \quad \text{or} \quad 2 |S_{11}|^2 = \frac{1}{2} \quad \text{or} \quad S_{11} = \frac{1}{2} \quad \dots(6.13)$$

$\therefore$  From Eq. 6.11 and 6.12,

$$S_{12} = -\frac{1}{2} \quad \dots(6.14)$$

$$\text{and} \quad S_{22} = \frac{1}{2} \quad \dots(6.15)$$

Substituting for  $S_{13}$ ,  $S_{11}$ ,  $S_{12}$  and  $S_{22}$  from Eq. 6.10 and Eqs. 6.13 to 6.15 in Eq. 6.5, we get

$$[S] = \begin{bmatrix} \frac{1}{2} & -\frac{1}{2} & \frac{1}{\sqrt{2}} \\ -\frac{1}{2} & \frac{1}{2} & \frac{1}{\sqrt{2}} \\ \frac{1}{\sqrt{2}} & \frac{1}{\sqrt{2}} & 0 \end{bmatrix} \quad \dots(6.16)$$

We know that  $[b] = [S] [a]$  (from Eq. 6.3)

$$\begin{bmatrix} b_1 \\ b_2 \\ b_3 \end{bmatrix} = \begin{bmatrix} \frac{1}{2} & -\frac{1}{2} & \frac{1}{\sqrt{2}} \\ -\frac{1}{2} & \frac{1}{2} & \frac{1}{\sqrt{2}} \\ \frac{1}{\sqrt{2}} & \frac{1}{\sqrt{2}} & 0 \end{bmatrix} \begin{bmatrix} a_1 \\ a_2 \\ a_3 \end{bmatrix}$$

$$b_1 = \frac{1}{2}a_1 - \frac{1}{2}a_2 + \frac{1}{\sqrt{2}}a_3 \quad (6.17)$$

$$b_2 = -\frac{1}{2}a_1 - \frac{1}{2}a_2 + \frac{1}{\sqrt{2}}a_3 \quad (6.18)$$

$$b_3 = \frac{1}{\sqrt{2}}a_1 + \frac{1}{\sqrt{2}}a_2 \quad (6.19)$$

$$a_3 \neq 0, a_1 = a_2 = 0.$$

Case 1 :

(i.e., Input is given at port ③ and no inputs at port ① and port ②).

Substituting these in Eqs. 6.17, 6.18 and 6.19, we get

$$b_1 = \frac{a_3}{\sqrt{2}}, b_2 = \frac{a_3}{\sqrt{2}} \text{ and } b_3 = 0$$

Let  $P_3$  (corresponding to  $a_3$ ) be the power input at port ③. Then this power divides equally between ports ① and ② in phase i.e.,  $P_1 = P_2$  (power outputs at the respective ports corresponding to  $b_1$  and  $b_2$ ).

$$P_3 = P_1 + P_2 = 2P_1 = 2P_2$$

But

The amount of power coming out of port ① or port ② due to input at port ③.

$$= 10 \log_{10} \frac{P_1}{P_3} = 10 \log_{10} \frac{P_1}{2P_1} = 10 \log_{10} \left( \frac{1}{2} \right)$$

$$= -10 \log_{10}^2 = -10(0.3010) \approx -3 \text{ dB}$$

Hence the power coming out of port ① or port ② is 3 dB down with respect to input power at port ③, hence the H-plane Tee is called as 3-dB splitter.

Further when  $TE_{10}$  mode is allowed to propagate into port ③, the electric field lines do not change their direction when they come out of port ① and ②, hence called H-plane Tee. i.e., The waves that come out of ports ① and ② are equal in magnitude and phase.

Case 2 :

$$a_1 = a_2 = a, a_3 = 0$$

$$b_1 = \frac{a}{2} - \frac{a}{2} + \frac{1}{\sqrt{2}}a_3 = \frac{a_3}{\sqrt{2}} = 0$$

$$b_2 = -\frac{a}{2} + \frac{a}{2} + \frac{1}{\sqrt{2}}a_3 = \frac{a_3}{\sqrt{2}} = 0$$

$$b_3 = \frac{a_1}{\sqrt{2}} = \frac{a_2}{\sqrt{2}} = \frac{a}{\sqrt{2}} + \frac{a}{\sqrt{2}}$$

i.e., The output at port ③ is addition of the two inputs at port ① and port ② and these are added in phase.

### ~~6.3.2 E-Plane Tee~~

A rectangular slot is cut along the broader dimension of a long waveguide and a side arm is attached as shown in Fig. 6.6. Ports ① and ② are the collinear arms and port ③ is the E-arm.

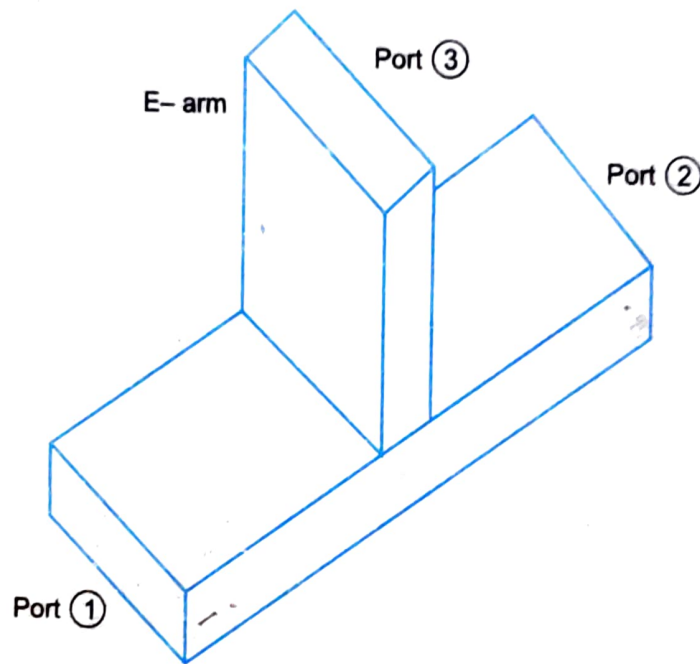


Fig. 6.6 E-plane Tee.

When  $TE_{10}$  mode is made to propagate into port ③, the two outputs at port ① and ② will have a phase shift of  $180^\circ$  as shown in Fig. 6.7. Since the electric field lines change their direction when they come out of port ① and ②, it is called a E-plane Tee. E-plane Tee is a voltage or series junction symmetrical about the central arm. Hence any signals that is to be split or any two signal that are to be combined will be fed from the E arm.

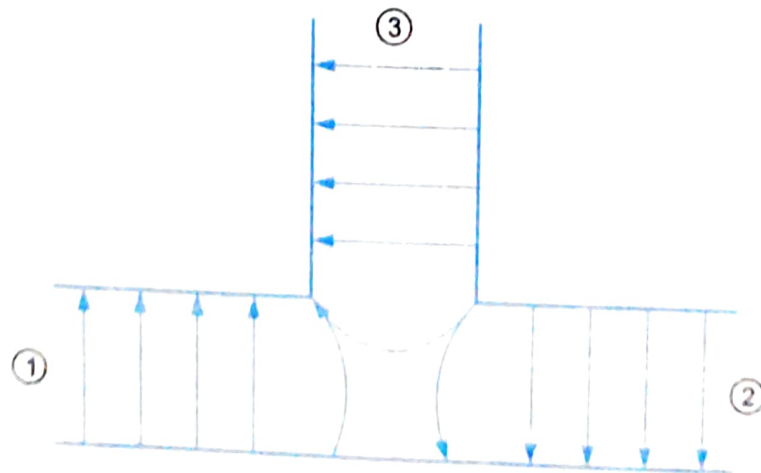


Fig. 6.7

The scattering matrix of an E-plane Tee can be used to describe its properties. In general, the power out of port ③ (side or E arm) is proportional to the difference between instantaneous powers entering from ports ① and ②.

Also, the effective value of the power leaving the E arm is proportional to the phasor difference between the powers entering ports ① and ②. When powers entering the main arms (ports ① and ②) are in phase opposition, maximum energy comes out of port ③ or E-arm.

Since it is a three port junction the scattering matrix can be derived as follows:

- [S] is a  $3 \times 3$  matrix since there are 3 ports.

$$[S] = \begin{bmatrix} S_{11} & S_{12} & S_{13} \\ S_{21} & S_{22} & S_{23} \\ S_{31} & S_{32} & S_{33} \end{bmatrix}$$

- The Scattering coefficient

$$S_{23} = -S_{13}$$

...(6.20)

Since outputs at ports ① and ② are out of phase by  $180^\circ$  with an input at port ③.

- If port ③ is perfectly matched to the junction.

$$S_{33} = 0$$

...(6.21)

- From symmetric property  $S_{ij} = S_{ji}$

$$S_{12} = S_{21}$$

$$S_{13} = S_{31}$$

$$S_{23} = S_{32}$$

...(6.22)

With the above properties (Eq. 6.21 and 6.22), [S] becomes,

$$[S] = \begin{bmatrix} S_{11} & S_{12} & S_{13} \\ S_{12} & S_{22} & S_{13} \\ S_{13} & S_{23} & 0 \end{bmatrix}$$

...(6.23)

- From unitary property,  $[S] \cdot [S]^* = [I]$

$$\text{i.e., } \begin{bmatrix} S_{11} & S_{12} & S_{13} \\ S_{12} & S_{22} & S_{13} \\ S_{13} & S_{23} & 0 \end{bmatrix} \begin{bmatrix} S_{11}^* & S_{12}^* & S_{13}^* \\ S_{12}^* & S_{22}^* & S_{13}^* \\ S_{13}^* & S_{23}^* & 0 \end{bmatrix} = \begin{bmatrix} 1 & 0 & 0 \\ 0 & 1 & 0 \\ 0 & 0 & 1 \end{bmatrix}$$

...(6.24)

$$R_1 C_1: |S_{11}|^2 + |S_{12}|^2 + |S_{13}|^2 = 1$$

...(6.25)

$$R_2 C_2: |S_{12}|^2 + |S_{22}|^2 + |S_{13}|^2 = 1$$

...(6.26)

$$R_3 C_3: |S_{13}|^2 + |S_{23}|^2 = 1$$

...(6.27)

$$R_3 C_1: S_{13} \cdot S_{11}^* + S_{13} \cdot S_{12}^* = 0$$

Equating Eqs. 6.24 and 6.25, we get

$$S_{11} = S_{22}$$

...(6.28)

From Eq. 6.26,

$$S_{13} = \frac{1}{\sqrt{2}}$$

...(6.29)

From Eq. 6.27,  $S_{13}(S_{11}^* - S_{12}^*) = 0$  or  $S_{11} = S_{12} = S_{22}$  ... (6.30)

Using these values (Eqs. 6.28 to 6.30) on Eq. 6.24.

$$|S_{11}|^2 + |S_{11}|^2 + \frac{1}{2} = 1$$

or  $2|S_{11}|^2 = \frac{1}{2}$  or  $S_{11} = \frac{1}{2}$  ... (6.31)

Substituting the values from Eq. 6.29 to 6.31, the [S] matrix of Eq. 6.23 becomes,

$$[S] = \begin{bmatrix} \frac{1}{2} & \frac{1}{2} & \frac{1}{\sqrt{2}} \\ \frac{1}{2} & \frac{1}{2} & \frac{-1}{\sqrt{2}} \\ \frac{1}{\sqrt{2}} & \frac{-1}{\sqrt{2}} & 0 \end{bmatrix} \quad \dots (6.32)$$

We know, (from Eq. 6.3)

$$[b] = [S][a]$$

$$\begin{bmatrix} b_1 \\ b_2 \\ b_3 \end{bmatrix} = \begin{bmatrix} \frac{1}{2} & \frac{1}{2} & \frac{1}{\sqrt{2}} \\ \frac{1}{2} & \frac{1}{2} & \frac{-1}{\sqrt{2}} \\ \frac{1}{\sqrt{2}} & \frac{-1}{\sqrt{2}} & 0 \end{bmatrix} \begin{bmatrix} a_1 \\ a_2 \\ a_3 \end{bmatrix} \quad \dots (6.33)$$

$$b_1 = \frac{1}{2}a_1 + \frac{1}{2}a_2 + \frac{1}{\sqrt{2}}a_3 \quad \dots (6.34)$$

$$b_2 = \frac{1}{2}a_1 + \frac{1}{2}a_2 - \frac{1}{\sqrt{2}}a_3 \quad \dots (6.35)$$

$$b_3 = \frac{1}{\sqrt{2}}a_1 - \frac{1}{\sqrt{2}}a_2 \quad \dots (6.36)$$

**Case 1 :**

$$a_1 = a_2 = 0 \quad a_3 \neq 0$$

$$b_1 = \frac{1}{\sqrt{2}}a_3; b_2 = -\frac{1}{\sqrt{2}}a_3; b_3 = 0$$

i.e., An input at port ③ equally divides between ① and ② but introduces a *phase shift* of  $180^\circ$  between the two outputs. Hence E-plane Tee also acts as a 3 dB splitter.

**Case 2 :**  $a_1 = a_2 = a, a_3 = 0$

Substituting again in Eqs. 6.34 to 6.36, we get

$$b_1 = \frac{a}{2} + \frac{a}{2}; b_2 = \frac{a}{2} + \frac{a}{2}; b_3 = \frac{1}{\sqrt{2}}a - \frac{1}{\sqrt{2}}a = 0$$

i.e., equal inputs at port ① and port ② result in no output at port ③

Case 3 :

$$a_1 \neq 0, a_2 = 0, a_3 = 0$$

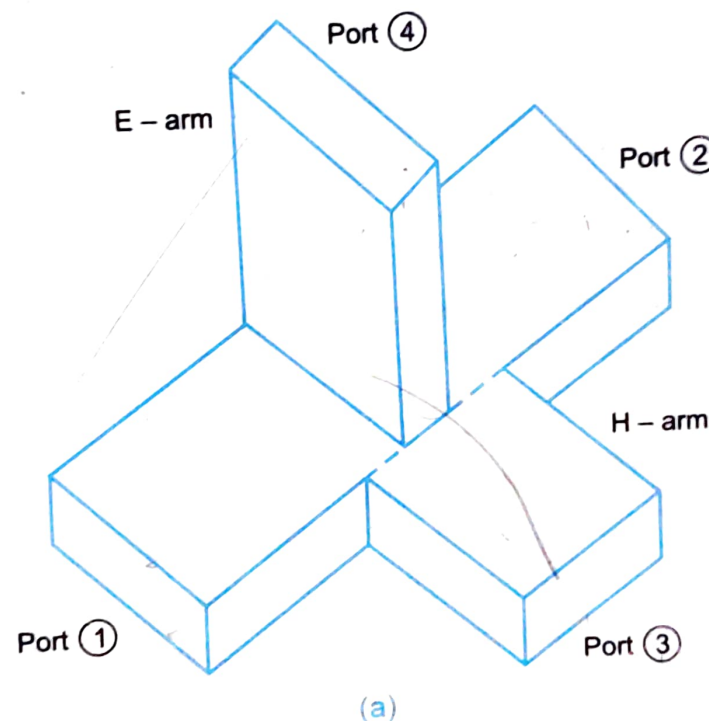
Hence,

$$b_1 = \frac{a_1}{2}; b_2 = \frac{a_1}{2}; b_3 = \frac{-a_1}{\sqrt{2}}$$

Similarly we can have all combinations of inputs and outputs.

### ~~6.3.5 E-H Plane (Hybrid or Magic) Tee~~

Here rectangular slots are cut both along the width and breadth of a long waveguide and side arms are attached as shown in Fig. 6.8a. Ports ① and ② are collinear arms, port ③ is the H-arm, and port ④ is the E-arm.



(a)

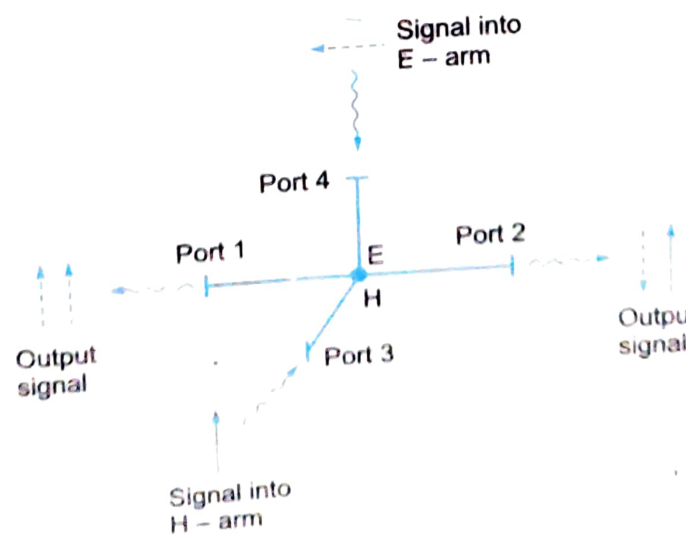


Fig. 6.8 (b)

Such a device became necessary because of the difficulty of obtaining a completely matched three port Tee junction. This four port hybrid Tee junction combines the power dividing properties of both H-plane Tee and E-plane Tee as shown in Fig. 6.8b and has the advantage of being completely matched at all its ports. This has several useful applications as will be seen later. Using the properties of E-H plane Tee, its scattering matrix can be obtained as follows.

- [S] is a  $4 \times 4$  matrix since there are 4 ports

i.e., 
$$[S] = \begin{bmatrix} S_{11} & S_{12} & S_{13} & S_{14} \\ S_{21} & S_{22} & S_{23} & S_{24} \\ S_{31} & S_{32} & S_{33} & S_{34} \\ S_{41} & S_{42} & S_{43} & S_{44} \end{bmatrix} \quad \dots(6.37)$$

- Because of H-plane Tee section

$$S_{23} = S_{13} \quad \dots(6.38)$$

- Because of E-plane Tee section

$$S_{24} = -S_{14} \quad \dots(6.39)$$

- Because of geometry of the junction an input at port ③ cannot come out of port ④ since they are isolated ports and vice versa.

$$S_{34} = S_{43} = 0 \quad \dots(6.40)$$

- From symmetric property,  $S_{ij} = S_{ji}$

$$\begin{aligned} S_{12} &= S_{21}; S_{13} = S_{31}; S_{23} = S_{32}; \\ S_{34} &= S_{43}; S_{24} = S_{42}; S_{41} = S_{14}; \end{aligned} \quad \dots(6.41)$$

- If ports ③ and ④ are perfectly matched to the junction.

$$S_{33} = S_{44} = 0 \quad \dots(6.42)$$

Substituting the above properties from Eqs. 6.38 to 6.42 in Eq. 6.37, we get

$$[S] = \begin{bmatrix} S_{11} & S_{12} & S_{13} & S_{14} \\ S_{12} & S_{22} & S_{23} & -S_{14} \\ S_{13} & S_{23} & 0 & 0 \\ S_{14} & -S_{14} & 0 & 0 \end{bmatrix} \quad \dots(6.43)$$

- From unitary property,  $[S][S]^* = [I]$

i.e., 
$$\begin{bmatrix} S_{11} & S_{12} & S_{13} & S_{14} \\ S_{12} & S_{22} & S_{23} & -S_{14} \\ S_{13} & S_{23} & 0 & 0 \\ S_{14} & -S_{14} & 0 & 0 \end{bmatrix} \cdot \begin{bmatrix} S_{11}^* & S_{12}^* & S_{13}^* & S_{14}^* \\ S_{12}^* & S_{22}^* & S_{23}^* & -S_{14}^* \\ S_{13}^* & S_{23}^* & 0 & 0 \\ S_{14}^* & -S_{14}^* & 0 & 0 \end{bmatrix} = \begin{bmatrix} 1 & 0 & 0 & 0 \\ 0 & 1 & 0 & 0 \\ 0 & 0 & 1 & 0 \\ 0 & 0 & 0 & 1 \end{bmatrix}$$

$$R_1C_1: |S_{11}|^2 + |S_{12}|^2 + |S_{13}|^2 + |S_{14}|^2 = 1 \quad \dots(6.44)$$

$$R_2C_2: |S_{22}|^2 + |S_{23}|^2 + |S_{13}|^2 + |S_{14}|^2 = 1 \quad \dots(6.45)$$

Such a device became necessary because of the difficulty of obtaining a completely matched three port Tee junction. This four port hybrid Tee junction combines the power dividing properties of both H-plane Tee and E-plane Tee as shown in Fig. 6.8b and has the advantage of being completely matched at all its ports. This has several useful applications as will be seen later. Using the properties of E-H plane Tee, its scattering matrix can be obtained as follows.

- [S] is a  $4 \times 4$  matrix since there are 4 ports

i.e.,

$$[S] = \begin{bmatrix} S_{11} & S_{12} & S_{13} & S_{14} \\ S_{21} & S_{22} & S_{23} & S_{24} \\ S_{31} & S_{32} & S_{33} & S_{34} \\ S_{41} & S_{42} & S_{43} & S_{44} \end{bmatrix} \quad \dots(6.37)$$

- Because of H-plane Tee section

$$S_{23} = S_{13} \quad \dots(6.38)$$

- Because of E-plane Tee section

$$S_{24} = -S_{14} \quad \dots(6.39)$$

- Because of geometry of the junction an input at port ③ cannot come out of port ④ since they are isolated ports and vice versa.

$$S_{34} = S_{43} = 0 \quad \dots(6.40)$$

- From symmetric property,  $S_{ij} = S_{ji}$

$$\begin{aligned} S_{12} &= S_{21}; S_{13} = S_{31}; S_{23} = S_{32}; \\ S_{34} &= S_{43}; S_{24} = S_{42}; S_{41} = S_{14}; \end{aligned} \quad \dots(6.41)$$

- If ports ③ and ④ are perfectly matched to the junction.

$$S_{33} = S_{44} = 0 \quad \dots(6.42)$$

Substituting the above properties from Eqs. 6.38 to 6.42 in Eq. 6.37, we get

$$[S] = \begin{bmatrix} S_{11} & S_{12} & S_{13} & S_{14} \\ S_{12} & S_{22} & S_{23} & -S_{14} \\ S_{13} & S_{23} & 0 & 0 \\ S_{14} & -S_{14} & 0 & 0 \end{bmatrix} \quad \dots(6.43)$$

- From unitary property,  $[S][S]^* = [I]$

i.e.,

$$\begin{bmatrix} S_{11} & S_{12} & S_{13} & S_{14} \\ S_{12} & S_{22} & S_{23} & -S_{14} \\ S_{13} & S_{23} & 0 & 0 \\ S_{14} & -S_{14} & 0 & 0 \end{bmatrix} \cdot \begin{bmatrix} S_{11}^* & S_{12}^* & S_{13}^* & S_{14}^* \\ S_{12}^* & S_{22}^* & S_{23}^* & -S_{14}^* \\ S_{13}^* & S_{23}^* & 0 & 0 \\ S_{14}^* & -S_{14}^* & 0 & 0 \end{bmatrix} = \begin{bmatrix} 1 & 0 & 0 & 0 \\ 0 & 1 & 0 & 0 \\ 0 & 0 & 1 & 0 \\ 0 & 0 & 0 & 1 \end{bmatrix}$$

$$R_1 C_1 : |S_{11}|^2 + |S_{12}|^2 + |S_{13}|^2 + |S_{14}|^2 = 1 \quad \dots(6.44)$$

$$R_2 C_2 : |S_{12}|^2 + |S_{22}|^2 + |S_{23}|^2 + |S_{14}|^2 = 1 \quad \dots(6.45)$$

## Cavity Resonators

...(6.46)

 $R_3 C_3$ :

$$|S_{13}|^2 + |S_{13}|^2 = 1 \quad \dots(6.46)$$

 $R_4 C_4$ :

$$|S_{14}|^2 + |S_{14}|^2 = 1 \quad \dots(6.47)$$

From Eq. 6.46 and Eq. 6.47,

$$S_{13} = \frac{1}{\sqrt{2}} \quad \dots(6.48)$$

$$S_{14} = \frac{1}{\sqrt{2}} \quad \dots(6.49)$$

Comparing Eqs. 6.44 and 6.45, we get

$$S_{11} = S_{22} \quad \dots(6.50)$$

Using these values from Eqs. 6.48 and 6.49 in Eq. 6.44, we get

$$|S_{11}|^2 + |S_{12}|^2 + \frac{1}{2} + \frac{1}{2} = 1$$

$$|S_{11}|^2 + |S_{12}|^2 = 0 \quad \dots(6.51)$$

$$S_{11} = S_{12} = 0 \quad \dots(6.52)$$

i.e.,

From Eq. 6.45,

$$S_{22} = 0$$

This means ports ① and ② are also perfectly matched to the junction. Hence in any four port junction, if any two ports are perfectly matched to the junction, then the remaining two ports are automatically matched to the junction. Such a junction where in all the four ports are perfectly matched to the junction is called a *Magic Tee*.

The  $[S]$  of Magic Tee is obtained by substituting the scattering parameters from Eqs. 6.48 to 6.52 in Eq. 6.43.

$$[S] = \begin{bmatrix} 0 & 0 & \frac{1}{\sqrt{2}} & \frac{1}{\sqrt{2}} \\ 0 & 0 & \frac{1}{\sqrt{2}} & -\frac{1}{\sqrt{2}} \\ \frac{1}{\sqrt{2}} & \frac{1}{\sqrt{2}} & 0 & 0 \\ \frac{1}{\sqrt{2}} & -\frac{1}{\sqrt{2}} & 0 & 0 \end{bmatrix} \quad \checkmark \quad \dots(6.53)$$

We know that,  $[b] = [S][a]$  (from Eq. 6.3)

i.e.,

$$\begin{bmatrix} b_1 \\ b_2 \\ b_3 \\ b_4 \end{bmatrix} = \begin{bmatrix} 0 & 0 & \frac{1}{\sqrt{2}} & \frac{1}{\sqrt{2}} \\ 0 & 0 & \frac{1}{\sqrt{2}} & -\frac{1}{\sqrt{2}} \\ \frac{1}{\sqrt{2}} & \frac{1}{\sqrt{2}} & 0 & 0 \\ \frac{1}{\sqrt{2}} & -\frac{1}{\sqrt{2}} & 0 & 0 \end{bmatrix} \begin{bmatrix} a_1 \\ a_2 \\ a_3 \\ a_4 \end{bmatrix}$$

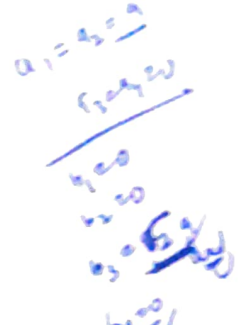
$$\left. \begin{array}{l} b_1 = \frac{1}{\sqrt{2}}(a_3 + a_4); \quad b_3 = \frac{1}{\sqrt{2}}(a_1 + a_2) \\ b_2 = \frac{1}{\sqrt{2}}(a_3 - a_4); \quad b_4 = \frac{1}{\sqrt{2}}(a_1 - a_2) \end{array} \right\} \quad \dots(6.54)$$

Using Eq. 6.54, we look at the properties of Magic Tee for some important cases.

**Case 1 :**  $a_3 \neq 0, a_1 = a_2 = a_4 = 0$

Substituting these in Eq. 6.54, we get

$$b_1 = \frac{a_3}{\sqrt{2}}; \quad b_2 = \frac{a_3}{\sqrt{2}}; \quad b_3 = b_4 = 0$$



This is the property of H-plane Tee.

**Case 2 :**  $a_4 \neq 0, a_1 = a_2 = a_3 = 0$

$$b_1 = \frac{a_4}{\sqrt{2}}; \quad b_2 = -\frac{a_4}{\sqrt{2}}; \quad b_3 = b_4 = 0$$

This is the property of E-plane Tee.

**Case 3 :**  $a_1 \neq 0, a_2 = a_3 = a_4 = 0$

$$b_1 = 0; \quad b_2 = 0; \quad b_3 = \frac{a_1}{\sqrt{2}}; \quad b_4 = \frac{a_1}{\sqrt{2}}$$

i.e., when power is fed into port ①, nothing comes out of port ② even though they are collinear ports (Magic !!). Hence ports ① and ② are called *isolated ports*. Similarly an input at port ③ cannot come out at port ①. Similarly E and H ports are isolated ports.

**Case 4 :**  $a_3 = a_4, a_1 = a_2 = 0$

$$\text{Then } b_1 = \frac{1}{\sqrt{2}}(2a_3); \quad b_2 = 0, \quad b_3 = b_4 = 0$$

This is nothing but the additive property. Equal inputs at ports ③ and ④ result in an output at port ① (in phase and equal in amplitude).

**Case 5 :**  $a_1 = a_2, a_3 = a_4 = 0;$

$$b_1 = 0 = b_2 = b_4; \quad b_3 = \frac{1}{\sqrt{2}}(2a_1)$$

that is equal inputs at ports ① and ② results in an output at port ③ (additive property) and no outputs at ports ①, ② and ④. This is similar to case 4.

### ~~6.3.4 Applications of Magic Tee~~

A magic Tee has several applications. A few of them have been discussed here.

(a) **Measurement of Impedance** : A magic Tee has been used in the form of a bridge, as shown in Fig. 6.9 for measuring impedance.

Microwave source is connected in arm ③ and a null detector in arm ④. The unknown impedance is connected in arm ② and a standard variable known impedance in arm ①. Using the properties

of Magic Tee, the power from microwave source ( $a_3$ ) gets divided equally between arms ① and ② ( $\frac{a_3}{\sqrt{2}}$ ) (to the unknown impedance and standard variable impedances). These impedances are not equal to characteristic impedance  $Z_0$  and hence there will be reflections from arms ① and ②. If  $\rho_1$  and  $\rho_2$  are the reflection coefficients, powers  $\frac{\rho_1 a_3}{\sqrt{2}}$  and  $\frac{\rho_2 a_3}{\sqrt{2}}$  enter the Magic Tee junction from arms ① and ② as shown in Fig. 6.9. The resultant wave into arm ④ i.e., the null detector can be calculated as follows :

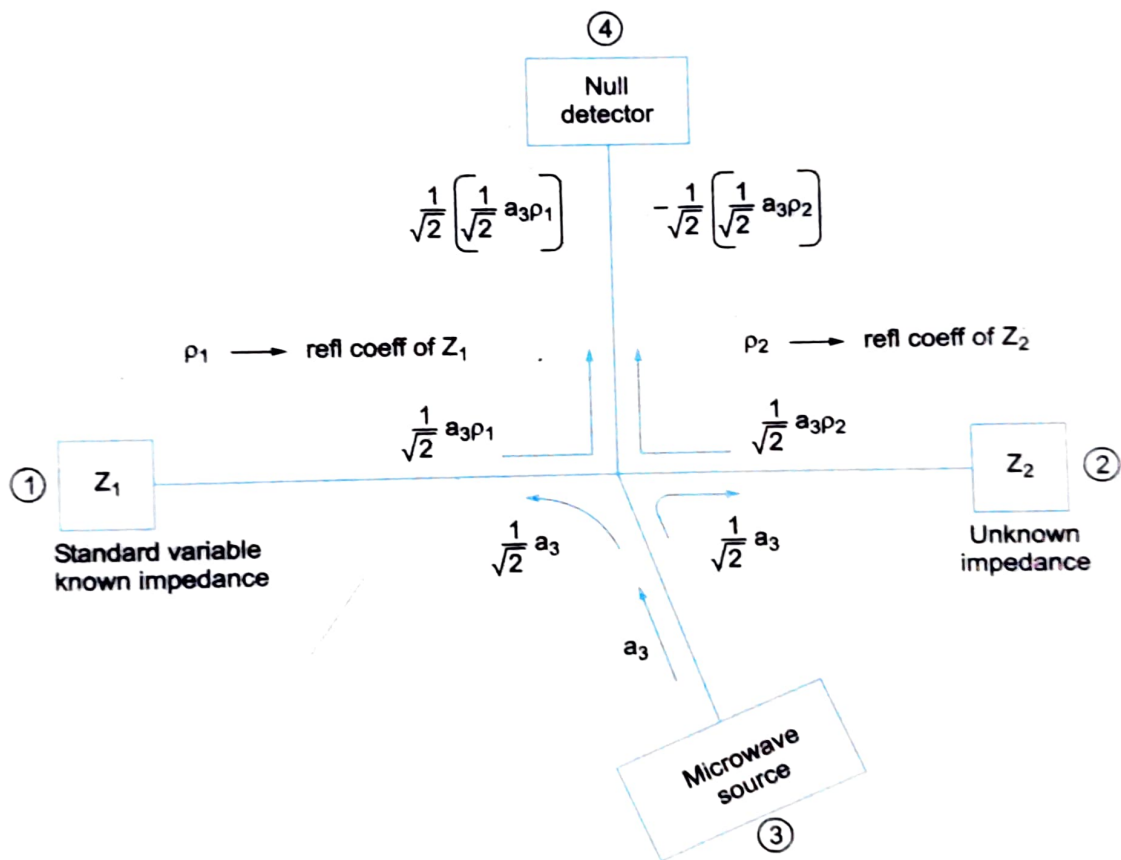


Fig. 6.9 Magic Tee for measurement of impedances.

The net wave reaching the null detector (Refer Fig. 6.9)

$$= \frac{1}{\sqrt{2}} \left( \frac{1}{\sqrt{2}} a_3 \rho_1 \right) - \frac{1}{\sqrt{2}} \left( \frac{1}{\sqrt{2}} a_3 \rho_2 \right) = \frac{1}{2} a_3 (\rho_1 - \rho_2) \quad \dots(6.55)$$

For perfect balancing of the bridge (null detection) Eq. 6.55 is equated to zero.

i.e.,

$$\frac{1}{2} a_3 (\rho_1 - \rho_2) = 0$$

or

$$\rho_1 - \rho_2 = 0 \quad \text{or} \quad \rho_1 = \rho_2$$

or

$$\frac{Z_1 + Z_2}{Z_1 - Z_2} = \frac{Z_3 + Z_4}{Z_3 - Z_4}$$

$$Z_1 = Z_2$$

i.e.,

$$R_1 + jX_1 = R_2 + jX_2$$

or

$$R_1 = R_2 \text{ and } X_1 = X_2.$$

Thus the unknown impedance can be measured by adjusting the standard variable impedance till the bridge is balanced and both impedances become equal.

**(b) Magic Tee as a Duplexer:** The transmitter and receiver are connected in ports ② and ① respectively, antenna in the E-arm or port ④ and port ③ of Magic Tee is terminated in a matched load as shown in Fig. 6.10. During transmission half the power reaches the antenna from where it is radiated into space. Other half reaches the matched load where it is absorbed without reflections. No transmitter power reaches the receiver since port ① and ② are isolated ports in a Magic Tee. During reception, half of the received power goes to the receiver and the other half to the transmitter are isolated during reception as well as during transmission.

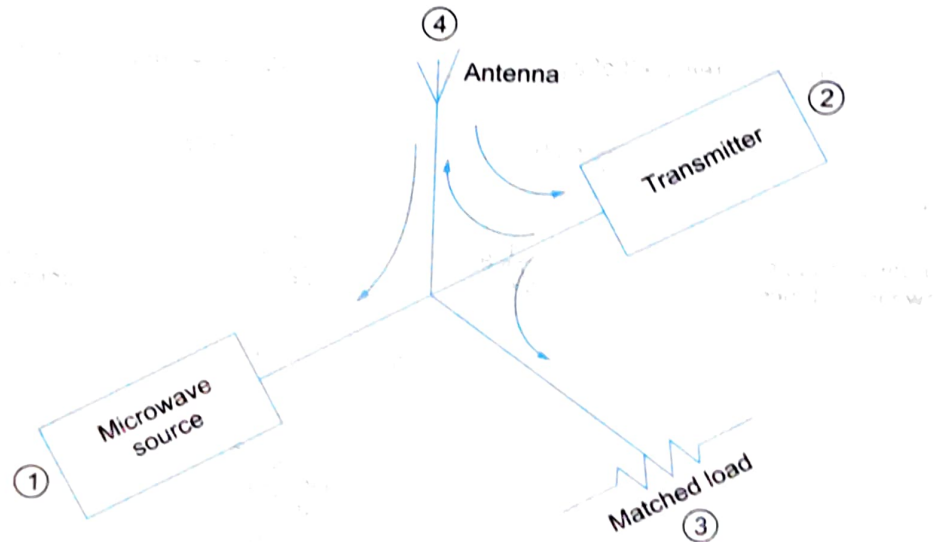


Fig. 6.10 Magic Tee as a Duplexer

**(c) Magic Tee as a Mixer:** A magic Tee can also be used in microwave receivers as a mixer where the signal and local oscillator are fed into the E and H arms as shown in Fig. 6.11.

Half of the local oscillator power and half of the received power from antenna goes to the mixer where they are mixed to generate the IF frequency.

$$IF = f_m \sim f_o$$

Magic Tee has many other applications such as a microwave discriminator, microwave bridge etc.

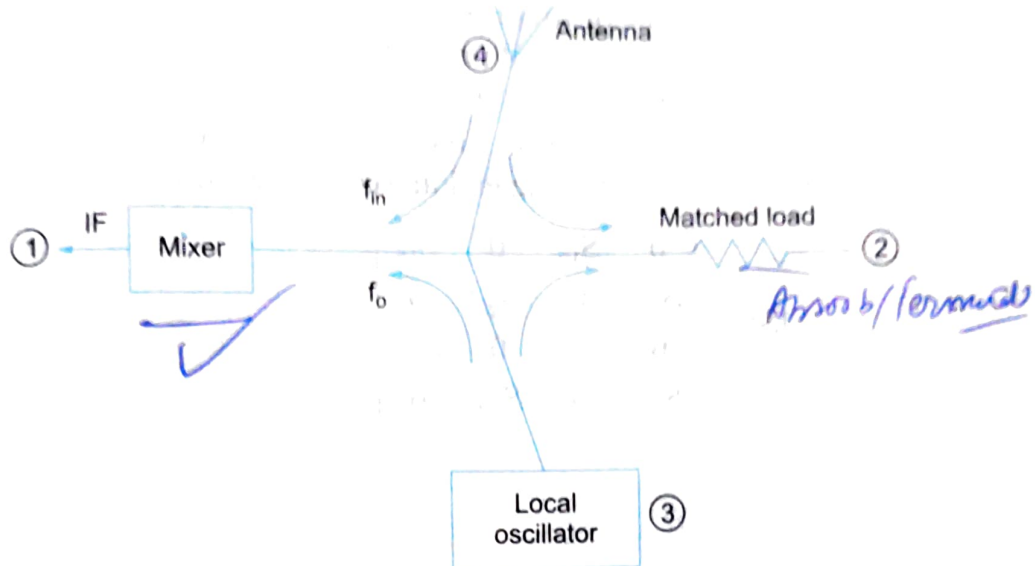


Fig. 6.11 Magic Tee as a mixer.

### ~~6.3.5 Rat race junction~~

This is a four port junction, the fourth port being added to a normal three port Tee. A typical rat race junction is shown in Fig. 6.12.

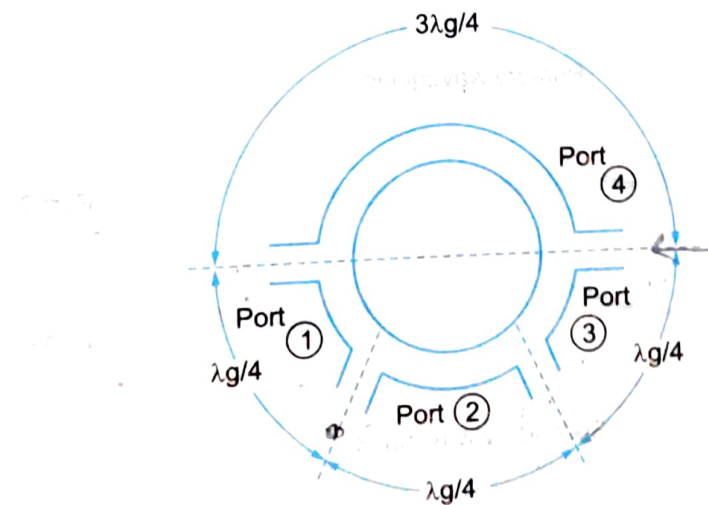


Fig. 6.12 Rat-race ring.

The four arms/ports are connected in the form of an angular ring at proper intervals by means of series (or parallel) junctions. These ports are separated by proper electrical lengths to sustain standing waves. For proper operation, it is necessary that the mean circumference of the total race be  $1.5 \lambda_g$  and that each of the four ports be separated from its neighbour by a distance of  $\lambda_g/4$ .

When power is fed into port ① it splits equally (in clockwise and anticlockwise directions) into ports ② and ④ and nothing enters port ③. At ports ② and ④ the powers combine in phase but at port ③ cancellation occurs due to  $\lambda_g/2$  path difference. For similar reasons any input applied at port ③ is equally divided between ports ② and ④ but the output at port ① will be zero. The rat race can

also be used for combining two signals or dividing a single signal into two equal halves. If two unequal signals are applied at port ①, an output proportional to their sum will emerge from ports ② and ④ while a differential output will appear at port ③.

The scattering matrix of a rat race junction (also called hybrid junction) can be written as shown below in ideal conditions (*i.e.*, neglecting leakage coupling values).

$$[S] = \begin{bmatrix} 0 & S_{12} & 0 & S_{14} \\ S_{21} & 0 & S_{23} & 0 \\ 0 & S_{32} & 0 & S_{34} \\ S_{41} & 0 & S_{43} & 0 \end{bmatrix} \quad \dots(6.56)$$

## 6.4 DIRECTIONAL COUPLERS

Directional couplers are flanged, built in waveguide assemblies which can sample a small amount of microwave power for measurement purposes. They can be designed to measure incident and/or reflected powers, SWR (standing Wave Ratio) values, provide a signal path to a receiver or perform other desirable operations. They can be unidirectional (measuring only incident power) or bi-directional (measuring both incident and reflected) powers. In its most common form, the directional coupler is a four port waveguide junction consisting of a primary main waveguide and a secondary auxiliary waveguide as shown in Fig. 6.13(a).

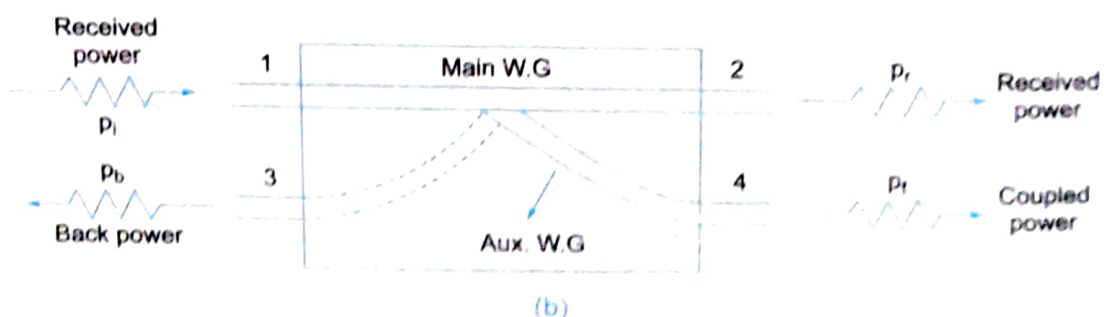
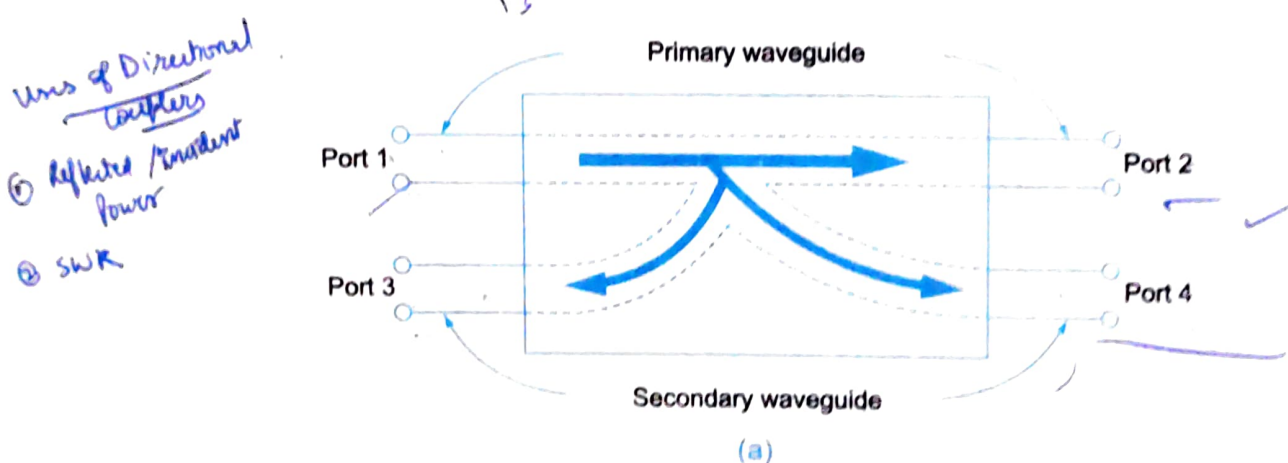


Fig. 6.13 (a) A schematic of a directional coupler (b) Directional coupler indicating powers

With matched terminations at all its ports, the properties of an ideal directional coupler can be summarized as follows.

1. A portion of power travelling from port ① to port ② is coupled to port ④ but not to port ③.
2. A portion of power travelling from port ② to port ① is coupled to port ③ but not to port ④ (bidirectional case).
3. A portion of power incident on port ③ is coupled to port ② but not to port ① and a portion of the power incident on port ④ is coupled to port ① but not to port ②. Also ports ① and ③ are decoupled as are ports ② and ④.

A small portion of input power at port ① is coupled to port ④ so that measurement of this small power is possible. Ideally no power should come out of port ③. Fig. 6.13b indicates the various input/output powers.

$P_i$  = incident power at port ①.

$P_r$  = received power at port ②.

$P_f$  = forward coupled power at port ④.

$P_b$  = back power at port ③.

The performance of a directional coupler is usually defined in terms of two parameters which are defined as follows.

**Coupling Factor C:** The coupling factor of a directional coupler (D.C.) is defined as the ratio of the incident power ' $P_i$ ' to the forward power ' $P_f$ ' measured in dB.

i.e.,

$$C = 10 \log_{10} \frac{P_i}{P_f} \text{ dB} \quad \dots(6.57)$$

**Directivity D:** The directivity of a D.C. is defined as the ratio of forward power ' $P_f$ ' to the back power ' $P_b$ ' expressed in dB.

i.e.,

$$D = 10 \log_{10} \frac{P_f}{P_b} \text{ dB} \quad \dots(6.58)$$

For a typical D.C.

$$C = 20 \text{ dB}, D = 60 \text{ dB}$$

i.e.,

$$C = 20 = 10 \log \frac{P_i}{P_f}$$

$$\therefore \frac{P_i}{P_f} = 10^2 = 100$$

or

$$P_f = \frac{P_i}{100}$$

Also,

$$D = 60 = 10 \log \frac{P_f}{P_b}$$

$$\therefore \frac{P_f}{P_b} = 10^6$$

*Coupling factor* is how much 1/P lower is being sampled  
*Directivity* is how well the coupler distinguishes between  
 forward & backward Traveling Power

or

$$P_b = \frac{P_f}{10^6} = \frac{P_i}{10^8} \quad \left( \text{since } P_f = \frac{P_i}{100} \right)$$

Since  $P_b$  is very small,  $\left(\frac{1}{10^8}\right) P_i$ , the power coming out of port ③ can be neglected.

The *Coupling factor* is a measure of how much of the incident power is being sampled while *directivity* is a measure of how well the directional coupler distinguishes between the forward and reverse traveling powers.

*Isolation*: Another parameter called *Isolation* is sometimes defined to describe the directive properties of a directional coupler. It is defined as the ratio of the incident power  $P_i$  to the back power  $P_b$  expressed in dB.

$$I = 10 \log_{10} \frac{P_i}{P_b} \text{ dB}$$

~~CD = I~~ ... (6.59)

It may be noted that isolation in dB equals coupling factor plus directivity.

In addition to the above parameters the *SWR*, frequency range and transmission loss are also specified for a directional coupler. Low *SWR* ensures minimum mismatch errors, wide frequency range eliminates the need for several octave band couplers to cover the broad band range and minimum transmission loss for significant power availability for measurement set up.

There are several types of directional couplers that have been developed like Two hole crossed guide couplers with common broad wall-sections (Fig. 6.14), branching guide couplers with a common wall instead of coupling holes (Fig. 6.15), short slot couplers (Fig. 6.16), bifurcated couplers (Fig. 6.17), loop directional coupler (Fig. 6.18), couplers made from parallel ground plane, metallic strips running internally within the waveguide structure.

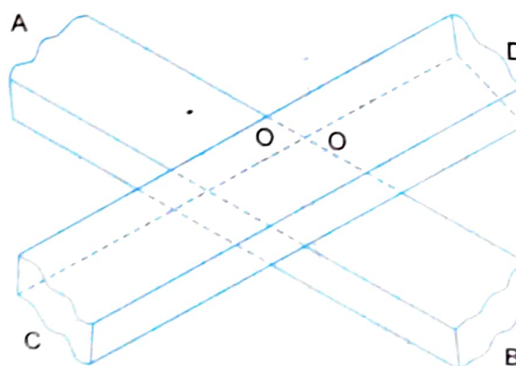


Fig. 6.14 Two hole crossguide coupler.

It may be noted that in most of the directional couplers only three of the four ports are used, the unwanted port is normally terminated in a matched load built into it. The two waveguides (primary and secondary) share a common wall. This common wall has got hole or holes for coupling the energy flowing into the main waveguide to the side waveguide and hence called a side hole coupler. A two hole directional coupler is most commonly used.

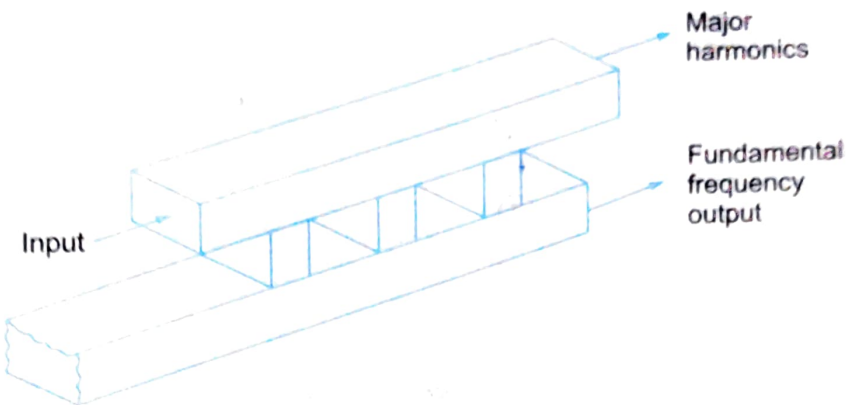


Fig. 6.15 Two hole branching guide coupler.

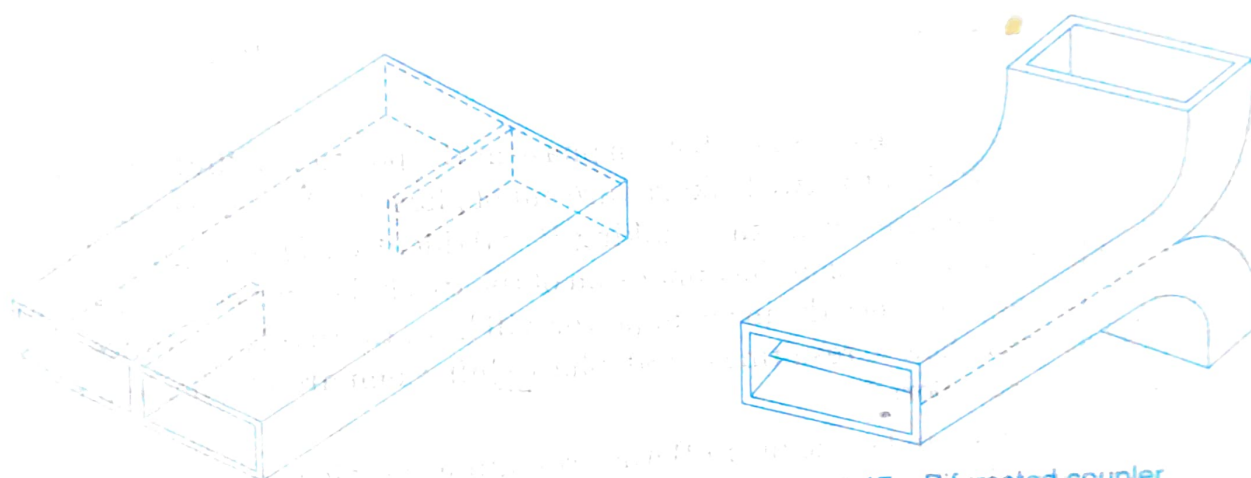


Fig. 6.16 Short-slot coupler.

Fig. 6.17 Bifurcated coupler.

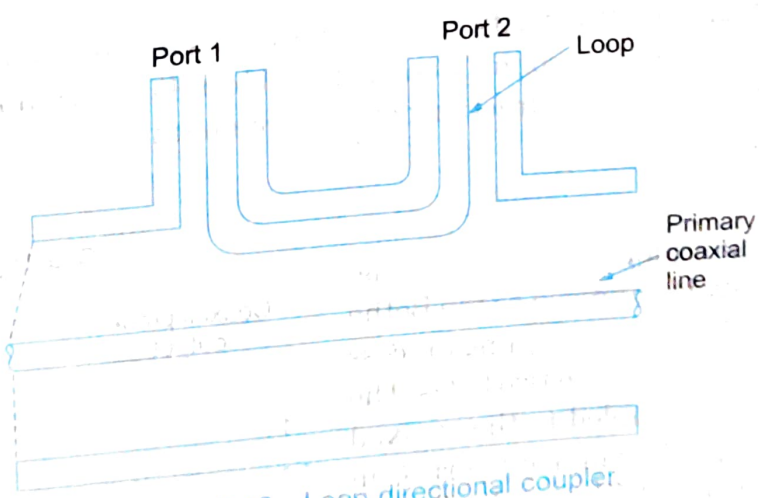


Fig. 6.18 Loop directional coupler.

### ~~11~~ Two-hole Directional Coupler

The principle of operation of a two-hole directional coupler is shown in Fig. 6.19. It consists of two guides the main and the auxiliary with two tiny holes common between them as shown. The two holes are at a distance of  $\lambda_g/4$  where  $\lambda_g$  is the guide wavelength.

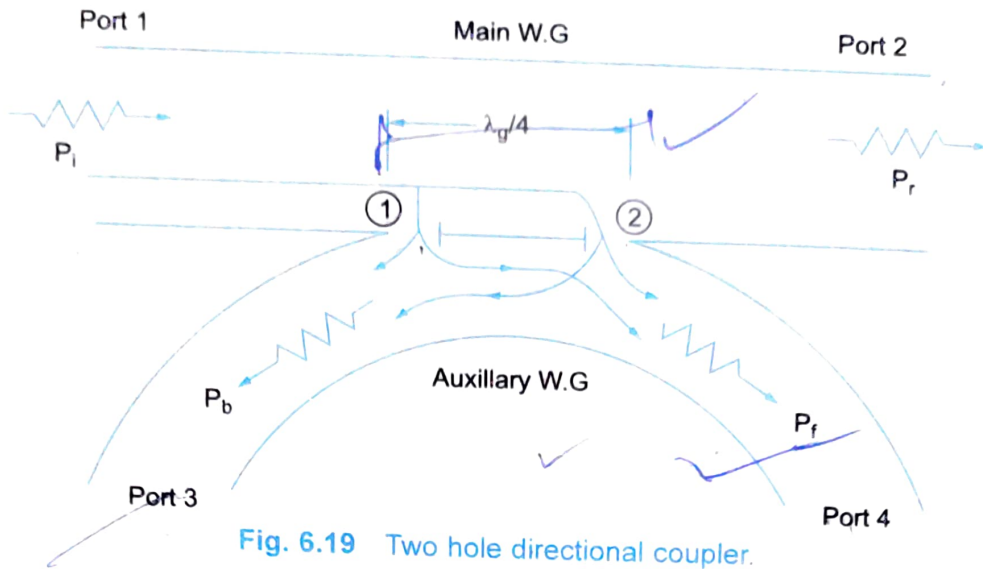


Fig. 6.19 Two hole directional coupler.

The two leakages out of holes ① and ② both in phase at the position of 2nd hole and hence they add up contributing to  $P_f$ . But the two leakages are out of phase by  $180^\circ$  at the position of the 1st hole and therefore they cancel each other making  $P_b = 0$  (ideally). The magnitude of the power coming out of 2 holes depends upon the dimension of the two holes. Since the distance between holes is  $\lambda_g/4$ ,  $P_b$  is made '0' (since the incident power will have to travel a distance of  $(\lambda_g/4 + \lambda_g/4)$  when it comes back from hole ② resulting in  $180^\circ$  phase shift. Compared to incident power leakage through hole ① entering port ③).

The number of holes can be one (as in Bethe crossguide coupler) or more than two (as in a Multi-hole coupler). The degree of coupling is determined by size and location of the holes in the waveguide walls.

Although a high degree of directivity can be achieved as a fixed frequency, it is quite difficult over a band of frequencies. In this connection, it should be realized that the frequency determines the separation of the two holes as a fraction of the wavelength.

#### 6.4.2 Bethe or Single-hole Coupler

A single-hole directional coupler is shown in Fig. 6.20. Here the directivity is improved as the Bethe coupler relies on a single hole for coupling process rather than the separation between two holes. The power entering port ① is coupled to the co-axial probe output and the power entering port ② is absorbed by the matched load. The auxiliary guide is placed at such an angle that the magnitude of the magnetically excited wave is made equal to that of the electrically excited wave for improved directivity. In this coupler, the waves in the auxiliary guide are generated through a single hole which includes both electric and magnetic fields. Because of the phase relationships involved in the coupling process, the signals generated by the two types of coupling cancel in the forward direction and reinforce in the reverse direction.

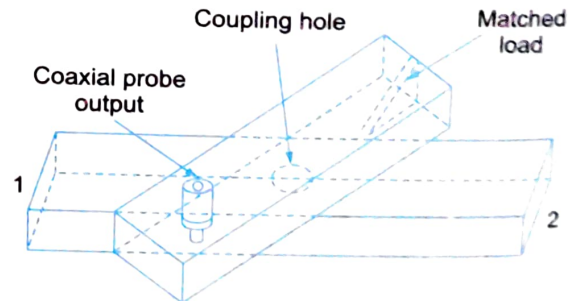


Fig. 6.20 Bethe or single-hole coupler

### 6.4.3 Scattering Matrix of a Directional Coupler

We use the properties of the directional coupler to arrive at the  $[S]$  matrix.

1. Directional coupler is a four port network. Hence  $[S]$  is a  $4 \times 4$  matrix.

$$\text{i.e., } [S] = \begin{bmatrix} S_{11} & S_{12} & S_{13} & S_{14} \\ S_{21} & S_{22} & S_{23} & S_{24} \\ S_{31} & S_{32} & S_{33} & S_{34} \\ S_{41} & S_{42} & S_{43} & S_{44} \end{bmatrix} \quad \dots(6.60)$$

2. In a directional coupler all four ports are perfectly matched to the junction. Hence the diagonal elements are zero.

$$\text{i.e., } S_{11} = S_{22} = S_{33} = S_{44} = 0 \quad \dots(6.61)$$

3. From symmetric property,  $S_{ij} = S_{ji}$

$$\begin{aligned} S_{23} &= S_{32}; S_{13} = S_{31}; S_{24} = S_{42}; \\ S_{34} &= S_{43}; S_{41} = S_{14}; \end{aligned} \quad \dots(6.62)$$

Ideally back power is zero ( $P_b = 0$ ) i.e., There is no coupling between port ① and port ②

$$\therefore S_{13} = S_{31} = 0 \quad \dots(6.63)$$

4. Also there is no coupling between port ② and port ④

$$\therefore S_{24} = S_{42} = 0 \quad \dots(6.64)$$

Substituting in Eq. 6.55, the values of scattering parameters as per Eqs. 6.56 to 6.59, we get

$$[S] = \begin{bmatrix} 0 & S_{12} & 0 & S_{14} \\ S_{12} & 0 & S_{23} & 0 \\ 0 & S_{23} & 0 & S_{34} \\ S_{14} & 0 & S_{34} & 0 \end{bmatrix} \quad \dots(6.65)$$

5. Since  $[S][S^*] = I$ , we get

$$\begin{bmatrix} 0 & S_{12} & 0 & S_{14} \\ S_{12} & 0 & S_{23} & 0 \\ 0 & S_{23} & 0 & S_{34} \\ S_{14} & 0 & S_{34} & 0 \end{bmatrix} \begin{bmatrix} 0 & S_{12}^* & 0 & S_{14}^* \\ S_{12}^* & 0 & S_{23}^* & 0 \\ 0 & S_{23}^* & 0 & S_{34}^* \\ S_{14}^* & 0 & S_{34}^* & 0 \end{bmatrix} = \begin{bmatrix} 1 & 0 & 0 & 0 \\ 0 & 1 & 0 & 0 \\ 0 & 0 & 1 & 0 \\ 0 & 0 & 0 & 1 \end{bmatrix}$$

$$R_1 C_1 : |S_{12}|^2 + |S_{14}|^2 = 1 \quad \dots(6.66)$$

$$R_2 C_2 : |S_{12}|^2 + |S_{23}|^2 = 1 \quad \dots(6.67)$$

$$R_3 C_3 : |S_{23}|^2 + |S_{34}|^2 = 1 \quad \dots(6.68)$$

$$R_1 C_3 : S_{12} S_{23}^* + S_{14} S_{34}^* = 0 \quad \dots(6.69)$$

Comparing Eq. 6.61 and 6.62,

$$S_{14} = S_{23} \quad \dots(6.70)$$

Comparing Eq. 6.62 and 6.63,

$$S_{12} = S_{34} \quad \dots(6.71)$$

Let us assume that  $S_{12}$  is real and positive = 'P'

$$S_{12} = S_{34} = P = S_{34}^* \quad \dots(6.72)$$

From Eqs. 6.69 and 6.72,

$$PS_{23}^* + S_{23}P = 0$$

$$P[S_{23} + S_{23}^*] = 0$$

Since,

$$P \neq 0, S_{23} + S_{23}^* = 0$$

$$S_{23} = jy$$

$$S_{23}^* = -jy$$

i.e.,  $S_{23}$  must be imaginary.

Let

$$S_{23} = jq = S_{14} \quad \dots(6.73)$$

Therefore,

$$S_{12} = S_{34} = P \quad \text{(transmission parameter)}$$

and

$$S_{23} = S_{14} = jq. \quad \text{Also, } P^2 + q^2 = 1$$

Substituting these values in Eq. 6.65, [S] matrix of a directional coupler is reduced to

$$[S] = \begin{bmatrix} 0 & P & 0 & jq \\ P & 0 & jq & 0 \\ 0 & jq & 0 & P \\ jq & 0 & P & 0 \end{bmatrix} \quad \dots(6.74)$$

## 6.5 WAVEGUIDE JOINTS

It is not possible to build a waveguide system in one piece and may require several sections connected by joints. These are the waveguide joints and must be constructed in such a way that a good connection is made between any two sections of a waveguide without any irregularities and without affecting the **E** and **H**-field patterns. Irregularities in a joint cause reflection effects, create standing waves and increase the attenuation. A rotating joint could be required as in a radar system where the transmitter/receiver is stationary and the antenna system is revolving.

There are several types of waveguide joints. Some of them are shown in Fig. 6.21. The semipermanent butt joints, a bolted flange (Fig. 6.20a) consists of two sections bolted together with a gasket to exclude moisture. For perfect mechanical alignment, it should be ensured that there are no bends or discontinuities and the ends of the waveguides and flanges must have mirror smooth finish to avoid reflection effects.

Figure 6.21b shows a quarter wavelength flange joint which uses no mechanical connection and an open circuit at point *B* creates a short circuit at point *A* due to the standing wave distribution between these points. The field patterns are not disturbed and no discontinuity exists but there is a possible leakage of energy through the open flange.

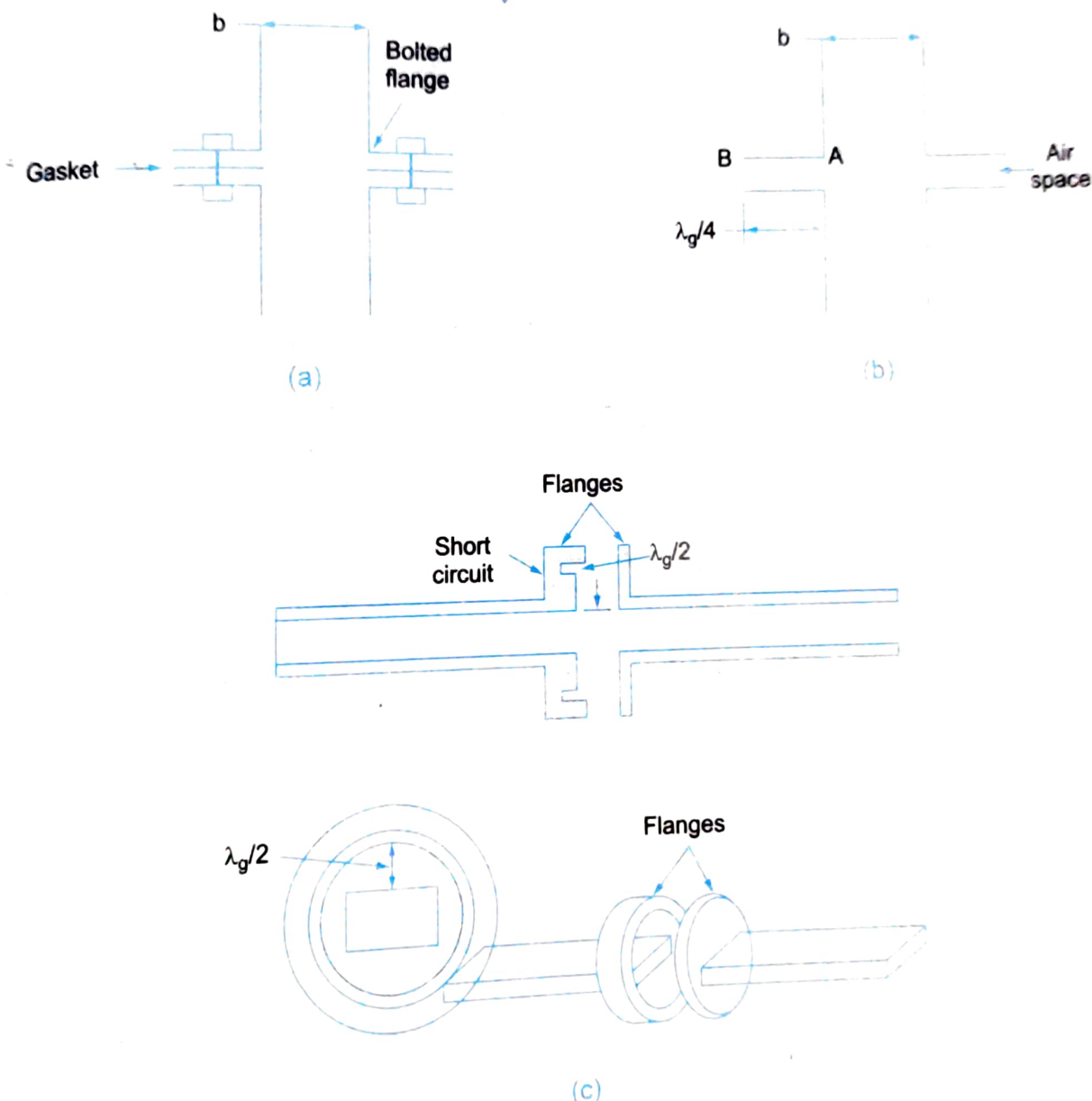
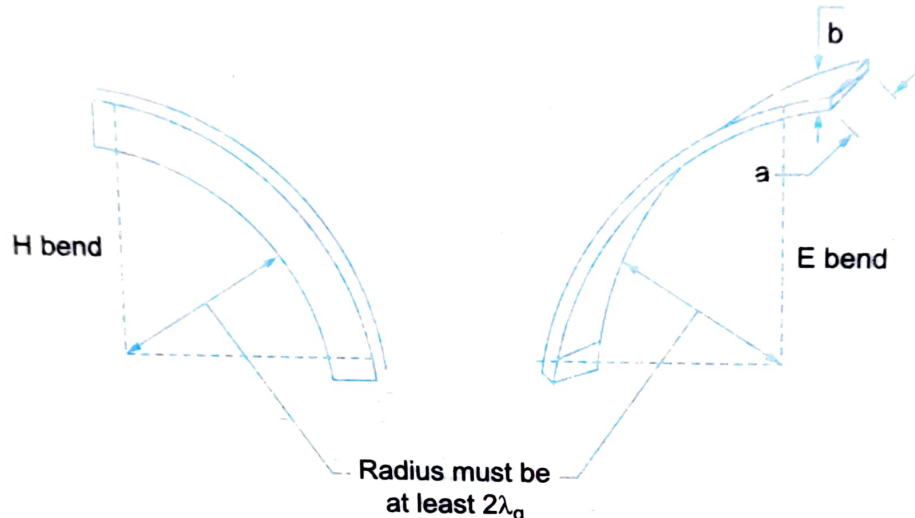


Fig. 6.21 (a) Bolted flange (b)  $\lambda_g/4$  Flange joint (c) Choke joint

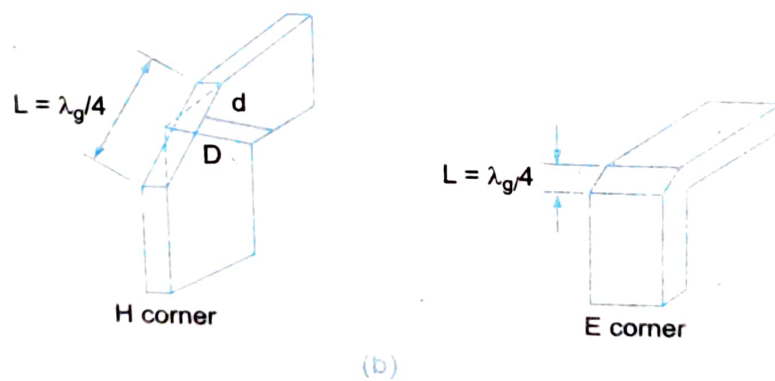
The choke joint (Fig. 6.21c) is superior to butt joint and is very widely used. It consists of flanges that are connected to the waveguide at its center. The right side flange is flat and the left side one is slotted,  $\lambda_g/4$  deep from the inner surface of the waveguide. This is positioned at a distance of  $\lambda_g/4$  from the point where the flanges are joined. Due to the  $\lambda_g/2$  length taken together, a short circuit is created at the place where the walls are joined together resulting in an electrical short. Mechanically they are separated by as much as one tenth of a wavelength and the area can be sealed with a rubber gasket for avoiding moisture.

Waveguide bend, corner and twist are shown in Fig. 6.22. These components are useful for changing the direction of the guide by a desired angle.

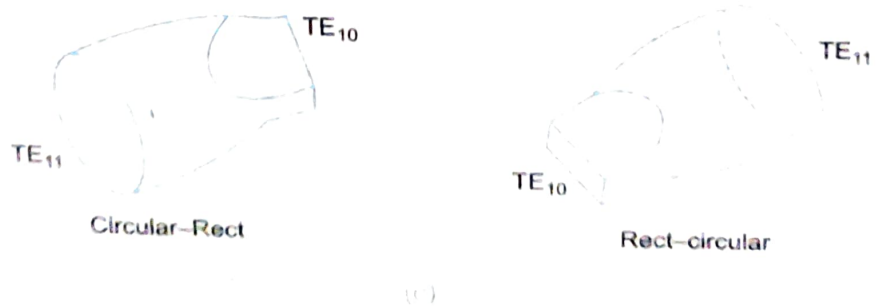
The bends can be *H* bend or *E* bend (Fig. 6.22a). If the bend is in the direction of the wide dimension the *H* lines are affected (*H* bend) and if the bend is in the direction of narrow dimension, the *E* lines are affected (*E* bend). The bending radius must be at least  $2\lambda_g$  to avoid SWR's greater than 1.05 and mean length as long as possible. ( $R_{\min} = 1.5 b$  an *E* bend and  $R_{\min} = 1.5 a$  for an *H* bend)



(a)



(b)



(c)

226

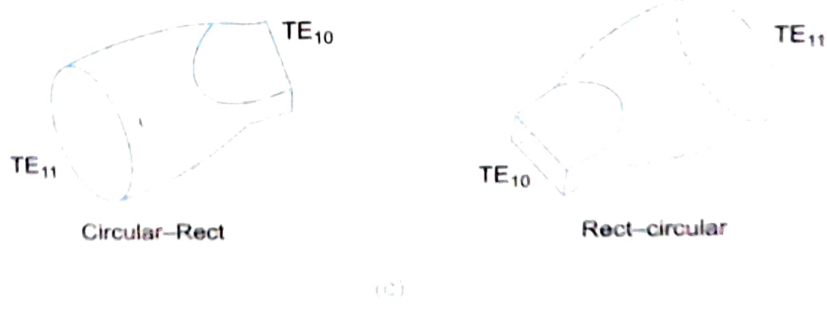
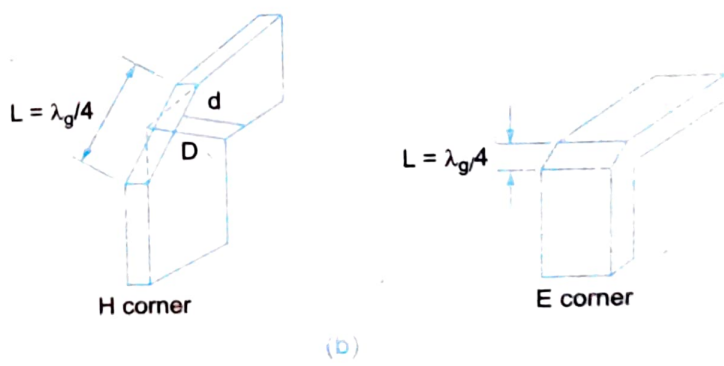
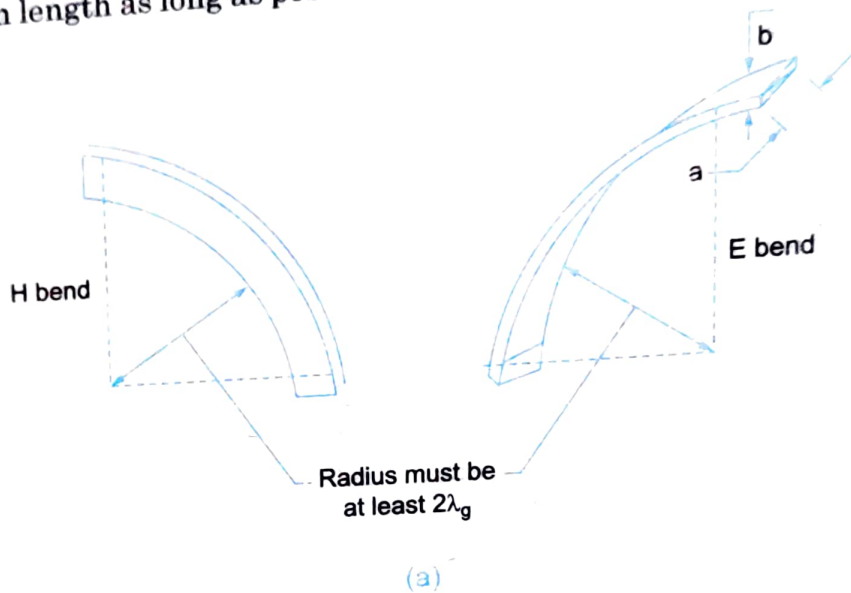
*Short note*

## 6.6

## WAVEGUIDE BENDS, CORNERS, TRANSITIONS AND TWISTS

Waveguide bend, corner and twist are shown in Fig. 6.22. These components are useful for changing the direction of the guide by a desired angle.

The bends can be *H* bend or *E* bend (Fig. 6.22a). If the bend is in the direction of the wide dimension the *H* lines are affected (*H* bend) and if the bend is in the direction of narrow dimension, the *E* lines are affected (*E* bend). The bending radius must be at least  $2\lambda_g$  to avoid SWR's greater than 1.05 and mean length as long as possible. ( $R_{\min} = 1.5 b$  an *E* bend and  $R_{\min} = 1.5 a$  for an *H*



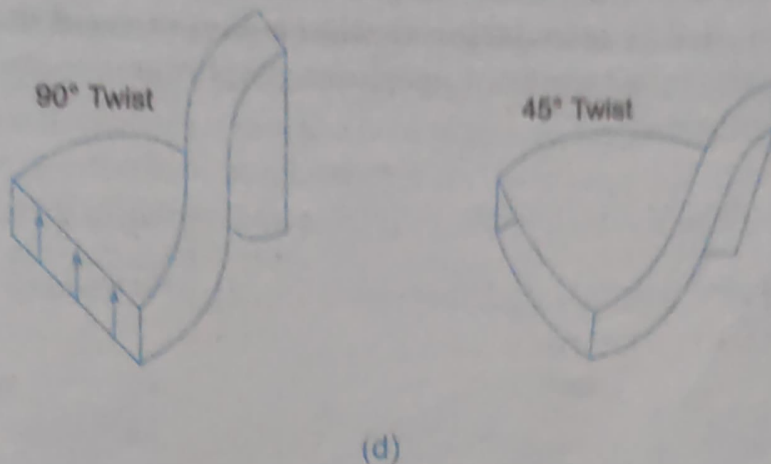


Fig. 6.22 (a) H bend and E bend, (b) H-plane corner and E-plane corner, (c) Circular to rectangular and rectangular to circular transitions (Tapers) (d) 90° twist and 45° twists.

bend for small reflections). Sharp 90° bends create total reflection resulting in infinite SWR. Therefore bends have to be gradual.

At lower frequencies a bend may have to be very long and in such cases, a corner would be preferred. A mitered 90° bend (shown in Fig. 6.22b) is a corner.

Mitered bends or corners are normally H-plane corners where  $d = 0.65 D$  as shown in Fig. 6.21c. Smaller values of  $d$  in a E-plane corner have the danger of arcing and hence not common. In order to minimise the reflections, the mean length  $L$  must be an odd number of quarter wavelength, so that reflected wave from both ends of the waveguide are completely cancelled.

$$\text{i.e., } L = (2n + 1) \frac{\lambda_g}{4} \text{ where } n = 0, 1, 2, \dots$$

Flexible waveguides are special bends that are made of ribbon brass which are edge interlocked so that the internal dimensions are preserved in any angular position. The exterior of such waveguides is coated with rubber to avoid dangers of oxidation and humidity.

Figure 6.21e shows waveguide transitions or tapers. These are required whenever it is required to join two waveguide sections that have different shapes for their cross-sectional areas. For example a circular to rectangular waveguide transition has a gradual taper that extends over a distance of more than  $2\lambda_g$ . Similarly rectangular to circular transition is also possible. If the circular waveguide carries the  $TE_{11}$  mode the rectangular waveguide will operate in the dominant  $TE_{10}$  mode and vice-versa. We can also have two rectangular waveguide tapers of different dimensions provided that there is a match between their characteristic impedances.

Waveguide twists such as 90° and 45° twists shown in Fig. 6.21d are helpful in converting vertical to horizontal polarizations or vice-versa. Twists can be incorporated along with bends also.

## 6.7 WAVEGUIDE IRISES

In any waveguide system, when there is a mismatch there will be reflections. In transmission lines, in order to overcome this mismatch lumped impedances or stubs of required value are placed at precalculated points. In waveguides too, some discontinuities are made use of for matching

purposes. Any susceptance appearing across the guide, causing mismatch (and production of standing waves) needs to be cancelled by introducing another susceptance of the same magnitude but of opposite nature. Irises (also called windows, apertures, diaphragms or obstacles) shown in Fig. 6.23 are made use of for the purpose.

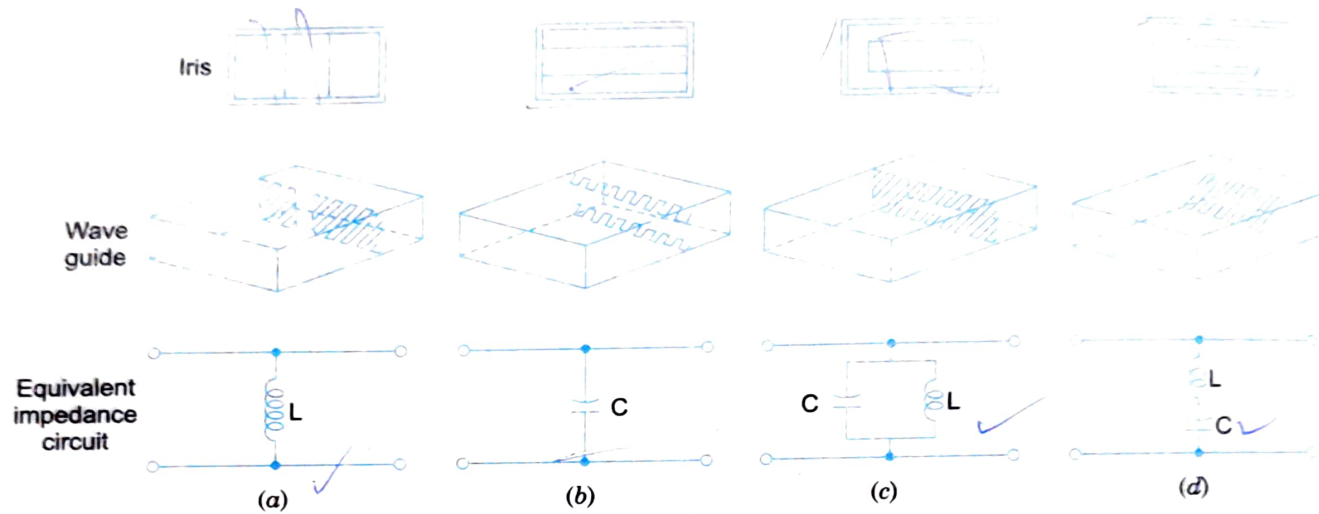


Fig. 6.23 Waveguide irises.

An inductive iris (Fig. 6.23a) allows a current to flow where none flowed before. The iris is placed in a position where the magnetic field is strong (or where electric field is relatively weak). Since the plane of polarisation of electric field is parallel to the plane of iris, the current flow due to iris causes a magnetic field to be set up. Energy storage of magnetic field takes place and there is an increase in inductance at that point of the waveguide.

In capacitive iris (Fig. 6.23b), it is seen that the potential which existed between the top and bottom walls of the waveguide now exists between surfaces which are closer and therefore the capacitance has increased at that point. The capacitive iris is placed in a position where the electric field is strong.

The inductive and capacitive irises if combined suitably (correctly shaped and positioned) the inductive and capacitive reactances introduced will be equal and the iris becomes a parallel resonant circuit (Fig. 6.23c). For the dominant mode, the iris presents a high impedance and the shunting effect for this mode will be negligible. Other modes are completely attenuated and the resonant iris acts as a band pass filter to suppress unwanted modes.

Figure 6.23d, shows a series resonant iris which is supported by a non-metallic material and is transpresent to the flow of microwave energy.

## 6.11 FERRITE DEVICES

Ferrites are non-metallic materials with resistivities ( $\rho$ ) nearly  $10^{14}$  times greater than metals and with dielectric constants ( $\epsilon_r$ ) around 10–15 and relative permeabilities of the order of 1000. They have magnetic properties similar to those of ferrous metals. They are oxide based compounds having general composition of the form  $\text{MeO} \cdot \text{Fe}_2\text{O}_3$  i.e., a mixture of a metallic and ferric oxide where  $\text{MeO}$  represents any divalent metallic oxide such as  $\text{MnO}$ ,  $\text{ZnO}$ ,  $\text{CdO}$ ,  $\text{NiO}$  or a mixture of these. They are obtained by firing powdered oxides of materials at  $1100^\circ\text{C}$  or more and pressing them into different shapes. This processing gives them the added characteristics of ceramic insulators so that they can be used at microwave frequencies.

Ferrites have atoms with large number of spinning electrons resulting in strong magnetic properties. These magnetic properties are due to the magnetic dipole moment associated with the electron spin. Because of the above properties, ferrites find application in a number of microwave devices to reduce reflected power, for modulation purposes and in switching circuits. Because of high resistivity they can be used upto 100 GHz.

Ferrites have one more peculiar property which is useful at microwave frequencies i.e., the non-reciprocal property. When two circularly polarised waves one rotating clockwise and other anticlockwise are made to propagate through ferrite, the material reacts differently to the two rotating fields, thereby presenting different effective permeabilities to both the waves. i.e.,  $\epsilon_{r1}, \mu_{r1}, \rho_1$  for left circularly polarised wave and  $\epsilon_{r2}, \mu_{r2}, \rho_2$  for the right circularly polarised wave.

### Faraday Rotation in Ferrites

Consider an infinite lossless medium. A static field  $B_o$  is applied along the  $z$ -direction. A plane TEM wave that is linearly polarised along the  $x$ -axis at  $t = 0$  is made to propagate through the ferrite in the  $z$ -direction. The plane of polarisation of this wave will rotate with distance, a phenomenon known as *Faraday Rotation*.

Any linearly polarised wave can be regarded as the vector sum of two counter rotating circularly polarised wave ( $E_0/2$  vectors shown in Fig. 6.30). The ferrite material offers different characteristics to these waves, with the result that the phase change for one wave is larger than the other wave resulting in rotation ' $\theta$ ' of the linearly polarized wave, at  $z = l$ .

It is observed that a rotation of 100 degrees or more per cm of ferrite length is typical for ferrites at a frequency of 10 GHz. If the direction of propagation is reversed, the plane of polarisation continues to rotate in the same direction i.e.,  $z = l$  to  $z = 0$ , the wave will arrive back at  $z = 0$  polarised at an angle  $2\theta$  relative to  $x$ -axis.

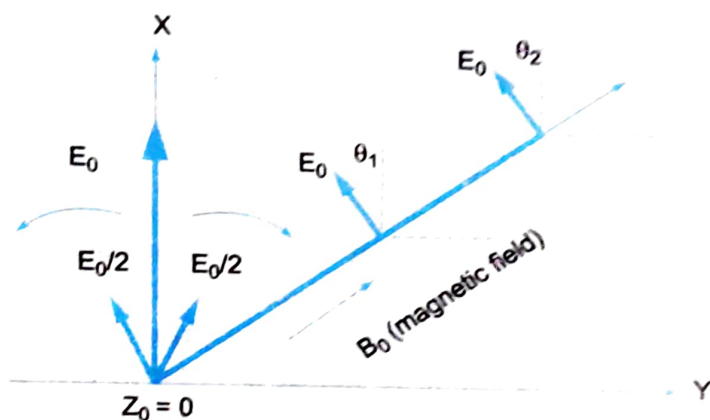


Fig. 6.30 Faraday rotation

In fact, the angle of rotation ' $\theta$ ' is given by

$$\theta = \frac{l}{2}(\beta_+ - \beta_-) \quad \dots(6.75)$$

where,  $l$  = length of the ferrite rod

$\beta_+$  = Phase shift for the right circularly polarised (component in clockwise direction) wave with respect to some reference.

$\beta_-$  = phase shift for the left circularly polarised (component in anticlockwise direction) wave with respect to the same reference.

In a practical ferrite medium, there will be finite losses. The propagation constant for circularly polarised wave will have unequal attenuation constants and unequal phase constant. Due to this, the direction of Faraday rotation will be different in the two regions above and below the resonant frequency ( $\omega_0$ ). A two port ferrite device is shown in Fig. 6.31 when a wave is transmitted from port ① port ②, it undergoes rotation in the anticlockwise direction as shown. Even if the same wave is allowed to propagate from port ② port ①, it will undergo rotation in the same direction (anticlockwise). Hence the direction of rotation of linearly polarised wave is independent of the direction of propagation of the wave.



Fig. 6.31

## ~~6.11.2 Microwave Devices which make use of Faraday rotation~~

We discuss three important devices which make use of faraday rotation

(a) Gyrorator

(b) Isolator

(c) Circulator

### (a) Gyrorator

It is two port device that has a relative phase difference of  $180^\circ$  for transmission from port ① port ② and 'no' phase shift ( $0^\circ$  phase shift) for transmission from port ② to port ① as shown in Fig. 6.32.

The construction of a gyrator is as shown in Fig. 6.32. It consists of a piece of circular waveguide carrying the dominant  $TE_{11}$  mode with transitions to a standard rectangular waveguide with dominant mode ( $TE_{10}$ ) at both ends. A thin circular ferrite rod tapered at both ends is located inside the circular waveguide supported by polyfoam and the waveguide is surrounded by a permanent magnet which generates dc magnetic field for proper operation of ferrite. To the input end a  $90^\circ$  twisted rectangular waveguide is connected as shown. The ferrite rod is tapered at both ends to reduce the attenuation and also for smooth rotation of the polarized wave.

**Operation :** When a wave enters port ① its plane of polarization rotates by  $90^\circ$  because of the twist in the waveguide. It again undergoes Faraday rotation through  $90^\circ$  because of ferrite rod and the wave which comes out of port ② will have a phase shift of  $180^\circ$  compared to the wave entering port ①.

But when the same wave ( $TE_{10}$  mode signal) enters port ②, it undergoes faraday rotation through  $90^\circ$  in the same anticlockwise direction. Because of the twist, this wave gets rotated back by  $90^\circ$  comes out of port ① with  $0^\circ$  phase shift as shown in Fig. 6.30. Hence a wave at port ① undergoes a phase shift of  $\pi$  radians (or  $180^\circ$ ) but a wave fed from port ② does not change its phase in a gyrator.

### (b) Isolator

An isolator is a 2 port device which provides very *small* amount of attenuation for transmission from port ① to port ② but provides *maximum* attenuation for transmission from port ② to port ①. This requirement is very much desirable when we want to match a source with a variable load.

In most microwave generators, the output amplitude and frequency tend to fluctuate very significantly with changes in load impedance. This is due to mismatch of generator output to the load resulting in reflected wave from load. But these reflected waves should not be allowed to reach the microwave generator, which will cause amplitude and frequency instability of the microwave generator.

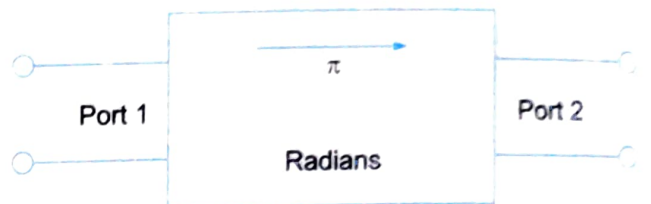


Fig. 6.32

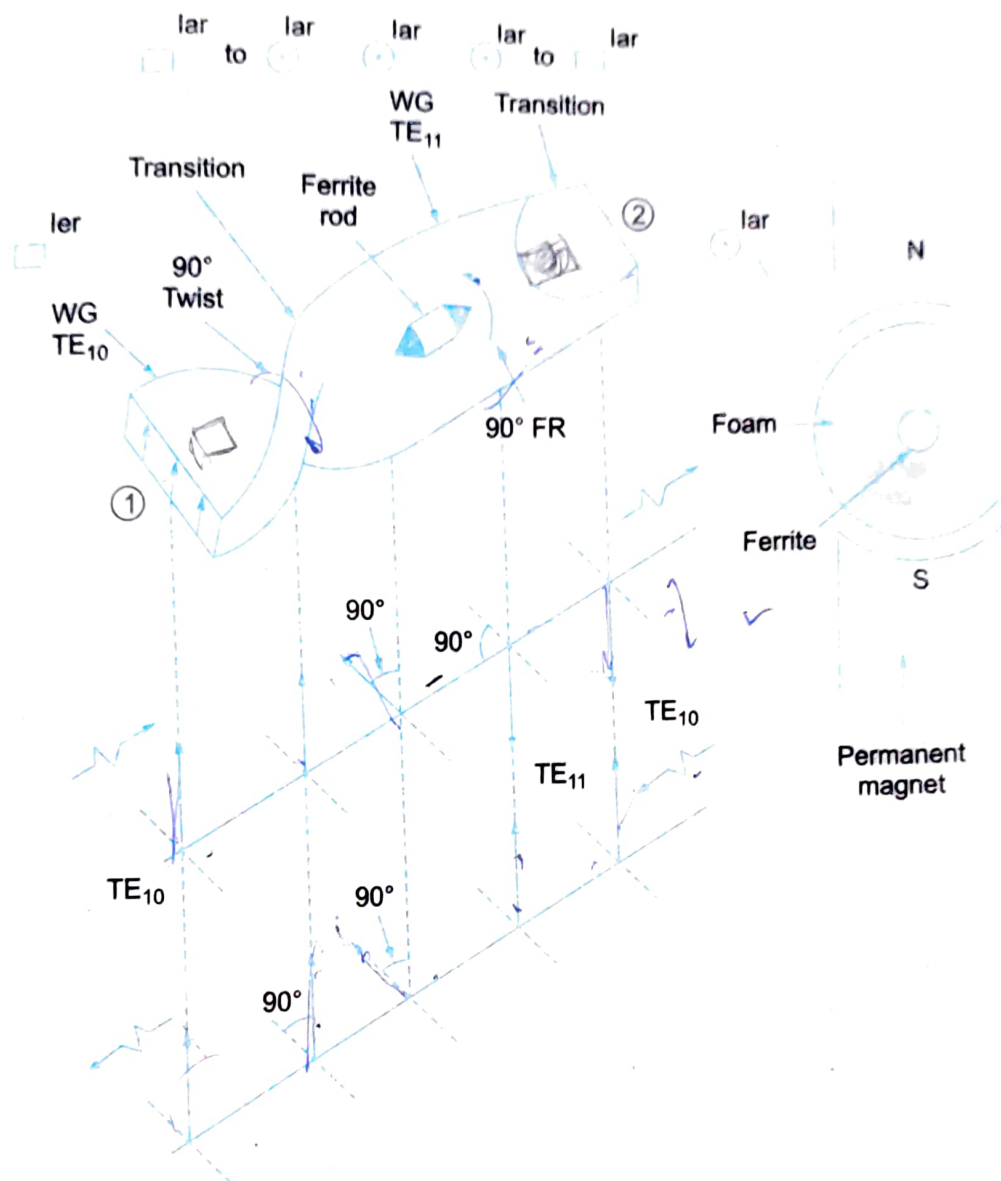


Fig. 6.33

When isolator is inserted between generator and load, the generator is coupled to the load with zero attenuation and reflections if any, from the load side are completely absorbed by the isolator without affecting the generator output. Hence the generator appears to be matched for all loads in the presence of isolator so that there is no change in frequency and output power due to variation in load. This is shown in Fig. 6.34.

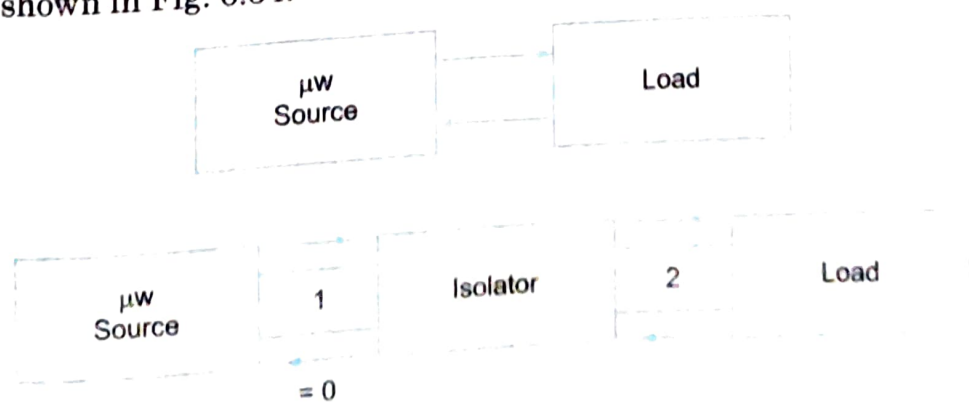


Fig. 6.34

**Construction :** The construction of isolator (Fig. 6.35) is similar to gyrator except that an isolator makes use of  $45^\circ$  twisted rectangular waveguide (instead of  $90^\circ$  twist) and  $45^\circ$  faraday rotation ferrite rod (instead of  $90^\circ$  in gyrator), a resistive card is placed along the larger dimension of the rectangular waveguide, so as to absorb an wave whose plane of polarisation is parallel to the plane of resistive card. The resistive card does not absorb any wave whose plane of polarization is perpendicular to its own plane.

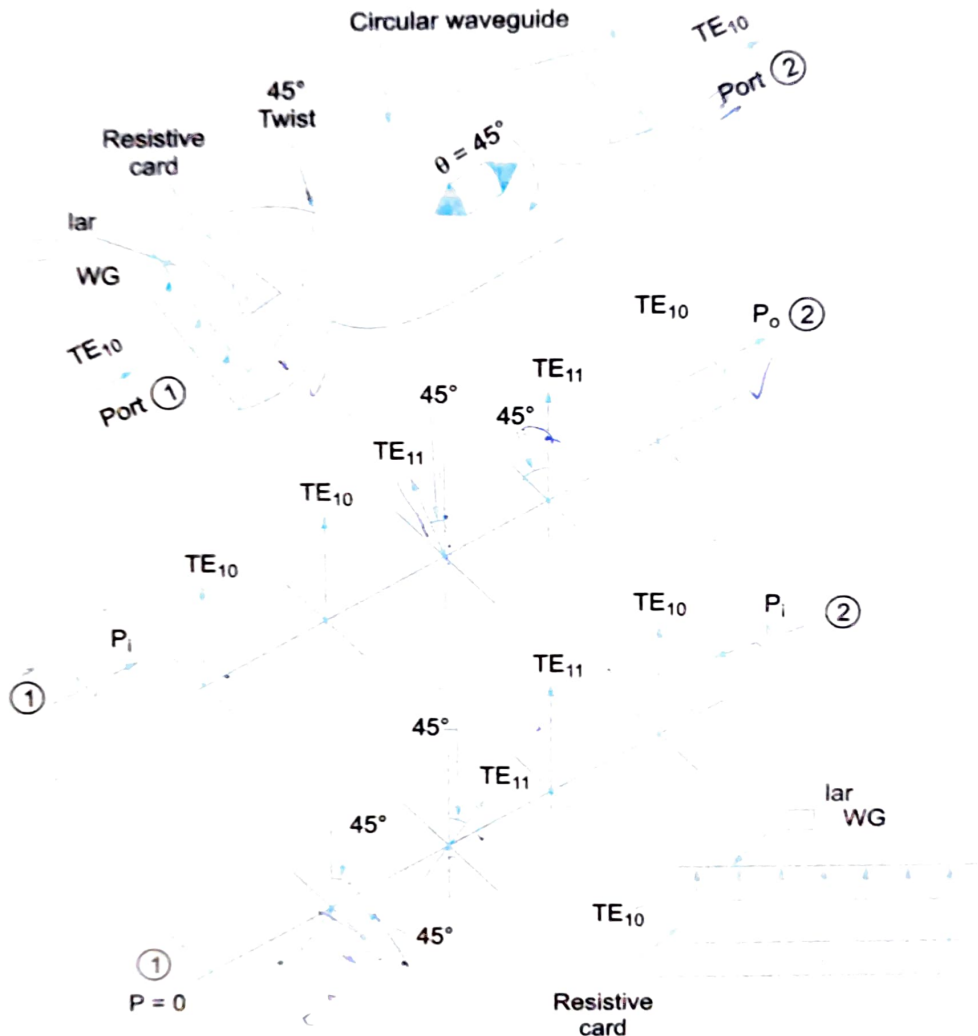


Fig. 6.35 Constructional details of isolator

**Operation :** A  $TE_{10}$  wave passing from port ① through the resistive card and is not attenuated. After coming out of the card, the wave gets shifted by  $45^\circ$  because of the twist in anticlockwise direction and then by another  $45^\circ$  in clockwise direction because of the ferrite rod and hence comes out of port ② with the same polarization as at port ① without any attenuation.

But a  $TE_{10}$  wave fed from port ② gets a pass from the resistive card placed near port ② since the plane of polarization of the wave is perpendicular to the plane of the resistive card. Then the wave gets rotated by  $45^\circ$  due to Faraday rotation in clockwise direction and further gets rotated by  $45^\circ$

in clockwise direction due to the twist in the waveguide. Now the plane of polarization of the wave will be parallel with that of the resistive card and hence the wave will be completely absorbed by the resistive card and the output at port ① will be zero. This power is dissipated in the card as heat. In practice 20 to 30 dB isolation is obtained for transmission from port ② to port ①.

### Circulator

A circulator is a four port microwave device which has a peculiar property that each terminal is connected only to the next clockwise terminal, i.e., port ① is connected to port ④ only and not to port ③ and ② and port ② is connected only to port ③ etc. This is shown in Fig. 6.36. Although there is no restriction on the number of ports, four ports are most commonly used. They are useful in parametric amplifiers, tunnel diode, amplifiers and duplexer in radars.

Construction : A four port Faraday rotation circulator is shown in Fig. 6.37. The power entering port ① is  $TE_{10}$  mode and is converted to  $TE_{11}$  mode because of gradual rectangular to circular transition. This power passes port ③ unaffected since the electric field is not significantly cut and is rotated through  $45^\circ$  due to the ferrite, passes port ④ unaffected (for the same reason as it passes port ③) and finally emerges out of port ②. Power from port ② will have plane of polarization already tilted by  $45^\circ$  with respect to port ①. This power passes port ④ unaffected because again the electric field is not significantly cut. This wave gets rotated by another  $45^\circ$  due to ferrite rod in the clockwise direction. This power whose plane of polarization is tilted through  $90^\circ$  finds port ③ suitably aligned and emerges out of it. Similarly port ③ is coupled only to port ④ and port ④ to port ①.

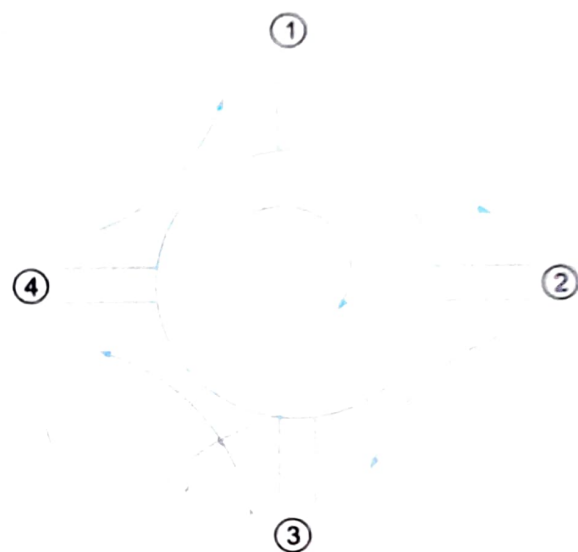


Fig. 6.36

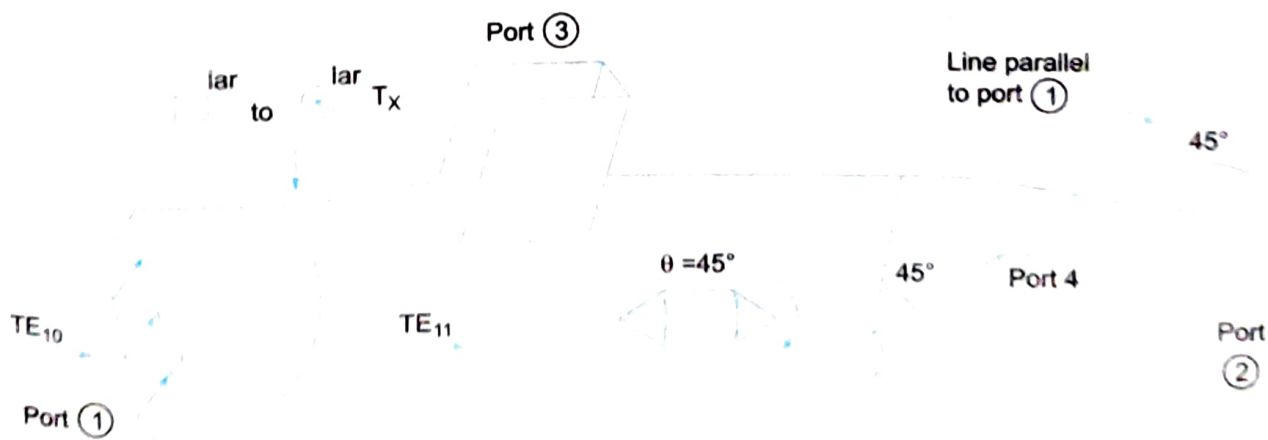


Fig. 6.37 Four port circulator

*Applications*

1. A circulator can be used as a duplexer for a radar antenna system as shown in Fig. 6.38.

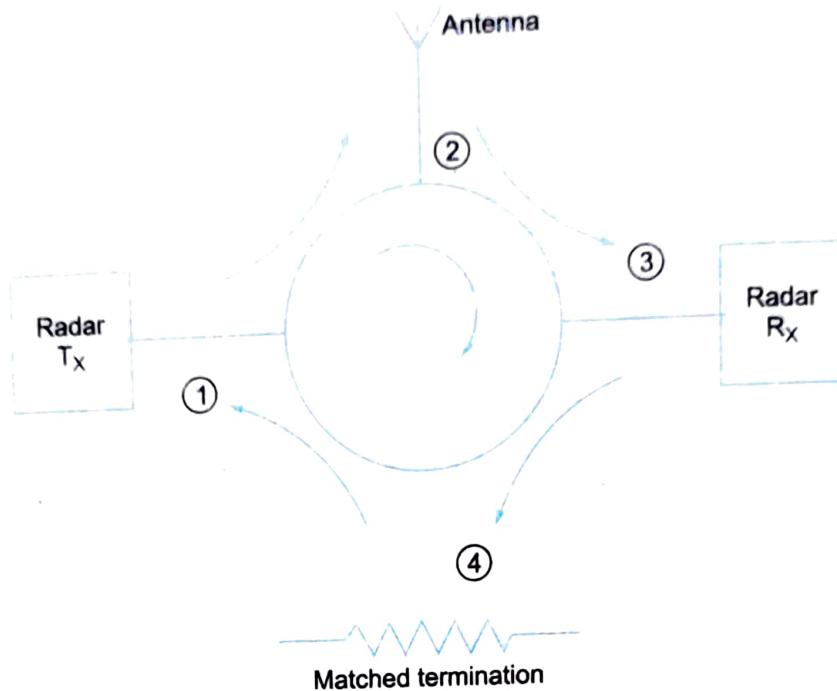


Fig. 6.38

Transmitter feeds the antenna while the received energy is directed to the receiver. The powerful radar transmitter is isolated from the sensitive receiver and also the same antenna can be used for both transmission and reception. This is the duplexer action being performed by a circulator.

2. We can have three port circulators, strip line circulators that can have several applications. Two three port circulators can be used in tunnel diode or parametric amplifiers as shown in Fig. 6.39.
3. Circulators can be used as low power devices as they can handle low powers only.

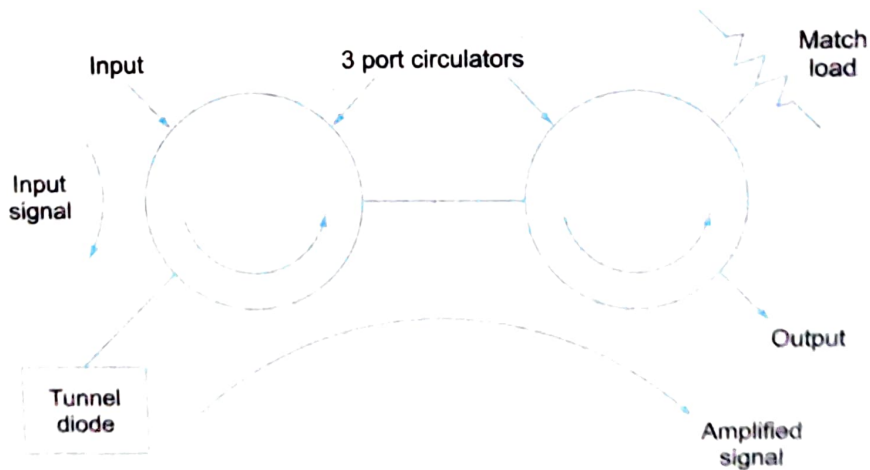


Fig. 6.39

## 6.16 PHASE SHIFTERS

Many applications require phase shifts to be introduced between two given positions in a waveguide system. The phase shift required may be fixed or variable. Since phase shift constant  $\beta$  is inversely proportional to guide wavelength  $\lambda_g$ , the magnitude of  $\lambda_g$  could be changed to obtain variable amounts of phase shift. Fixed amounts of phase shifts can be obtained by use of capacitive/inductive irises in the waveguide or by inserting dielectric rods across the diameters of a circular waveguide or by reducing wider dimension of a rectangular waveguide.

The physical construction of a phase shifter is same as that of a vane attenuator (to be described later). It consists of a dielectric slab or vane specially shaped to minimise reflection.

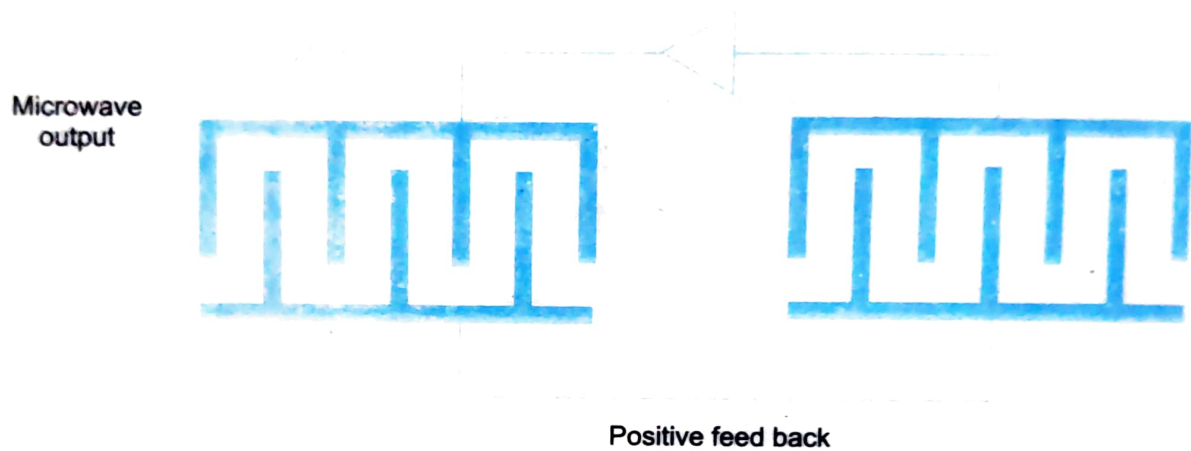


Fig. 6.46 SAW resonator

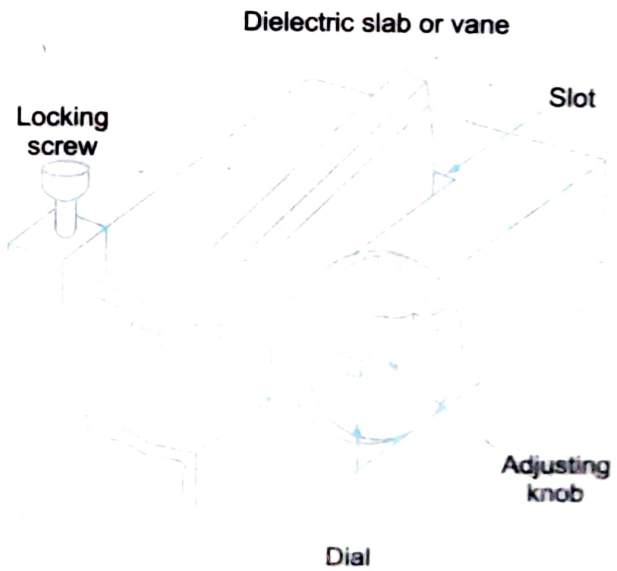


Fig. 6.47 Dielectric slab or vane phase shifter

effects, inserted through longitudinal slot cut along the wider dimension of a waveguide as shown in Fig. 6.46. This dielectric slab is made of some low loss material (polyfoam) with  $\epsilon_r > 1$ . It may be noted that, higher the dielectric constant of a medium the more slowly a microwave signal travels through it. Since most of the microwave signal in a waveguide travels through the center of the waveguide, movement of a dielectric slab with  $\epsilon_r > 1$  towards the centre of the waveguide means that microwave signal moves more slowly the nearer the slab gets to the center. The electric field distribution in the broader dimension of the waveguide will be modified by the dielectric slab so that it is distorted from sinusoidal to that indicated in Fig. 6.47.

If the vane is inserted deeper, there is more change in the medium and there is a greater phase shift. The electric field distribution also shows that the dielectric has the same effect of increasing the broader dimension of the waveguide which reduces the wavelength in the waveguide. The amount of phase shift is maximum when the slab is at the centre and minimum when it's adjacent to the wall of the waveguide if the dielectric vane is placed such that the vane's inside dimension is parallel to the direction of the electric flux lines.

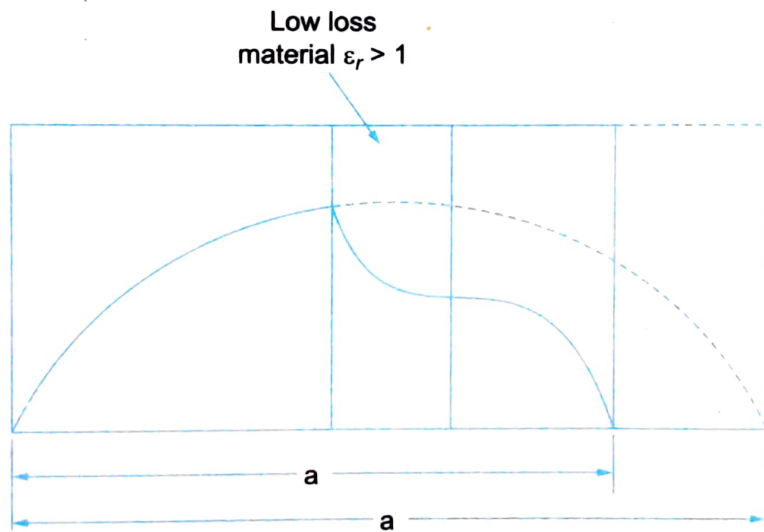


Fig. 6.48 Electric field distribution.

In the above dielectric vane variable phase shifters the phase shift is changed continuously from one value to another and hence they are also termed as analog phase shifters. If a fixed (rather than variable) phase shift is produced, then we name them as digital/discrete phases shifters. Digital phase shifters are mostly used in phased array antennas whereas analog phase shifters are used in bridges and instruments.

A precision phase shifter can be realised by a rotary phase shifter useful in microwave measurement. It basically consists of three circular waveguide sections all of which contain one dielectric vane. The centre section is rotatable providing the required phase shift. It works on the principle of converting a linearly polarised  $TE_{11}$  mode into a circularly polarised mode.

Alternately, ferrite phase shifters utilise Faraday rotation for providing the necessary amount of phase shift as in the case of Gyrator (discussed earlier) which provides  $180^\circ$  phase shift in one direction and  $0^\circ$  phase shift in the reverse direction.

## # 6.15 MICROWAVE ATTENUATORS

For perfect matching sometimes we require that the microwave power in a waveguide be absorbed completely without any reflection and also insensitive to frequency. For this we make use of attenuators.

Attenuators are commonly used for measuring power gain or loss in dBs, for providing isolation between instruments, for reducing the power input to a particular stage to prevent overloading and also for providing the signal generators with a means of calibrating their outputs accurately so that precise measurement could be made. Attenuators can be classified as fixed or variable (continuous or step variation) types.

Fixed Attenuators are used where fixed amount of attenuation is to be provided. If such a fixed attenuator absorbs all the energy entering into it, we call it as a waveguide terminator. This normally consists of a short section of a waveguide with a tapered plug of absorbing material at the end. The tapering is done for providing a gradual transition from the waveguide medium to the absorbing medium thus reducing the reflection occurring at the media interface. Figure 6.49 shows such a fixed attenuator where a dielectric slab consisting of glass slab coated with aquadog or carbon film has been used as a plug.

Here the lossy dielectric or vane shown is V-shaped and can occupy the whole of the waveguide.

Variable attenuators provide continuous or step wise variable attenuation. For rectangular waveguides, these attenuators can be flap type or vane type. For circular waveguides rotary type is used.

Shorting plate

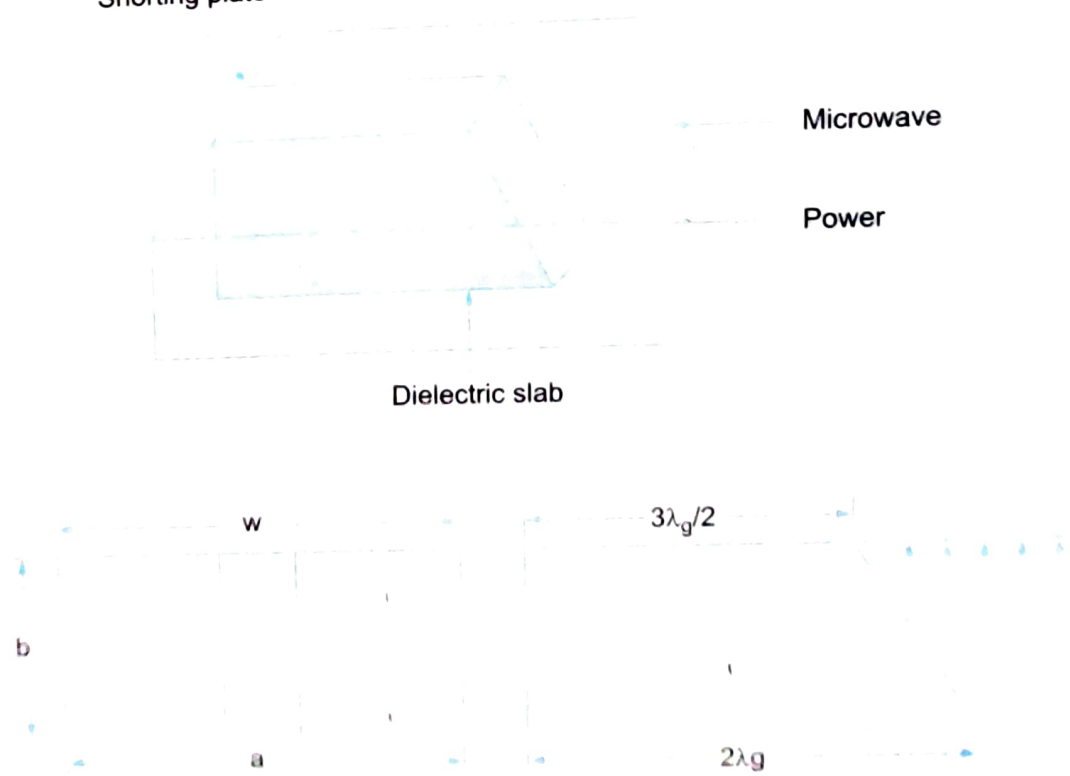


Fig. 6.49 Fixed attenuator

The flap type attenuator shown in Fig. 6.50, consists of a resistive element or disc inserted into a longitudinal slot cut along the centre of the wider dimension of the guide. The flap is mounted on the hinged arm allowing it to descent into the centre of the waveguide. The degree of attenuation is determined by the depth of insertion of the flap.

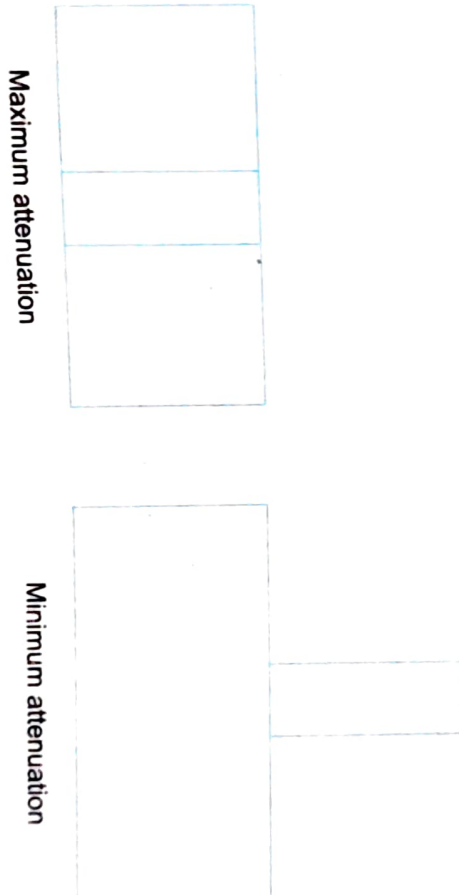
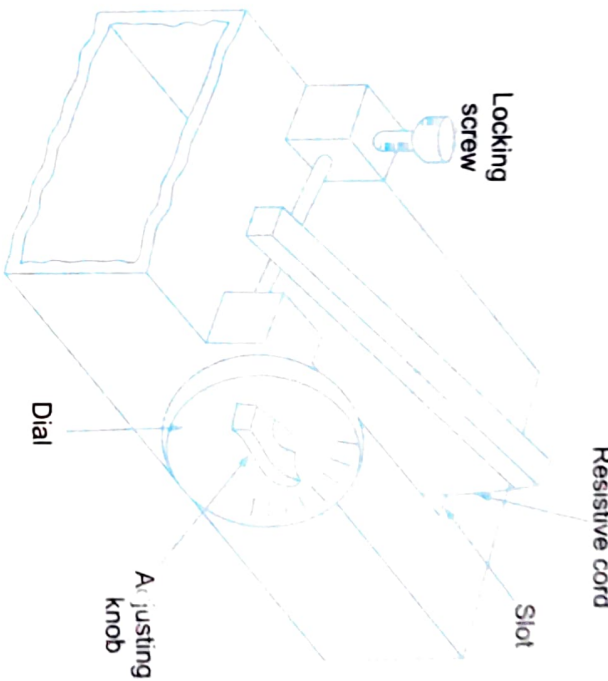


Fig. 6.50 Flap attenuator

However the flap attenuator dial needs to be calibrated against a standard as it is not a precision attenuator.

The vane type attenuator, (Fig. 6.51) basically consists of a glass vane with a coating of aquadog or carbon similar to a fixed vane attenuator. If this vane used at the centre is made movable, it can be used as a variable attenuator. The vane positioned at the centre of the waveguide can be moved laterally from the centre, where it provides maximum attenuation to the edges where the attenuation is considerably reduced since the electric field lines are always concentrated at the centre of the

waveguide. The vane is tapered at both ends for matching the attenuator to the waveguide. An adequate match is obtained if the taper length is made equal to  $\lambda_g/2$ . The amount of attenuation is frequency sensitive and also has to be calibrated against a precision (standard) attenuator.

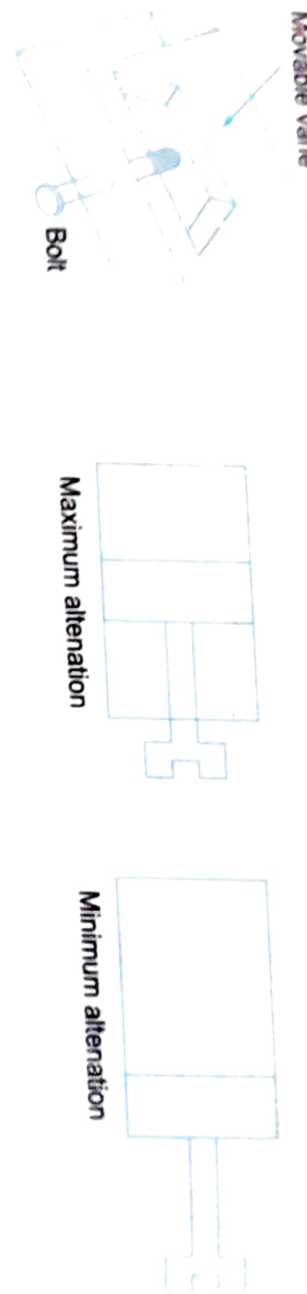


Fig. 6.51 Movable vane attenuator.

A resistive rotary vane attenuator provides precision attenuation with an accuracy of  $\pm 2.1\%$  of the indicated attenuation over the operating frequency range. It consists of three vanes. The central vane rotating type placed in the central section of a circular waveguide arrangement tapered at both ends. The other two vanes are in the rectangular sections as shown in Fig. 6.52.

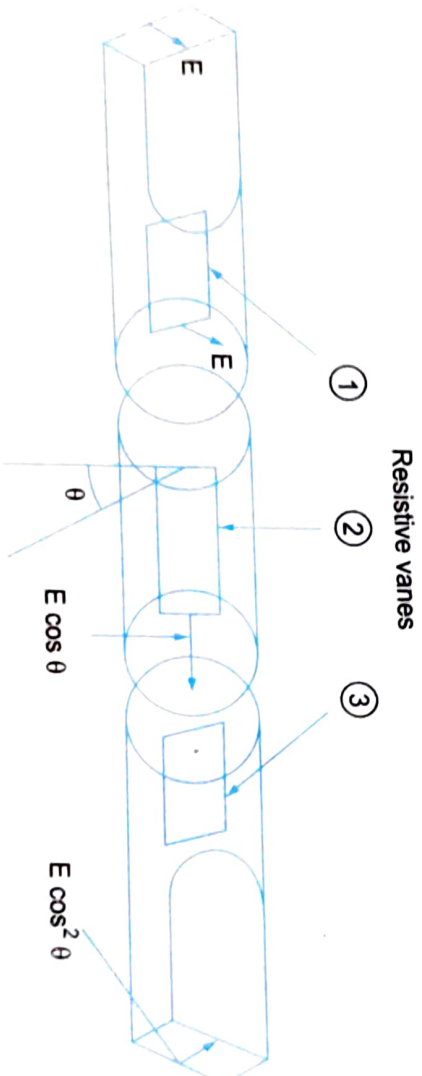


Fig. 6.52 Rotary wave precision attenuator.

When all the three vanes are aligned their planes are at  $90^\circ$  to the direction of electric field. Hence there is no (or zero) attenuation. Vane 1 prevents any horizontal polarisation and hence electric field at the output of vane 1 is vertically polarised. The centre vane 2 is rotating type and if it is rotated by an angle  $\theta$ , the  $E \sin \theta$  component is attenuated and  $E \cos \theta$  component is present at the output of vane 2 and the final output of the attenuator becomes  $E \cos^2 \theta$ , which has the same polarisation as the input wave. The attenuation due to this rotary vane attenuator is then equal to  $20 \log \cos^2 \theta = 40 \log \cos \theta$  that is independent of frequency and is precise.

# 7

# Microwave Measurements

## 7.1 INTRODUCTION

### Low Frequency Measurement vs. Microwave Measurements

- At low frequency, it is convenient to measure voltage and current and use them to calculate power. However at microwave frequencies, they are difficult to measure and since they vary with position in a transmission line, are of little value in determining power. Therefore at microwave frequencies, it is more desirable and simpler to measure power directly.
- At low frequency, circuits use lumped elements which can be identified and measured. At microwave frequencies circuit elements are distributed and as such it is usually not important to know what element make up a line. It is possible and also satisfactory to measure the impedance of a circuit without regard to the individual distributed elements making up that circuit.
- Unlike low frequency measurements, many quantities measured at microwave frequencies are relative and it is not necessary to know their absolute values.
- Further for power measurement, it is usually sufficient to know the ratio of two powers (or their difference in dBs) rather than exact input or output powers.

The following parameters can be conveniently measured at microwave frequencies (1) Frequency (2) Power (3) Attenuation (4) Voltage Standing Wave Ratio (VSWR) (5) Phase (6) Impedance (7) Insertion loss (8) Dielectric constant (9) Noise factor.

## 7.2 MICROWAVE BENCH-GENERAL MEASUREMENT SET-UP

The general set up for measurement of any parameter in microwaves is normally done by a microwave bench. Such a set up is shown in Fig. 7.1. The signal generator is a microwave

source whose output is of the order of milliwatts. It could be a Gunn diode oscillator (Chapter 8), a backward wave oscillator or a reflex klystron tube (Chapter 7). It can provide either a continuous wave (CW) or square wave modulated at an audio rate which is normally 1 kHz. In some cases it may have provision for sweep oscillator which allows the output cases it may have provision for sweep oscillator which allows the output frequency to be varied periodically. The *precision attenuator* can provide 0 to 50 dB attenuation above its insertion loss. The *variable flat attenuator* is also used in addition, whose calibration can be checked against readings of the precision attenuator. A frequency meter is used for direct reading of frequency that consists of single cylindrical cavity which can be adjusted to resonance and is slot coupled to the waveguide. The slotted line carriage has just been described. The *crystal detector*, inserted in the *E* probe of the slotted line is contained in the crystal detector mount at the end of the waveguide run (as discussed in chapter 4), is used to detect the modulated signal. the SWR (Standing Wave Ratio) indicator is basically a sensitive tuned voltmeter that provides direct reading of the SWR or its equivalent value in decibels.

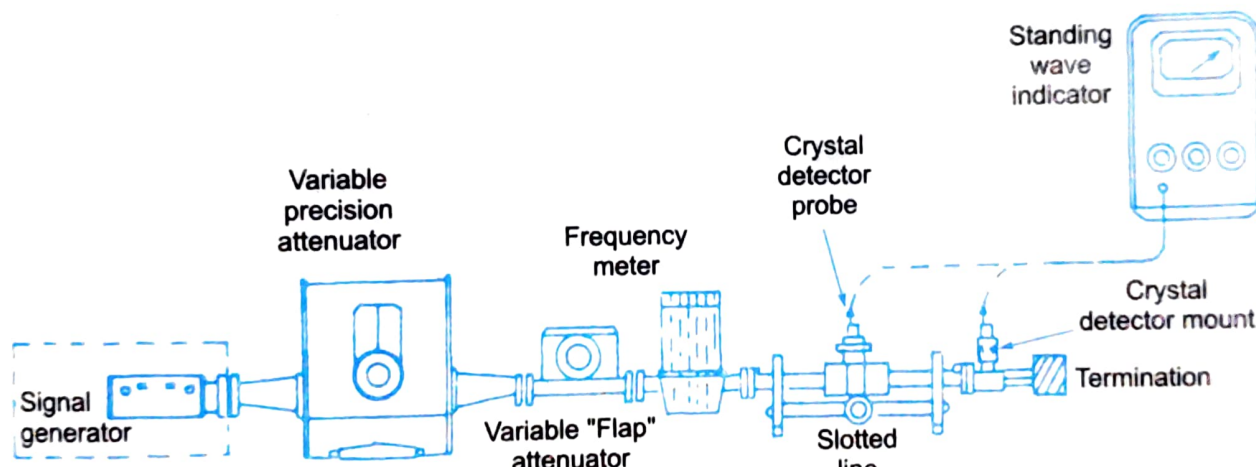


Fig. 7.1. General set-up of microwave bench.

### 7.3 MEASUREMENT DEVICES AND INSTRUMENTATION

Before different parameters can be measured it shall be appropriate if the several devices and instrumentation that are normally used are discussed. Here, we give a brief descriptions of some of the devices and instruments such as Slotted line carriage, Tunable detector, VSWR meter, Power meter, Wave meter, Spectrum analyser, Network analyser (Scalar and Vector) etc.

#### 7.3.1 Slotted Line

A coupling probe moving along the waveguide can be used to detect the standing wave pattern present inside the waveguide. It is basically used for measuring the standing wave ratio. It consists of a slotted section of a transmission line (waveguide) a travelling probe carriage and facility for attaching detecting instruments (Fig. 7.2). The slot is made in the centre of the broad face of the

waveguide parallel to the axis of the waveguide. For the dominant mode travelling inside the waveguide, the slot does not radiate any power. A small probe inserted through the slot senses the relative field strength of the standing wave pattern inside the waveguide. This probe is on a carriage plate which moves on the top surface of the waveguide. The probe is connected to a crystal detector so that the output from the detector is proportional to the square of the input voltage at that position of the probe. As the position of the probe is moved along the waveguide slot, it gives an output proportional to the standing wave pattern inside the waveguide. Since the crystal is a square law device, the square root of the ratio of maximum output to the minimum output when the probe carriage or travelling probe is moved along the slot gives the VSWR (Voltage Standing Wave Ratio). For noting the positions, the precision built probe carriage has a centimeter scale with a vernier reading of 0.1 mm. least count.

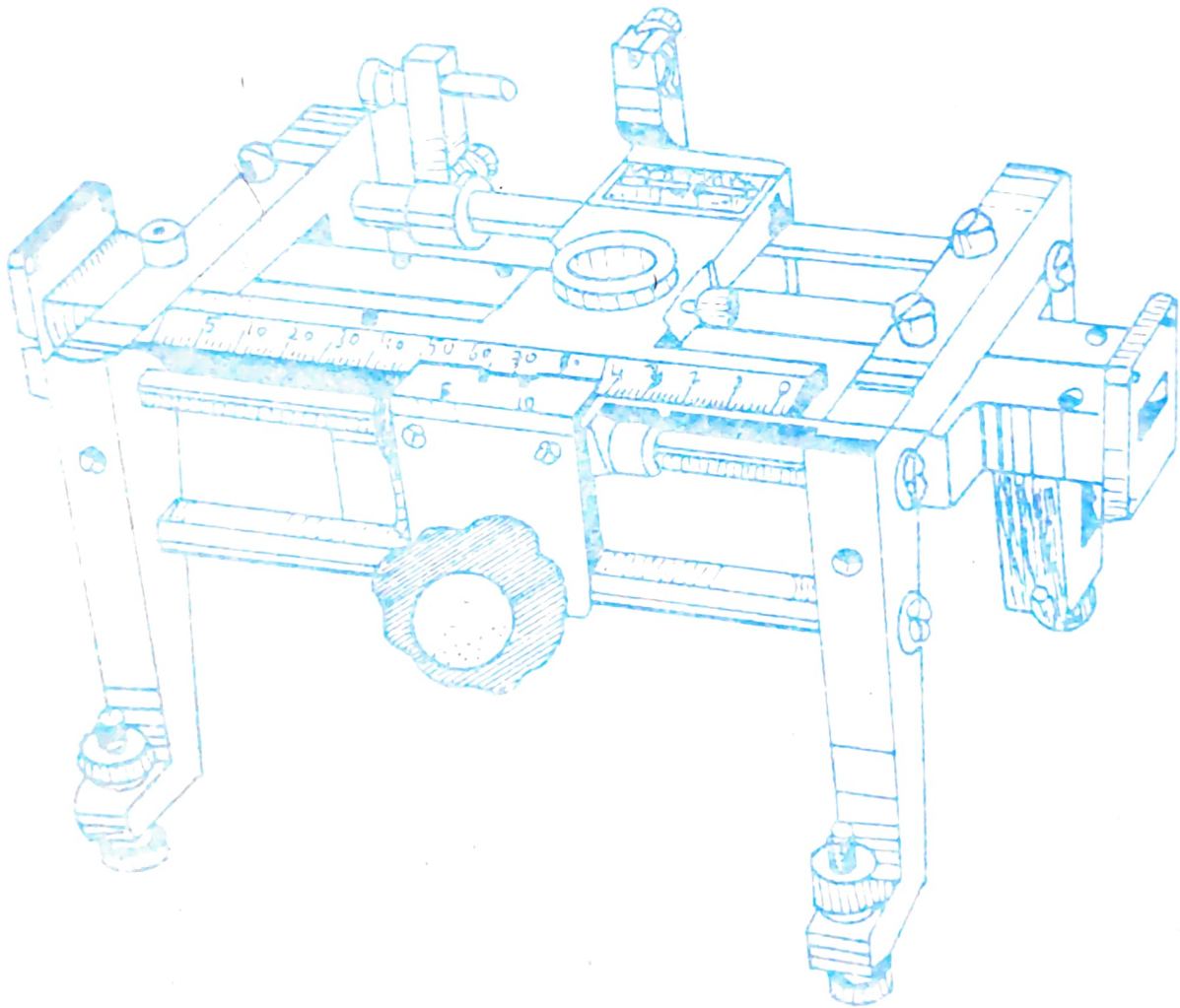


Fig. 7.2 Slotted line

Thus the slotted line carriage with a tunable detector can be employed to obtain the low frequency modulating signal on an oscilloscope (or VSWR meter, that will be dealt in next section).

The probe extends into the slot coming quite close to the inner conductor of the line but not touching it. This loose coupling between line and probe is adequate for measurement purposes.

The slotted line will have same characteristic impedance as the main line to which it is connected in series. It has a length slightly greater than half wavelength at the lowest frequency of operation. It permits convenient and accurate measurement of the position and size of the first voltage maximum from the load and any subsequent ones without significantly interfering with the quantities being measured.

Further it is necessary that the probe be quite thin as compared to the wavelengths and the depth also be small enough to avoid any field distortion. The slotted line carriage with tunable detector can be used to measure impedance, reflection coefficient and return loss in addition to SWR, standing wave pattern and frequency of the generator being used.

### 7.3.2 Tunable Detector

As mentioned in 7.3.1, the tunable detector helps detect the low frequency square wave modulated microwave signal. This is made possible by use of a non-reciprocal detector diode mounted in the microwave transmission line. The detector diode can be point contact type or metal-semiconductor Schottky Barrier diode (SBD). The details of these diodes is given in the chapter on solid state microwave devices (Chapter 8). A tunable stub is used to match the detector to the microwave transmission system and there are three different types

1. Tunable waveguide detector,
2. Tunable co-axial detector, and
3. Tunable probe detector.

The various tunable detectors/mounts are shown in Fig. 7.3.

### 7.3.3 VSWR Meter

A VSWR meter basically consists of a high gain, high  $Q$ , low noise voltage amplifier normally tuned at a fixed frequency (1 kHz) at which the microwave signal is modulated. The VSWR meter uses the detected signal out of the microwave detector as its input, amplifies the same and provides the output on a calibrated voltmeter. The meter itself can be calibrated in terms of VSWR. In this case, the probe carriage is moved to give maximum deflection on the VSWR meter by adjusting the pad. This full scale deflection (FSD) corresponds to a VSWR of 1 as shown in Fig. 7.4. As an example, an FSD of 10 mV corresponds to a VSWR of 1. The travelling probe is adjusted to get minimum reading on the meter. It this corresponds to 5 mV, then

$$\text{VSWR} = \frac{10 \text{ mV}}{5 \text{ mV}} = 2. \text{ If it is } 3.3 \text{ mV, VSWR} = 3, \text{ if it is } 2.5 \text{ mV, VSWR} = 4. \text{ If it is } 1 \text{ mV, VSWR}$$

$= 10$  etc. i.e. Such a calibrated VSWR meter gives an expanded scale upto a VSWR of 2 but for  $\text{VSWR} > 10$ , the meter will be congested and the measurement will not be accurate for VSWR's  $> 10$ . Hence this method is not useful for VSWR's  $> 10$ .

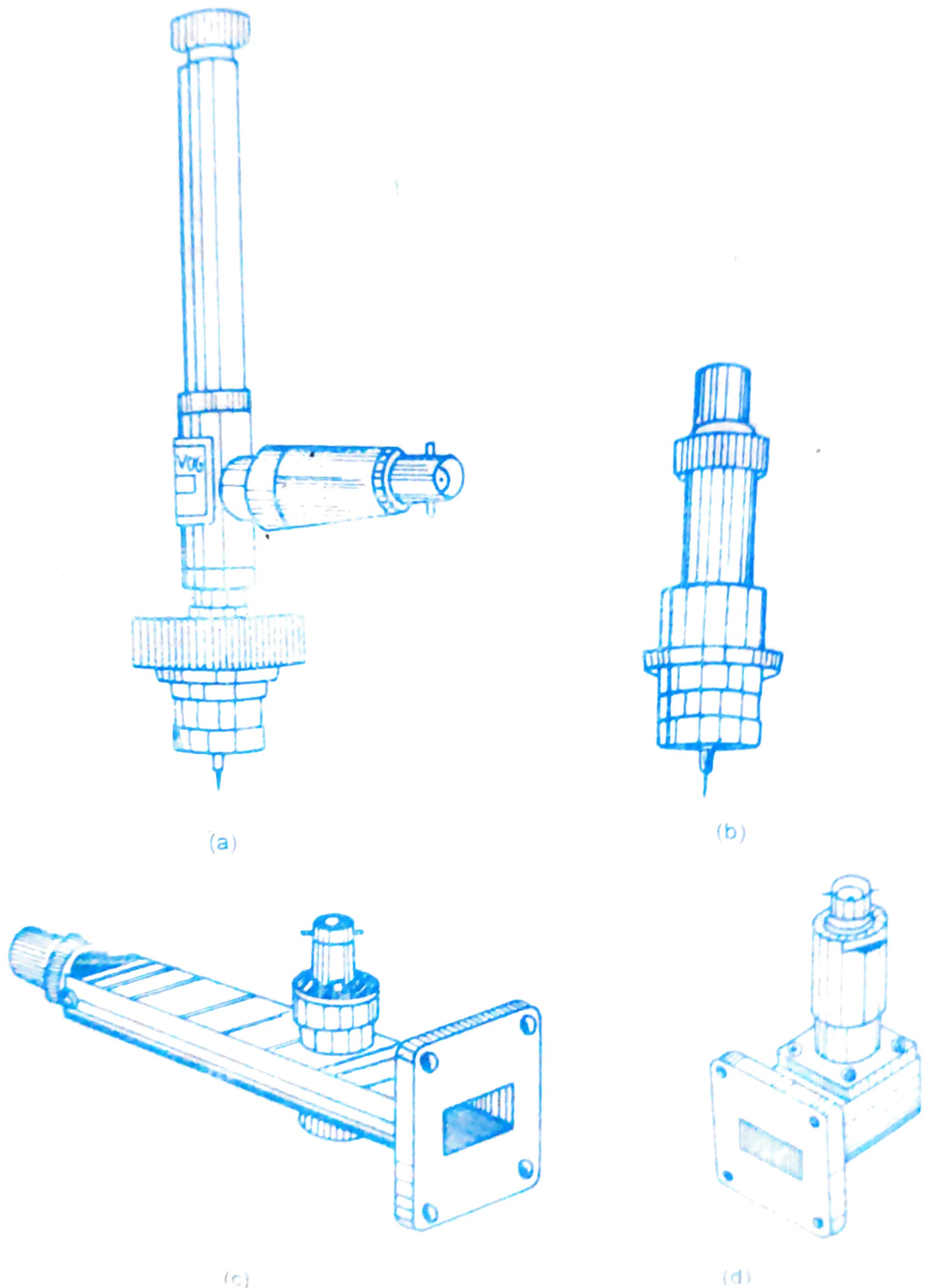


Fig. 7.3 (a) Tunable probe; (b) fixed board band-tuned probe;  
(c) tunable waveguide detector; and (d) fixed waveguide matched detector mount

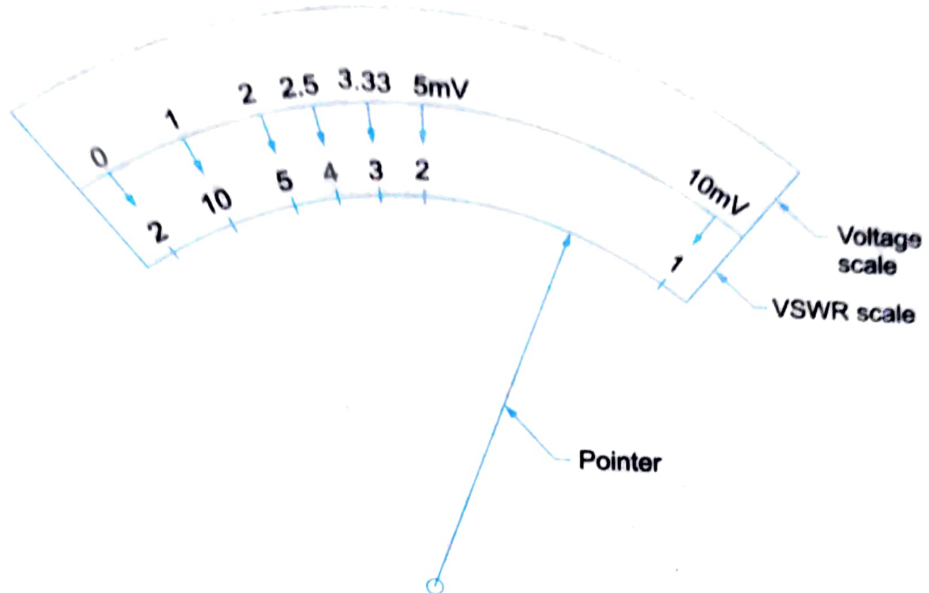


Fig. 7.4 VSWR meter.

The actual VSWR meter looks like that of Fig. 7.5. It has a gain control to adjust the reading to a desired value, by fine or coarse adjusting knobs. Normally, the overall gain is about 125 dB that can be adjusted in steps of 10. Also there are three scales on the VSWR meter—normal SWR, expanded SWR, and dB scales. The normal SWR scale can be used when the VSWR is between 1

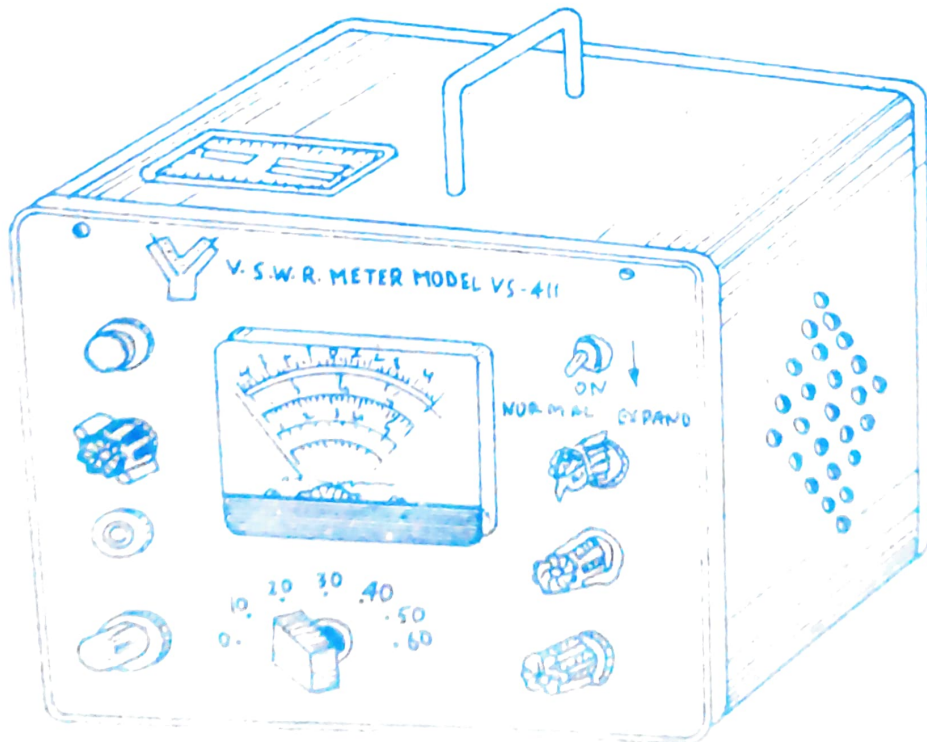


Fig. 7.5 VSWR meter

and 4. For VSWR's between 3 and 10 the bottom of normal SWR scale can be used. The expanded SWR scale is graduated from 1 to 1.3 and hence can be used whenever the VSWR is less than 1.3 for an accurate reading. The dB scale is at the bottom along with an expanded dB (between 0 to 2 dB) for measuring VSWR directly in dBs. The input selector switch is provided for different input crystal low current (4.5 mA) or high current (8.75 mA) bolometer bias.

### 7.3.4 Power Meter

A microwave power meter shown in Fig. 7.6a basically consists of a power sensor that converts the microwave power into heat energy. The temperature change so produced provides an output current in the low frequency circuit that indicates power. The sensors used for power measurements are the Schottky barrier diode, bolometer and the thermocouple. Here we discuss the Schottky barrier diode and the thermocouple sensor. (The bolometer and calorimeter techniques are discussed in section 7.4)

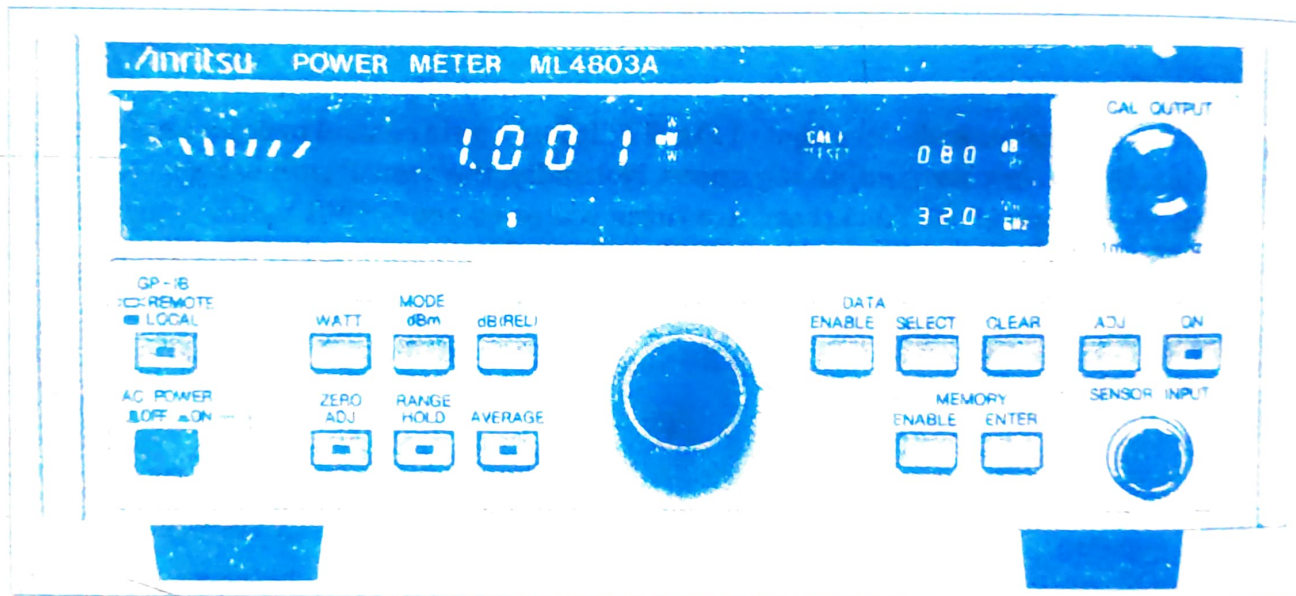


Fig. 7.6 (a) Power meter.

### Schottky barrier diode (SBD) sensor

A zero biased SBD sensor is used as a square law detector for measurement of power. The SBD sensor circuit is shown in Fig. 7.6b wherein the circuit is so defined that the input matching is not affected by diode resistance. The output of the circuit is proportional to the input RF power. These SBD detectors can be used to measure power levels as low as 70 dBm, meaning that they can be employed to measure only low microwave powers (less than 10 mW).

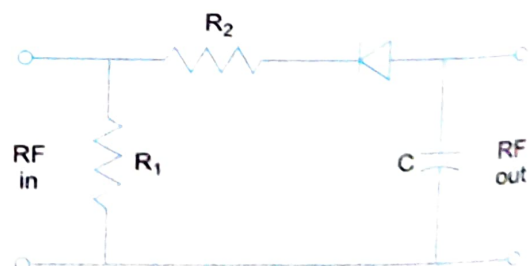


Fig. 7.6 (b) Schottky barrier diode sensor

## Thermocouple sensor

A thermocouple power sensor can also be used to measure microwave power as shown in Fig. 7.6c. We know that when the two ends of a thermocouple (consisting of a junction of two dissimilar metal or semiconductors—*n*-type silicon) are heated up differently by absorption of microwaves they produce an emf across them. This is done in a thin film tantalum-nitride resistive load deposited on a silicon substrate which forms one electrode of the thermocouple as shown in Fig. 7.6c. The emf produced will be proportional to the RF microwave input power being measured. Capacitor  $C_2$  is an RF bypass capacitor and capacitor  $C_1$  is the input coupling capacitor for dc blocking. The figure shows dual thermocouples that are parallelly connected. The overall emf generated by these thermocouples get added and appear across  $C_2$  that is connected to a dc voltmeter. The dc voltmeter can be calibrated to read the input microwave power directly. Generally, the microwave power is square wave modulated. If the average power of this signal is known, the peak power can be calculated since  $P_{\text{peak}} = P_{\text{av}} \cdot T/\tau$  where  $\tau$  is the pulselength,  $T$  is the period and  $P_{\text{av}}$  is the average microwave power.

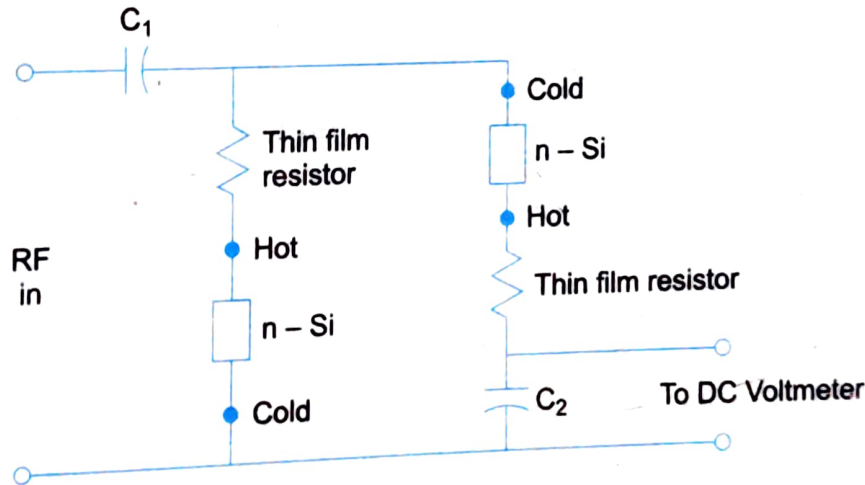


Fig. 7.6 (c) Thermocouple sensor.

### 7.3.5 Wave Meter

A wave meter is typically constructed of a cylindrical cavity resonator with a variable short circuit termination. The shorting plunger is used to change the resonance frequency of the cavity by changing the cavity length. The wave meter axis is so placed that it is perpendicular to the broad wall of the waveguide as shown in Fig. 7.7a.

The dominant mode  $\text{TM}_{011}$  is normally used in wave meter. The most suitable mode however is  $\text{TE}_{011}$  because of its higher  $Q$  and absence of axial current. The  $\text{TM}_{010}$  mode is excited in the cavity through the coupling hole by magnetic field coupling. Any possible oscillation due to plunger can be avoided by placing a block of polytron—an absorbing material, at the back of the tuning plunger. The various plunger positions result in different cavity resonant frequencies. This tuning can be calibrated in terms of frequency by use of known frequency inputs and observing a dip in the power meter. The power meter can be connected at the output side of the waveguide.

Quality factor of 1000–5000 will result in accuracies as small as 1% to 0.005%. The absorption cavity characteristics and its analog equivalent is shown in Fig. 7.7b and c. A resonant cavity wavemeter is the microwave analog to tuned resonant circuit. There are two types—*transmission cavities* which pass only the signal frequency to which they are tuned and *absorption cavities* which *attenuate* the signal frequency to which they are tuned. The absorption type is preferred for laboratory frequency measurement. Cavity wave meters are rugged, simple and highly accurate. Accuracies upto 99.9% can be achieved. The resonant frequency of the cavity wavemeter is determined primarily by the physical dimensions  $a$ ,  $b$ ,  $d$  and the mode is determined by  $m$ ,  $n$ ,  $p$  as given by

$$f_0 = \frac{c}{2} \sqrt{\left(\frac{m}{a}\right)^2 + \left(\frac{n}{b}\right)^2 + \left(\frac{p}{d}\right)^2}$$

They should have high effective  $Q$ 's for good accuracy.

A micrometer type frequency meter using absorption type cavity wavemeter is shown in Fig. 7.7d.  
A direct reading frequency meter is shown in Fig. 7.7e.

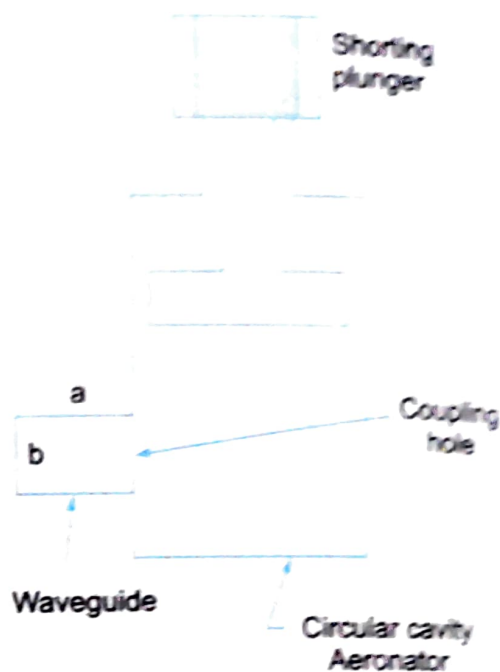


Fig. 7.7 (a) Wave meter

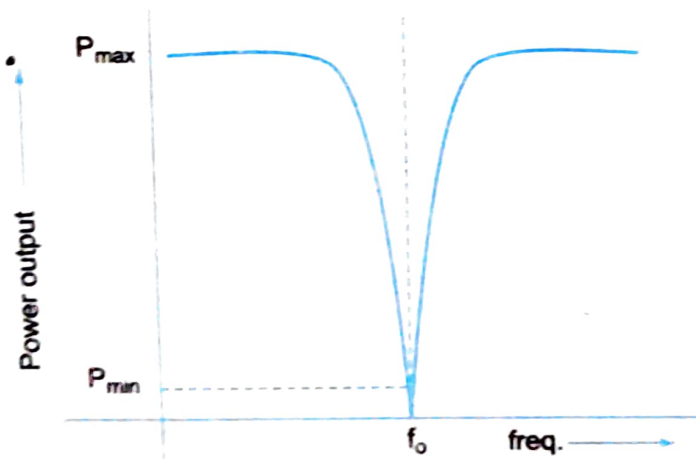


Fig. 7.7 Absorption cavity (b) Characteristics and (c) Analog-equivalent

### 7.3.6 Spectrum Analyser

A spectrum analyser is a frequency domain instrument which gives a display of the frequency spectrum of the input signal (in contrast to an oscilloscope which is a time domain instrument that gives a plot of signal amplitude vs time). The spectrum analyser gives a plot of frequency vs signal amplitude (amplitude of the Fourier transform of the input signal). Spectrum analysers are particularly useful at RF and microwave frequencies for analysing the spectrum of the signal source, antenna or signal distribution. It also helps as a diagnostic tool to establish compliance for the RFI

EMI (Radio frequency interference/Electromagnetic interference) requirements. A spectrum analyser is basically a broad band superhet receiver (shown in Fig. 7.8) that provides a plot of frequency vs amplitude i.e. signal spectrum as explained above. The local oscillator is electronically swept back and forth between two frequency limits at a linear rate. The input attenuation limits the input signal power so as to keep it within the normal operating range of the instrument (normally 0 to 10 dBm). The input tracking filter provides image frequency rejection. The sawtooth sweep voltage waveform moves the spot on the CRT horizontally. This movement is performed in synchronism with the frequency sweep so that the horizontal position is a function of the frequency of the local oscillator. The vertical deflection of the spot gives the amplitude of the input IF signal. The frequency sweep's range and rate, IF amplifier bandwidth and centre frequency are critical for the design of a spectrum analyser. The bandwidth is kept minimum and sweep speed quite low for better resolution and also to provide sufficient time for build up of voltage at the receiver. IF frequency is chosen quite high to avoid image frequency ( $f_{si} = f_s \pm 2f_i$ ) then the range of frequencies to be covered should be as small as possible. The bandwidth of the IF amplifier determines the bandwidth and hence resolution of the spectrum analyser.

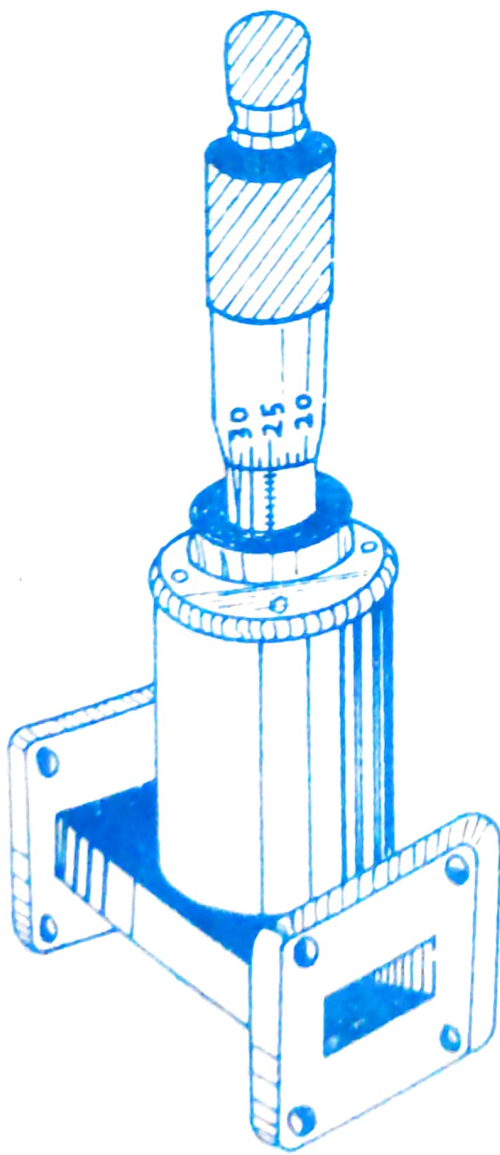


Fig. 7.7 (d)

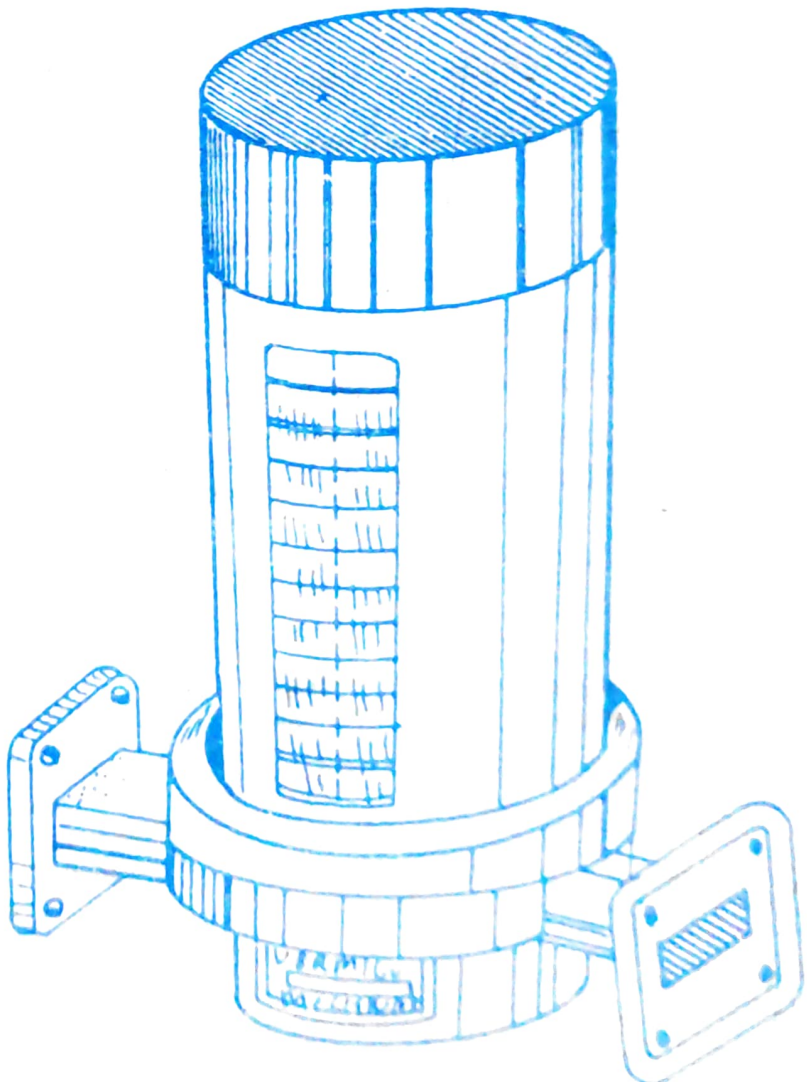


Fig. 7.7 (e)

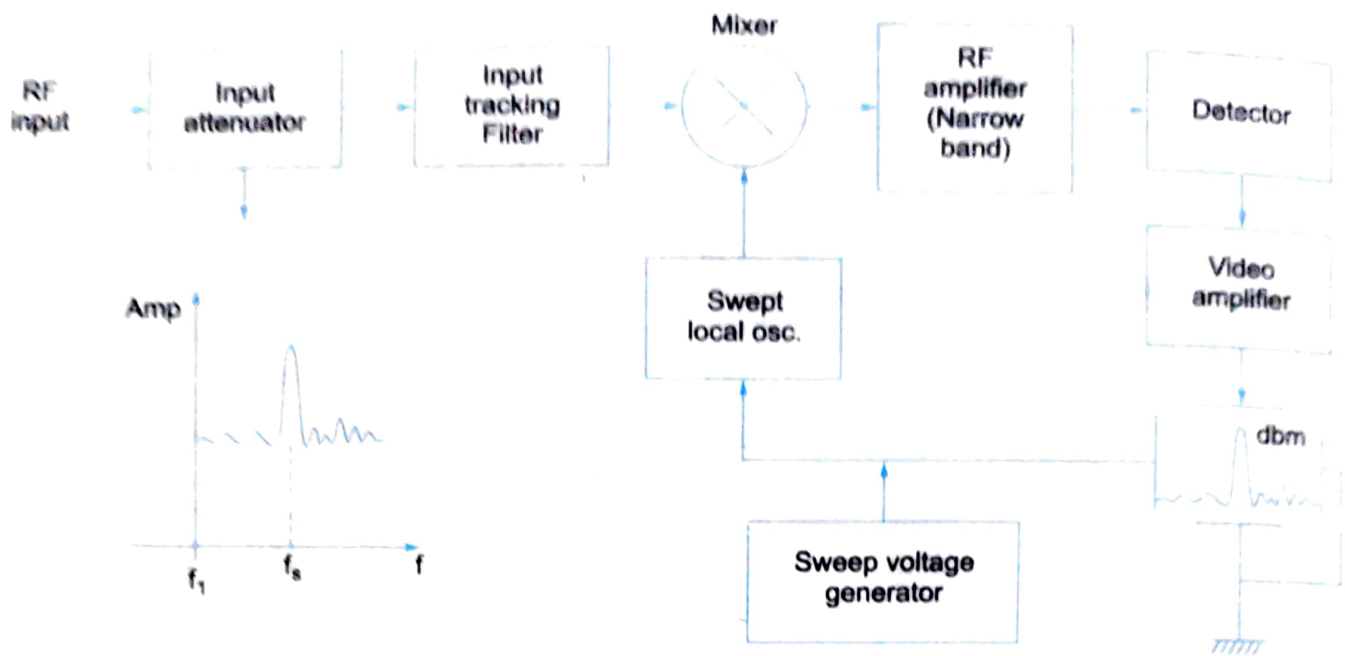


Fig. 7.8

### 7.3.7 Network Analyser

A network analyser is a network system that measures both amplitude and phase of a microwave signal over a wide frequency range in a reasonably small time. We may mention here that the slotted line could measure the amplitude and phase of a microwave signal only at a single frequency. Moreover to make measurements at broad band frequencies using slotted line is both time consuming and costly in terms of manpower.

In a network analyser, the basic principle of measurement is to generate an accurate reference signal and compare this with respect to the test signal whose amplitude and phase are to be measured. A block schematic of a network analyser is shown in Fig. 7.9.

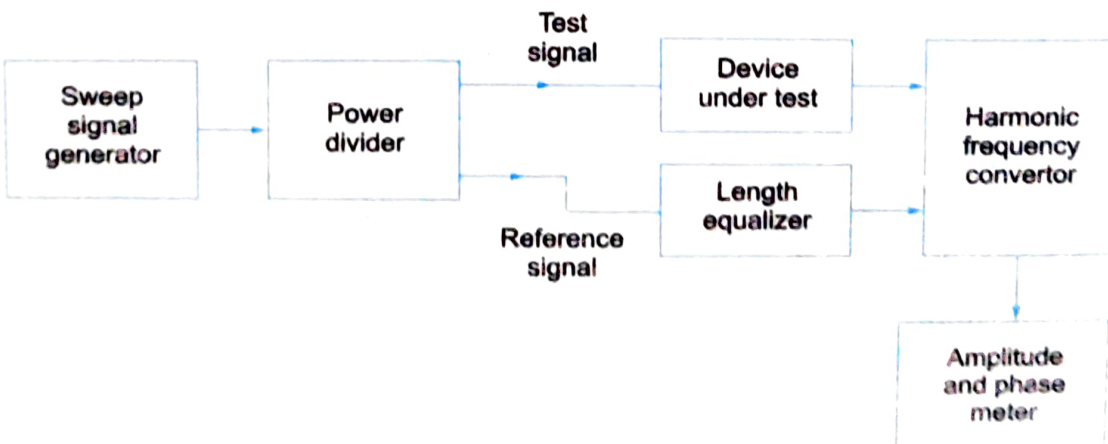


Fig. 7.9 Network analyser

A sweep signal generator feeds a power divider or splitter that converts into two signals the test signal and the reference signal. The device under test (DUT) is fed with the test signal and length equalizer (phase equalising line) takes in the reference signal. These test and reference signals are then converted to standard IF frequency by a harmonic frequency converter. The output of the harmonic frequency converter is then used to determine the amplitude and phase of the test signal.

The harmonic frequency converter consists of a phase locked loop shown in Fig. 7.10. The local oscillator tracks the reference signal frequency making error possible swept frequency measurement. The double mixer arrangement first converts the memory RF test signal to a first IF of 10 MHz and then a second IF of 278 kHz.

A network analyser is quite useful for measurement of both passive as well as active microwave component or network parameters. It is used for measurement of both impedance (reflection) and gain (transmission) characteristics of microwave devices. It uses a stimulus response method for testing over the frequency range of interest. As these parameters are a function of frequency with complex variables (having both magnitude and phase), a swept frequency measurement becomes imminent.

A network analyser can be scalar or vector. A scalar network analyser provides only magnitude characteristics of microwave devices as a function of frequency. A vector network analyser can measure complex reflection or transmission characteristics of microwave devices. The principle of measurement in both these methods is the same in that they compare the incident or input power with the transmitter or reflected waves depending upon the parameter to be measured. The ratio of the relevant signals is used to determine the scattering matrix of the DUT.

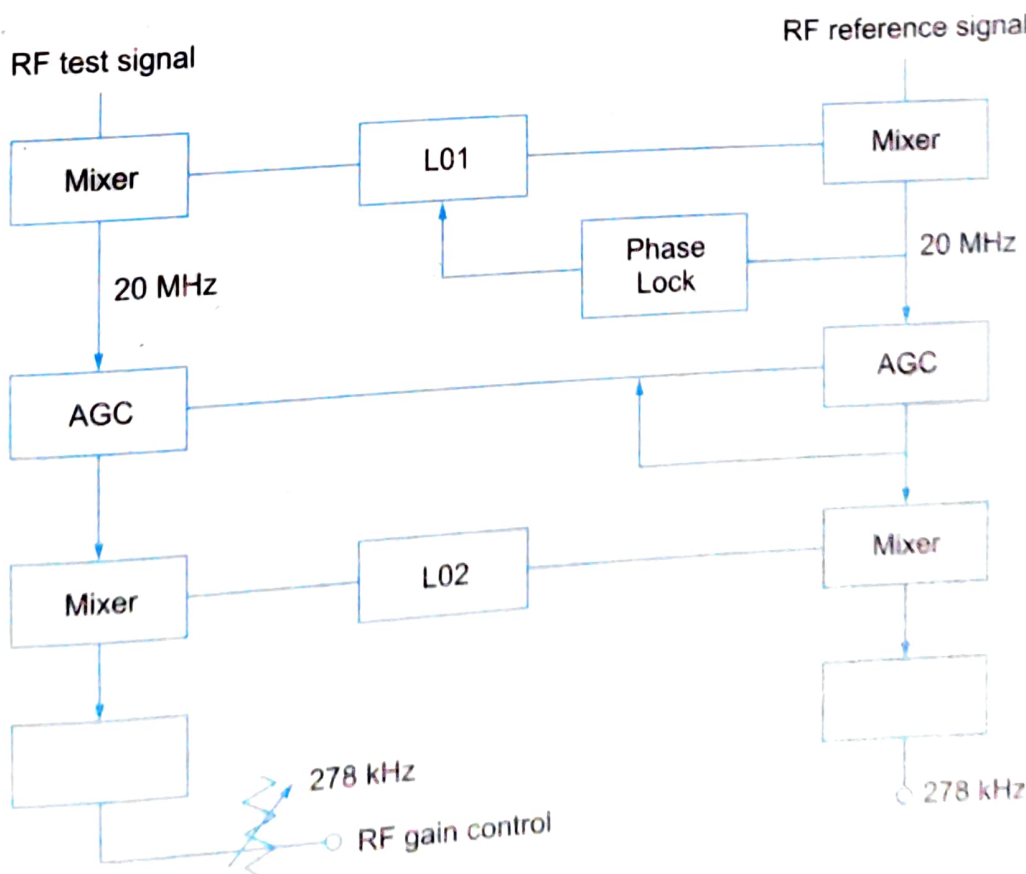


Fig. 7.10 Harmonic frequency converter

As explained earlier, we have a signal source, power splitter, receiver/detector and a processor/display components. The DUT transmits or reflects the stimulating or incident signal from the signal source which are used in the measurement of magnitude and phase of individual components of the test signal. The receiver and display could be a harmonic generator and the amplitude/phase meter which have already been described. However in place of power splitter, we might have as well used a directional coupler or a higher impedance probe.

### 7.3.8 Test Set up for Reflection-Transmission Measurement

A reflection-transmission unit is normally employed for measurement of reflection and transmission. A reflection-transmission unit is shown in Fig. 7.11.

For transmission measurement, the reference line length is balanced and for reflection measurements the DUT is compared to the sliding short. A good balance between the channels can be maintained by use of accurately matched directional couplers in the bridge.

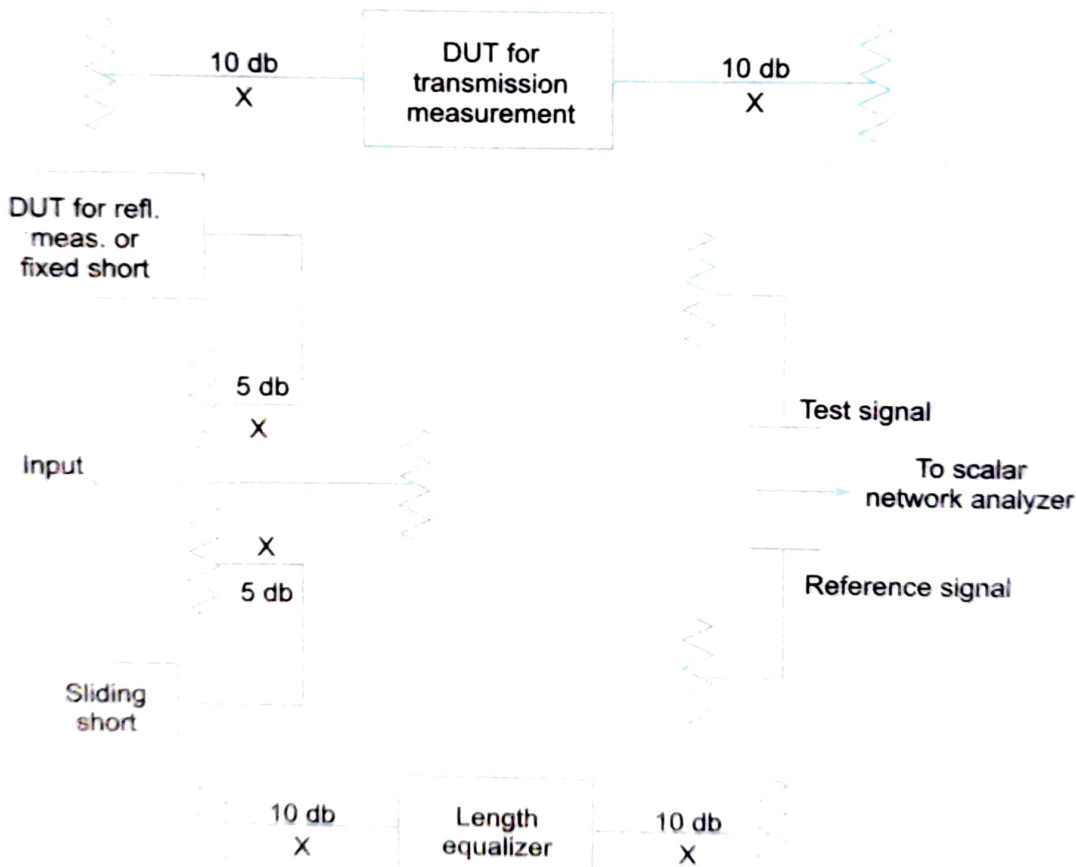


Fig. 7.11 Test set up for reflection-transmission measurement

As explained earlier, we have a signal source, power splitter, receiver/detector and a processor/display components. The DUT transmits or reflects the stimulating or incident signal from the signal source which are used in the measurement of magnitude and phase of individual components of the test signal. The receiver and display could be a harmonic generator and the amplitude phase meter which have already been described. However in place of power splitter, we might have as well used a directional coupler or a higher impedance probe.

### 7.3.8 Test Set-up for Reflection-Transmission Measurement

A reflection-transmission unit is normally employed for measurement of reflection and transmission. A reflection-transmission unit is shown in Fig. 7.11.

For transmission measurement, the reference line length is balanced and for reflection measurements the DUT is compared to the sliding short. A good balance between the channels can be maintained by use of accurately matched directional couplers in the bridge.

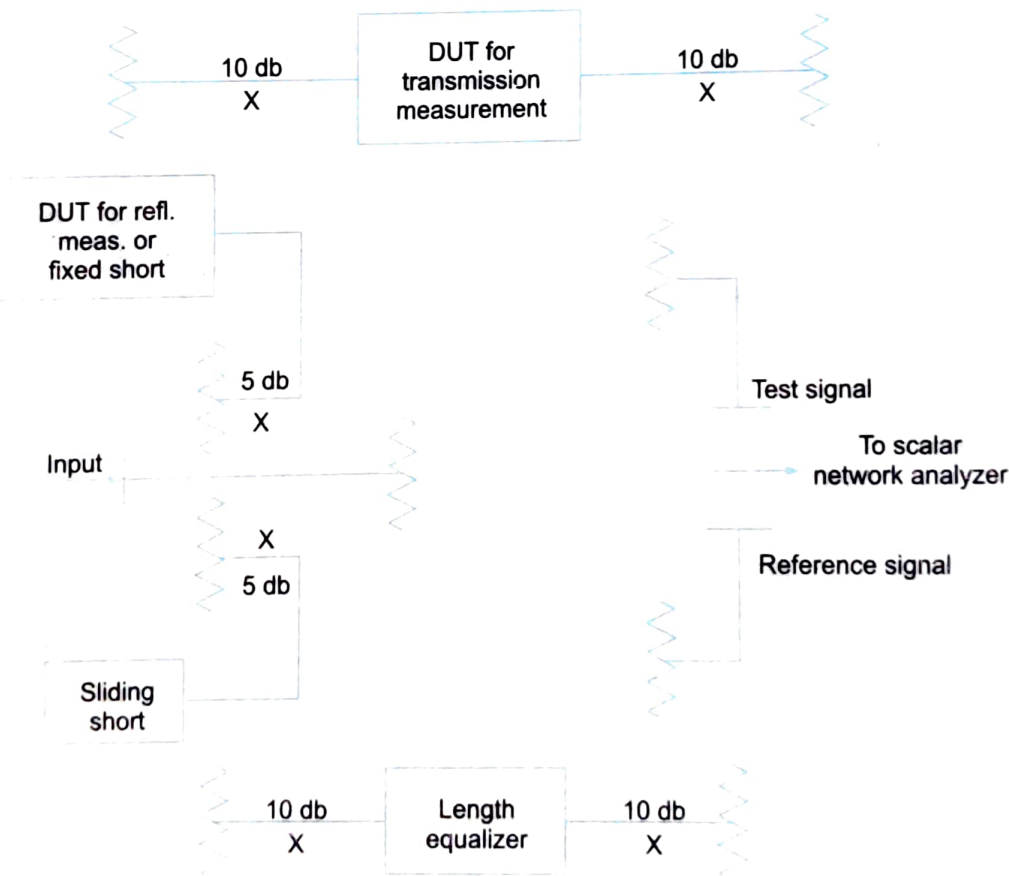


Fig. 7.11 Test set-up for reflection-transmitter measurement

### 7.3.9 Test Set-up for S-Parameter Measurement

It is possible to measure S-parameters using network analyser for a two port network. Such a scheme is shown in Fig. 7.12. The S-parameters of a two port network (DUT) can be obtained by measuring the amplitude and phase from the ports through the dual directional coupler as per Fig. 7.12a and b by interchanging the RF signal source and the load positions.

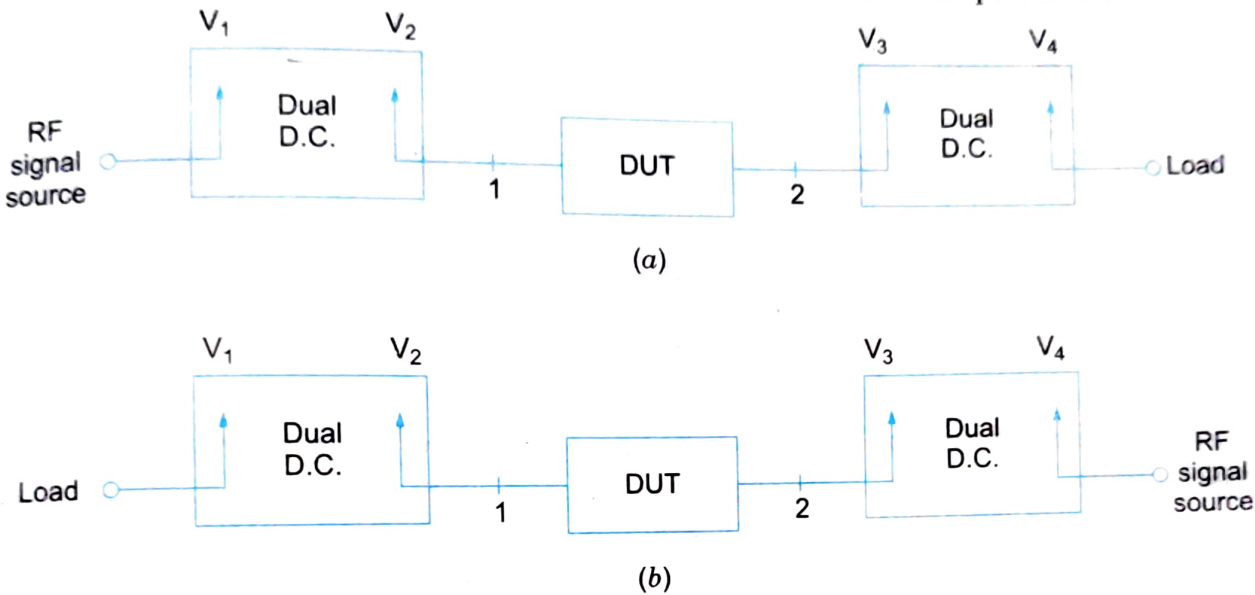


Fig. 7.12

From Fig. 7.12a

$$S_{11} = \frac{V_2}{V_1} (\phi_2 - \phi_1)$$

$$S_{21} = \frac{V_3}{V_1} (\phi_3 - \phi_1)$$

For measuring  $S_{22}$  and  $S_{12}$ , the RF signal source and load are interchanged as shown in Fig. 7.12b.

$$S_{22} = \frac{V_3}{V_4} (\phi_3 - \phi_4)$$

$$S_{12} = \frac{V_2}{V_4} (\phi_2 - \phi_4)$$

Thus with a scalar network analyser, it is possible to measure the transmitted and reflected signal magnitudes. Also, it can be employed to characterize many of the microwave devices such as antennas, amplifiers, RF bridges, attenuators, mixers, couplers, receivers, up/down converters, power-dividers etc.

A vector network analyser on the other hand can measure complex transmission-reflection characteristics of several microwave devices as a function of frequency, i.e., it measures both magnitude and phase information. It also compares the incident RF signal with the transmitted and reflected signals for measurement purpose. The major difference between vector network

analyser and scalar network analyser is the receiver architecture, complexity and detection technique. In a scalar network analyser, a diode detector is employed whereas the vector network analyser employs a multichannel receiver that is linear in its conversion characteristics. The broadband swept signal is converted to a fixed IF by employing fundamental or harmonic mixing. Magnitude of the signal can be measured in each of the receiver channels while phase relationship between any two receiver channels could also be measured. Thus complex impedances, phase delay characteristics, electrical delay, group delay and distance to fault in transmission structure measurements can be easily performed using vector network analyser.

## 7.4 FREQUENCY MEASUREMENT

Microwave frequency can be measured by either electronic or mechanical techniques.

### 7.4.1 Electronic Techniques

These techniques generally are more accurate but expensive. Frequency counters or high frequency heterodyne systems can be used. Here the unknown frequency is compared with harmonics of a known lower frequency is compared with harmonics of a known lower frequency by use of a low frequency generator, a harmonic generator and a mixer as shown in Fig. 7.13.

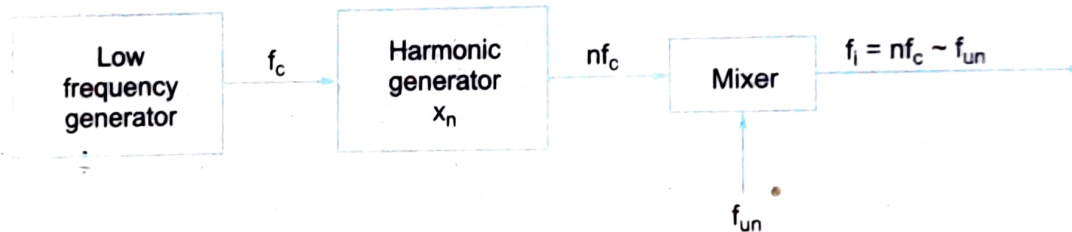


Fig. 7.13 Measurement of frequency-electronic method.

## 7.5 MEASUREMENT OF POWER

The microwave power inside a waveguide is invariant with position of measurement and the power measured is the average power. The technique used to measure power depends on whether the power to be measured is low or high. Thus we divide the measurement of power into three categories.

- (a) Measurement of low power (0.01 mW–10 mW)
  - Bolometer technique
- (b) Measurement of medium microwave power (10 mW–1 W)
  - Calorimetric Technique
- (c) Measurement of high microwave power (> 10 W)
  - Calorimetric Watt meter

### Measurement of low microwave power

Devices such as bolometers and thermocouples whose resistance changes with the applied power are capable of measuring low microwave powers. Bolometers are most widely used among these.

Bolometer is a simple temperature sensitive device whose resistance varies with temperature. These are of two types viz *Barretters* and *Thermistors*. *Barretters* have positive temperature coefficient and their resistance increases with an increase in temperature as shown in Fig. 7.14. It basically consists of a short length of fine platinum wire mounted in a cartridge, like an ordinary fuse. It is very delicate device. Thermistors have negative temperature coefficient of resistance and their resistance decreases with increase in temperature as shown in Fig. 7.15. Thermistors are basically semiconductor materials.

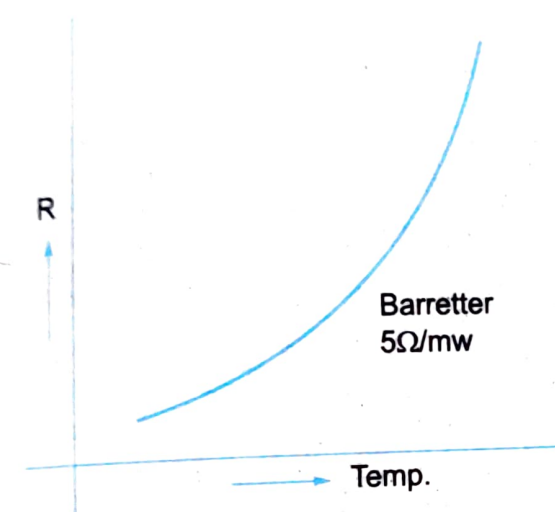


Fig. 7.14

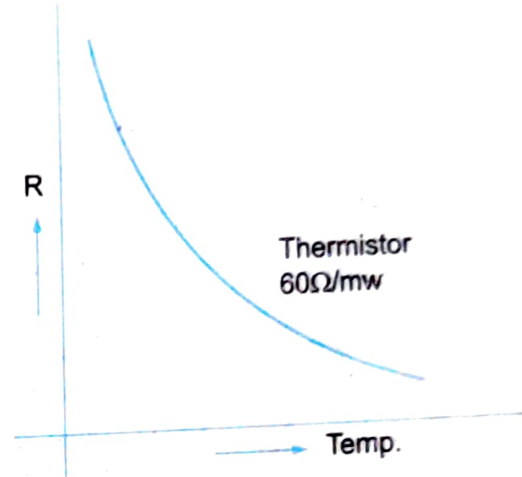


Fig. 7.15

A bolometer such as crystal diode is a square law device and it produces a current that is proportional to the applied power i.e. square of the applied voltage, rather than the applied voltage. Bolometer is mounted inside the waveguide as shown in Fig. 7.16, where the bolometer itself is used as a load, with the operation resistance as  $R_1 \Omega$ . Now the low microwave power which is to be measured is applied. Some power is absorbed in the bolometer load and dissipated as heat and the resistance changes to  $R_2$ . This change in resistance ( $R_1 \sim R_2$ ) is proportional to the microwave power which can be measured using a bridge. Inaccuracy is introduced due to bolometer non-linear characteristics.

In the *balanced bolometer bridge* technique, the bolometer itself is made to be one of the arms of the bridge as shown Fig. 7.17.

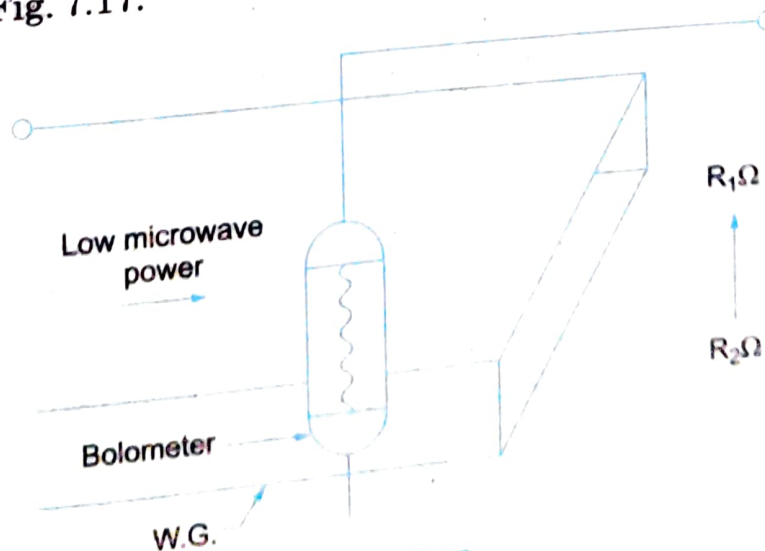


Fig. 7.16

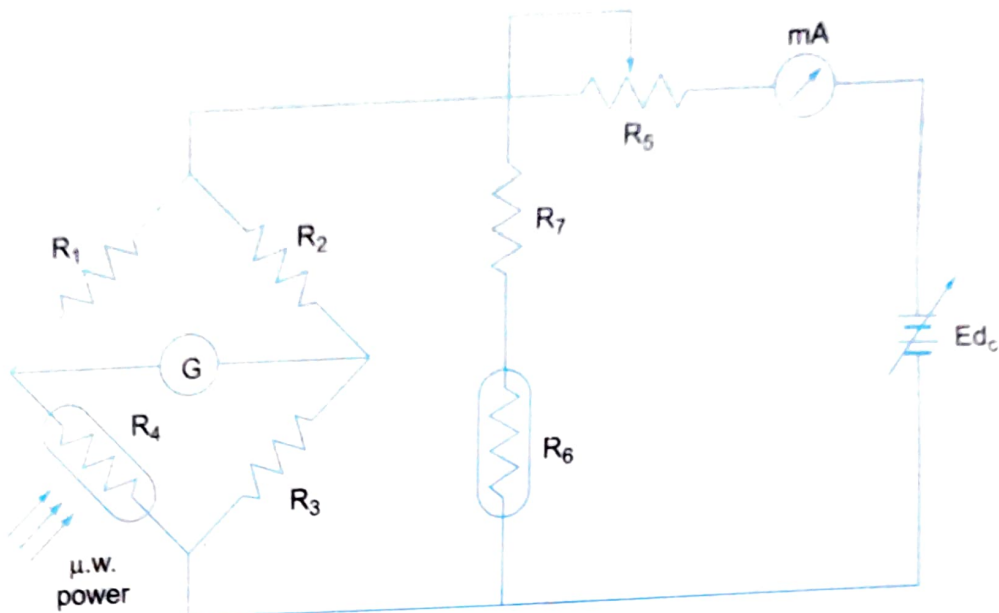


Fig. 7.17

Initially, the bridge is balanced by adjusting  $R_5$ , which varies the dc power applied to the bridge and the bolometer element is brought to a predetermined operating resistance before microwave power is applied. Let the voltage of the battery be  $E_1$  at balance. The microwave power is now applied and this power gets dissipated in the bolometer. The bolometer heats up and it changes its resistance. Therefore the bridge becomes unbalanced. The applied dc power is changed to  $E_2$  to get back the balance and this change in dc battery voltage ( $E_1 - E_2$ ) will be proportional to the microwave power. Alternately the detector 'G' can be directly calibrated in terms of microwave power so that when the bridge is unbalanced, the detector reads the microwave power directly.

**Errors.** Since bolometers are *temperature* sensitive some form of temperature compensation has to be used to avoid errors. By  $R_6$  and  $R_7$  resistors this can be achieved.  $R_6$  is identical and close to  $R_3$  i.e. both are bolometer elements as shown and subjected to the same ambient temperature. If temperature changes and reduces the resistance  $R_3$  (even in the absence of applied microwave power) this will not be interpreted as a microwave power change because the resistance  $R_6$  will be equally reduced. Thus more current will flow through it and hence lesser amount will flow through the bridge i.e. the current through  $R_3$  will be lowered and so will its temperature thus restoring the balance.

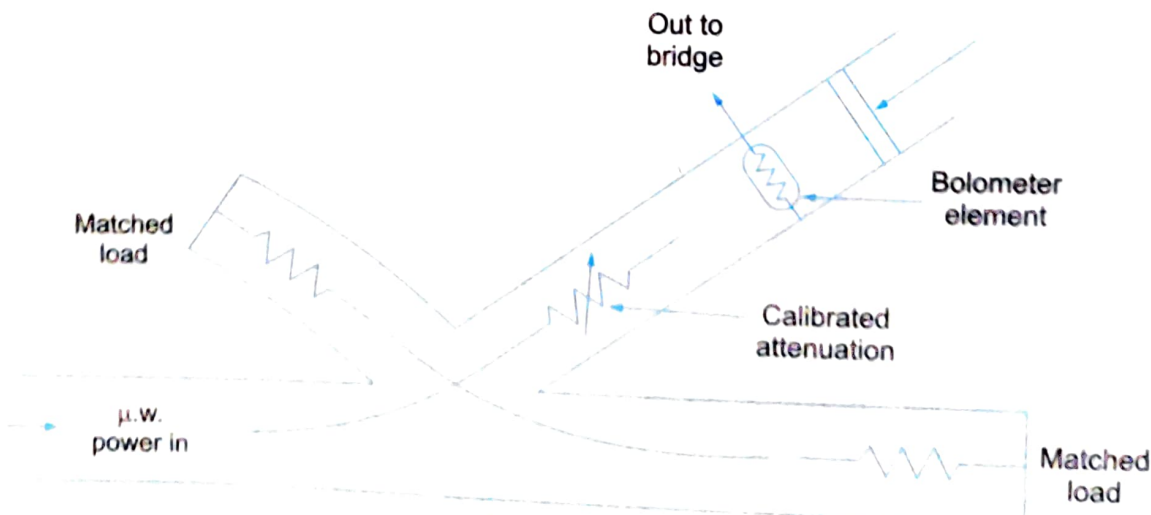


Fig. 7.18

**Limitations.** Barretters and Thermistors, both are limited in their power handling ability to about 10 mW, so that powers greater than 10 mW cannot be measured with them directly. However power measurement range can be increased by using a directional coupler as shown in Fig. 7.18.

If a 20 dB directional coupler and a 10 dB attenuator is used then the power received by the bolometer element will be 30 dB down (1/1000th of the power fed to the matched termination). This method extends the range of power by 1000 times. The only limitation of this method being the limited power handling capacity of directional coupler itself.

### (b) Measurement of medium power

Medium power as already stated is in the range of 10 mW to 10 W. Such powers can be measured by calorimetric techniques. The principle is very simple wherein the temperature rise of a special load monitored which is proportional to the power responsible for the rise as shown in Fig. 7.19. The special load must necessarily have high specific heat. Water happens to be a good load. Knowing mass, specific heat and temperature rise at a fixed and known rate of fluid flow, the power can be measured. Alternately rate of temperature rise with a fixed quantity of fluid also can be adopted for measurement of power.

The normally used method is the self balancing bridge technique. Figure 7.20 illustrates this technique.

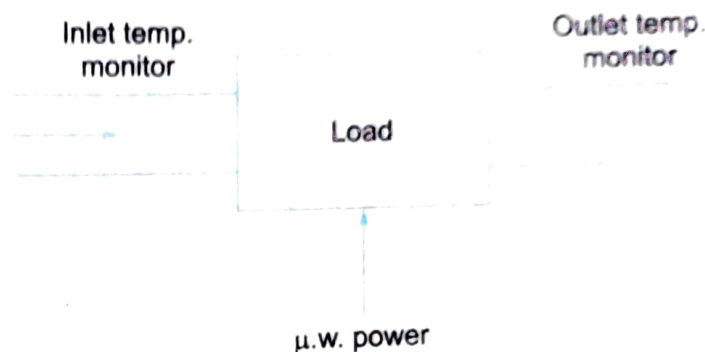


Fig. 7.19

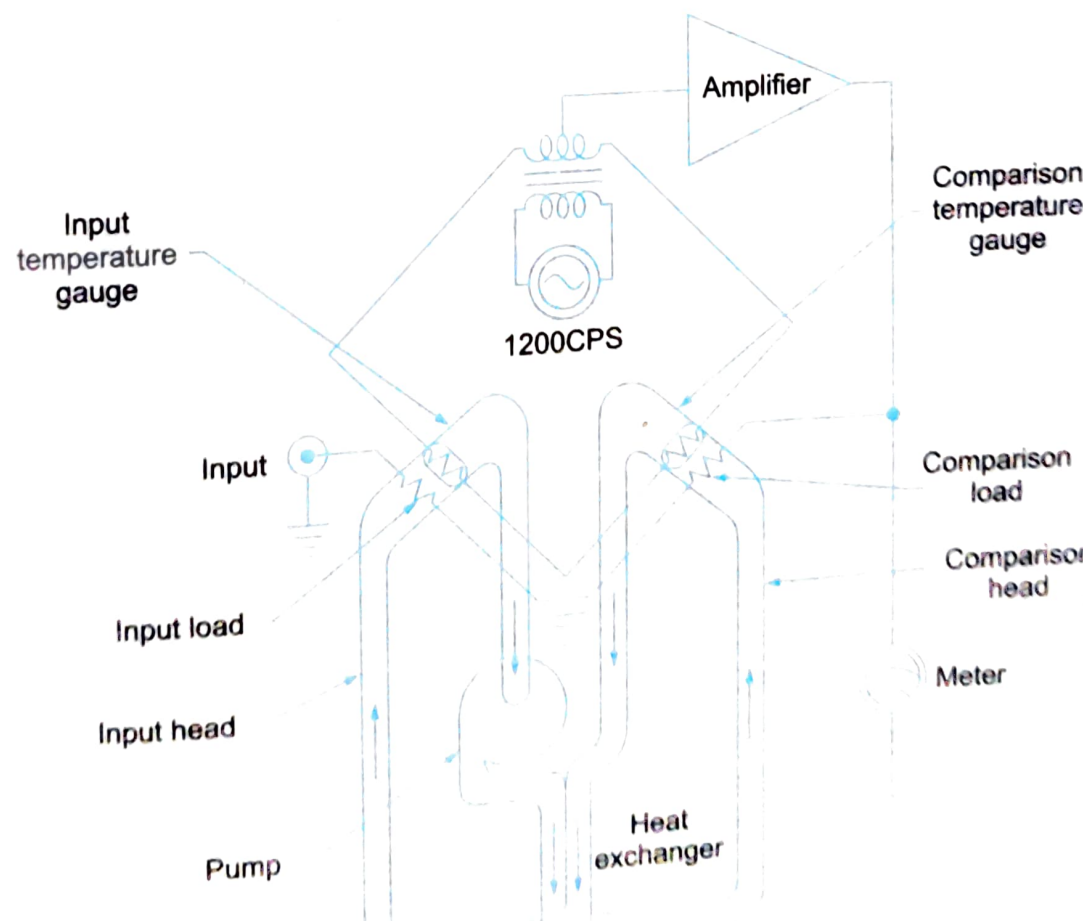


Fig. 7.20

It consists of identical temperature sensitive resistors or gauges in two arms, an indicating meter and two load resistors. The input load resistor senses the unknown input microwave power and the comparison head is associated with the comparison power. The input load power and input temperature gauge are placed close to each other so that the heat generated in the input load resistor raises the temperature of the gauge. This results in unbalancing the bridge. The signal due to the imbalance is amplified and then applied to the comparison load resistor which is placed closer to the comparison gauge. Hence, the heat generated in comparison load resistor is transferred to its gauge and the bridge is rebalanced. The meter measures the amount of power that is supplied to the comparison load in order to rebalance the bridge. It can be calibrated directly in terms of input microwave power. It is necessary that the characteristics of the two gauges be matched and also the heat transfer characteristics from each load be same for equal power dissipation in the two loads.

For quick balancing of the bridge and for efficient heat transfer from loads to the gauges, the components are immersed in an oil stream. Since the flow rates are the same through the two heads (that are having identical characteristics), the accuracy of power measurement is within  $\pm 5\%$ . To maintain constant temperature, the streams are passed through a parallel flow heat exchanger just before they enter the heads. The error signal is amplified by an amplifier and the 1200 Hz source and meter separated by means of a transformer which form the other arms of the bridge.

### (c) High Power

Any power between 10 W to 50 kW is considered high power. These are normally measured by calorimetric watt meters. These meters can be either dry type or flow type.

A dry type calorimeter normally consists of a co-axial cable which is filled by a dielectric with a high hysteresis loss. The flow type uses circulating water, oil or any liquid which is a good absorber of microwaves. The fluid after flowing through the load experiences a temperature rise due to microwave energy. The difference between the temperature ( $T_1$ ) of a known quantity of liquid before entering the load and the temperature ( $T_2$ ) after it emerges is a measure of the power which has been absorbed. Knowing the rate of the fluid flow the exact value of power can be calculated by using the equation

$$P = \frac{RK_p(T_2 - T_1)}{4.18} \quad \dots (7.1)$$

where,  $P$  = measured power in watts,

$R$  = rate of flow in  $(\text{cm}^3/\text{s})$

$K$  = specific heat in  $\text{cal/g}$

$\rho$  = specific gravity in  $\text{g/cm}^3$

and  $(T_2 - T_1)$  is the temperature difference in  $^\circ\text{C}$ .

It may be noted that in calorimeter measurements heat losses do occur due to conduction and radiations, resulting in erroneous measurement of power. Also errors in flow determination, calibration and thermal inertia etc cannot be neglected for accurate measurement.

## 7.6 ATTENUATION MEASUREMENT

Microwave components and devices almost always provide some degree of attenuation. Attenuation is the ratio of input power to the output power and is normally expressed in decibels.

$$\text{i.e. } \text{Attenuation (in dBs)} = 10 \log \frac{P_{\text{in}}}{P_{\text{out}}} \quad \dots(7.2)$$

where,  $P_{\text{in}}$  = input power and  $P_{\text{out}}$  = output power.

The amount of attenuation can be measured by two methods.

- (a) Power Ratio method
- (b) RF Substitution method.

### 7.6.1 Power Ratio Method

This method involves measuring the input power and output power with and without the device whose attenuation is to be measured as shown in set up 1 and set up 2 of Figs. 7.21 and 7.22. The powers are measured in each set up as  $P_1$  and  $P_2$ . The ratio of power  $P_1/P_2$  expressed in decibels gives the attenuation as in Eq. 7.2.

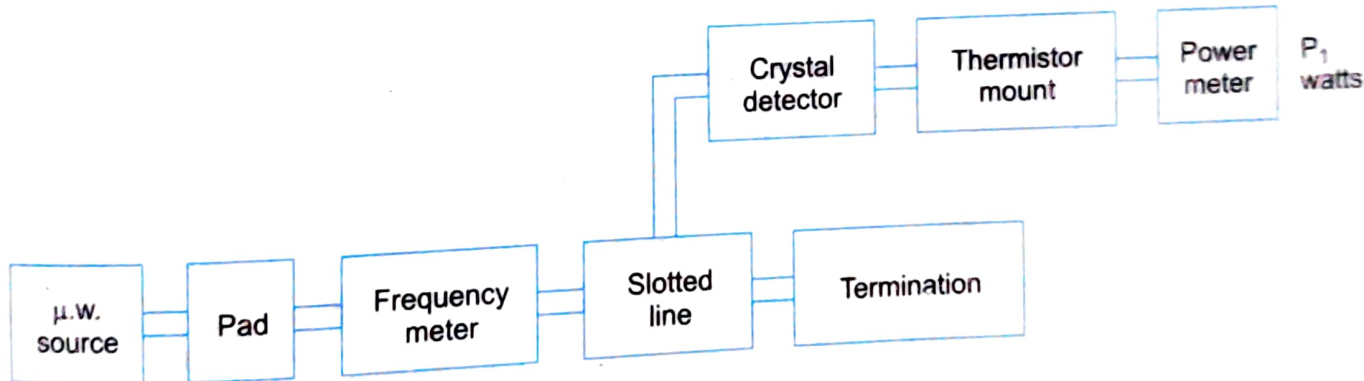


Fig. 7.21 Set up 1, power ratio method.

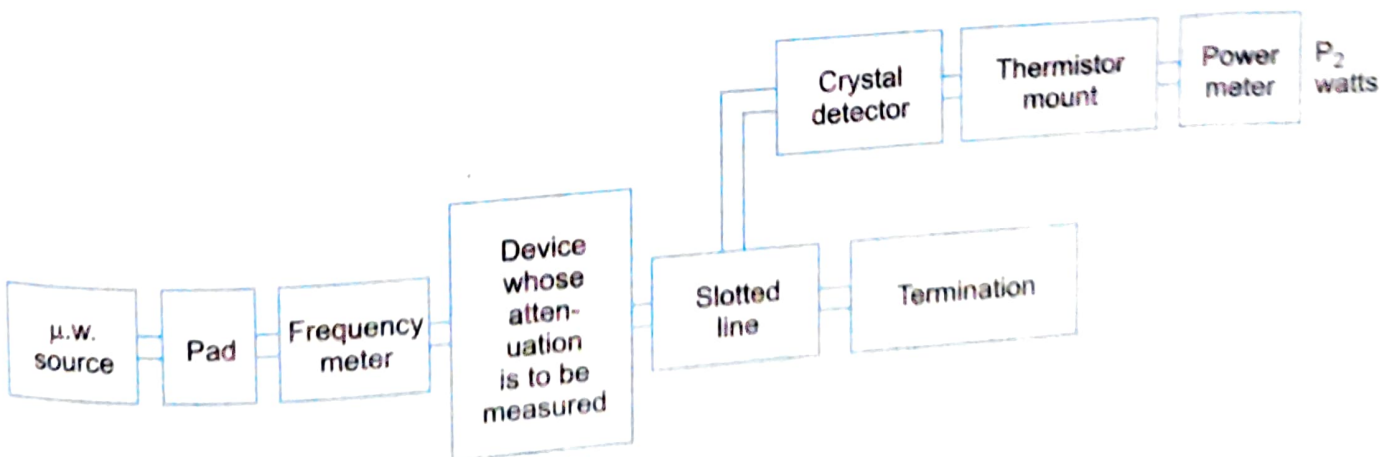


Fig. 7.22 Set up 2, power ratio method

The drawback of this method is that the attenuation measured corresponds to two power positions on the power meter with a square law crystal detector characteristics as shown by Fig. 7.23. Due to non-linear characteristics the two powers measured and the attenuation calculated will not be accurate particularly if the attenuation of the network is large and if the input power is low.

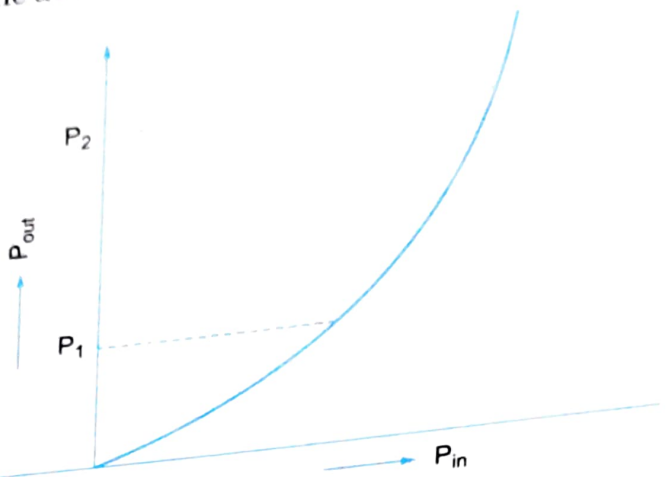


Fig. 7.23 Square law characteristics of crystal diode

### 7.6.2 RF Substitution Method

This method overcomes the drawback of power ratio method since here we measure attenuation at a single power position. The method consists of measuring the output power say ' $P$ ' by including the network whose attenuation is to be measured in set up 1 as shown in Fig. 7.24.

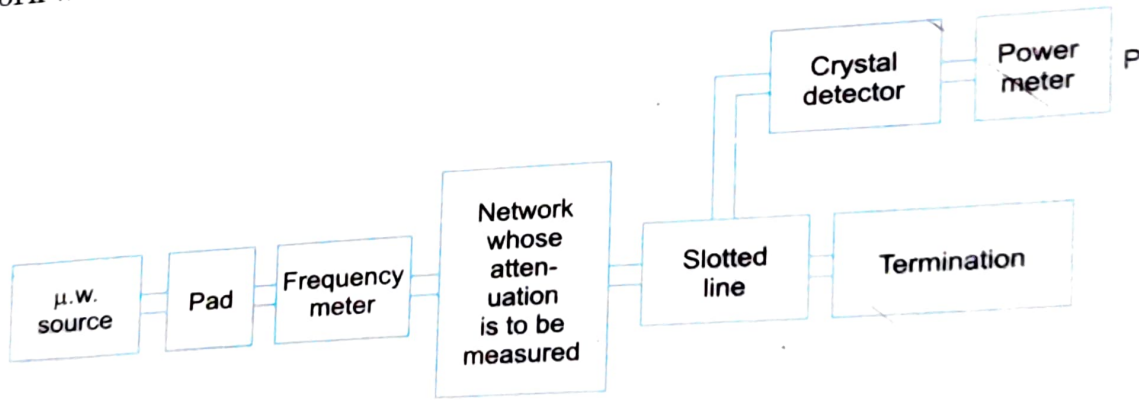


Fig. 7.24 Set up 1, RF substitution method.

In set up 2 (Fig. 7.25) this network is replaced by a precision calibrated attenuator which can be adjusted to obtain the same power ' $P$ ' as measured in set up 1. Under this condition the attenuation read on the precision attenuator would give attenuation of the network directly.

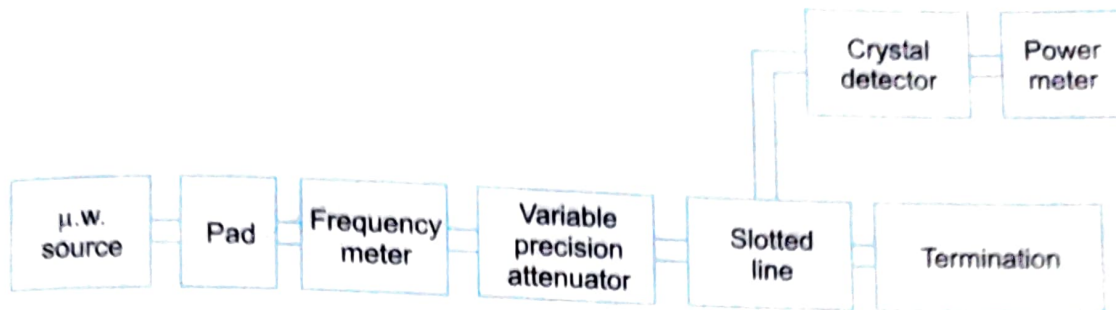


Fig. 7.25 Set up 2, RF substitution method.

## 7.7 MEASUREMENT OF PHASE SHIFT

The phase shift introduced by a microwave network can be measured by using the set up shown in Fig. 7.26. For determining the phase shift we must have an approximate idea of the network's electrical length as it is not possible to distinguish between one quarter wavelength and say, five quarter wavelengths.

Each wavelength ( $\lambda_g$ ) corresponds to a phase shift of  $2\pi$  radians. Knowing the approximate electrical length of the network phase shift can be determined to a fairly accurate value as follows.

Amplitude modulation of the source is done with a 1 kHz sine wave generator and the output is split up into two equal parts using the H-plane Tee junction, one going to the unknown network whose accurate phase shift is to be measured and the other to the comparison adjustable precision phase shifter. The standard phase shifter is now adjusted until the two demodulated 1 kHz sine waves on the CRO are in phase as shown by Fig. 7.27 and the relative phase shift of the two networks are now equal. The dial reading on the precision phase shifter now gives the phase shift offered by the device as shown by Fig. 7.28.

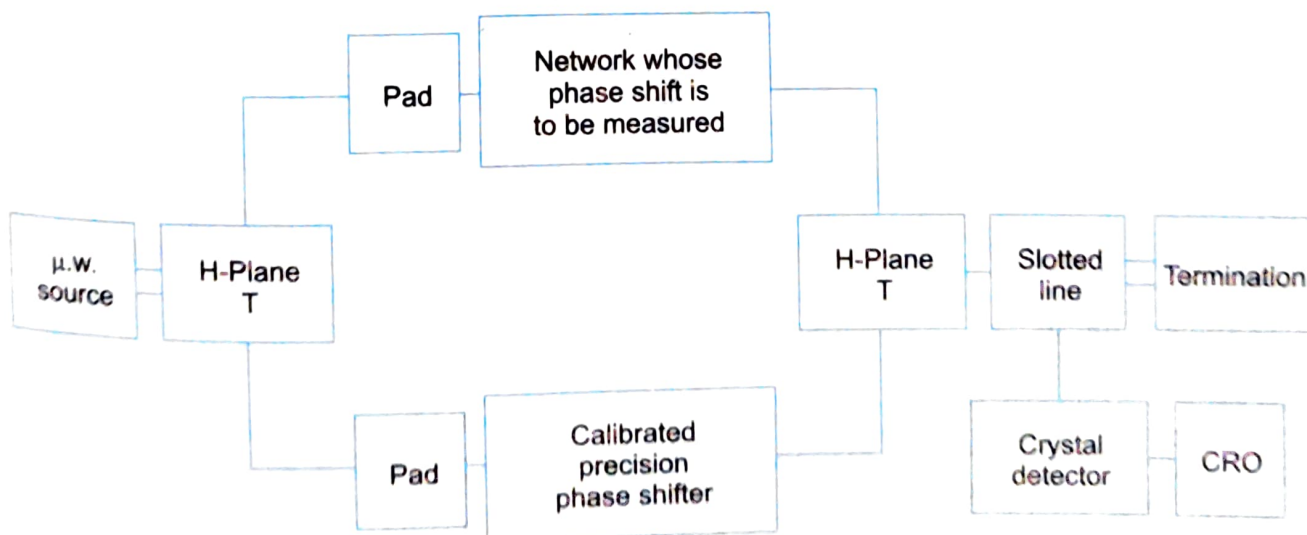


Fig. 7.26 Measurement of phase shift

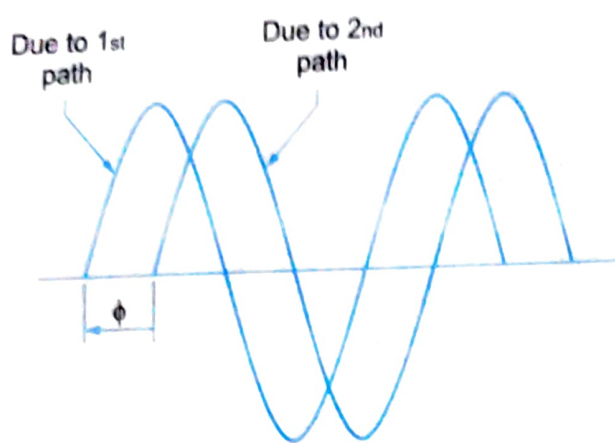


Fig. 7.27 Output of CRO.

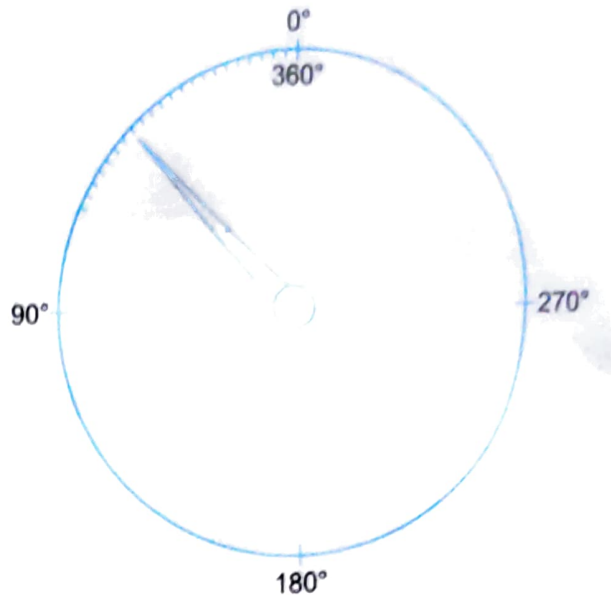


Fig. 7.28 Calibrated dial of the standard precision variable phase shifter.

For example the preliminary measurement showed the phase shift of the unknown network to be in the vicinity of  $3\lambda_g = 1080^\circ$  and the reading on the calibrated precision phase shifter is  $15^\circ$ . Then the total phase shift must be  $1080^\circ + 15^\circ = 1095^\circ$ . If the reading is  $320^\circ$ , then the total phase shift must be

$$[1080^\circ - (360 - 320)] = [1080^\circ - 40^\circ] = 1040^\circ.$$

## 7.8 MEASUREMENT OF VOLTAGE STANDING WAVE RATIO (VSWR)

Any mismatched load leads to reflected waves resulting in standing waves along the length of the line. The ratio of maximum to minimum voltage gives the VSWR as shown by Fig. 7.29.

i.e.

$$S = \frac{V_{\max}}{V_{\min}} = \frac{1 + \rho}{1 - \rho}$$

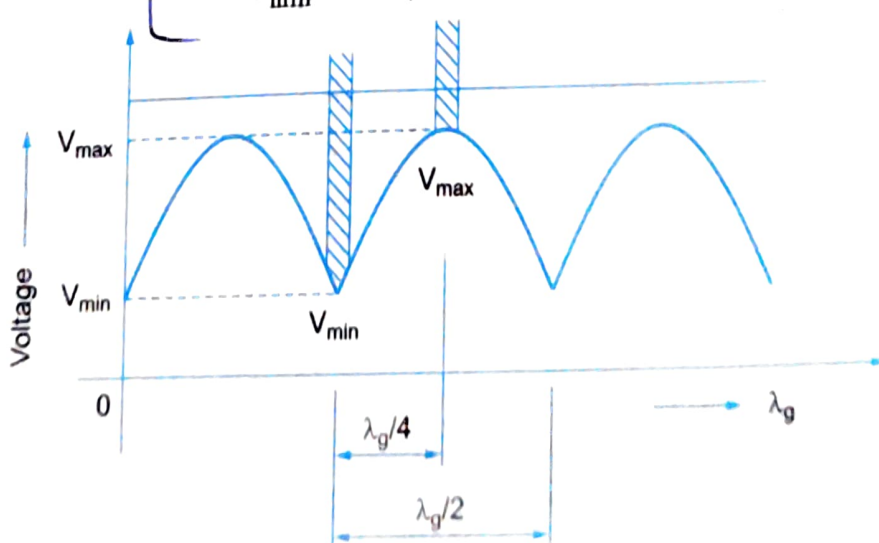


Fig. 7.29

where,  $\rho$  = reflection coefficient =  $\frac{P_{\text{reflected}}}{P_{\text{incident}}}$

$S$  varies from 1 to  $\infty$   
as  $\rho$  varies from 0 to  $\infty$   
Hence minimum value of  $S$  is unity.

T=

### 7.8.1 Measurement of Low VSWR's ( $S < 10$ )

Values of VSWR not exceeding 10 are very easily measured with the set up shown in Fig. 7.30 and can be read off directly on the VSWR meter calibrated as shown in Fig. 7.31. The measurement basically consists of simply adjusting the attenuator to give an adequate reading on the meter, which is a D.C. millivoltmeter. The probe on the slotted waveguide is moved to get maximum reading on the meter (corresponding to  $V_{\max}$ ). The attenuation is now adjusted to get full scale reading. This full scale reading is noted down. Next the probe on the slotted line is adjusted to get minimum reading on the meter (corresponding to  $V_{\min}$ ). The ratio of first reading to the second (i.e.  $V_{\max}/V_{\min}$ ) gives the VSWR.

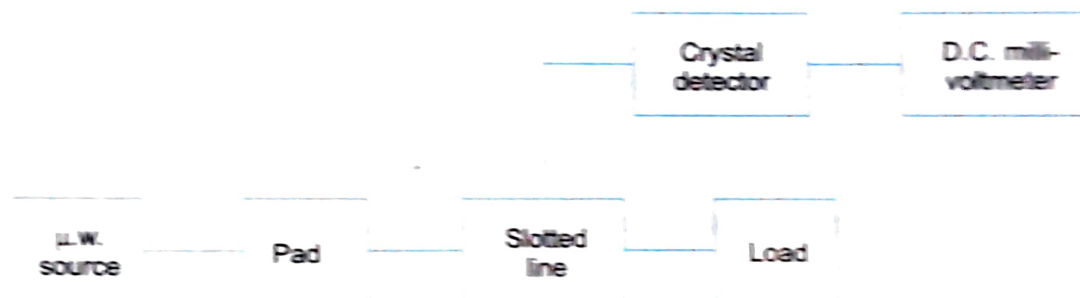


Fig. 7.30

The meter itself can be calibrated in terms of VSWR. In this case, the probe carriage is moved to give maximum deflection on the VSWR meter by adjusting the pad. This full scale deflection (FSD) corresponds to a VSWR of 1. As an example, a FSD of 10 mV corresponds to a VSWR of 1. The travelling probe is adjusted to get minimum reading on the meter. If this corresponds to 5 mV,

then  $\text{VSWR} = \frac{10 \text{ mV}}{5 \text{ mV}} = 2$ . If it is 3.3 mV,  $\text{VSWR} = 3$ , if it is 2.5 mV,  $\text{VSWR} = 4$ . If it is 1 mV,  $\text{VSWR} = 10$  etc. i.e. Such a calibrated VSWR meter gives an expanded scale upto an VSWR of 2 but for  $\text{VSWR} > 10$ , the meter will be congested and the measurement will not be accurate for VSWR's  $> 10$ . Hence this method is not useful for VSWR's  $> 10$ .

### 7.8.2 Measurement of High VSWR ( $S > 10$ )

For VSWR's  $> 10$ , we use what has come to be known as the *double minimum method*. In this method, the probe is inserted to a depth where the minimum can be read without difficulty. The probe is then moved to a point where the power is twice the minimum. Let this position be denoted by  $d_1$ . The probe is then moved to twice the power point on the other side of the minimum (say  $d_2$ ) as shown in Fig. 7.31, we get

$$2P_{\min} \propto V_x^2$$

$$\frac{1}{2} = \frac{V_{\min}^2}{V_x^2}$$

or

$$V_x^2 = 2(V_{\min})^2$$

or

$$V_x = \sqrt{2} V_{\min}$$

Further for TE<sub>10</sub> mode,  $\lambda_c = 2a$

$$\lambda_o = c/f$$

$$\lambda_g = \frac{\lambda_o}{\sqrt{1 - (\lambda_o / \lambda_c)^2}}$$

Then VSWR can be calculated using the empirical relation,

$$\boxed{\text{VSWR} = \frac{\lambda_g}{\pi(d_2 - d_1)}}$$

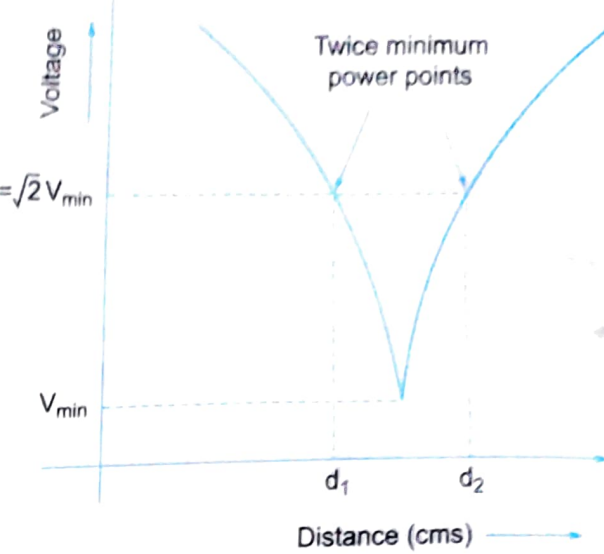


Fig. 7.31

## 7.9 MEASUREMENT OF IMPEDANCE

Impedance at microwave frequencies can be measured using any of the following 3 methods.

- (a) using Magic T (as already discussed in Magic T applications)
- (b) using slotted line and
- (c) using reflectometer.

### 7.9.1 Measurement of Impedance using Slotted Line

Incident and reflected waves will be present proportional to the *mismatch* of the load under test (whose impedance is to be measured) resulting in standing waves. Using slotted waveguide and with the load  $z_L$  in the circuit given by Fig. 7.32, the position of  $V_{\max}$  and  $V_{\min}$  can be accurately determined.

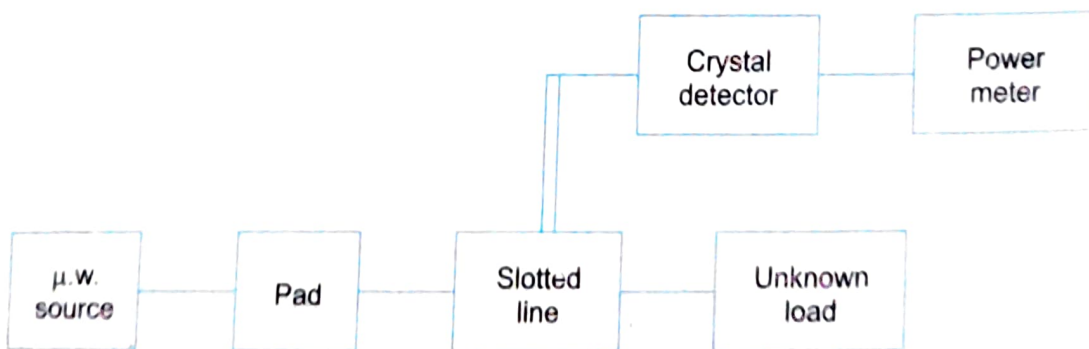


Fig. 7.32 Set up 1. Impedance measurement using slotted line

Now the load  $z_L$  is replaced by a short circuit as shown by Fig. 7.33 and the shift in minimum is measured. If the minimum is shifted to the left, then the impedance is *inductive* and if it shifts to the right, it is *capacitive* (Fig. 7.34). Unknown impedance can be obtained by usual methods using the data recorded and a smith chart. Both impedance and reflection coefficient can be obtained in *magnitude* and *phase*.

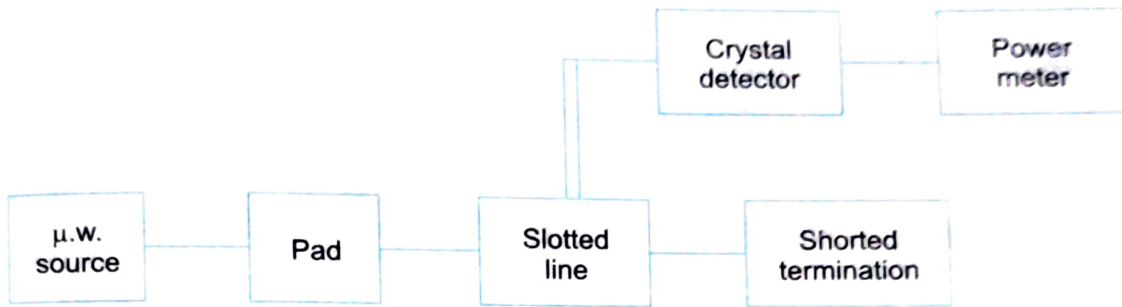


Fig. 7.33 Set up 2, impedance measurement using slotted line.

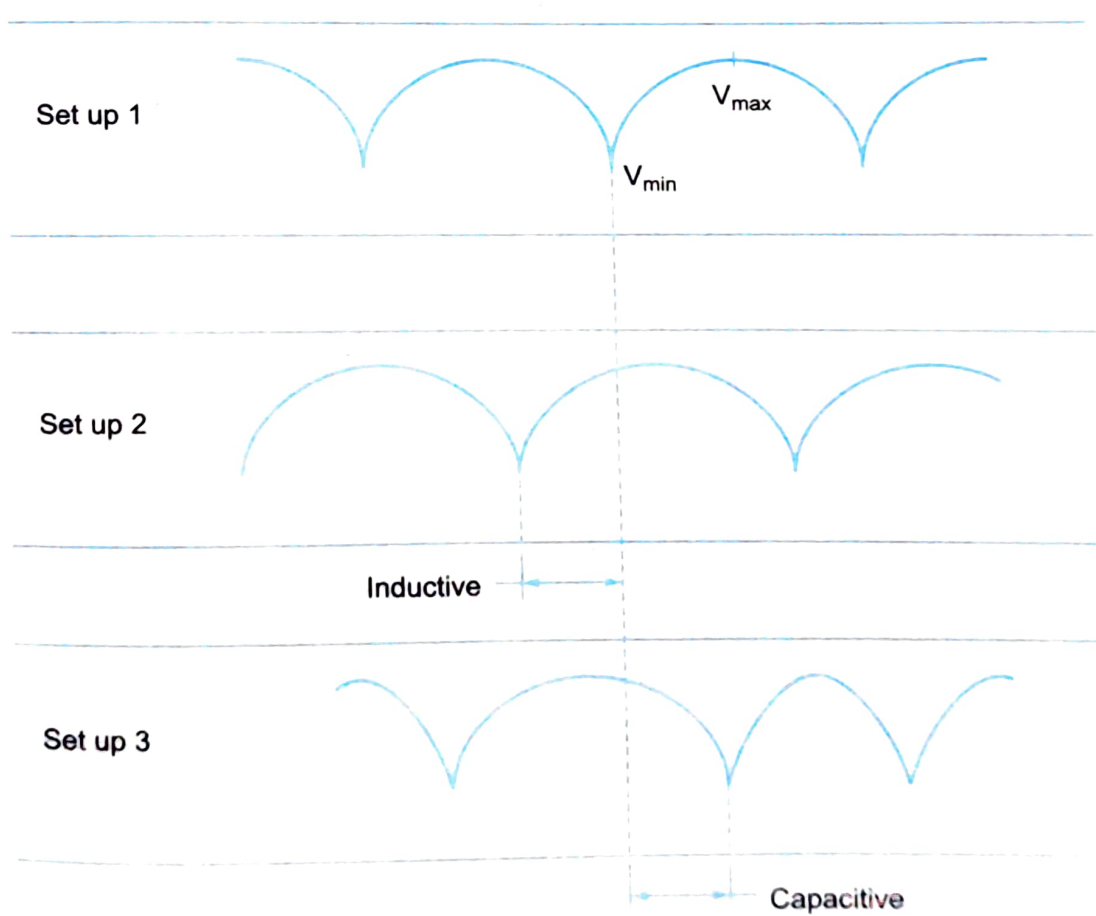


Fig. 7.34 Output standing waves of set up 1 and 2.

### 7.9.2 Measurement of Impedance using Reflectometer

The reflectometer indicates magnitude of impedance but not the phase angle, whereas a slotted line waveguide measurement gives both. A typical set up for reflectometer technique is shown in Fig. 7.35 where two directional couplers are used to sample the incident power  $P_i$  and the reflected power  $P_r$  from load. Both the directional couplers are identical (except their direction). The magnitude of the reflection coefficient  $\rho$ , can be directly obtained on the reflectometer from which impedance can be calculated.

From reflectometer reading we have,

$$\rho = \sqrt{\frac{P_r}{P_i}}$$

Knowing  $\rho$  we can calculate VSWR and impedance by using the relations

$$S = \frac{1 + \rho}{1 - \rho} \quad \text{and} \quad \frac{z - z_g}{z + z_g} = \rho$$

where  $z_g$  is the known wave impedance and  $z$  is unknown impedance.

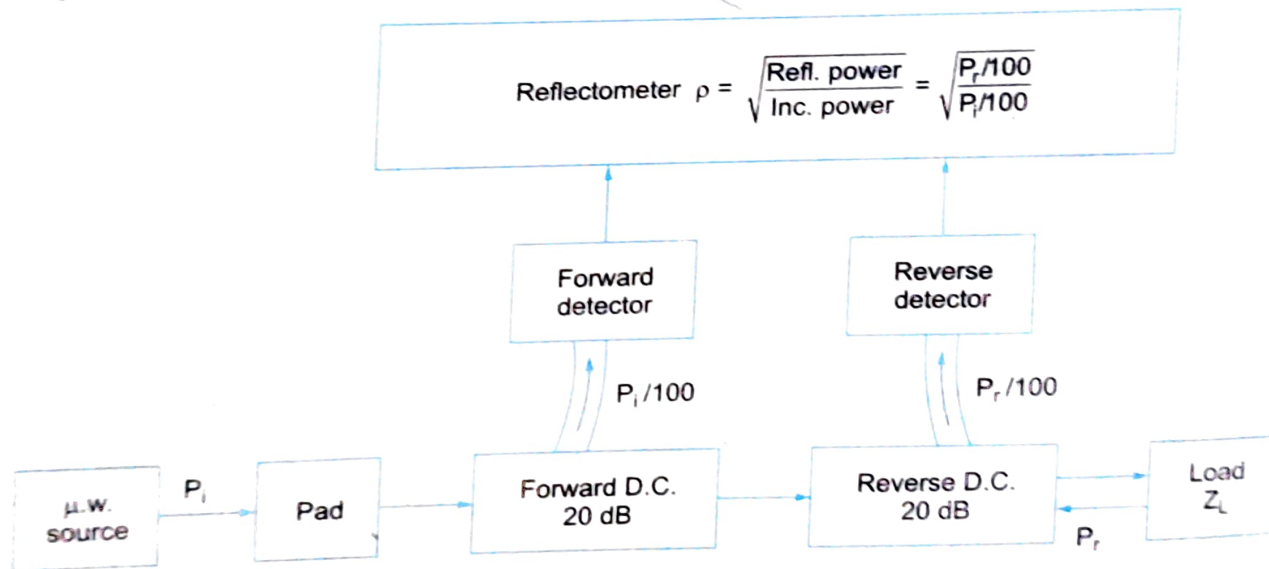


Fig. 7.35 Set up for measuring impedance using reflectometer.

Due to directional property of the couplers, there will be no interference between forward and reverse waves. The input power is kept to a low level by means of pad. The reflectometer accuracy is greatest at low VSWR (i.e. low reflection coefficient).

# 8

# *Microwave Tubes and Circuits*

## **8.1 INTRODUCTION**

At microwave frequencies, the size of electronic devices required for generation of microwave energy becomes smaller and smaller. This results in lesser power handling capability and increased noise levels. Electronic devices such as tubes and transistors will be required even at microwave frequencies. As expected, the tubes can provide higher output powers while transistors (Semi-conductor devices) are smaller have lesser noise, better reliability with reduced output power levels.

Conventional triodes, tetrodes and pentodes are useful only at low microwave frequencies. Special tubes would be required even at UHF frequencies (300–3000 MHz) as conventional tubes have certain limitations at microwave frequencies which will be discussed in section 8.2. However all tubes including UHF tubes are bound to fail at higher microwave frequencies due to their limitations at these frequencies.

In this chapter we shall discuss the most important microwave tubes such as two cavity klystron, multicavity klystron, reflex klystron, travelling wave tube, backward wave oscillator and the magnetron as well as the UHF tubes.

## **8.2 HIGH FREQUENCY LIMITATIONS OF CONVENTIONAL TUBES**

To see whether or not a conventional device like a triode or a transistor works satisfactorily at higher frequencies say UHF or at microwave frequencies, we can consider a simple oscillator and try to increase the operating frequency. In this process one would quite naturally proceed to reduce the tank circuit parameters i.e., either  $L$  or  $C$ . But what is the limit upto which one can decrease the value of the tank circuit elements? The natural answer is one can go upto the limit wherein still the operational frequency of the oscillator is decided by the external circuit components

(i.e.,  $L$  and  $C$  components of the tank circuit). At this point, the device parameters like the inter electrode capacitance and lead inductance are negligible. As the frequency of operation is made higher than this, these device parameters start taking dominating part in the circuit and affect the operation of the oscillator i.e., the circuit condition required for operation as an oscillator or as an amplifier may not be satisfied and the device at these frequencies becomes useless as an oscillator or as an amplifier. There are other reasons too, i.e., conventional devices (tubes or transistors) cannot be used for frequencies  $> 100$  MHz because of the following effects

1. Inter electrode capacitance effect
2. Lead inductance effect
3. Transit time effect
4. Gain bandwidth limitation
5. Effect due to RF losses (the conductance/skin depth or  $I^2R$  losses and the dielectric losses), and
6. Effect due to radiation losses.

### 8.2.1 Inter Electrode Capacitance (IEC) Effect

As frequency increases, the reactance  $X_c = 1/2 \pi f C$ , decreases and the output voltage decreases due to shunting effect. Because at higher frequencies  $X_c$  becomes almost a short.  $C_{gp}$ ,  $C_{gk}$  and  $C_{pk}$  are the IEC's which come into effect and are shown in Fig. 8.1.

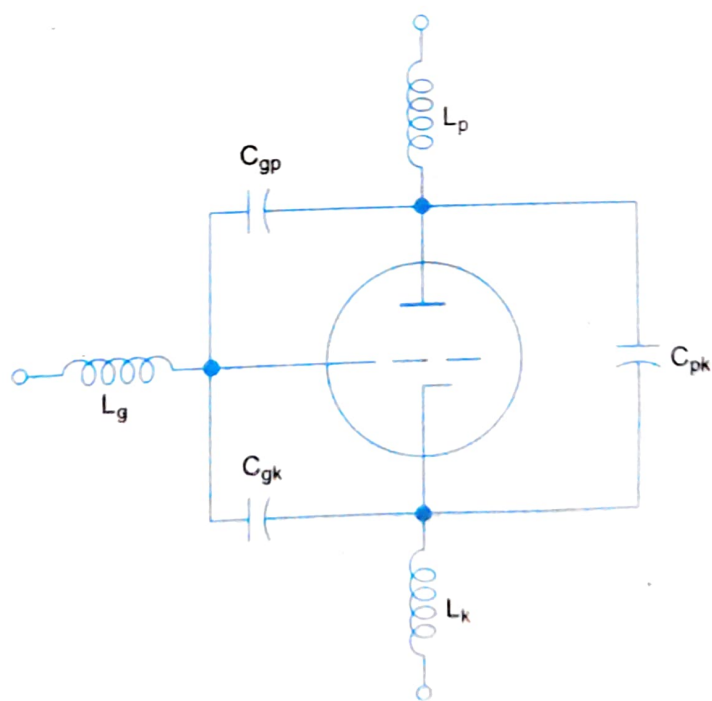


Fig. 8.1

The effect of IEC can be minimised by reducing the IEC's  $C_{gk}$ ,  $C_{pk}$  and  $C_{gp}$ . These can be reduced by decreasing the area of the electrodes (since  $C = \epsilon_0 \epsilon_r A/d$ ) i.e., by using smaller electrodes or by increasing the distance between electrodes.

### 8.2.2 Lead Inductance (LI) Effect

As frequency increases, the reactance  $X_L = 2\pi f L$ , increases and hence the voltages appearing at the active electrodes are less than the voltages at the base pins. This results in reduced gain for the tube amplifier.  $L_k$ ,  $L_p$  and  $L_g$  are the lead inductances that limit the performance of the tube and are shown in Fig. 8.1.

The effect of LI can be minimised by decreasing  $L$ . Since  $L$  is proportional to reactance ( $L = l/\mu_0 \mu_r A$ ),  $L$  can be decreased by using larger sized short leads without base pins i.e., by increasing 'A' and decreasing 'l'. This however reduces the power handling capability.

### 8.2.3 Transit Time Effect

Transit time is the time taken for the electron to travel from cathode to anode as shown in Fig. 8.2.

$$\text{i.e.,} \quad \text{Transit time} = \tau = \frac{d}{v_0}$$

where,  $d$  = distance between anode and cathode

$v_0$  = velocity of electrons.

Static energy of electrons =  $eV$

$$\text{Kinetic energy} = \frac{1}{2}mv_0^2$$

Under equilibrium, Static energy = Kinetic energy

$$\text{i.e.,} \quad eV = \frac{1}{2}mv_0^2$$

$$\text{or} \quad v_0 = \sqrt{\frac{2eV}{m}} \quad \dots(8.1)$$

$$\therefore \quad \tau = \frac{d}{\sqrt{\frac{2eV}{m}}} \quad \dots(8.2)$$

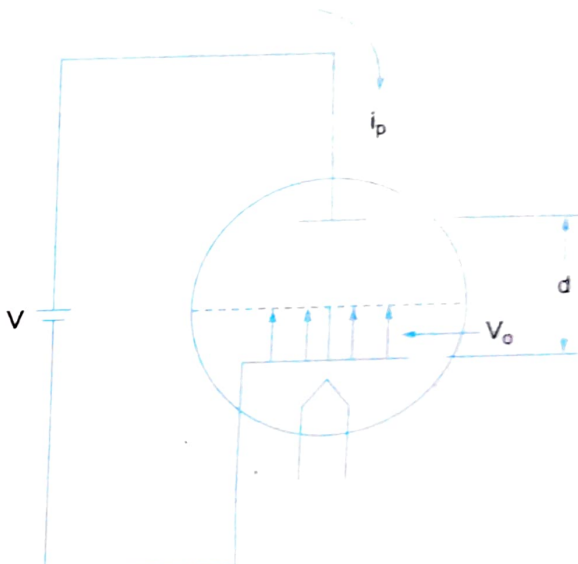


Fig. 8.2

At low frequencies, transit time is negligible compared to the period of the signal as shown in Fig. 8.3.

$$g_m = \frac{\Delta i_p}{\Delta V_g}$$

i.e., both  $V_g$  and  $i_p$  are in phase. Therefore the plate current ' $i_p$ ' responds immediately or instantaneously to changes in control grid voltage ' $V_g$ ' i.e.,  $V_g$  and  $i_p$  are in phase.

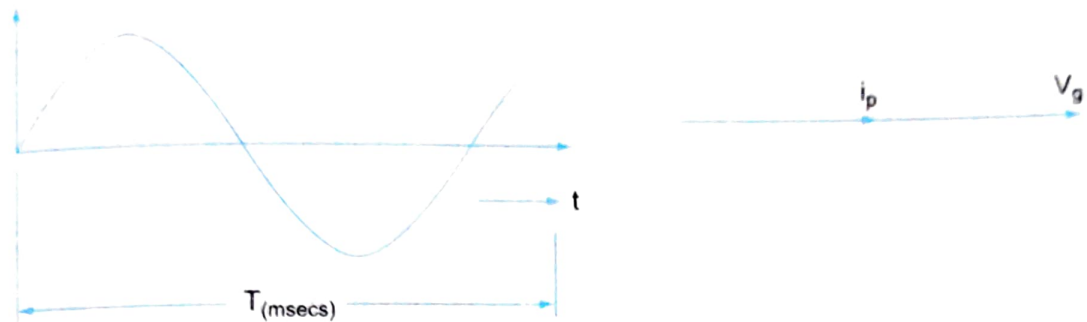


Fig. 8.3

At high frequencies the transit time ' $\tau$ ' is comparable with the period of the signal which is very small-nano seconds, as shown in Fig. 8.4.

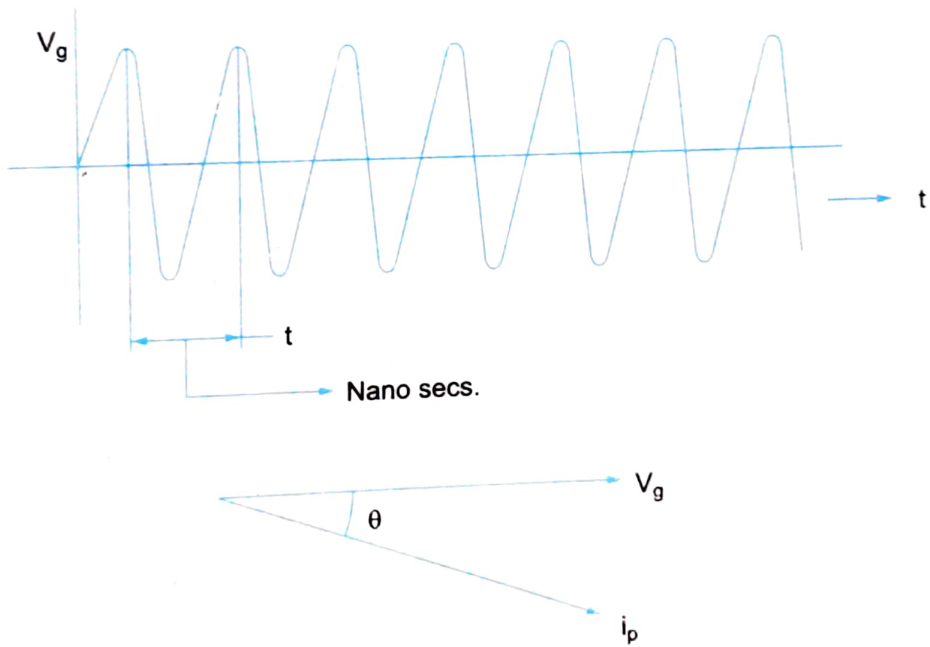


Fig. 8.4

i.e.,  $i_p$  lags  $V_g$  and  $g_m$  becomes a complex quantity. Therefore change in plate current occurs after a finite delay with respect to change in control grid voltage  $V_g$ . Hence the plate current lags behind the control grid voltage or in other words the transconductance ' $g_m$ ' becomes a complex quantity as now it has a lagging phase angle. The gain then becomes complex (since  $A = -g_m r_p R_L/r_p + R_L$ ) even for a resistive load and real gain falls. It can be shown that  $Y_{in} = \omega^2 L_k g_m C_{gk} + j\omega C_{gk}$  (as in the next section 8.2.4). This equation shows that grid circuit absorbs power even if the grid is negative with respect to cathode and is proportional to the square of the frequency.

## Remedy for Transit Time Effect

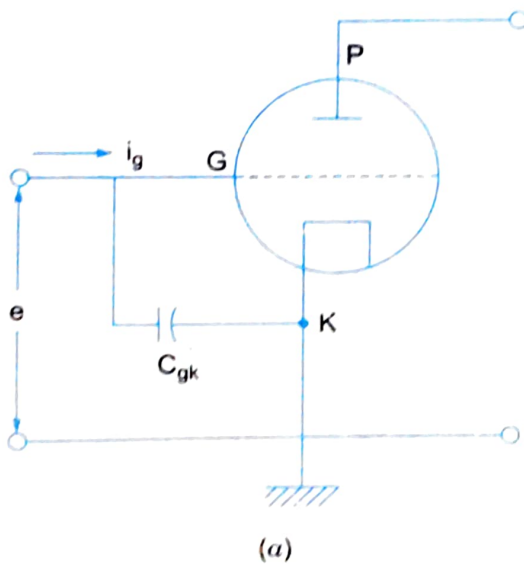
To minimise transit time ( $\tau = d / \sqrt{2 eV/m}$ ),  $d$ , the separation between electrodes can be decreased (but this increases IEC) and the plate to cathode potential 'V' can be increased (this can not be increased indefinitely). Therefore a trade off between IEC and transit time is a must.

### 8.2.4 Combined Effect of LI, IEC and Transit Time

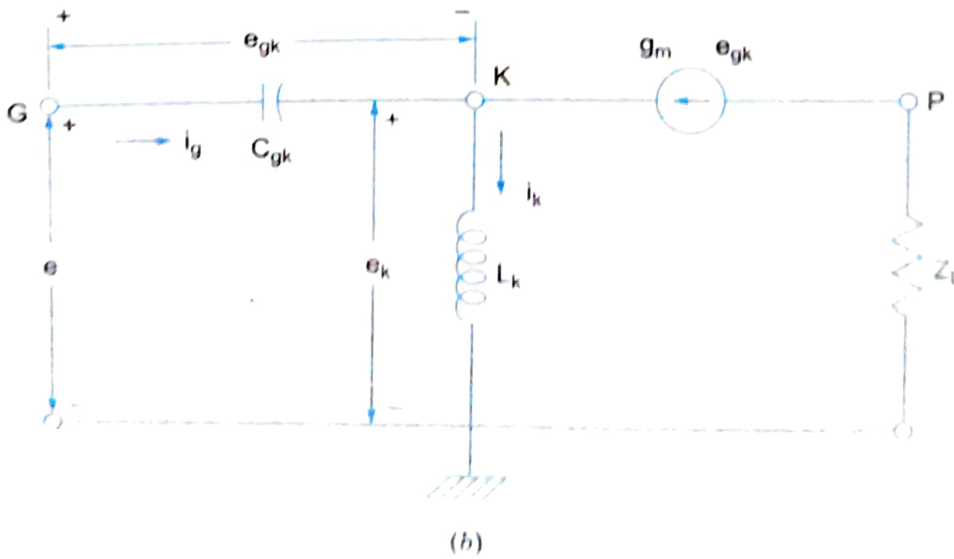
Assuming that the effect of  $L_p$ ,  $L_g$ ,  $C_{gp}$ ,  $C_{ph}$  and  $r_p$  are negligible, the equivalent circuit of the tube can be shown as in Fig. 8.5a and b. Now we shall prove that the input admittance  $y_{in}$  is directly proportional to square of the angular frequencies.

At low frequencies,  $X_L = 2\pi f L$  is so small that effect of  $L_k$  can also be neglected. Referring to Fig. 8.5b,

$$y_{in} = \frac{i_g}{e} \quad \dots (8.3)$$



(a)



(b)

Fig. 8.5

$$e = i_g \cdot X_{C_{gk}}$$

$$y_{in} = \frac{i_g}{i_g X_{C_{gk}}} = j\omega C_{gk} \quad (\text{i.e., } y_{in} \text{ is imaginary at low frequencies})$$

At high frequencies,  $L_k$  is also considered.

Applying KVL,

$$e = e_{gk} + e_k \quad \dots(8.4)$$

Applying KCL,

$$i_k = i_g + g_m e_{gk} \quad \dots(8.5)$$

We have,

$$e_{gk} = i_g \cdot X_{C_{gk}} = \frac{i_g}{j\omega C_{gk}}$$

$$i_g = j\omega C_{gk} e_{gk} \quad \dots(8.6)$$

$$e_k = i_k \cdot X_{Lk} = j\omega L_k i_k$$

$$e_k = j\omega L_k \cdot (i_g + g_m e_{gk}) \quad \dots(8.7)$$

From Eqs. 8.4, 8.6 and 8.7,

$$\begin{aligned} e &= e_{gk} + e_k \\ e &= e_{gk} + j\omega L_k i_g + j\omega g_m e_{gk} L_k \\ &= e_{gk} + j\omega L_k (j\omega C_{gk} e_{gk}) + j\omega g_m e_{gk} L_k \\ e &= e_{gk} [1 + j\omega g_m L_k - \omega^2 L_k C_{gk}] \end{aligned} \quad \dots(8.8)$$

Substituting for  $e$  and  $i_g$  from Eqs. 8.8 and 8.6 in Eq. 8.3, we get

$$y_{in} = \frac{i_g}{e} = \frac{j\omega C_{gk} \cdot e_{gk}}{e_{gk} [(1 - \omega^2 L_k C_{gk}) + j\omega L_k g_m]} \quad \dots(8.9)$$

$$y_{in} = \frac{j\omega C_{gk}}{1 - \omega^2 L_k C_{gk}} \left[ \frac{1}{1 + \left( \frac{j\omega L_k g_m}{1 - \omega^2 L_k C_{gk}} \right)} \right] \quad \dots(8.9)$$

We know that,

$$\frac{1}{1+x} = (1+x)^{-1} = 1-x+x^2-x^3+\dots \approx 1-x$$

(from binomial series)

$$y_{in} = \frac{j\omega C_{gk}}{1 - \omega^2 L_k C_{gk}} \left[ 1 - \frac{j\omega L_k g_m}{1 - \omega^2 L_k C_{gk}} \right]$$

If,  $\omega^2 L_k C_{gk} \ll 1$  (assumption)  
then  $1 - \omega^2 L_k C_{gk} \approx 1$ .

$$y_{in} \approx (j\omega C_{gk}) (1 - j\omega L_k g_m)$$

$$y_{in} \approx \underline{\omega^2 L_k C_{gk} g_m} + j\omega C_{gk}$$

i.e.,  $y_{in}$  above has a real and an imaginary component. Real component is the conductive component which absorbs power from the signal source, the amount of which is proportional to square of the frequency. One more observation one can make from the Fig. 8.5a, is that a part of the signal input is dropped across ' $L_k$ ' or in other words the net voltage available for amplification which appears actually across the active part of grid and cathode goes on decreasing as the frequency of operation

is increased. That is, the output voltage or the amplification of the amplifier goes on decreasing at higher and higher frequencies.

### 8.2.5 Gain Bandwidth Limitation

Maximum gain is achieved when the tuned circuit is at resonance. Referring to the equivalent circuit in Fig. 8.6, we have by transfer function,

$$\text{Gain, } G = \frac{V_o(s)}{V_i(s)} = Z_o(s)$$

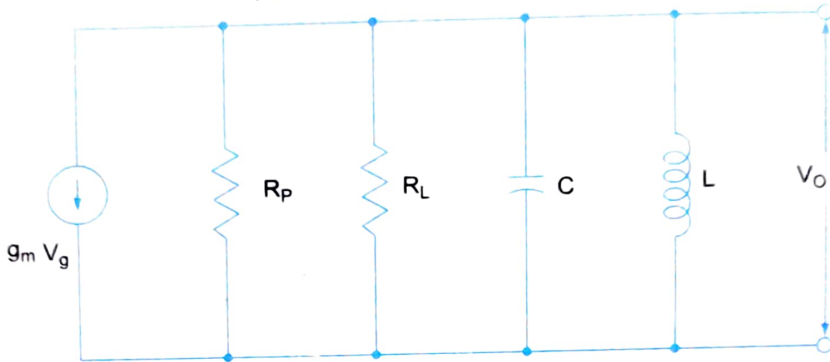


Fig. 8.6 Equivalent circuit.

Applying Laplace transform to the parallel circuit and replacing  $R_L$  and  $R_P$  by  $R = \frac{1}{R_L} + \frac{1}{R_P}$ ,

$$\frac{1}{Z_o(s)} = Y_o(s) = Cs + \frac{1}{Ls} + \frac{1}{R} = \frac{s^2 LCR + Ls + R}{RLs}$$

or

$$Z_o(s) = \frac{s/C}{s^2 + \frac{s}{CR} + \frac{1}{LC}}$$

The characteristic equation is given by the denominator  $s^2 + \frac{1}{CR}s + \frac{1}{LC}$ . The roots of the quadratic equation give the extreme frequencies  $\omega_1$  and  $\omega_2$  for calculating the bandwidth.

$$\omega_1 = -\frac{G}{2C} - \sqrt{\left(\frac{G}{2C}\right)^2 - \frac{1}{LC}}$$

$$\omega_2 = -\frac{G}{2C} + \sqrt{\left(\frac{G}{2C}\right)^2 - \frac{1}{LC}}$$

where  $G = \frac{1}{R}$ .

$$\text{Bandwidth, } BW = \omega_2 - \omega_1 = \frac{G}{C} \text{ for } \left(\frac{G}{2C}\right)^2 \gg \frac{1}{LC}.$$

The maximum gain at resonance is  $A_{\max} = g_m/G$ .

$$\therefore \text{Gain bandwidth product} = A_{\max} \cdot BW = \frac{g_m}{G} \times \frac{G}{C} = \frac{g_m}{C}.$$

The gain bandwidth product is thus independent of frequency. As  $gm$  and  $C$  are fixed for a particular tube or circuit, higher gain can be achieved at the cost of bandwidth only. In microwave circuit, this restriction/limitation can be overcome by use of  
 (i) re-entrant cavities  
 (ii) slow wave tubes  
 for a larger gain over a larger bandwidth.

### 8.2.6 Effect Due to RF Losses

#### (a) Skin effect losses (or conductor or $I^2R$ losses)

These losses come into play at higher frequencies at which the current has the tendency to confine itself to a smaller cross-section of the conductor towards its outer surface (Refer Fig. 8.7).

$$\delta = \text{skin depth} = \sqrt{2/\omega\mu\sigma}$$

i.e.,  $\delta \propto \frac{1}{\sqrt{\omega}}$  and  $\delta \propto A_{\text{eff}}$ ,

where  $A_{\text{eff}}$  is the effective area over which current flows.

$$A_{\text{eff}} \propto 1/\sqrt{f}$$

and

$$R = \frac{\rho l}{A_{\text{eff}}}$$

$$R = \frac{\rho l}{1/\sqrt{f}} = \rho l \sqrt{f} \quad \dots(8.11)$$

i.e., As  $f$  increases  $R$  increases.

Hence losses will increase at higher frequencies. These losses can be reduced by increasing the size of the conductors.

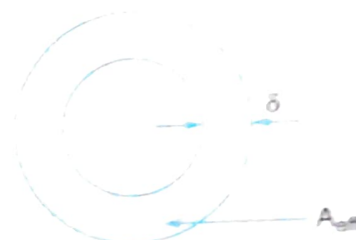


Fig. 8.7

#### (b) Dielectric losses

This occurs in various types of insulating materials used in the device i.e., spacers, glass envelope, silicon or plastic encapsulations etc. The loss in any of these material is in general given by

$$P = \pi f \cdot V_o^2 \epsilon_r \tan \sigma \quad \dots(8.12)$$

where,  $\epsilon_r$  = relative permittivity of the dielectric and

$\delta$  = loss angle of the dielectric.

As  $f$  increases the power loss increases. The remedy for this is to eliminate the tube base and to reduce the surface area of glass.

### 8.2.7 Radiation Losses

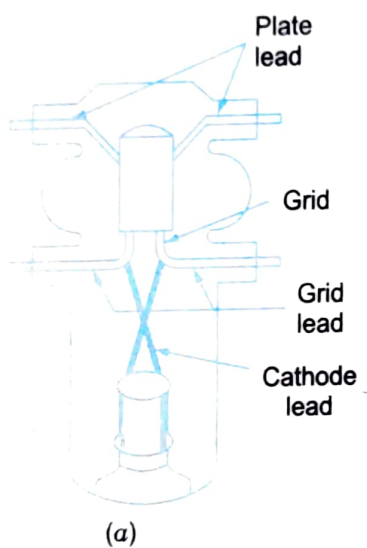
Whenever the dimensions of the wire approaches the wavelength ( $\lambda = c/f$ ), it will emit radiation that is, radiation losses increase with increase in frequency. The remedy for this is to use proper shielding of the tubes and its circuitry.

### 8.3 SPECIAL TUBES AT UHF (300-3000 MHz)

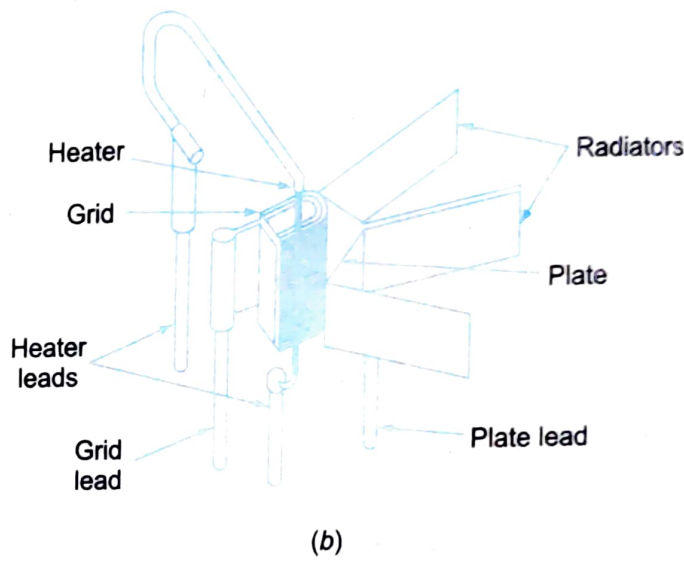
We have seen that reduction of transit time, LI and IEC cannot be done simultaneously since the requirements are conflicting in nature. Hence some compromise has to be done in design as regard to the requirement of power handling capacity, transit time, lead inductances and device capacitances. Special tubes have been designed taking these into consideration, known as UHF tubes—the ACORN tube, pencil triodes and light house tubes.

#### 8.3.1 ACORN Tube

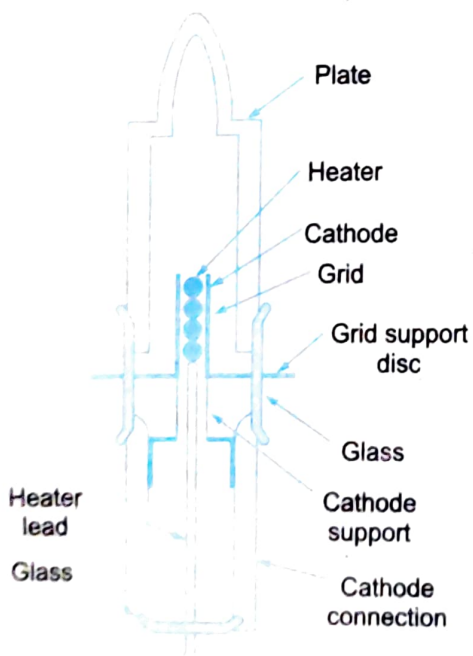
These are corn sized UHF tubes capable of handling frequencies upto 12 MHz. They have small electrodes of conventional shape and type.



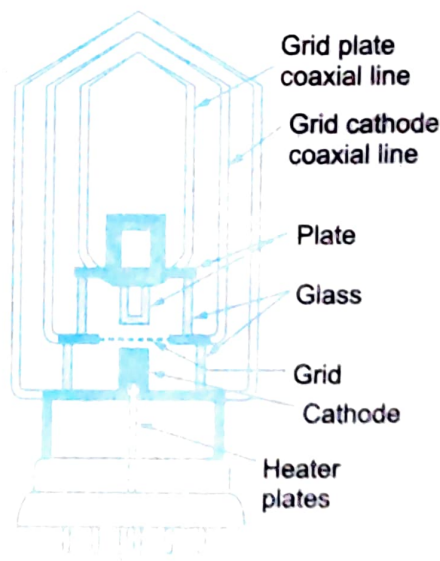
(a)



(b)



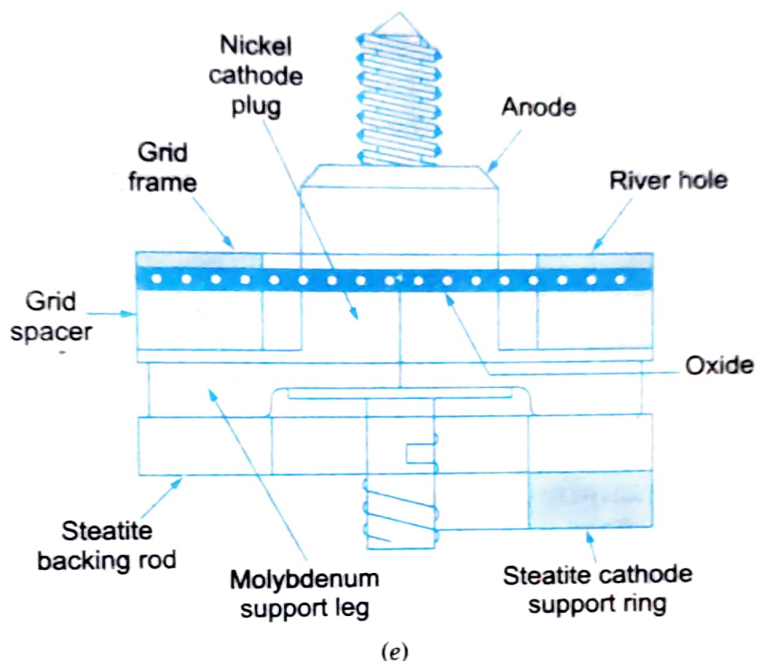
(c)



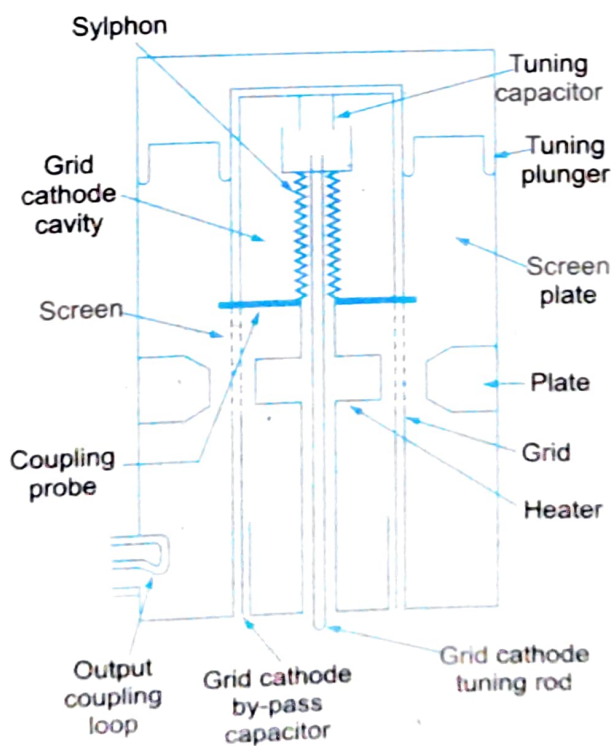
(d)

UHF tubes (a) Acorn tube, (b) Light house tube, (c) Pencil triode, (d) Light house UHF

The small capacitance is due to small electrodes and low lead inductance is due to thick multiple leads brought out radially from the lower end of the electrode assembly. This is shown in Fig. 8.8c. Tube base is eliminated to reduce dielectric losses. This is a low power device as the size is very small. These are basically designed for use in low power oscillators and amplifier circuits.



(e)



(d)

Fig. 8.8 Some UHF tubes (e) Close-spaced triode (f) Resonatron

### 8.3.2 Disk Seal Tube or Light House Tube

This is a larger tube capable of handling large powers and is the most important of UHF tubes. It can operate upto 3000 MHz. Beyond this, transit time effects come into picture and hence cannot be used. Lead inductances and IEC can be reduced considerably by making the electrodes of metal discs which are sealed in a glass envelope as shown in Fig. 8.8d. Because of its shape, it is known as Light house tube. The anode and grid are cylindrical with fairly large volumes but with low active surface areas. All the electrodes are solid and firmly attached to the body of the tube. The large area of the electrodes permit good power dissipation and low inductance. The efficiency and high frequency limits are better compared to ACORN tube since the electrodes form the body of the tube.

### 8.3.3 Pencil Triodes

These are more or less similar to conventional triodes in construction with the only difference that the electrodes are in the form of cylinders or flat flanges. Note that this is nothing but extension of the idea of multiple lead construction where the number of leads are now increased to infinity. This results in the minimum possible lead inductance and substantial increase in the power handling capacity. These can be operated in conjunction with co-axial lines and capacity. These can be operated in conjunction with coaxial lines and cavity resonators so that operations around 4000 MHz are easily realizable, using these devices. Materials used here are of high grade so that losses due to  $I^2R$  and dielectric losses are reduced to the minimum.

Other tubes shown in figure such as the door knob (Fig. 8.8b), close-spaced triode (Fig. 8.8e) and the resnatron (Fig. 8.8f) are not frequently used. Table 8.1 shows the various types of UHF tubes that are commercially available with their ratings, applications and their usefulness in present days.

## 8.4 MICROWAVE TUBES

As already stated microwave tubes are constructed so as to overcome the limitations of conventional and UHF tubes. They differ from them in that they make use of the transit time effect rather than fight it ("if you can't beat them join them"!). In fact, large transit time is required for their operation. The basic principle of operation of the microwave tubes involves transfer of power from a source of dc voltage to a source of dc voltage by means of a current density modulated electron beam. The same is achieved by accelerating electrons in a static electric field and retarding them in an ac field. The density modulation of the electron beam allows more electrons to be retarded by ac field than accelerated by ac field which therefore makes possible a net energy to be delivered to the ac electric field. The various types of microwave tubes that are available differ from each other in

- (i) their mechanism of producing density modulation
- (ii) the acceleration and retardation of electrons in the ac field and
- (iii) the retardation of electrons by a short gap or over an extended region.

Table 8.1 UHF Tubes - Performance Parameters

Sr. No.	Type	Power output	Frequency	Typical applications	Remarks
1	Acorn	a few mW	upto 1200 MHz	Low power oscillators	Obsolete - being replaced by solid state devices.
2	Door-knob	-do-	upto 1700 MHz	-do-	-do-
3	Disk-seal tubes:				
(a)	Pencil triodes 5794 5675	500 mW 570 mW 5 W	1680 MHz 1700 3 GHz	Oscillators	Amplifier
(b)	Light house tubes: 2C40/39	Power gain 10-14 (Avg. 3 or 4)	3000 MHz (operation extended up to 6 GHz)	Oscillators & Amplifiers	Firmly entrenched due to high powers and its easy adaptability for coaxial line resonators
(c)	Close-spaced triodes: 416-A	Power gain of 10 dB	4 GHz	Amplifier & Frequency convertor	In use and not likely to be replaced
4	Resnatron	50 to 75 kW (cw)	350 to 625 MHz	High power oscillators	-do-

The most important microwave tubes that are considered in this chapter include klystron amplifier (two cavity, multicavity), klystron oscillator (reflex klystron), the travelling wave tube amplifier, magnetron oscillators, backward wave oscillators etc.

### 8.5 KLYSTRONS #

A klystron is a vacuum tube that can be used either as a generator or as an amplifier of power at microwave frequencies. This was invented by Russel H. Varian at Stanford University in 1939 in association with his brother S.P. Varian. We study a two cavity klystron amplifier, multicavity klystron, two cavity klystron oscillators and reflex klystron in this section.

### 8.5.1 Two Cavity Klystron Amplifier

A two cavity klystron amplifier is shown in Fig. 8.9 which is basically a velocity modulated tube. Here a high velocity electron beam is formed, focussed and sent down along a glass tube through an input cavity (buncher), a field free drift space and an output cavity (catcher) to a collector electrode/anode. The anode is kept at a positive potential with respect to cathode. The electron beam passes through a gap 'A' consisting of two grids of the buncher cavity separated by a very small distance and two other grids of the catcher cavity with a small gap 'B'. The input and output are taken from the tube via resonant cavities with the aid of coupling loops.

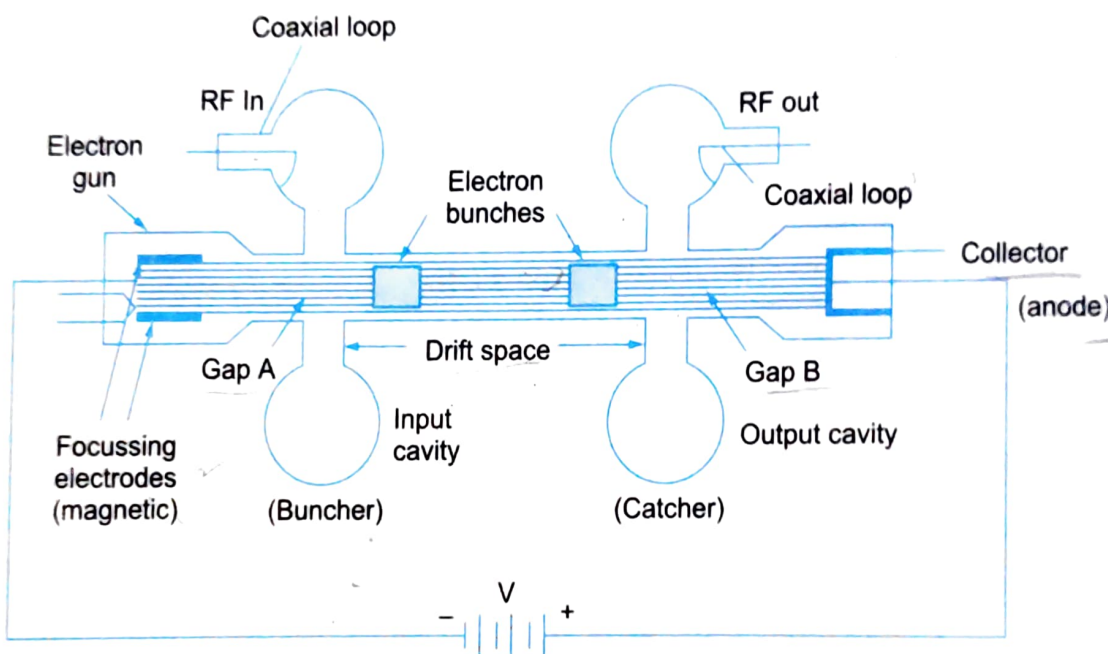


Fig. 8.9 Two cavity klystron amplifier.

### Operation

The RF signal to be amplified is used for exciting the input buncher cavity thereby developing an alternating voltage of signal frequency across the gap A.

Let us now consider the effect of this gap voltage on the electron beam passing through gap A. The situation is best explained by means of an Applegate diagram shown in Fig. 8.10. At point B on the input RF cycle, the alternating voltage is zero and going positive. At this instant, the electric field across gap A is zero and an electron which passes through gap A at this instant is unaffected by the RF signal. Let this electron be called the reference electron  $e_R$  which travels with an unchanged velocity  $v_o = \sqrt{2 eV/m}$  where V is the anode to cathode voltage.

At point 'C' of the input RF cycle an electron which leaves gap A later than reference electron  $e_R$ , called the late electron  $e_L$  is subjected to maximum positive RF voltage and hence travels towards gap B with an increased velocity ( $v > v_o$ ) and this electron tries to overtake the reference electron  $e_R$ .

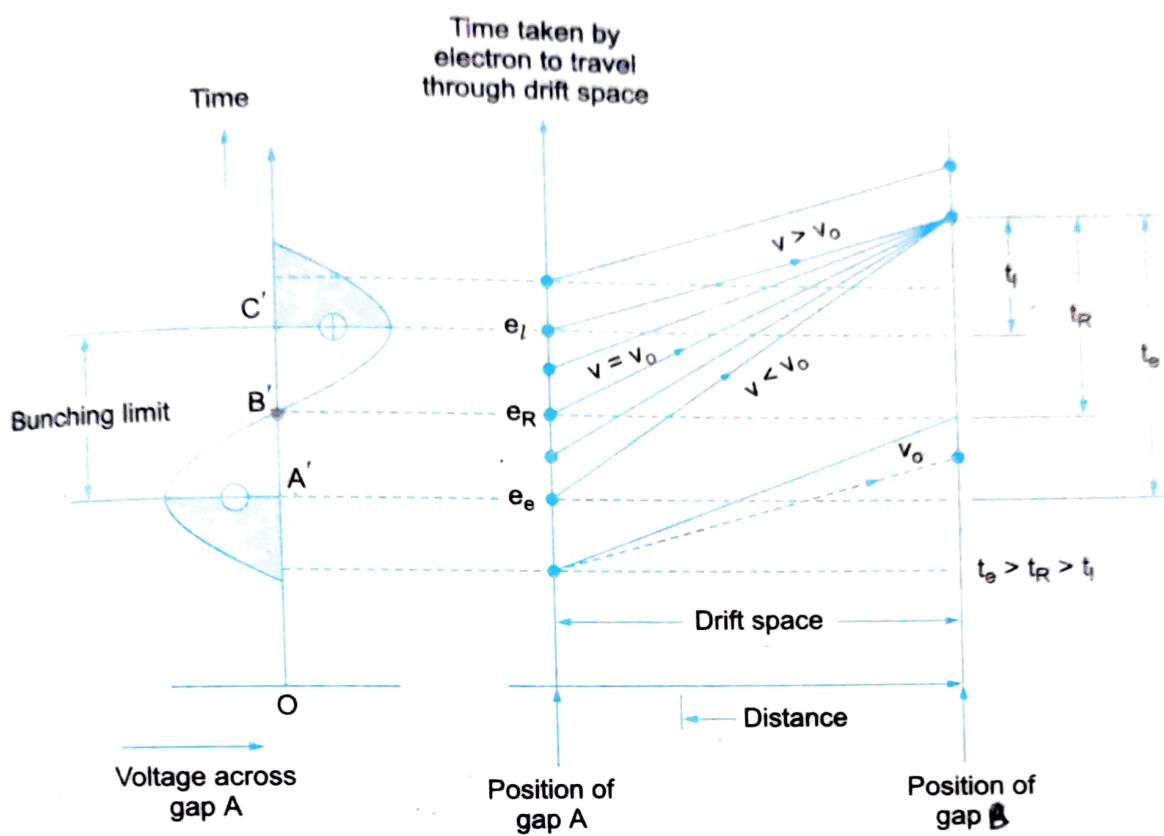


Fig. 8.10 Apple gate diagram of a klystron amplifier.

Similarly an early electron  $e_e$  that passes the gap 'A' slightly before the reference electron  $e_R$  is subjected to a maximum negative field. Hence this early electron is decelerated and travels with a reduced velocity  $v_o$ . This electron  $e_e$  falls back and reference electron  $e_R$  catches up with the early electron.

Therefore the velocity of electron varies in accordance with *RF* input voltage, resulting in *velocity modulation* of the electron beam.

As a result of these actions, the electrons in the bunching limit (between points 'A' and 'C') gradually bunch together as they travel down the drift space, from gap A to gap B. The pulsating stream of electrons pass through gap B and excite oscillations in the output cavity (catcher). The density of electrons passing the gap B vary cyclically with time, that is the electron beam contains an ac current and is current modulated. The drift space converts the velocity modulation into current modulation.

Bunching occurs only once per cycle centered around the reference electron. With proper design (optimum gap widths, anode to cathode voltage, drift space length etc), a little *RF* power applied to the buncher cavity results in large beam currents at the catcher cavity with a considerable power gain.

### Performance Characteristics

1. Frequency : 250 MHz to 100 GHz. (60 GHz nominal)
2. Power : 10 kW–500 kW (CW) 30 MW (pulsed)

3. Power gain : 15 dB–70 dB (60 dB nominal)
4. Bandwidths: Limited (because cavity resonators are being used) 10–60 MHz—generally used in fixed frequency applications.
5. Noise figure : 15–20 dB (Sometimes greater than 25 dB)
6. Theoretical efficiency : 58% (30–40% nominal)

Multicavity klystrons use more than two cavities (upto 6), with more bunching, voltage amplification and hence power gain,  $\eta$  and BW.

## Applications

1. As power output tubes
  - (a) In UHF TV transmitters
  - (b) In troposphere scatter transmitters
  - (c) Satellite Communication ground stations
  - (d) Radars transmitters
2. As power oscillator (5–50 GHz) if used as a klystron oscillator.

## Mathematical Analysis of a Klystron Amplifier

Let the dc voltage between cathode and anode be  $V_0$  and  $v_0$  be the velocity of the electron,  $L$  be the drift space length and the RF input signal to be amplified by the klystron be  $V_s$ .

Then,

$$v_0 = \sqrt{\frac{2eV_0}{m}} = 0.593 \times 10^6 \sqrt{v_0} \text{ m/sec} \quad \dots(8.13)$$

$$V_s = V_1 \sin \omega t \quad \dots(8.14)$$

where,  $V_1$  = amplitude of the signal and  $V_1 \ll V_0$  is assumed.

The energy of the electron at the time of leaving buncher cavity (Refer Fig. 8.11) is given by

$$\frac{1}{2}mv_1^2 = e(V_0 + V_1 \sin \omega t_1)$$

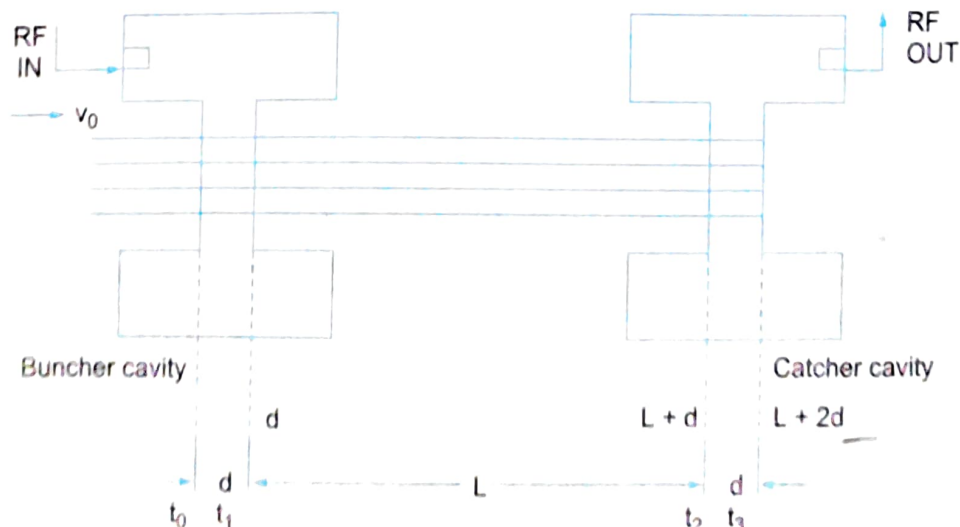


Fig. 8.11

i.e.,

$$v_1 = \sqrt{\frac{2e(V_0 + V_1 \sin \omega t_1)}{m}}$$

$$= \sqrt{\frac{2eV_0}{m}} \cdot \sqrt{1 + \frac{V_1}{V_0} \sin \omega t_1}$$

Since

$$V_1 \ll V_0, \quad v_1 = v_0 \left( 1 + \frac{V_1}{V_0} \sin \omega t_1 \right)^{1/2}$$

Expanding binomially and neglecting higher powers of  $\sin \omega t$ , we get

$$v_1 = v_0 \left( 1 + \frac{V_1}{2V_0} \sin \omega t_1 \right) \quad \dots(8.15)$$

This is the equation of velocity modulation.

$$\omega t_1 = \omega t_0 + \frac{\theta_g}{2}$$

where  $\theta_g$  is the phase angle of the RF input voltage during which the electron is accelerated (refer Fig. 8.12)

$$\theta_g = \omega t = \omega (t_1 - t_0) = \frac{\omega d}{v_0} \quad \dots(8.16)$$

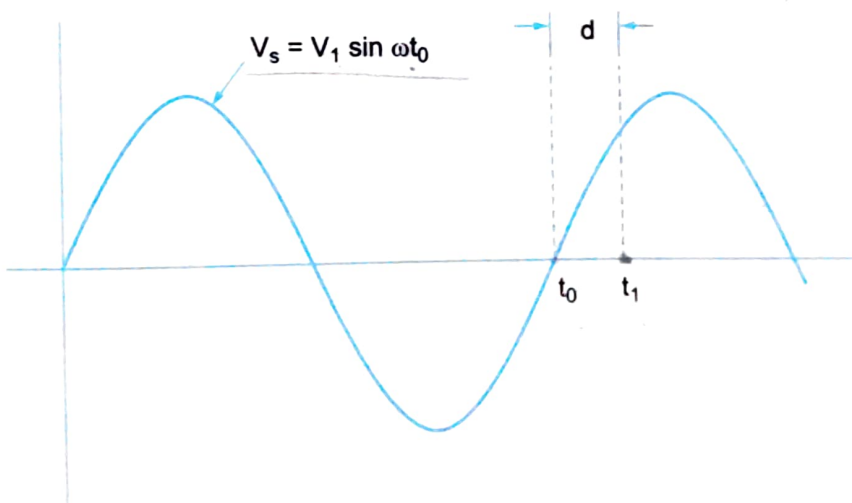


Fig. 8.12

### Bunching Process of the Electron Beam

Maximum velocity occurs at  $\pm \pi/2$  so that

$$v_{1(\max)} = v_0 \left( 1 + \frac{V_1}{2V_0} \right) \quad \dots(8.17)$$

and minimum velocity at  $\pm \pi/2$ , so that

$$v_{1(\min)} = v_0 \left( 1 - \frac{V_1}{2V_0} \right) \quad \dots(8.18)$$

If the distance in the drift space at which the bunching occurs from the buncher grid at time  $t_0$  is  $L_1$ , (Fig. 8.13)

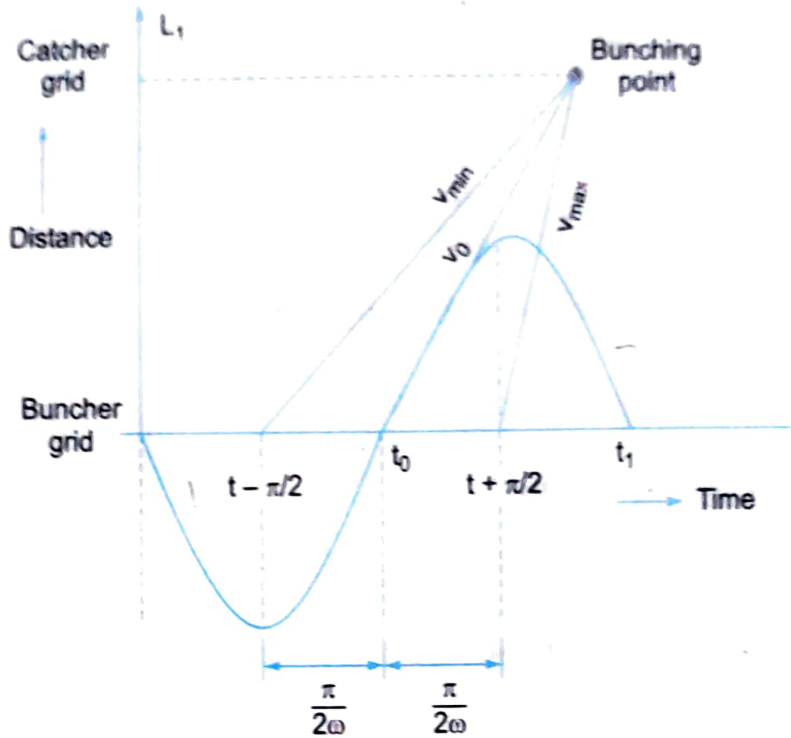


Fig. 8.13

$$L_1 = v_0 (t_1 - t_0) \quad \dots(8.19)$$

The distance  $L_1$  at  $t_{-\pi/2} = v_{\min} (t_1 - t_{-\pi/2})$   $\dots(8.20)$

The distance  $L_1$  at  $t_{+\pi/2} = v_{\max} (t_1 - t_{+\pi/2})$   $\dots(8.21)$

$$\left. \begin{aligned} t_{-\pi/2} &= t_0 - \pi/2\omega \\ t_{+\pi/2} &= t_0 + \pi/2\omega \end{aligned} \right\}$$

$$\left. \begin{aligned} L_1 &= v_0 (t_1 - t_0) \\ L_1 &= v_0 (t_1 - t_0 + \frac{\pi}{2\omega}) \\ L_1 &= v_0 (t_1 - t_0 - \frac{\pi}{2\omega}) \end{aligned} \right\} \dots(8.22)$$

From Eqs. 8.17 to 8.19 and 8.22, we get

$$L_1 \text{ at } t_{-\pi/2} = v_0 \left( 1 - \frac{V_1}{2V_0} \right) \left( t_1 - t_0 + \frac{\pi}{2\omega} \right) \quad \dots(8.23)$$

$$L_1 \text{ at } t_{+\pi/2} = v_0 \left( 1 + \frac{V_1}{2V_0} \right) \left( t_1 - t_0 - \frac{\pi}{2\omega} \right) \quad \dots(8.24)$$

$$L_1 = v_0 (t_1 - t_0) + v_0 \left[ \frac{\pi}{2\omega} - \frac{V_1}{2V_0} (t_1 - t_0) - \frac{V_1}{2V_0} \frac{\pi}{2\omega} \right]$$

For maximum value,

$$L_1 = v_0 (t_1 - t_0) + v_0 \left[ \frac{\pi}{2\omega} - \frac{V_1}{2V_0} (t_1 - t_0) - \frac{V_1}{2V_0} \frac{\pi}{2\omega} \right]$$

If the distance has to be the same for  $-\pi/2$ ,  $0$ ,  $+\pi/2$  bunches,  $L_1$  for all three should be equal to  $v_0 (t_1 - t_0)$

$$\frac{\pi}{2\omega} - \frac{V_1}{2V_0}(t_1 - t_0) - \frac{V_1}{2V_0} \frac{\pi}{2\omega} = 0$$

$$\begin{aligned} - (t_1 - t_0) &= \frac{\pi}{2\omega} \left[ \frac{V_1}{2V_0} - 1 \right] \cdot \frac{2V_0}{V_1} \\ &= \frac{\pi}{2\omega} - \frac{\pi V_0}{\omega V_1} \end{aligned}$$

As  $\frac{V_0}{V_1}$  is very high,  $\frac{\pi}{2\omega}$  can be neglected.

$$t_1 - t_0 \approx \frac{\pi V_0}{\omega V_1}$$

Substituting this in Eq. 8.19, we get

$$L_1 = v_0 \left( \frac{\pi V_0}{\omega V_1} \right) \quad \dots(8.26)$$

Bunching occurs as the RF signal changes from  $-\pi/2$  to  $+\pi/2$ , i.e.,  $\pi$ . For a value of  $\pi = 3.682$ , optimum bunching occurs and

$$L_{\max} = 3.682 \frac{v_0 V_0}{\omega V_1} \quad \dots(8.27)$$

If beam coupling coefficient of input cavity is  $\beta$ , given by

$$\beta = \frac{\sin(\theta_g/2)}{\theta_g/2}$$

(average gap transit angle)

$$\text{where } \theta_g = \frac{\omega d}{v_0}$$

Then,  $L_{\max}$  is given by

$$L_{\max} = 3.682 \frac{v_0 V_0}{\omega \beta V_1}$$

$$V_1 = \frac{v_0 \times 3.682}{\beta \left( \frac{\omega d}{v_0} \right)} \quad \dots(8.28)$$

Efficiency is given by  $\eta = \frac{P_{\text{out}}}{P_{\text{in}}}$

### Output Power ( $P_{\text{out}}$ )

At the catcher cavity,

$$\text{RF voltage} = V_2 \sin \omega t_2$$

$$\begin{aligned} \text{Energy given by the electron to the bunch} \\ = (-e) V_2 \sin \omega t_2 = -e V_2 \sin \omega t_2 \end{aligned}$$

The average energy given to the *RF* field in a cycle

$$P_{av} = \frac{1}{2\pi} \int_{\omega t_1}^{\omega t_2} (-eV_2 \sin \omega t_2) d\omega t_1 \quad \dots(8.29)$$

In the field free space between cavities, the transit time for velocity modulated electron is given by

$$\begin{aligned} T = t_2 - t_1 &= \frac{L}{v_1} = \frac{L}{v_0 \left( 1 + \frac{V_1}{V_0} \right) \sin \omega t_1}^{1/2} \\ &= \frac{L}{v_0} \left[ 1 - \frac{V_1}{2V_0} \sin \omega t_1 \right] \end{aligned} \quad \dots(8.30)$$

Multiplying by  $\omega$ ,

$$\omega T = \omega (t_2 - t_1) = \frac{\omega L}{v_0} \left[ 1 - \frac{V_1}{2V_0} \sin \omega t_1 \right] \quad \dots(8.31)$$

In the above equation,  $\frac{L}{v_0} = T_0$ , the transit time without *RF* voltage  $V_1$  in buncher cavity and  $\frac{\omega L}{v_0} = \omega T_0 = \theta_0 = 2\pi N$  is the transit angle without *RF* voltage  $V_1$  in buncher cavity (or it is due to dc voltage  $V_0$ ) and  $N$  is the number of electron transit cycles in drift space.

The bunching parameter  $X$  of a klystron is defined by the equation,

$$X = \frac{V_1}{2V_0} \theta_0 \quad \dots(8.32)$$

which is a dimensionless quantity and proportional to input power.

Eq. 8.29 can be written using Eq. 8.31,

$$P_{av} = \frac{-eV_2}{2\pi} \int_0^{2\pi} \sin(\omega t_1 + T) d\omega t_1$$

$$i.e., \quad P_{av} = \frac{-eV_2}{2\pi} \int_0^{2\pi} \sin \left[ \omega t_1 + \theta_0 \left( 1 - \frac{V_1}{2V_0} \sin \omega t_1 \right) \right] d\omega t_1$$

This is a Bessel function and its solution is given by,

$$P_{av} = -eV_2 J_1(X) \sin \theta_0 \quad \dots(8.33)$$

where,  $J_1(X)$  = Bessel function of the first order for the argument  $X$  (Eq. 8.32).

For  $N$  electron transit cycles,

$$\text{Energy transferred} = NP_{av} = -Ne V_2 J_1(X) \sin \theta_0;$$

$$Ne = I_0, \text{ the output current.}$$

$$\text{Energy transferred} = -I_0 V_2 J_1(X) \sin \theta_0 \quad \dots(8.34)$$

Maximum value of  $J_1(X) = 0.58$  for  $X = 1.84$  (from Bessel function tables).

For maximum energy transfer,

$$\begin{aligned} P_{\max} &= I_0 V_0 (0.58) \sin \theta_0 \\ \sin \theta_0 &= 1, \theta_0 = 2n\pi - \pi/2 \end{aligned}$$

The output power,  $P_{\text{out}} = P_{\max} = 0.58 I_0 V_0$

(8.35)

### Input Power ( $P_{\text{in}}$ )

The input power is basically the dc input given by

$$P_{\text{in}} = I_0 V_0$$

The efficiency ( $\eta$ ) therefore is given by Eqs. 8.35 and 8.36

$$\eta = \frac{P_{\text{out}}}{P_{\text{in}}} = \frac{0.58 I_0 V_0}{I_0 V_0} = 0.58 \frac{V_0}{V_0} \quad (8.37)$$

As  $V_0$  is always less than  $V_0$ , the maximum efficiency that can be attained is 0.58 or 58%. Further efficiency is a function of the transit angle and is maximum for a catcher gap transit angle of  $\theta_g = \theta_0 = -\pi/2$  and is zero for  $\theta_g = \pi/2$ .

However, practical efficiencies are only 15 to 30% with CW powers of 500 kW and pulsed powers of 30 MW at 10 GHz and power gain of 10–20 dB.

Also for maximum power transfer, the electron gun anode voltage required is given by  $(V_1/V_0)_{\max}$ . We know

$$X = \frac{V_1}{2V_0} \theta_0$$

For maximum transfer of energy,  $X = 1.84$ ,  $\theta_0 = 2n\pi - \pi/2$

$$\left( \frac{V_1}{V_0} \right)_{\max} = \frac{2 \times 1.84}{2n\pi - \pi/2} = \frac{3.68}{\left( 2n\pi - \frac{\pi}{2} \right)} \quad (8.38)$$

### 8.5.2 Multicavity Klystron

As explained in the previous section, gains of about 10 to 20 dB are typical with two-cavity tubes. A higher overall gain can be achieved by connecting several two cavity tubes in cascade, feeding the output of each of the tubes to the input of the succeeding one. Instead, multiple number of cavities can be used as in a multicavity klystron shown in Fig. 8.14.

Here, each of the intermediate cavities act as a buncher with the passing electron beam inducing an enhanced RF voltage than the previous cavity. With four cavities, power gains of around 50 dB can be easily achieved. The cavities can all be tuned to the same frequency (synchronous tuning) for narrow band operation. Bandwidth can be improved by stagger tuning of cavities upto about 80 MHz of course with reduction in gain (to about 45 dB). This stagger tuning is employed in UHF klystrons for TV transmitter output tubes and in satellite earth station transmitters as power amplifiers at 6 GHz.

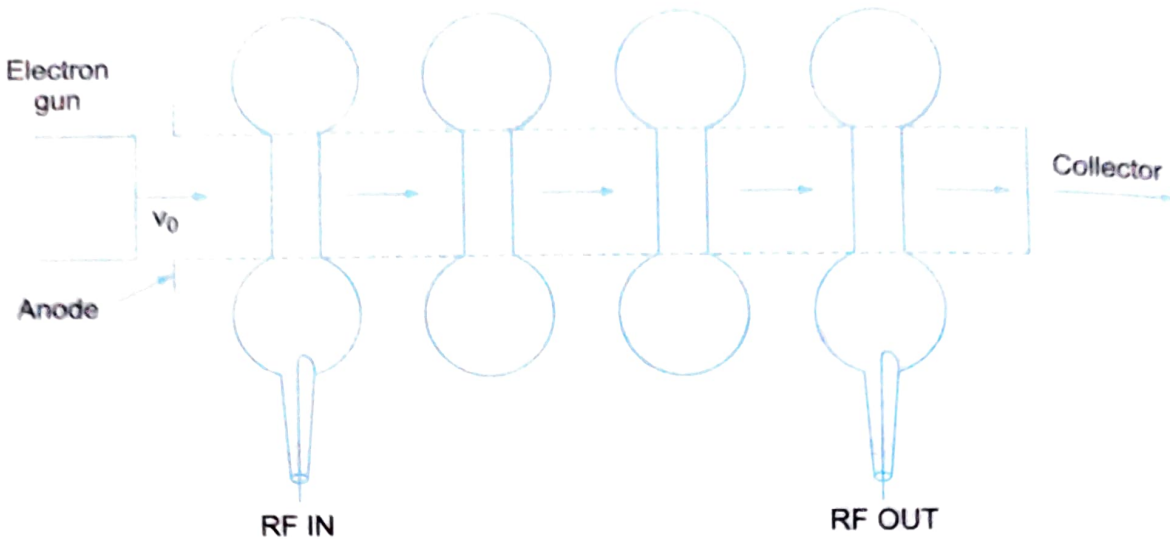


Fig. 8.14 Multicavity klystron (4 cavity).

### ~~8.5.3 Two Cavity Klystron Oscillator~~

A klystron amplifier can be converted into an oscillator by feeding back a part of the catcher output into the buncher in proper phase so as to satisfy Barkhausen criterion. The schematic is same as klystron amplifier (Fig. 8.7) except that a feedback loop needs to be added. The feedback must be adjusted to give correct polarity and amplitude which basically depends on the cavity tuning and the various dc voltages. If  $\theta$  is the phase shift in the resonators and the feedback cable, the criterion for oscillation is (since  $A\beta = 1 \angle 2\pi n$  radians where  $n$  is any integer including zero.)

$$\theta + \alpha + \frac{\pi}{2} = 2\pi n \text{ radians} \quad \dots(8.39)$$

where  $\alpha + \pi/2$  is the phase angle between the zeroes of buncher and catcher voltages. If the two resonators oscillate in same phase, then  $\theta = 0$ . Maximum power output is obtained by substituting for  $\theta = 0$  in Eq. 8.39 for obtaining  $\alpha = 2\pi n - (\pi/2)$ . i.e., If the two resonators oscillate in time phase, the condition that  $\alpha = 2\pi n - (\pi/2)$  not only becomes a requirement for maximum power output but also for obtaining sustained oscillations. However, the two resonators in general need not have oscillate in time phase.

Also, a small change in dc accelerating voltage causes a change in frequency since the transit angle  $\alpha$  varies. In that case the frequency of oscillation will shift in such a way as to yield a new value of  $\theta$  so as to satisfy Eq. 8.39. Since two resonators having the same resonant frequency are coupled here, the input impedance looking into either resonator circuits will vary with frequency as shown in Fig. 8.15.

Oscillations can be obtained over a somewhat wide range if the resonators are over coupled. Critically coupled klystron oscillator has almost a linear variation in frequency with accelerating voltage making frequency modulation possible. High frequency stability of oscillator is obtained by controlling the temperature of the resonators and also by use of regulated power supplies.

Tuning of the oscillator is done by adjusting the grid voltage, dc accelerating voltage and the tuning of the two resonators.

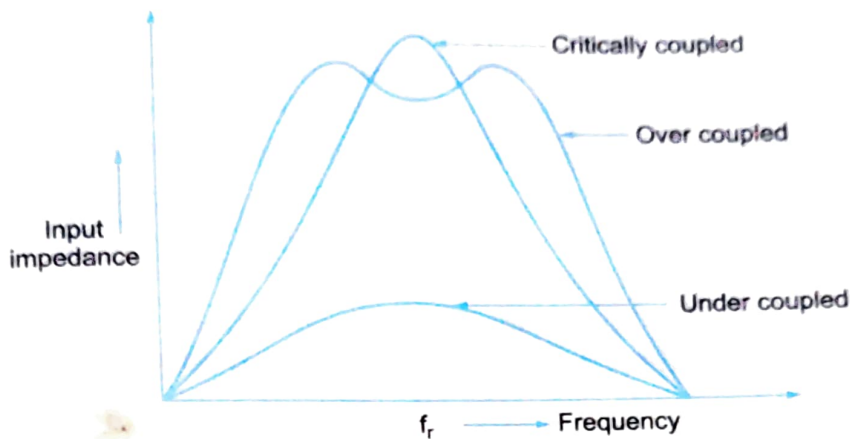


Fig. 8.15 Frequency vs impedance.

### ~~8.54~~ Reflex Klystron

The reflex klystron is a single cavity variable frequency microwave generator of low power and low efficiency.

This is most widely used in applications where variable frequency is desired as

1. in radar receivers
2. local oscillator in microwave receivers
3. signal source in microwave generator of variable frequency
4. portable microwave links and
5. pump oscillator in parametric amplifier.

### Construction

It consists of an electron gun, a filament surrounded by cathode and a focussing electrode at cathode potential as shown in Fig. 8.16. The electron beam is accelerated towards the anode cavity.

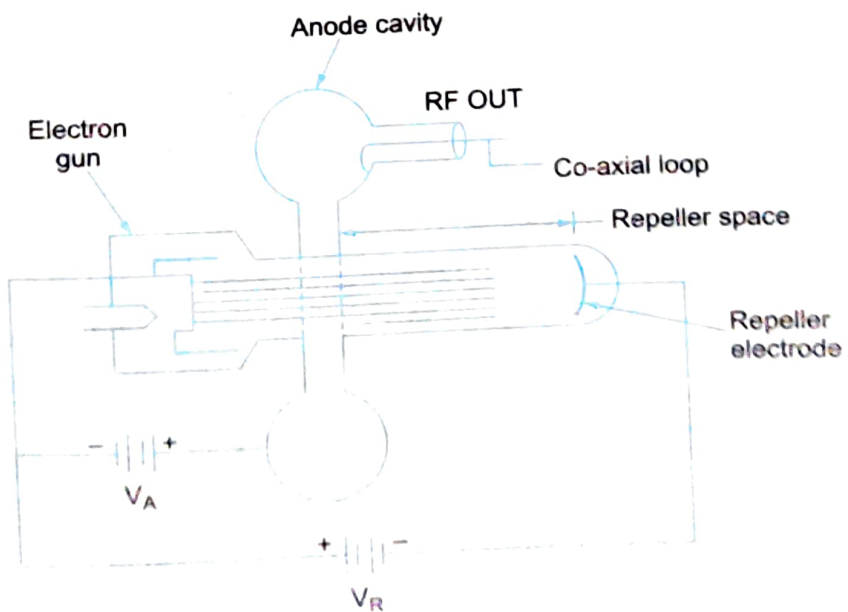


Fig. 8.16 Constructional details of reflex klystron.

(at positive potential). After passing the gap in the cavity, electrons travel towards a repeller electrode which is at a high negative potential  $V_R$ . The electrons never reach the repeller because of the negative field and are returned back towards the gap. Under suitable conditions, the electrons give more energy to the gap than they took from the gap on their forward journey and oscillations are sustained.

### Operation

It is assumed that the oscillations are set up in the tube initially due to noise or switching transients and these oscillations are sustained by device operation. This can be explained again by applegate diagram, shown in Fig. 8.17.

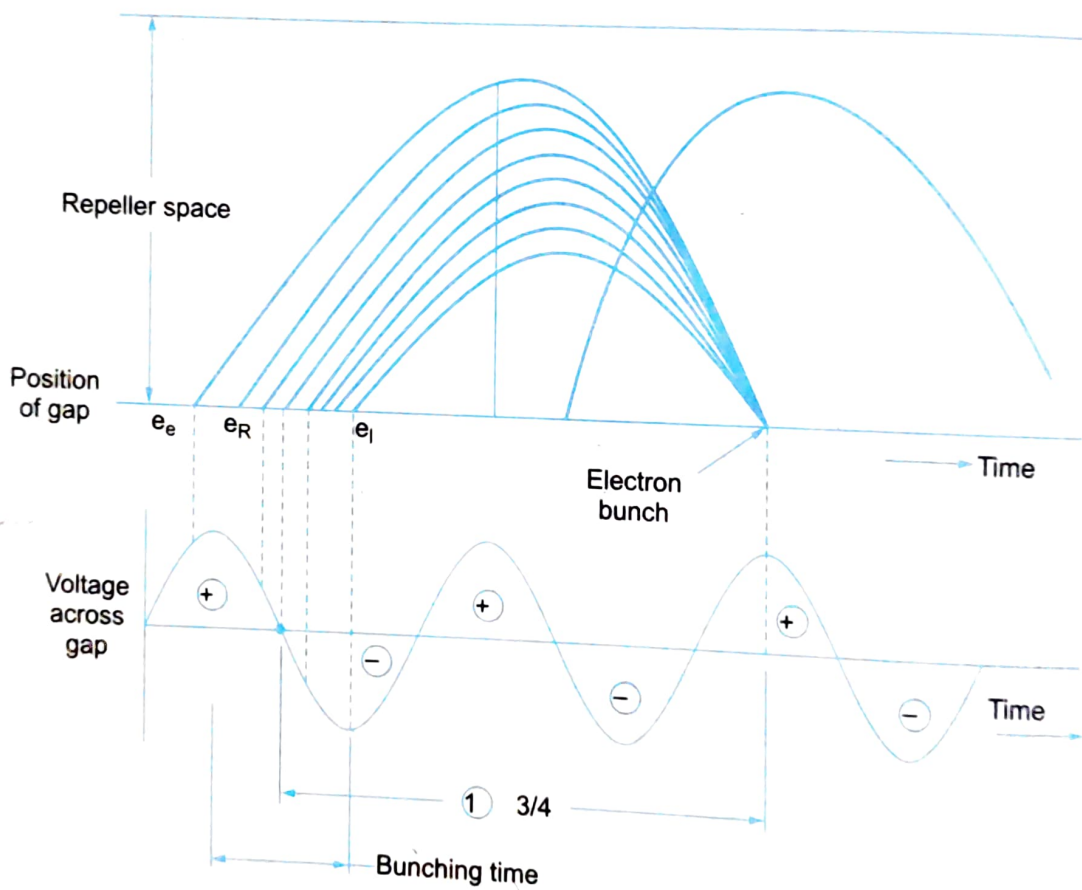


Fig. 8.17 Applegate diagram

The RF voltage that is produced across the gap by the cavity oscillations act on the electron beam to cause velocity modulation. ' $e_R$ ' is the reference electron that passes through the gap when the gap voltage is '0' and going negative. Electron ' $e_R$ ' is unaffected by the gap voltage. This moves towards the repeller and gets reflected by the negative voltage on the repeller. It returns and passes through the gap for a second time.

The early electron ' $e_e$ ' that passes through the gap before the reference electron ' $e_R$ ' experiences a maximum positive voltage across the gap and this electron is accelerated. It moves with greater velocity and penetrates deep into repeller space. The return time for electron ' $e_e$ ' is greater as the depth of penetration into the repeller space is more. Hence  $e_e$  and  $e_R$  appear at the gap for the second time at the same instant.

The late electron ' $e_l$ ' that passes the gap later than reference electron ' $e_R$ ' experiences a maximum negative voltage and moves with a retarding velocity. The return time is shorter as the penetration into repeller space is less and catches up with  $e_R$  and  $e_o$  electrons forming a bunch. Bunches occur once per cycle centred around the reference electron ' $e_R$ ' and these bunches transfer maximum energy to the gap to get sustained oscillations.

For oscillations to be sustained, the time taken by the electrons to travel into the repeller space and back to the gap (called transit time) must have an optimum value. This factor is not important in a klystron amplifier but it assumes a great importance here.

The most optimum departure time is obviously centered on the reference electron which is at  $180^\circ$  point of sine wave voltage across the resonator gap. The cavity resonator spends energy in accelerating the electrons and gains energy in retarding them. As there are as many retarded electrons as accelerated the total energy outlay is nil. From this discussion, it is clear that the best possible time for electrons to return to the gap is at a time at which the voltage then existing across the gap will apply maximum retardation to them. This is when the gap voltage is positive maximum. This causes electrons to fall through the maximum negative voltage between the gap grids, thus giving up the maximum amount of energy to the gap. Thus it appears that the best time for electrons to return to the gap is at the  $90^\circ$  point of sine wave gap

voltage. Returning of electrons after  $1\frac{3}{4}$  or  $2\frac{3}{4}$  or  $3\frac{3}{4}$  cycles etc. satisfies the above requirements. In general, the optimum transit time should be

$$T = n + \frac{3}{4} \quad \dots(8.40)$$

where  $n$  is any integer.

This depends on repeller and anode voltages.

## Operating Characteristics

**1. Voltage Characteristics:** Oscillations can be obtained only for specific combinations of anode and repeller voltages that give a favourable transit time ( $T = n + 3/4$ ).

The shaded areas show possible oscillation combinations and heavy lines show optimum combinations. Each value of  $n = 1, 2, 3, \dots$  is said to correspond to a different mode for the reflex klystron oscillator. The earlier the mode the larger the output power, which is obviously an advantage. But the voltages required are also higher as shown in Fig. 8.18 leading to insulation problems and the possibilities of lower efficiencies. As a result the modes corresponding to  $n = 2$  or  $n = 3$  are most widely used.

**2. Power Output and Frequency Characteristics:** The mode curves and frequency characteristics are shown in Fig. 8.19. The frequency of resonance of the cavity decides the frequency of oscillation. Variations of repeller voltage slightly changes the frequency. This amounts to electronic tuning of reflex klystron and this is also depicted in Fig. 8.19. This makes it possible to use reflex klystron as a voltage tuned oscillator or frequency modulated oscillator.

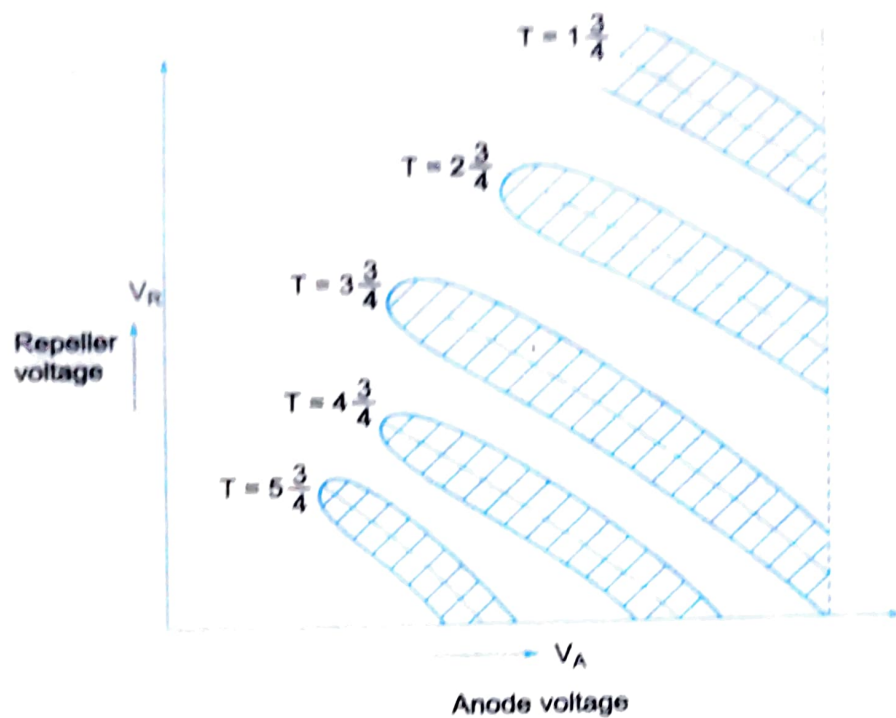


Fig. 8.18 Voltage characteristics of reflex klystron

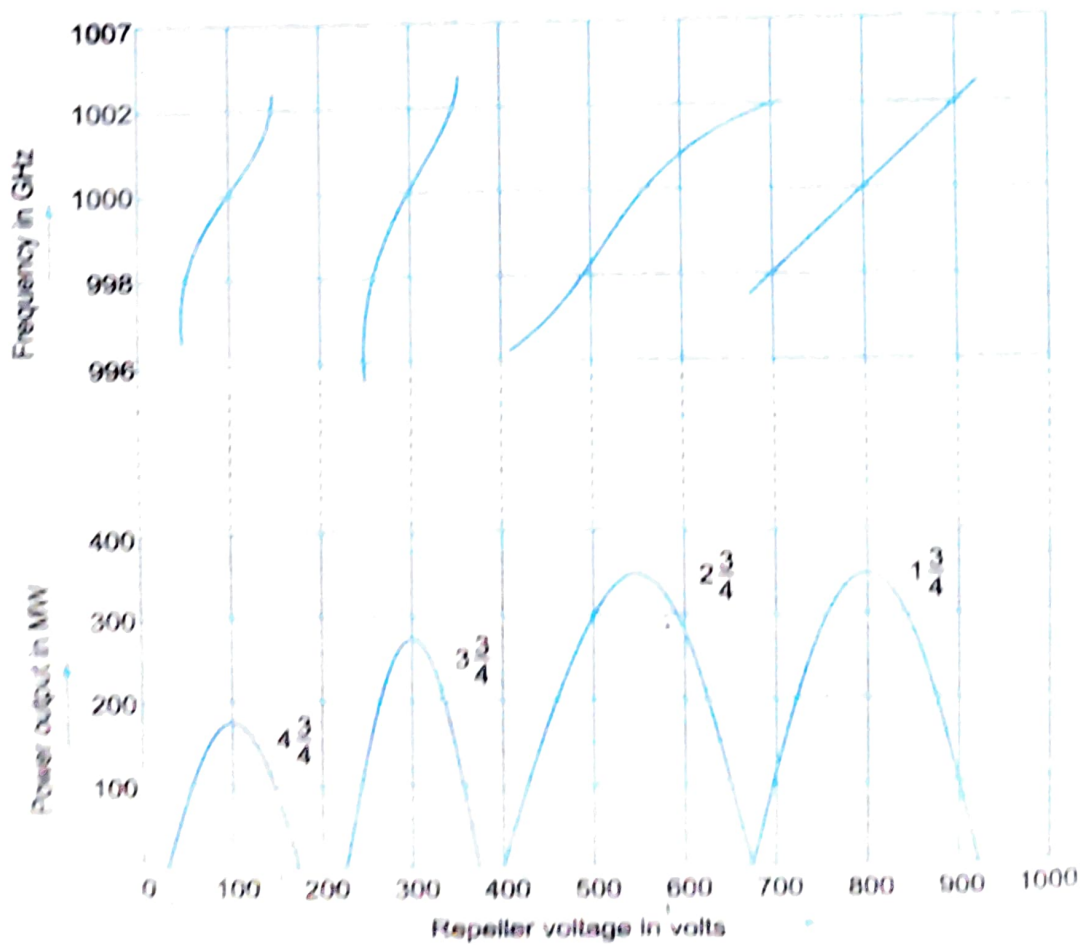


Fig. 8.19 Power output and frequency characteristics of reflex klystron

**Mathematical Analysis** We shall refer to Fig. 8.20 for the mathematical analysis of a klystron.

Symbols used

$V_0$  = electron gun anode voltage

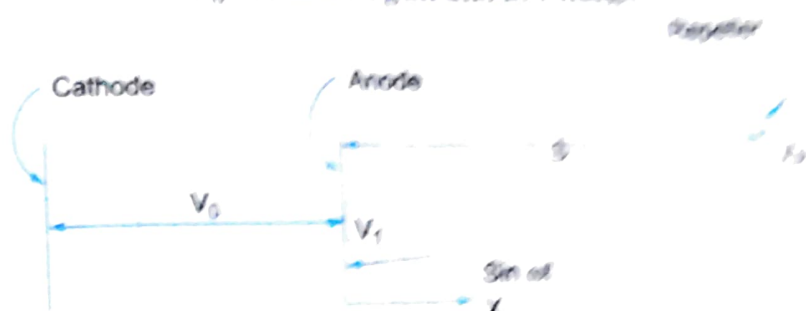


Fig. 8.20

$V_1 \sin \omega t$  = RF voltage at cavity gap

$V_R$  = Repeller voltage with respect to cathode.

$s$  = distance between cavity gap and repeller electrode

$v_0$  = velocity of electron in gun.

$v_1$  = velocity due to RF voltage in addition to the electron accelerating voltage  $V_0$

$t_0$  = time for electron entering cavity gap at  $x = 0$

$t_1$  = time for same electron leaving cavity gap at  $x = s$

$t_2$  = time for same electron returned by retarding field at  $x = s$

## Calculations

$$v_0 = \sqrt{\frac{2eV_0}{m}} \quad (\text{since } \frac{1}{2}mv_0^2 = eV_0)$$

$$v_1 = V_0 \sqrt{\frac{1 + V_1}{V_0}} \sin \omega t$$

(voltage now is  $V_0 + V_1 \sin \omega t$ ,  $V_1 \ll V_0$ )

Voltage between repeller and anode

$$= V_R - (V_0 + V_1 \sin \omega t) = V_R - V_0 - V_1 \sin \omega t$$

Retarding electrostatic field between repeller and anode is given by

$$E = -\frac{(V_R - V_0)}{s}$$

$$\text{Force on electron} = -eE = +e \frac{(V_R - V_0)}{s}$$

Also, force on electrons = mass × acceleration =  $\frac{md^2x}{dt^2}$  ... (8.45)

Equating Eqs. 8.44 and 8.45,

$$\begin{aligned} m \frac{d^2x}{dt^2} &= \frac{+e}{s} (V_R - V_0) \\ \frac{d^2x}{dt^2} &= \frac{e}{ms} (V_R - V_0) \end{aligned} \quad \dots (8.46)$$

Integrating Eq. 8.46 once,

$$\frac{dx}{dt} = \frac{e}{ms} (V_R - V_0) t + C \quad \dots (8.47)$$

At  $t = t_1$ ,

$$\frac{dx}{dt} = v_1$$

$$\therefore v_1 = \frac{e}{ms} (V_R - V_0) t_1 + C$$

$$C = v_1 - \frac{e}{ms} (V_R - V_0) t_1$$

Substituting for 'C' in Eq. 8.47, we get

$$\frac{dx}{dt} = \frac{e}{ms} (V_R - V_0) (t - t_1) + v_1 \quad \dots (8.48)$$

Integrating Eq. 8.48, once again,

$$x = \frac{e}{2ms} (V_R - V_0) (t - t_1)^2 + v_1 t + C_1 \quad \dots (8.49)$$

At  $x = 0$ , i.e., at the point of return from repeller space;  $t = t_2$

$$0 = \frac{e}{2ms} (V_R - V_0) (t_2 - t_1)^2 + v_1 t_2 + C_1$$

or

$$C_1 = -\frac{e}{2ms} (V_R - V_0) (t_2 - t_1)^2 - v_1 t_2$$

Using this value of  $C_1$  in Eq. 8.49, we get

$$x = \frac{e}{2ms} (V_R - V_0) [(t - t_1)^2 - (t_2 - t_1)^2] + v_1 (t - t_2)$$

Again when  $t = t_1$ ,  $x = 0$ ,

i.e.,  $-\frac{e}{2ms} (V_R - V_0) (t_2 - t_1)^2 - v_1 (t_2 - t_1) = 0$

$(t_2 - t_1)$  is the round trip transit time and is given by

$$(t_2 - t_1) = \frac{-2ms v_1}{e (V_R - V_0)} \quad \dots (8.50)$$

The transit angle ' $\omega t$ ' is defined as transit angle at time 't'.

$$\omega(t_2 - t_1) = \frac{-2msv_1\omega}{e(V_R - V_0)} \quad \dots(8.51)$$

$$\omega t_2 = \omega t_1 - \frac{2msv_1\omega}{e(V_R - V_0)}$$

or

From Eq. 8.42,

$$v_1 = v_0 \left( 1 + \frac{V_1}{V_0} \sin \omega t \right)^{1/2}$$

Since  $V_1 \ll V_0$ ,

$$v_1 \approx v_0 \left( 1 + \frac{V_1}{2V_0} \sin \omega t \right)$$

Substituting for  $v_1$  in Eq. 8.51,

$$\omega t_2 = \omega t_1 - \frac{2ms\omega}{e(V_R - V_0)} \cdot v_0 \left( 1 + \frac{V_1}{2V_0} \sin \omega t \right) \quad \dots(8.52)$$

Let  $-\frac{2ms\omega v_0}{e(V_R - V_0)} = \omega T'_0 X = \theta'_0$  ...(8.53)

where  $\theta'_0$  is the round trip dc transit angle of centre of bunch electron.

where  $X'$  is the bunching parameter. (8.54)

Substituting in Eq. 8.52,

$$\omega t_2 = \omega t_1 + \theta'_0 \left( 1 + \frac{V_1}{2V_0} \sin \omega t \right) \quad \dots(8.55)$$

### Relation between Peppeller voltage and Accelerating voltage

Considering Eq. 8.55 and when  $V_1 \ll V_0$  (i.e., for the centre bunch of electrons which is unaffected by RF),

$$\omega t_2 = \omega t_1 + \theta'_0$$

Also, for maximum transfer of energy, the modes are  $1\frac{3}{4}$  cycles apart

i.e.,

$$2\pi(n - 1/4) \text{ where } n - 1/4 = 3/4, 1\frac{3}{4} \text{ etc.}$$

$$2\pi(n - 1/4) = 2\pi n - \pi/2$$

$\therefore$  The optimum value of  $\theta'_0$  is

$$\theta'_0 = (2\pi n - \pi/2) \quad \dots(8.56)$$

From Eq. 8.53,

$$\theta_0 = -\frac{2ms\omega}{e(V_R - V_0)} \cdot v_0 \quad \text{or} \quad v_0 = -\frac{e(V_R - V_0)}{2ms\omega} \cdot \theta'_0.$$

$$v_0^2 = \frac{e^2 (V_R - V_0)^2 (\theta'_0)^2}{4\omega^2 m^2 s^2}$$

We know that

$$\frac{1}{2}mv_0^2 = eV_0$$

$$\text{or} \quad V_0 = \frac{m}{2e} \cdot v_0^2$$

Substituting for  $v_0^2$  from Eq. 8.57

$$V_0 = \frac{m}{2e} \cdot \frac{e^2 (V_R - V_0)^2 (\theta'_0)^2}{4\omega^2 m^2 s^2}$$

$$\text{where } \theta'_0 = 2\pi n - \frac{\pi}{2} \quad (\text{from Eq. 8.56})$$

$$\therefore \frac{V_0}{(V_R - V_0)^2} = \frac{m}{2e} \frac{e^2}{4\omega^2 m^2 s^2} \left(2\pi n - \frac{\pi}{2}\right)^2$$

Simplifying,

$$\frac{V_0}{(V_R - V_0)^2} = \frac{1}{8} \cdot \frac{1}{\omega^2 s^2} \frac{e}{m} \left(2\pi n - \frac{\pi}{2}\right)^2$$

Eq. 8.58 provides the relationship between  $V_0$  and  $V_R$ .

**Expression for change in frequency due to repeller voltage variation (Electron of Reflex klystron)**

Eq. 8.58 can be rewritten as,

$$(V_R - V_0)^2 = \frac{8ms^2 V_0}{\left(2\pi n - \frac{\pi}{2}\right) \cdot e} \cdot \omega^2$$

Differentiating  $V_R$  with respect to  $\omega$ .

$$2(V_R - V_0) \frac{dV_R}{d\omega} = \frac{16ms^2 V_0}{(2\pi n - \pi/2)^2 \cdot e} \cdot \omega$$

or

$$\frac{dV_R}{d\omega} = \frac{8ms^2 V_0 \omega}{2 \left(2\pi n - \frac{\pi}{2}\right)^2 \cdot (V_R - V_0)}$$

We can resubstitute the value of  $(V_R - V_0)$  as,

$$(V_R - V_0) = \sqrt{\frac{8ms^2 V_0 \omega^2}{e(2\pi n - \pi/2)^2}}$$

and obtain a value of  $dV_R/d\omega$  as,

$$\begin{aligned}\frac{dV_R}{d\omega} &= \frac{8ms^2V_{00}}{e(2\pi n - \pi/2)^2} \times \sqrt{\frac{e(2\pi n - \pi/2)^2}{8ms^2V_{00}^2}} \\ &= \sqrt{\frac{8ms^2V_0}{e}} \cdot \frac{1}{(2\pi n - \pi/2)} \\ \frac{dV_R}{df} &= \frac{2\pi s}{(2\pi n - \pi/2)} \sqrt{\frac{8mV_0}{e}} \quad \dots(8.59)\end{aligned}$$

This is a very useful relationship for electronic tuning of reflex klystron i.e., repeller voltage is crucial for frequency of oscillation. If repeller voltage (usually 2 kV) is varied by even 2%, frequency will vary quite considerably. For example, typically if  $V_R = 2000$  V,  $V_0 = 500$  V, drift space = 2 cm, Mode  $n = 1$ ,  $f = 2$  GHz and variation in  $V_R = 2\%$ , then

$$\begin{aligned}df &= dV_R \left( 2\pi \cdot \frac{s}{(2\pi n - \pi/2)} \sqrt{\frac{8mV_0}{e}} \right) \\ &= \frac{2}{100} \times 2000 \left( 2\pi \times \frac{2}{100} \times \frac{1}{(2\pi - \pi/2)} \right) \sqrt{\frac{8 \times 9 \times 10^{-31} \times 500}{1.6 \times 10^{-19}}}\end{aligned}$$

10 MHz

As variation in frequency is quite sensitive to repeller voltage adjustment and also it may draw large current and get overheated, some precautions need to be taken. The precautions include, application of repeller voltage prior to application of anode voltage and connection of a protective diode across the klystron (anode of diode to repeller and cathode of diode to klystron cathode) so that repeller can never become positive.

The tuning range exceeding 2 to 1 in the range of 1GHz to 11GHz are possible in reflex klystrons.

### Efficiency of Reflex klystron

V. Imp

Similar to klystron amplifier, maximum power is transferred to the output when the returning bunched electrons arrive at the cavity and when the field is at antinode power output.

DC power supplied by beam voltage  $V_0$  is

... (8.60)

$$P_{dc} = V_0 I_0$$

AC power delivered (from Eq. 8.33),

$$P_{ac} = I_0 V_2 J_1(X) \sin \theta'_0$$

As the current flows in the negative direction, the negative sign becomes positive and  $\sin \theta'_0$  is 1 and  $V_2$  is  $V_1$  being single and same cavity.

... (8.61)

$$P_{ac} = I_0 V_1 J_1(X)$$

where  $X' = \frac{V_1}{2V_0} \cdot \theta'_0 \left( = 2n\pi - \frac{\pi}{2} \text{ from Eq. 8.56} \right)$

$$\frac{V_1}{V_0} = \frac{2X'}{(2n\pi - \pi/2)}$$

Substituting for  $V_1$  in Eq. 8.61.

$$P_{ac} = \frac{2V_0 I_0 \cdot X' J_1(X')}{(2n\pi - \pi/2)} \quad \dots(8.61)$$

$$\text{Efficiency} = \frac{P_{ac}}{P_{dc}} = \frac{2V_0 I_0 X' J_1(X')}{V_0 I_0 (2n\pi - \pi/2)}$$

$$\eta = \frac{2X' J_1(X')}{(2n\pi - \pi/2)} \quad \dots(8.62)$$

The factor  $X' J_1(X')$  reaches a maximum value of 1.252 at  $X' = 2.408$  and  $J_1(X') = 0.52$ . The maximum power output is obtained when  $n = 2$  or  $1\frac{3}{4}$  mode.

Maximum theoretical efficiency is

$$\eta_{th(max)} = \frac{2(2.408)(0.52)}{2\pi(2) - \pi/2} = 22.78\% \quad \dots(8.63)$$

The practical values however are around 20%.

### Power output in terms of repeller voltage $V_R$

$$P_{out} = \frac{2V_0 I_0 X' J_1(X')}{2n\pi - \pi/2}$$

$$2n\pi - \frac{\pi}{2} = \theta'_0 = \omega T'_0 = \frac{2ms\omega}{e(V_R - V_0)} v_0$$

The negative sign is not taken as electron bunch travels in the reverse direction,  $-x$ .

$$P_{out} = \frac{2V_0 I_0 X' J_1(X')}{2ms \cdot \omega v_0} \times (V_R - V_0) e$$

Eliminating  $v_0$

$$P_{out} = \frac{2V_0 I_0 X' J_1(X')}{\omega s} \times (V_R - V_0) \sqrt{\frac{e}{2mV_0}}$$

For maximum value of  $X' J_1(X') = 1.75$ , we get

$$P_{max} = \frac{1.25 V_0 I_0 (V_R - V_0)}{\omega s} \times \sqrt{\frac{e}{2mV_0}} \quad \dots(8.63)$$

## Equivalent Circuit of Reflex Klystron

The equivalent circuit of a reflex klystron is shown in Fig. 8.21. It consists of the klystron in parallel with beam loading conductance  $G_b$ , copper cavity losses  $G_o$ , load conductance  $G_L$  and parallel tuned circuit.

The electronic admittance is given by

$$Y_e = \frac{I_2}{V_2}$$

where  $I_2$  and  $V_2$  are output current and voltage respectively.

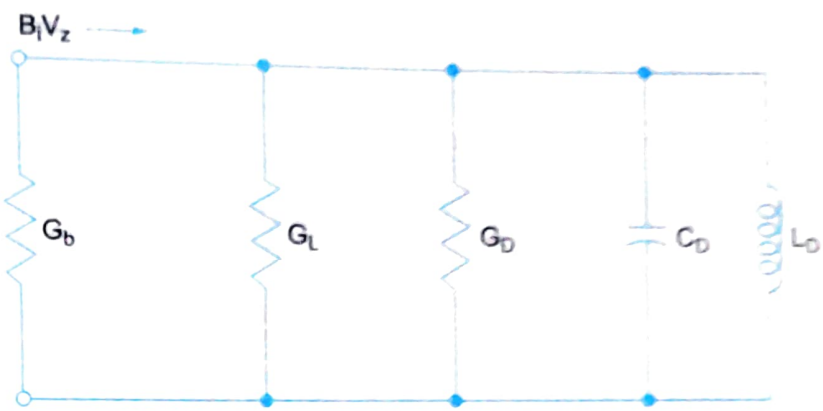


Fig. 8.21 Equivalent circuit of reflex klystron.

i.e.,

$$Y_e = \frac{2I_0 J_1(X'_1) \cdot e^{-j\theta'_0}}{V_1 e^{-j\pi/2}}$$

(since  $I_2 = 2 I_0 J_1(X'_1) \cdot e^{-j\theta'_0}$  in exponential form and  $V_2 = V_1 e^{-j\pi/2}$ )

Putting

$$V_1 = \frac{2V_0 X'}{\theta'_0}$$

$$Y_e = \frac{I_0}{V_0} \frac{\theta'_0}{X'} e^{j(\pi/2 - \theta'_0)} \quad \dots(8.66)$$

Oscillations will take place when the net conductance is less than zero (negative resistance).

$$Y_e = G_e + jB_e$$

$$\text{For oscillation, } | -G_e | \geq G$$

$$\text{where } G = \frac{1}{R_{sh}} = G_0 + G_L + G_b.$$

and

$R_{sh}$  = shunt resistance

A rectangular plot of  $G_e + jB_e$  will be a spiral (Fig. 8.22). The electronic admittance  $Y_e$  is a function of transit angle  $\theta'_0$ . Its phase is  $\pi/2$  when  $\theta'_0$  is 0.

$$n = 1, \theta'_0 = 2\pi n - \frac{\pi}{2} = \frac{3\pi}{2}; n = 2, \theta'_0 = \frac{7\pi}{2};$$

$$n = 3, \theta'_0 = \frac{11\pi}{2}; n = 4, \theta'_0 = \frac{15\pi}{2}.$$

Practically the reflex klystron oscillations are possible, upto  $n = 7$

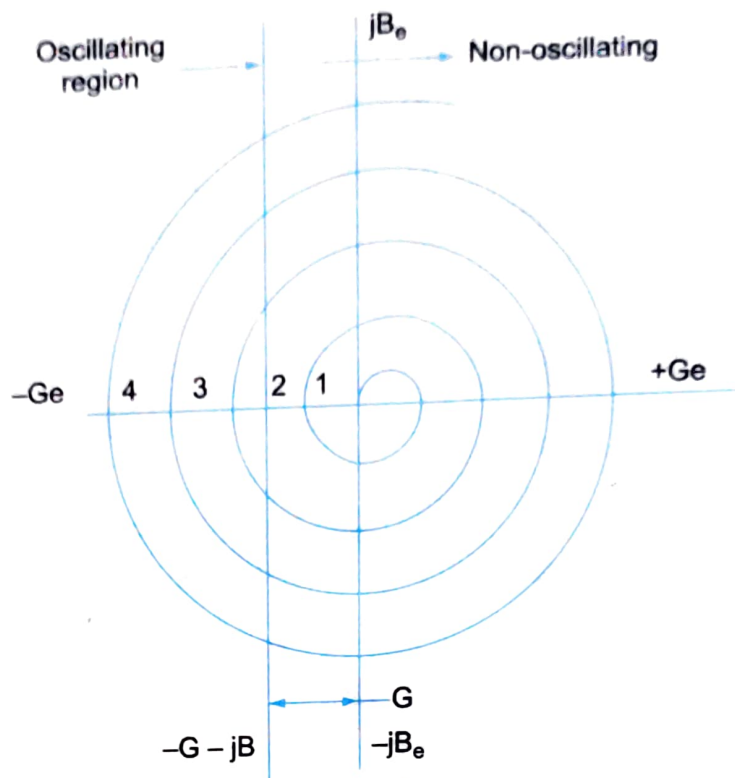


Fig. 8.22

### Performance characteristics of reflex klystron

1. Frequency range : 4 to 200 GHz
2. Output power : 1.0 mW to 2.5 W
3. Theoretical  $\eta$  : 22.78%
4. Practical  $\eta$  : 10% to 20%
5. Tuning range : 5 GHz at 2 watts to 30 GHz at 10 mW.

### B.6 TRAVELLING WAVE TUBE (TWT)

The travelling wave tube is a new type of tube which has displayed considerable promise as a broad band amplifier, proposed by Pierce and others in 1946. These amplifiers are different from klystron amplifiers in the following ways.

Klystrons are essentially narrow band devices as they utilise cavity resonators to velocity modulate the electron beam over a narrow gap whereas TWT's are broad band devices in which there are no cavity resonators. The interaction space in a TWT is extended and the electron beam exchanges energy with the RF wave over the full length of the tube.

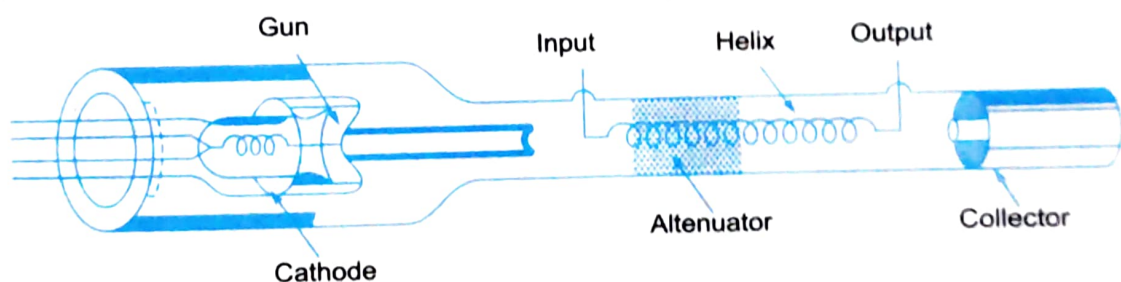
The TWT makes use of distributed interaction between an electron beam and a travelling wave. To prolong the interaction between an electron beam and the RF field it is necessary to ensure that

they are both traveling in the same direction with nearly the same velocity. Thus it differs from the klystron in which the electron beam travels and the RF field remains stationary.

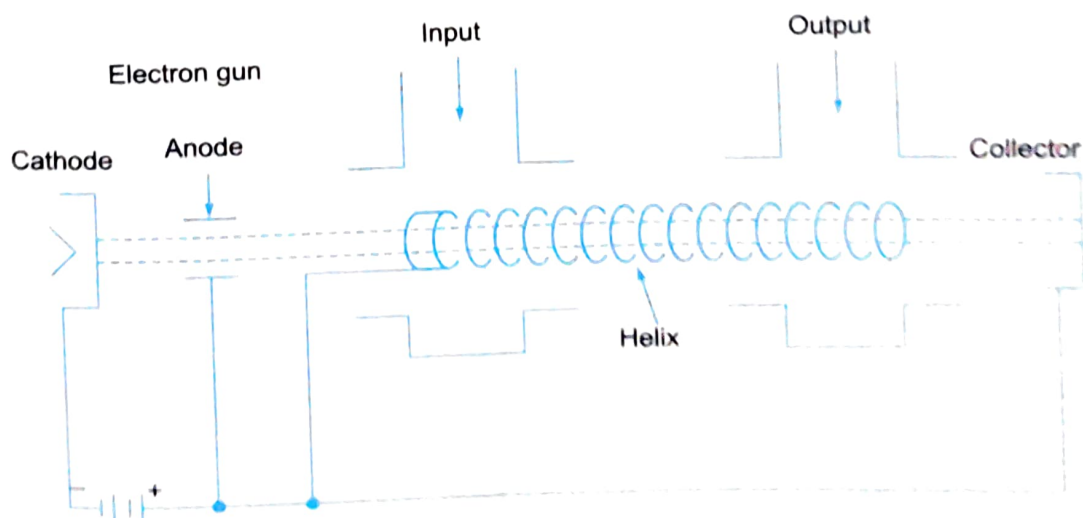
The electron beam travels with a velocity governed by the anode voltage (typically  $0.1 v_c$ , where  $v_c$  is the velocity of light in vacuum). The RF field propagates with a velocity equal to velocity of light  $v_c$ . The interaction between the RF field and the moving electron beam will take place only when the RF field is retarded by some means. Normally slow wave structures are utilised to retard the RF field, like helix or a waveguide arrangement.

### 8.6.1 Constructional Features of TWT

The physical construction of a typical TWT alongwith the schematic electrode arrangement is shown in Fig. 8.23. It has an electron gun as used in klystrons, which is used to produce a narrow constant velocity electron beam. This electron beam is in turn passed through the centre of a long axial helix. A magnetic focussing field is provided to prevent the beam from spreading and to guide it through the center of the helix. Helix is a loosely wound thin conducting helical wire, which acts as a slow wave structure.



(a)



(b)

Fig. 8.23 (a) Physical construction of TWT (b) schematic electrode arrangement

The signal to be amplified is applied to the end of the helix adjacent to the electron gun. The amplified signal appears at the output or other end of the helix under appropriate operating conditions.

### 8.6.2 Operation

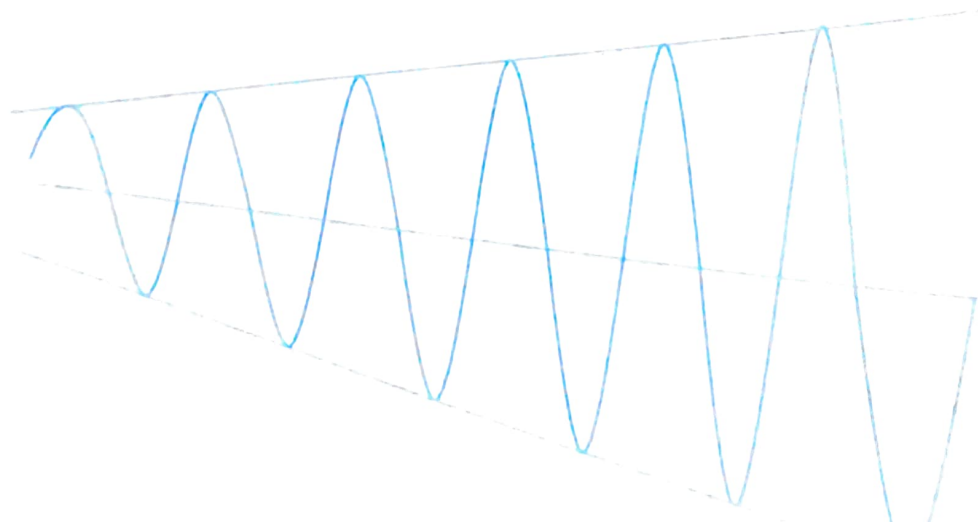
When the applied *RF* signal propagates around the turns of the helix, it produces an electric field at the centre of the helix. The *RF* field propagates with velocity of light. The axial electric field due to *RF* signal travels with velocity of light multiplied by the ratio of helix pitch to helix circumference. When the velocity of the electron beam travelling through the helix approximates the rate of advance of the axial field, then interaction takes place between them in such a way that on an average the electron beam delivers energy to the *RF* wave on the helix.

Thus, the signal wave grows and amplified output is obtained at the output of the TWT. The axial phase velocity  $v_p$  is given by,

$$v_p = v_c (\text{Pitch}/2\pi r) \quad \dots(8.67)$$

where  $r$  is the radius of the helix and is essentially constant over a range of frequencies and this characteristic of helix slow wave structure enables TWT to have broadband operation. Helix, since it provides the least change in  $v_p$  with frequency, is preferred over other slow wave structures for TWT.

The TWT may be thought of as a limiting case of the multicavity klystron which has a very large number of closely spaced gaps with a phase change that propagates from left to right at approximately the same velocity as the electron beam. When the axial field is zero, electron velocity is unaffected. This happens at the point of node of the axial electric field. At a point where the axial field is positive antinode, the electron coming against it is accelerated and tries to catch up with the later electron which encounters the nodal *RF* axial field. At a later point where the axial *RF* field is negative antinode, the electrons referred before tend to overtake. The electrons get velocity modulated. As a result of energy transfer from the electron to the *RF* field in phase with the *RF*



field at the axis, a second wave is induced on the helix. This produces an axial electric field that lags behind the original electric field by  $\lambda/4$ . Bunching continues to take place. The electrons in the bunch encounter retarding field and deliver energy to the wave on the helix. The output becomes larger than the input and amplification results. Thus, the energy increase in the RF is a continuous process as shown in Fig. 8.24.

### Mathematical Analysis

Consider a helix that is characterised by a structure which is electrically smooth (sheath helix). The conductivity of a smooth sheath helix in the direction of helix wire is specified to be infinite and that in the direction perpendicular to the helix wire is zero. A simpler solution can be thought of by using these boundary conditions for a wave that is guided by the helix. As we have seen, helix supports a slow wave with an axial phase velocity  $v_p = v_c \times \sin \psi$  where  $\psi$  is the helix angle given by  $\tan^{-1} \left( \frac{P}{2\pi r} \right)$ . (Refer Fig. 8.25) with  $P$  as pitch of the helix,  $r$ , radius of helix and  $v_c$  as the velocity of the wave propagating along the helix.

The wave travelling along the helix has a longitudinal component of electric field which causes velocity modulation of the electron beam. This velocity modulation causes bunching of electrons at regular intervals of one wavelength as shown in Fig. 8.26.

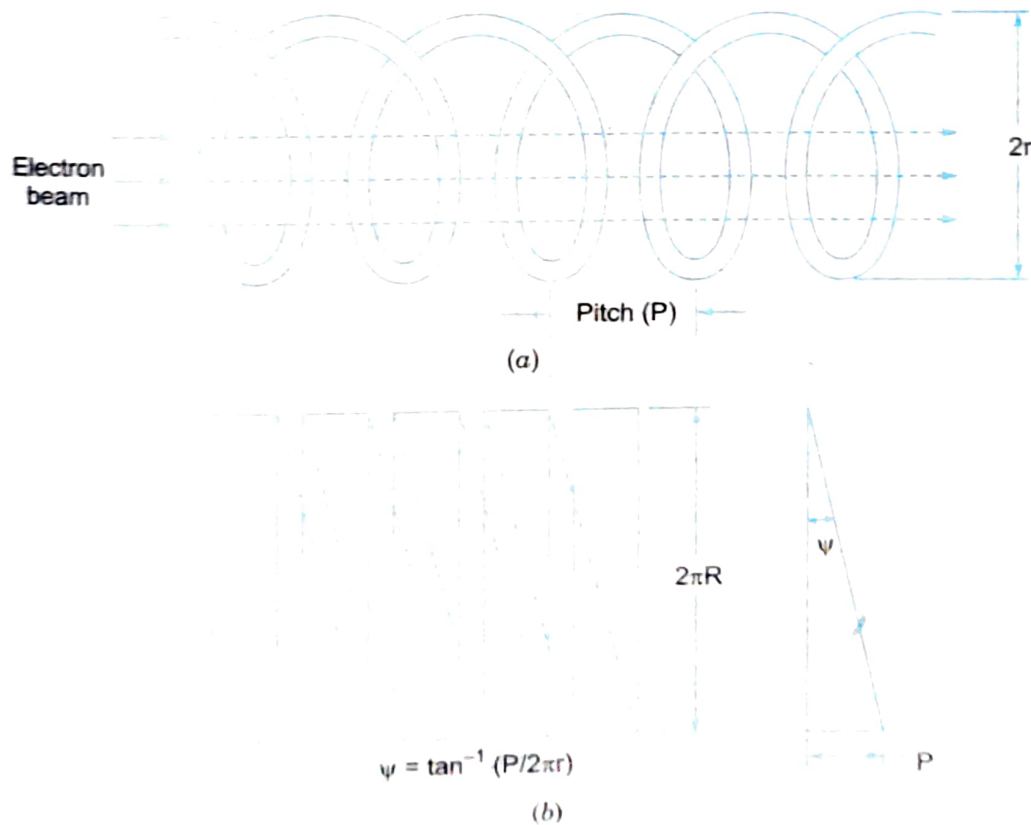


Fig. 8.25

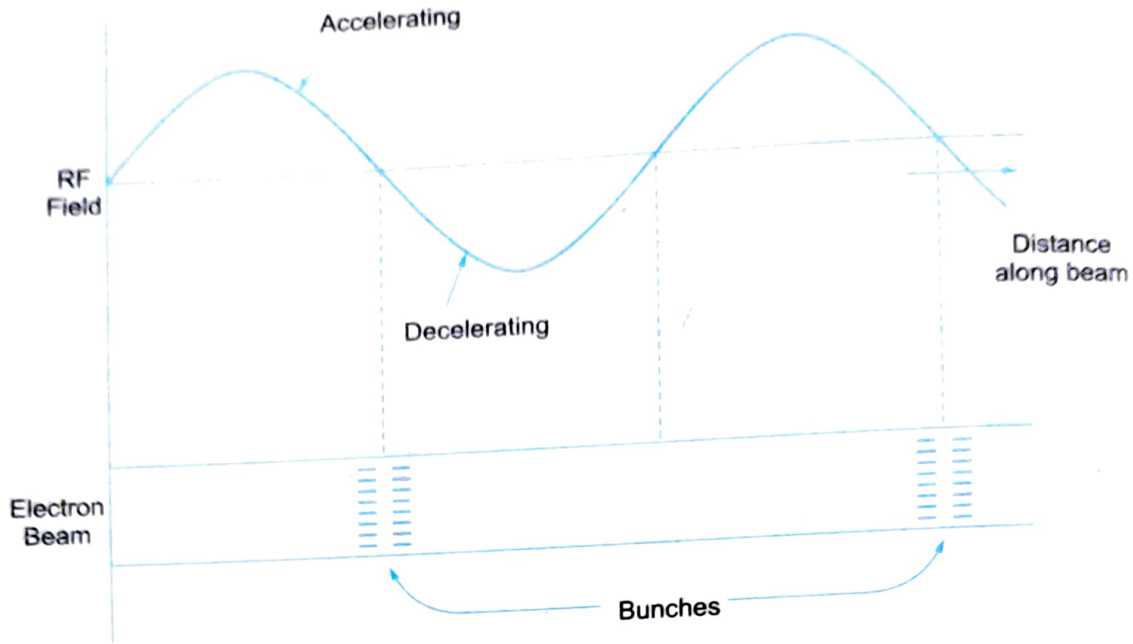


Fig. 8.26

When the *RF* wave and the electron beam are moving with similar velocities, a continuous interaction between the wave and the beam takes place resulting in bunches and these bunches grow as the beam moves further in the helix. This cumulative interaction can be explained in terms of space charge waves on the beam.

In addition to velocity modulation, the beam will also experience a fluctuation in charge density and current density. These are known as space charge waves on the electron beam. We shall carry out a small signal analysis of the same.

Let  $v_0, \rho_0, J_{z0}$  represent static *RF* velocity, charge density and current density and  $v_1, \rho_1, J_{z1}$  their corresponding time varying equivalents. We can hence write,

$$\begin{aligned} v &= v_0 + v_1 e^{j(\omega t - \beta z)} \\ \rho &= \rho_0 + \rho_1 e^{j(\omega t - \beta z)} \\ J_z &= j_{z0} + J_{z1} e^{j(\omega t - \beta z)} \end{aligned} \quad \dots(8.68)$$

Also, the electric field in  $z$  direction is given by

$$E_z = E_{z1} e^{j(\omega t - \beta z)}$$

We know that, current density is given by

$$J_z = \rho v$$

Substituting for  $\rho$  and  $v$  from Eq. 8.68, we get

$$J_z = \rho_0 v_0 + (\rho_1 v_0 + \rho_0 v_1) e^{j(\omega t - \beta z)} + \rho_1 v_1 e^{2j(\omega t - \beta z)} \quad \dots(8.69)$$

The last term being very small can be neglected.

$$\begin{aligned} J_z &= \rho_0 v_0 + (\rho_1 v_0 + \rho_0 v_1) e^{j(\omega t - \beta z)} \\ &= J_{z0} + J_{z1} e^{j(\omega t - \beta z)} \end{aligned} \quad \dots(8.70)$$

where  $J_{z0} = \rho_0 v_0$  and  $J_{z1} = \rho_1 v_0 + \rho_0 v_1$

The electric field  $E_z$  causes the electron motion and hence by law of electron, we have

$$\frac{e}{m} E_z = \frac{dv}{dt} = \frac{\partial V}{\partial z} \frac{dz}{dt} + \frac{\partial V}{\partial t}$$

By differentiating the above equation, we can show that

$$\frac{e}{m} E_{z_1} = jv_1 v_0 \left( \frac{\omega}{v_0} - \beta \right) \quad \dots(8.71)$$

The continuity equation ( $\Delta \cdot J_z = -\partial \rho / \partial t$ ) can be used to have a relationship between space derivative of current and time derivative of charge.

$$\dots(8.72)$$

i.e.,

Using Eqs. 8.70 and 8.72,  $\rho_1$  can be eliminated and the resulting value of  $v_1$  when substituted in Eq. 8.71 gives the relationship between  $E_{z_1}$  and  $J_{z_1}$ .

$$E_{z_1} = \frac{jmv_0^2}{\epsilon\mu_0\omega} \left( \beta - \frac{\omega}{v_0} \right)^2 J_{z_1} \quad \dots(8.73)$$

$$D_z = j \frac{v_0^2}{\omega_p^2 \omega} (\beta - \beta_0)^2 J_{z_1} \quad \dots(8.74)$$

where  $D_z$  = electric flux density in  $z$  direction

$$\beta_0 = \frac{\omega}{v_0} \text{ and } \omega_p^2 = \frac{e\mu_0}{m\varepsilon_0}$$

$f_p = \omega_p / 2\pi$  is the plasma frequency whose value is dependant on the electron density in the beam and can be written as

$$f_p = 8.98 \times 10^3 [n_e]^{1/2} \quad \dots(8.75)$$

where  $n_e$  = electron density in particles per cu. cm.

(For low power TWT's  $f_p$  is of the order of  $10^8$  Hz)

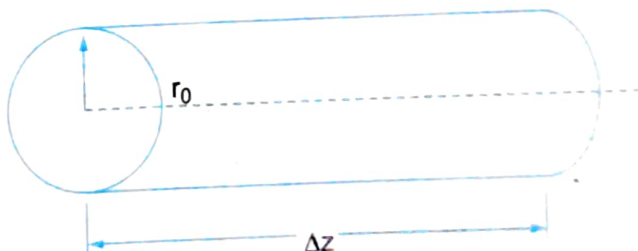


Fig. 8.27

We now consider a small section of electron beam (Fig. 8.27).

Applying divergence theorem  $\left( \iiint \left( J + \frac{\partial D}{\partial t} \right) da = 0 \right)$  to the closed area in Fig. 8.27

$$\left( \frac{\partial J_z}{\partial z} + j\omega \frac{\partial D_z}{\partial z} \right) \Delta z \cdot \pi r_0^2 + j\omega D_r 2\pi r_0 \Delta z = 0$$

Using Eq. 8.74, for  $D_z$ , we have

$$J_{z_1} = \frac{-2\omega\beta_p^2}{\beta r_0} \frac{D_r}{(\beta - \beta_0)^2 - \beta_p^2} \quad \dots(8.76)$$

where  $\beta_p = \frac{\omega_p}{v_0}$

$D_r$ , in general being a finite quantity, there is a singular value of  $\beta$  at which the current becomes large. This results in current resonance with a propagation constant  $\beta = \frac{\omega \pm \omega_p}{v_0}$ . This also shows that the electron beam will possess two space charge waves even in the absence of RF excitation. These waves, known as slow and fast space charge waves travel with velocities given by

$$v = \frac{\omega}{\omega \pm \omega_p} v_0 \quad \dots(8.77)$$

In presence of an RF field, these two waves interact with the RF signal all along the slow wave circuit.

If the slow wave structure can be thought of as a transmission line with series impedance ( $Z$ ) and shunt admittance ( $Y$ ), we have

$$j\beta_1 = (YZ)^{1/2} \quad \dots(8.78)$$

where  $\beta_1$  = phase constant for the slow wave circuit.

The coupling between the beam and the slow wave structure can be obtained by connecting a displacement current  $di$  as shown in Fig. 8.28.

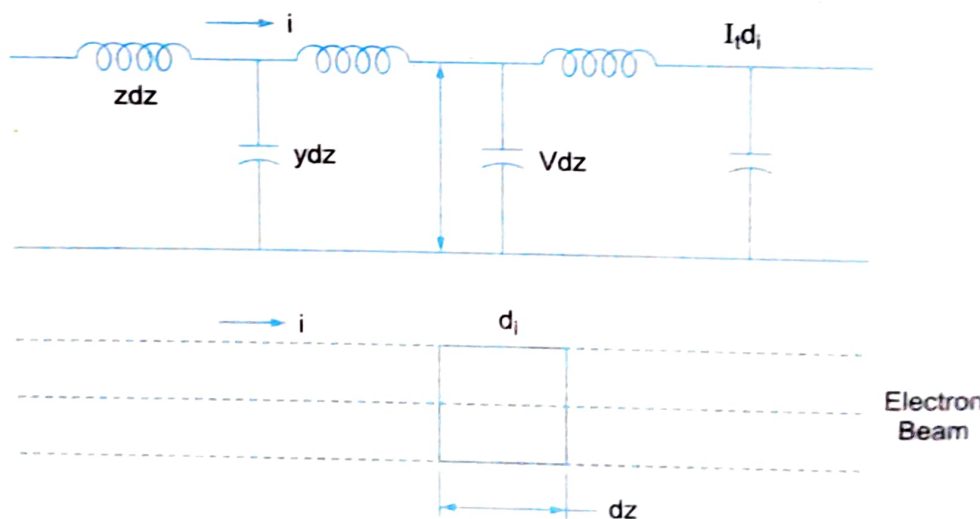


Fig. 8.28

$$dV = -IZdz$$

$$dI = -VYdz - di$$

where  $di = \left(\frac{\partial i}{\partial z}\right) dz$  and  $i$  is the beam current  $= J_{z_1} \pi r_0^2$ .

we know,  $\frac{d}{dz} = -j\beta$  and relation between  $\beta$  and  $\beta_1$  becomes

$$(\beta^2 - \beta_1^2) V = j\beta Z_i = j\beta Z J_{z_1} \pi r_0^2 \quad \dots(8.79)$$

Voltage  $V$  is proportional to transverse component of electric field expressed in terms of  $J_{z_1}$  (Eq. 8.76).

Substituting for  $J_{z_1}$  in Eq. 8.79,

$$(\beta^2 - \beta_1^2) = \frac{-A}{(\beta - \beta_0)^2 - \beta_p^2} \quad \dots(8.80)$$

where  $A = \frac{-2 \omega \beta_p^2 \times \epsilon_0 E_r}{r_0 V} \pi r_0^2$ , a constant and  $Z = jX$ .

Since Eq. 8.80 is a fourth order equation in  $\beta$ , it has four roots. Since  $\beta_p \ll \beta_0$ , there will be three forward wave solutions and one backward wave solution corresponding to  $(\beta + \beta_1)$ . If  $(\beta + \beta_1)$  is replaced by  $2\beta_1$ , Eq. 8.80 can be written as,

$$(\beta - \beta_1)(\beta^2 - 2\beta\beta_0 + \beta_p^2) = -(A/2\beta_1) \quad \dots(8.81)$$

If

$$\begin{aligned} \beta_1^2 &= \beta_0^2 - \beta_p^2, \\ (\beta - \beta_1)^3 &= -(A/2\beta_1) \end{aligned} \quad \dots(8.82)$$

This equation corresponds to three values of  $\beta$

$$\begin{aligned} \beta &= \beta_1 + b \left( \cos \frac{\pi}{3} + j \sin \frac{\pi}{3} \right) \\ \beta &= \beta_1 + b(\cos \pi + j \sin \pi) \end{aligned} \quad \dots(8.83)$$

and

$$\beta = \beta_1 + b \left( \cos \frac{5\pi}{3} + j \sin \frac{5\pi}{3} \right)$$

where  $b = (A/2\beta_1)^{1/3}$ .

These three values of  $\beta$  correspond to three types of waves along  $z$ .

1.  $e^{-j(\beta_1 + 0.5b)z} e^{-0.866 bz}$

which represents a wave that is attenuated exponentially as it travels.

2.  $e^{-j(\beta_1 + b)z}$

which represents an unattenuated wave and

3.  $e^{-j(\beta_1 + 0.5b)z} e^{+0.866 bz}$

which represents a wave that grows exponentially as it travels.

For large values of  $z$ , the wave in 3. dominates the other two waves 1. and 2. and this is responsible for amplification in the helix TWT.

The kinetic energy (KE) of the electrons is the real source for the increase in electro-magnetic energy associated with the growth of the helix wave. As the bunches continuously slow down as they travel down the tube, the helix wave gains energy at the expense of the KE of the electrons. It may be noted that in a TWT the bunches travel faster than the wave on the helix. The gain of the TWT is given by,

$$G = -9.54 + 47.3 CN \text{ (dB)} \quad \dots(8.84)$$

where,  $C = \text{gain parameter} = k \left( \frac{I_0}{V_0} \right)^{1/3}$

$N = \text{helix length in wavelengths} = Z/\lambda_s$ .

$\lambda_s = v_p/f$

$k = \text{constant}$

$v_p = \text{axial phase velocity}$

$I_0 = \text{dc beam current}$

$V_0 = \text{dc beam voltage}$

The gain will be maximum when the beam velocity is approximately in synchronism with the axial wave velocity  $v_p$ .

There is always a chance of feed back from output to input and also there could be some spurious signals generated within the TWT. These may cause parasitic oscillations in the TWT. These can be suppressed by coating the inside glass wall of the TWT with aquadog which acts as an attenuator. This helps in absorption of spurious signals and all parasitics (although some absorption of the desired signal also might occur, reducing amplification) and is quite effective. Normally the attenuator is kept at the input end of the tube since the attenuator attenuates both forward and reverse waves but then the latter are more heavily attenuated than the former.

The high frequency limit of a TWT can be increased by decreasing the helix diameter. i.e., The lower and higher frequency limits are due to the size limitations in a TWT. At low frequencies, the gain is limited by the helix length.

## Performance Characteristics of TWT

1. Frequency of operation : 0.5 GHz to 95 GHz.
2. Power outputs : 5 mW (10–40 GHz) (Low power TWT)  
250 kW (CW) at 3 GHz (High Power TWT)  
10 MW (pulsed) at 3 GHz
3. Efficiency : 5 to 20% (30% with depressed collector)  
(A depressed collector is a set of collector rings maintained at successively higher potentials to effectively slow down the electron beam that still possesses a considerable KE).
4. Noise figure : 4–6 dB (Low Power TWT 0.5 to 16 GHz)  
25 dB (High Power TWT at 40 GHz).

## Applications of TWT

1. Low noise RF amplifier in broad band microwave receivers.
2. Repeater amplifier in wide band communication links and coaxial cables (Long Distance Telephony).
3. Due to long tube life (50,000 hours against 1/4th for other types), TWT is used as power output tube in communication satellites.

4. Continuous wave high power TWT's are used in troposcatter links (due to larger power and larger bandwidths).
5. Airborne and shipborne pulsed high power radars ECM ground based radars use a TWT.

## 8.7 BACKWARD WAVE OSCILLATOR

$\alpha$

Backward wave oscillator (BWO) is a microwave continuous wave (CW) oscillator with excellent tuning capability and frequency coverage range. BWO is similar in construction and operates on the same principle of electron beam–RF field interaction, generally employing a helical slow wave structure. It can be thought of as a short, thick TWT.

### 8.7.1 Operation

The electron beam from the electron-gun cathode is focussed by an axial magnetic field. If transients have resulted in starting *RF* oscillations, these travel through the helix and interact with the electron beam. Bunching takes place increasing in completeness from the cathode to the collector and interchange of energy between the electron beam and the *RF* wave occurs exactly in the same way as in TWT. Since BWO does not have an attenuator, there will be oscillations due to reflections from an imperfectly terminated collector end of the helix. The reflected wave results in a backward wave.

The interaction between *RF* and the electron beam is different in BWO (as against TWT). The growing *RF* wave travels in a direction opposite to that of the electron beam. A  $\omega$ - $\beta$  curve called the dispersion curve is shown in Fig. 8.29, where  $\omega$  is the angular frequency and  $\beta$  is the phase constant. The growing *RF* wave has a group velocity in the backward direction. In the direction *OB* (Refer to Fig. 8.28), phase velocity  $v_p (= \omega/\beta)$  and group velocity  $d\omega/d\beta$  are *positive*. This is the case in TWT. In the portion *BC*, the beam velocity of the electron  $v_p$ , phase velocity of the *RF* wave  $\omega/\beta$  are positive but the group velocity  $d\omega/d\beta$  is *negative*. Interaction takes place during the backlash region *BC* (in Fig. 8.28). In fact BWO, can be thought of as a feed back loop akin to low frequency circuit as shown in Fig. 8.30.

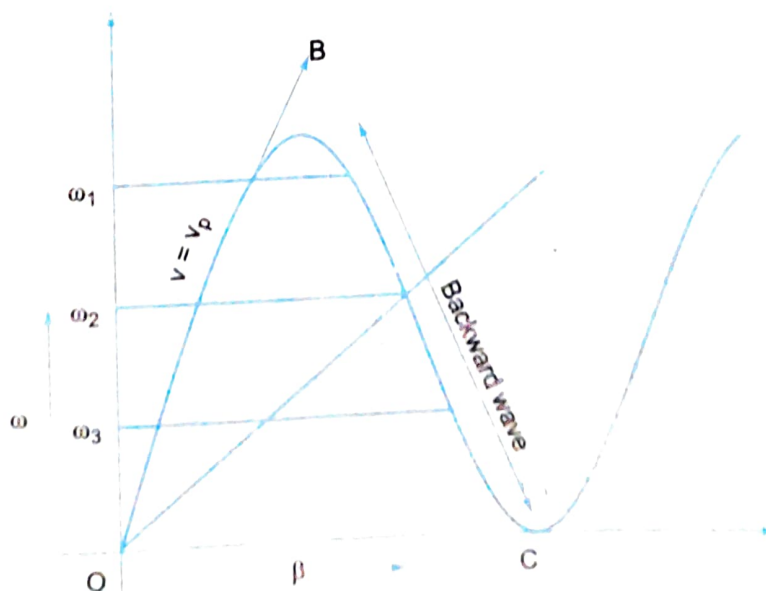


Fig. 8.29

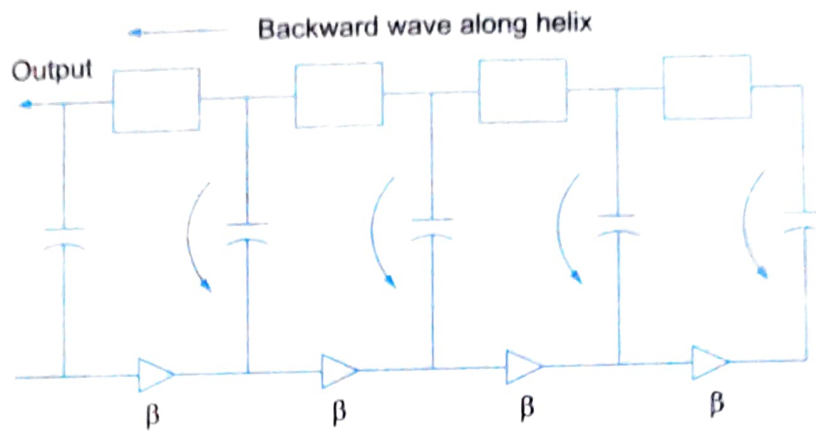


Fig. 8.30

The figure (Fig. 8.30) shows several regenerative loops that function as an amplifier with  $\beta > 1$  the feed back factor in the looping of the output to input. Each regenerative loop functions as an amplifier or oscillator and is designed such that the phase shift around the loop is  $2\pi$  radians. The forward circuit is the helix along which the wave moves. The feed back circuit is the  $\beta$ -circuit in feedback amplifier. Connecting the output to input when the amplifier gain becomes sufficiently large (compared to the transmission loss), positive feed back takes place and the  $\beta$ -circuit loop oscillates at the frequency for which the total delay is  $2\pi$  radians.

The RF field velocity modulates the electron beam which moves towards the collector end of the tube forming a bunch. This bunch now provides energy to the helix RF wave in the backward direction. This looping continues until there is sufficient energy in the RF wave. The frequency of oscillation of a BWO can be varied by varying the voltage controlling the beam velocity and the amplitude of oscillations by changing the electron beam current (voltage of the electron gun anode).

## Performance Characteristics of BWO

1. Frequency range : 1 GHz to 1000 GHz.
2. Power output : 10 mW to 150 mW (CW)  
20 W (at high frequencies)  
250 kW (pulsed) with duty cycle < 1 sec
3. Tuning range : upto about 40 GHz.

## Applications of BWO

BWO can be used as

1. Signal sources in instruments and transmitters.
2. Broad band noise source (for enemy radar confusion).
3. A noiseless oscillator with good bandwidth in the frequency range 3–9 GHz.

## 8.8 MAGNETRONS

The tubes discussed earlier (viz. klystron, reflex klystron, TWT and BWO) are linear beam tubes generally called *O* tubes or original type. The other type of microwave tubes are cross field tubes in which the electric and magnetic fields are perpendicular to each other. The principal tube in this type, called the *M*-type is the *Magnetron*.

The magnetron was invented by Hull in 1921 and an improved high power magnetron was developed by Randall and Boot around 1939. Magnetrons provide microwave oscillations of very high peak power.

It may be noted in klystrons that the electrons carrying energy are in contact with the *RF* field in the resonant cavity only for a short duration. However, if the electrons can be made to interact with *RF* field for a longer duration higher efficiency can be obtained. This has been done in TWT and in magnetron also the same technique is utilised.

There are three types of magnetrons.

1. Negative Resistance type
2. Cyclotron frequency type
3. Travelling Wave or Cavity type.

*Negative resistance Magnetrons* make use of negative resistance between two anode segments but have low efficiency and are useful only at low frequencies (< 500 MHz).

*Cyclotron frequency magnetrons* depend upon synchronism between an alternating component of electric and periodic oscillation of electrons in a direction parallel to this field. These are useful only for frequencies greater than 100 MHz.

*Cavity magnetrons* depend upon the interaction of electrons with a rotating electro-magnetic field of constant angular velocity. These provide oscillations of very high peak power and hence are very useful in radar applications. This being the most useful one, we shall study this in detail.

### 8.8.1 Cavity Magnetron

It is a diode usually of cylindrical configuration with a thick cylindrical cathode at the centre and a coaxial cylindrical block of copper as anode. In the anode block are cut a number of holes and slots which act as resonant anode cavities. The space between the anode and cathode is the interaction space and to one of the cavities is connected a coaxial line or waveguide for extracting the output. It is a cross field device as the electric field between anode and cathode is radial whereas the magnetic field produced by a permanent magnet is axial. The permanent magnet is placed such that the magnetic lines are parallel to the vertical cathode and perpendicular to the electric field between cathode and anode. The construction is shown in Fig. 8.31a and b.

Electric Field Between  
Cathode & Anode Radial

Magnetic Field Produced  
by Permanent Magnet  
Axial

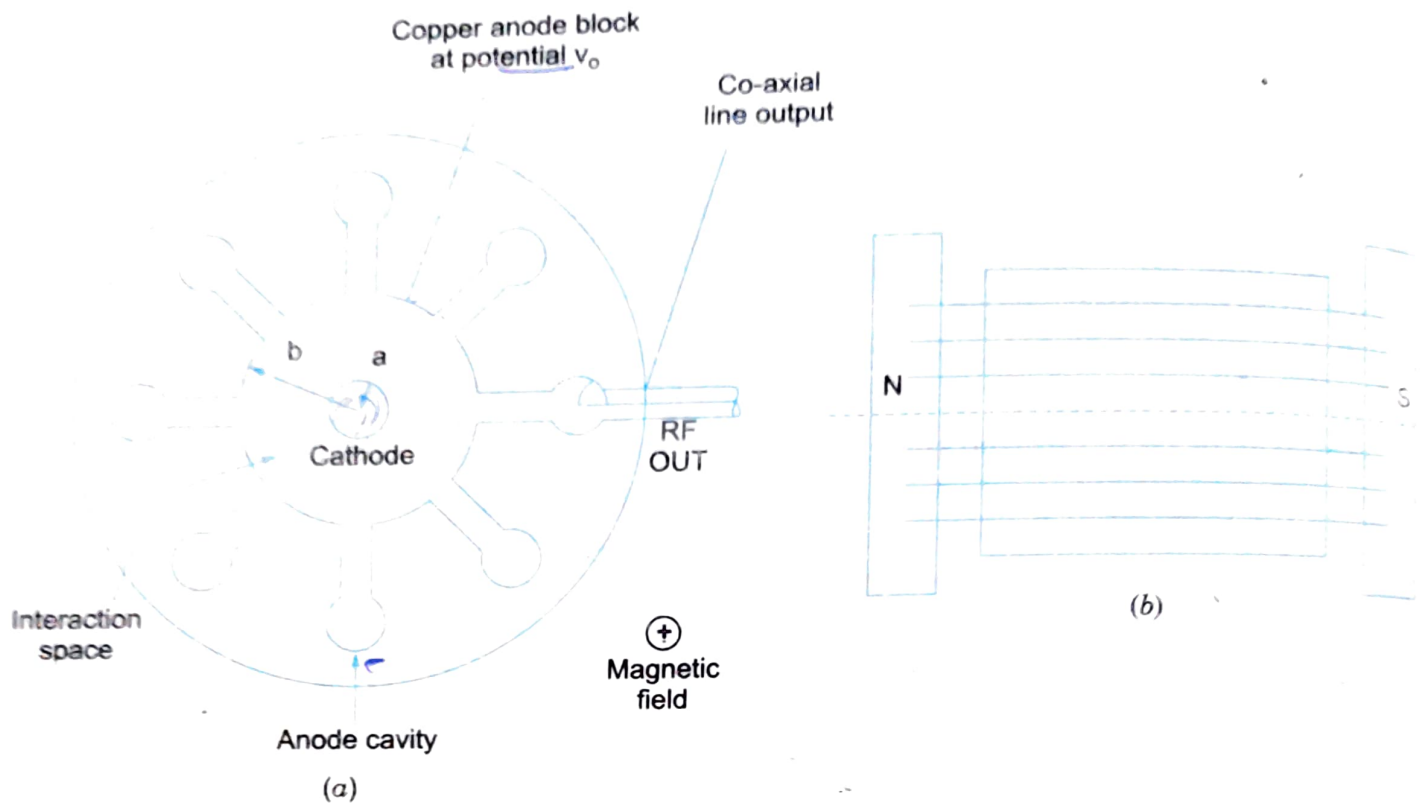


Fig. 8.31 (a) Constructional detail of cavity magnetron. (b) Magnetic flux lines in magnetron

## Operation

The cavity magnetron shown in Fig. 8.31 has 8 cavities, that are tightly coupled to each other. We know, in general that a  $N$ -cavity tightly coupled system will have  $N$ -modes of operation each of which is uniquely characterised by a combination of frequency and phase of oscillation relative to the adjacent cavity. In addition, these modes must be self consistent so that the total phase shift around the ring of cavity resonators is  $2n\pi$  where  $n$  is an integer. For example, a phase shift should be  $40^\circ$  between cavities of a 8-cavity magnetron will mean that the first cavity is out of phase with itself by  $320^\circ$ ! The correct minimum phase shift should be  $45^\circ$  ( $45 \times 8 = 360^\circ$ ). Therefore if  $\phi_v$  represents the relative phase change of the ac electric field across adjacent cavities, then,

$$\boxed{\phi_v = \frac{2\pi n}{N}} \quad \text{where } n = 0, \pm 1, \pm 2, \dots, \pm \left(\frac{N}{2} - 1\right), \pm \frac{N}{2}. \quad \dots(8.85)$$

i.e.,  $N/2$  mode of resonance can exist if  $N$  is an even number.

$$\text{If } n = \frac{N}{2},$$

$$\phi_v = \pi$$

This mode of resonance is called the  $\pi$ -mode

$$\text{If } n = 0, \quad \phi_v = 0.$$

This is the zero mode, meaning there will be no RF electric field between anode and cathode (called the fringing field) and is of no use in magnetron operation.

To understand the operation of cavity magnetron, we must first look at how the electrons behave in the presence of closed electric and magnetic fields.

Depending on the relative strengths of the electric and magnetic fields the electrons emitted from the cathode and moving towards the anode will traverse through the interaction space as shown in Fig. 8.32.

In the absence of magnetic field ( $B = 0$ ), the electron travels straight from the cathode to the anode due to the radial electric field force acting on it (indicated by the trajectory 'a' in Fig. 8.32). If the magnetic field strength is increased slightly (i.e., for moderate value of  $B$ ) it will exert a lateral force bending the path of the electron

as shown by path 'b' in Fig. 8.32. The radius of the path is given by  $R = \frac{mv}{eB}$ , that varies directly with electron velocity and inversely as the magnetic field strength.

If the strength of the magnetic field is made sufficiently high so as to prevent the electrons from reaching the anode (as shown by path 'c' and those inside in Fig. 8.33) the anode current becomes zero. The magnetic field required to return electrons back to cathode just grazing the surface of the anode is called the critical magnetic field ( $B_c$ ), the cut-off magnetic field. If the magnetic field is made larger than the critical field ( $B > B_c$ ), the electron experiences a greater rotational force and may return back to cathode quite faster. All such electrons may cause back heating of the cathode. This can be avoided by switching off the heater supply after commencement of oscillation. This is done to avoid fall in the emitting efficiency of the cathode.

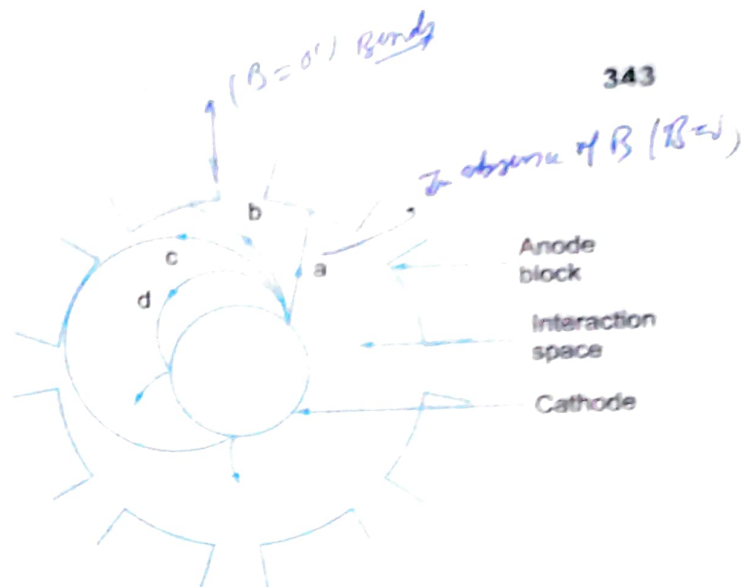


**Fig. 8.32** Electron trajectories in the presence of crossed electrical and magnetic fields. (a) No magnetic field (b) Small magnetic field (c) Magnetic field =  $B_c$  (d) Excessive magnetic field

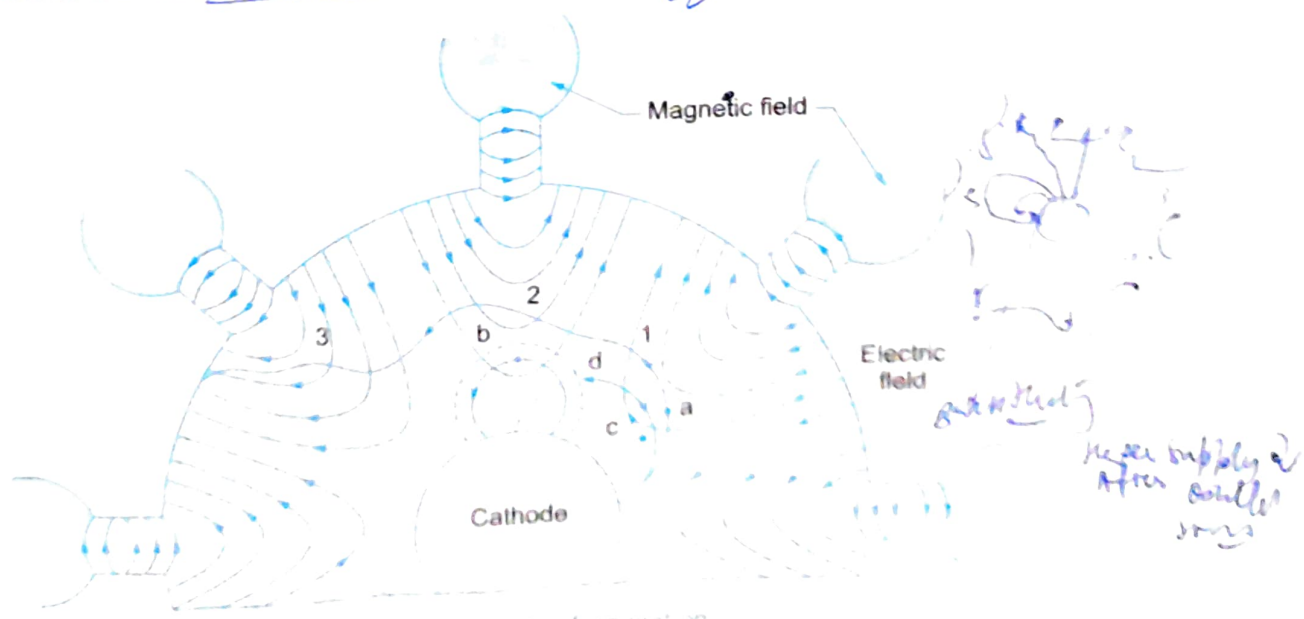


**Fig. 8.33** Anode of magnetron

*self sustained oscillation will be generated if only adjacent anodes are there*

All the above explanation is for a static case in the absence of the RF field in the cavity of magnetron.

Assuming RF oscillations to have been initiated due to some noise transient within the magnetron, the oscillations will be sustained by device operation. As pointed out earlier self consistent oscillations will be obtained if the phase difference between adjacent anode poles is  $n\pi/4$ , where  $n$  is an integer.  $n = 4$  results in  $\pi$ -mode of operation which is shown in Fig. 8.33. Here the anode poles are  $\pi$  radians apart in phase. The dotted electron paths refer to the case of static fields with no RF field. The solid paths refer to the electron trajectories in the presence of RF oscillations in the interaction space. The electron 'a' is seen to be slowed down in presence of oscillations thus transferring energy to the oscillations, during its longer journey from cathode to anode. Such electrons which participate in transferring energy to the RF field are called favoured electrons and are responsible for bunching-effect. An electron 'b' is accelerated by the RF field and instead of imparting energy to the oscillations takes energy from oscillations resulting in increased velocity. Hence bends more sharply, spends very little time in the interaction space and is returned back to the cathode. Such electrons are called unfavoured electrons which do not participate in the bunching process rather they are harmful in the sense they cause back heating. Similarly an electron 'c' which is emitted a little later to be in correct position moves faster and tries to catch up with electron 'a' and an electron emitted at 'd' will be slowed down to fall back in step with electron 'a'. This results in all favoured electrons like 'a', 'c', 'd' to form a bunch and are confined to spokes or electron clouds. One for each two anodes as shown in Fig. 8.34. The process is called the phase focussing effect corresponding to a bunch of favoured electrons around the reference electrons 'a'. The spokes so formed in the  $\pi$ -mode rotate with an angular velocity corresponding to two poles per cycle.

The phase focussing effect of these favoured electrons imparts enough energy to the RF oscillations so that they are sustained.

### Mathematical Analysis

Cylindrical Magnetron being the most commonly used magnetrons, we will deal with its mathematical analysis (rather than parallel plate magnetron which is not very commonly used).

Let the cathode and anode radius be 'a' and 'b' respectively and  $\phi$  the angular displacement of the electron bends. Being a cross field device electric and magnetic fields are perpendicular to each other and the path of the electrons in the presence of this cross field is naturally parabolic. (Refer Fig. 8.35)

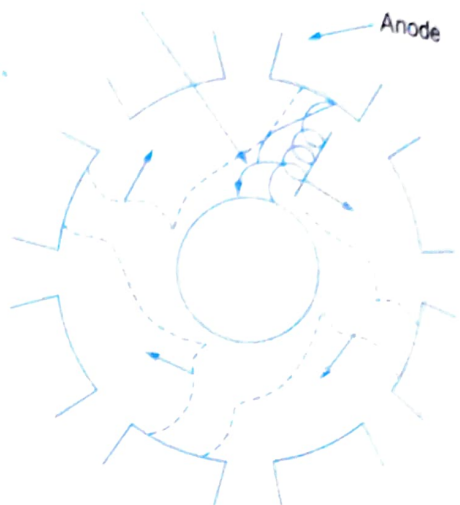
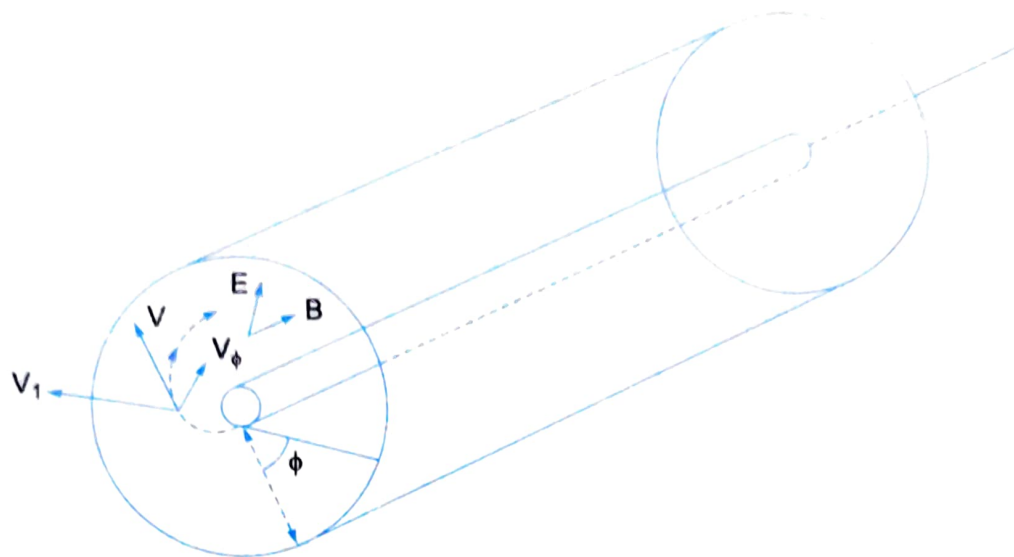


Fig. 8.34 Phase focussing effect



**Fig. 8.35** Diagram for analysis of cylindrical magnetron.

Force acting on the electron is

$$F = Bev$$

In the direction of  $\phi$ , the force component  $F_\phi$  is given by,

$$F_\phi = eBv_p$$

where  $v_p$  = velocity in the direction of the radial distance  $\rho$  from the centre of the cathode cylinder.  
Torque in  $\phi$  direction is

$$T_\phi = \rho F_\phi = e\rho v_p B \quad \dots(8.86)$$

Angular momentum = angular velocity  $\times$  moment of inertia

$$= \frac{d\phi}{dt} \times m\rho^2$$

$$\text{Time rate of angular momentum} = \frac{d}{dt} \left( \frac{d\phi}{dt} \times m\rho^2 \right) \quad \dots(8.87)$$

which gives the Torque in  $\phi$  direction.

Equating Eq. 8.87 and Eq. 8.86, (the two values of Torque in  $\phi$  direction).

$$\frac{d}{dt} \left[ \left( \frac{d\phi}{dt} \right) m\rho^2 \right] = e \cdot \rho \cdot v_p \cdot B$$

$$2 m\rho \frac{d\phi}{dt} + m\rho^2 \frac{d^2\phi}{dt^2} = e \cdot \rho \cdot v_p \cdot B \quad \dots(8.88)$$

i.e.,

$$v_p = \frac{d\rho}{dt}$$

We know that

$$\rho v_p = \rho \cdot \frac{d\rho}{dt}$$

$$\int \rho \cdot \frac{d\rho}{dt} = \frac{\rho^2}{2}$$

Integrating Eq. 8.88 with respect to 't'.

$$2m\rho \cdot \dot{\phi} + m\rho^2 \cdot \frac{d\phi}{dt} = eB \cdot \frac{\rho^2}{2}$$

For a particular direction  $\phi$ ,  $m\rho \dot{\phi}$  can be thought of as a constant.

$$m\rho^2 \frac{d\phi}{dt} + C = eB \cdot \frac{\rho^2}{2}$$

Now applying boundary conditions (i.e., at surface of the cathode  $\rho = a$  and  $\frac{d\phi}{dt} = 0$  being angular velocity at emission), we can determine the value of constant 'C'.

$$0 + C = \frac{e \cdot B \cdot a^2}{2} \text{ or } C = \frac{eBa^2}{2}$$

Substituting the value of 'C' in Eq. 8.89,

$$m\rho^2 \frac{d\phi}{dt} = \frac{eB}{2}(\rho^2 - a^2)$$

or 
$$\frac{d\phi}{dt} = \frac{eB}{2m} \left( 1 - \frac{a^2}{\rho^2} \right)$$

when  $\rho = a$ , (i.e., at cathode),  $\frac{d\phi}{dt}$  approaches 0.

and when  $\rho >> a$ ,  $\frac{d\phi}{dt}$  approaches  $(\omega)_{\max}$  (Maximum angular velocity).

i.e., 
$$\left( \frac{d\phi}{dt} \right)_{\max} = (\omega)_{\max} = \frac{eB}{2m} = \frac{eB_c}{2m}$$

where  $B = B_c$  is the cut-off magnetic flux density.

We know from conservation of energy that

Potential energy of electron = Kinetic energy of electron

i.e., 
$$eV_0 = \frac{1}{2}mv^2$$

$$eV_0 = \frac{m}{2}(v_\rho^2 + v_\phi^2)$$

where  $v_\rho$  and  $v_\phi$  are components in  $\rho$  and  $\phi$  directions in cylindrical co-ordinates.

$$v_\rho = \frac{d\rho}{dt} \quad \text{and} \quad v_\phi = \rho \cdot \frac{d\phi}{dt}$$

Rewriting Eq. 8.91, (substituting for  $v_\rho$  and  $v_\phi$ ),

$$eV_0 = \frac{m}{2} \left[ \left( \frac{d\rho}{dt} \right)^2 + \rho^2 \left( \frac{d\phi}{dt} \right)^2 \right]$$

From Eq. 8.90,

$$\begin{aligned} \left( \frac{d\phi}{dt} \right) &= (\omega)_{\max} \left( 1 - \frac{a^2}{\rho^2} \right) \\ eV_0 &= \frac{m}{2} \left[ \left( \frac{d\rho}{dt} \right)^2 + \rho^2 (\omega)_{\max}^2 \left( 1 - \frac{a^2}{\rho^2} \right)^2 \right] \end{aligned} \quad \dots(8.92)$$

At anode,  $\rho = b$ ,  $\frac{d\rho}{dt} = 0$ . Substituting these boundary conditions in Eq. 8.92,

$$\frac{m}{2} \left[ b^2 \cdot (\omega)_{\max}^2 \left( 1 - \frac{a^2}{b^2} \right)^2 \right] = eV_0 \quad \dots(8.93)$$

Also,  $(\omega)_{\max}^2 = \left( \frac{eB_c}{2m} \right)^2$  (from Eq. 8.90).

where  $B_c$  is the cut-off value of the magnetic flux density.

Substituting for  $(\omega)_{\max}^2$  in Eq. 8.74,

$$\frac{m}{2} b^2 \left( \frac{eB_c}{2m} \right)^2 \times \left( 1 - \frac{a^2}{b^2} \right)^2 = eV_0.$$

i.e., 
$$\frac{e^2 B_c^2 b^2}{8m} \left( 1 - \frac{a^2}{b^2} \right)^2 = eV_0$$

or 
$$B_c = \frac{(8V_0 m/e)^{1/2}}{b \left( 1 - \frac{a^2}{b^2} \right)}$$

Since  $b >> a$  and  $\frac{a^2}{b^2}$  can be neglected,

$$B_c = \frac{1}{b} \sqrt{\frac{8mV_0}{e}} \quad \dots(8.94)$$

At this cut-off value of magnetic field, the electron grazes the anode and the value of this magnetic field can be obtained by the knowledge of anode voltage. Equation 8.94 is called the Hull's cut-off voltage equation.

## Sustained Oscillations in Magnetron

The cavities of magnetron are of high  $Q$  and transient switching is good enough to start oscillations. When anode voltage is applied, the electrons from cathode deflect towards the anode. As they gain velocity, the axial magnetic field acts on them. The radial direction (due to electric field) of electrons is now changed and are deflected with a tangential velocity due to magnetic field. Due to the RF field in the interaction space, the tangential velocity of the electrons experience a drag or opposition slowing them in the process. In losing velocity, the electrons give off their energy to the RF field. As the velocity of the electrons is less, the deflection force of the magnetic field on them also is reduced and hence these electrons (favourable electrons only) move towards the anode instead of curving back to the cathode in spite of  $B > B_c$ .

The spacing between the anodes is so adjusted that it is equivalent to half cycle of the frequency and hence when the electrons reach the second anode the polarity of *RF* reverses. The electrons continue to slow down since the energy acquired by them in falling through the dc anode to cathode voltage is delivered to the *RF* oscillating wave. The electrons finally reach the anode after having slowed down almost to a dead spot having delivered the kinetic energy acquired from anode to cathode voltage.

In the presence of the cross field, let us consider one such favourable electron. The outward centrifugal force must equal the magnetic force on this electron.

$$\text{i.e., } \frac{mv^2}{r} = eVB$$

where,  $r$  = radius of cycloidal path.

$$\text{Angular velocity, } \omega = \frac{v}{r} = \frac{eB}{m}$$

$$\text{Period of one revolution, } T = \frac{2\pi}{\omega} = \frac{2\pi m}{eB}$$

Therefore for oscillations to occur, the feedback should be in phase or integral multiples of radians. If there are  $N$ -cavities, the phase should be

$$\phi = \frac{2\pi n}{N}$$

where  $n$  = an integer indicating  $n$ th mode of oscillation. As already discussed, magnetron oscillator are operated in the  $\pi$ -mode so that  $\phi = \pi$ . In the  $\pi$  mode the *RF* fields in successive cavities are in antiphase, as shown in Fig. 8.32.

The angular velocity of the *RF* field in the interaction space is given by,

$$\frac{d\phi}{dt} = \frac{\omega}{\beta}$$

The condition for maximum transfer of energy from the electrons to the *RF* field takes place when the cyclotron frequency of electron is equal to angular velocity of the *RF* wave.

i.e.,

$$\frac{\omega}{\beta} = \frac{d\phi}{dt} \quad \text{or} \quad \omega = \beta \frac{d\phi}{dt} = \frac{eB}{m}$$

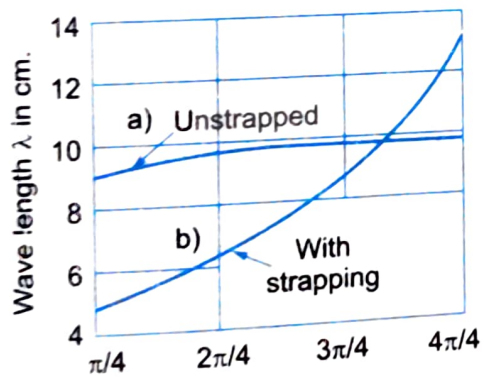
... (8.95)

## Mode jumping in Magnetron

The resonant modes of magnetron are very close to each other and there is always a possibility of mode jumping (Fig. 8.36a). i.e., The weaker modes have frequencies differing very little from the dominant mode and the purity of vibrations may be lost. Mode jumping hence must be avoided. A magnetron in which no effort is made to separate the dominant mode (mostly the  $\pi$ -mode) from other modes is said to be unstrapped. A method commonly employed to avoid mode jumping is known as strapping.

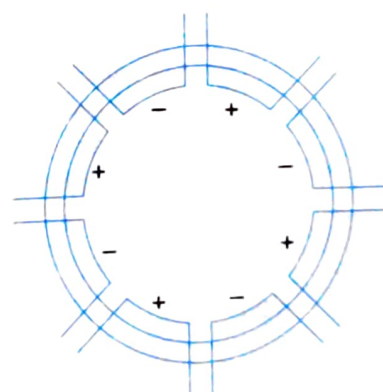
Strapping means to connect alternate anode plates with two conducting rings of heavy gauge touching the anode's poles at the dots as shown in Fig. 8.36b. This is done in order to make the  $2\pi$  anode poles together (0,  $2\pi$ ,  $4\pi$  and  $6\pi$  anode cavities). Strapping helps in achieving only the dominant mode (here  $\pi$ -mode) in the magnetron. However strapping may cause power loss in the conducting rings. Also, at higher frequencies it will be difficult to maintain the RF field within the interaction space and strapping may introduce stray effects.

A magnetron which needs no strapping is the *rising sun magnetron* shown in Fig. 8.36c. Here the anode cavities are designed to be dissimilar and only the dominant mode with  $2\pi$  phase will be effective. The adjacent cavities oscillate at widely different frequencies and hence separation will be quite effective.

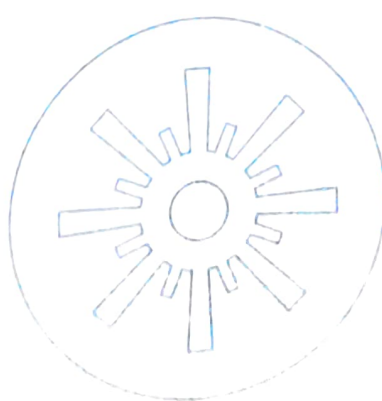


Mode (designated by phase difference between adjacent anode poles)

(a)



(b)



(c)

Fig. 8.36 (a) Mode jumping in magnetron strapped/unstrapped modes  
 (b) strapping scheme for  $\pi$ -mode (c) rising sun magnetron

## Frequency Pushing and Pulling

Similar to reflex klystron, it is possible to change the resonant frequency of magnetron by changing the anode voltage. This process referred to as frequency *pushing* is due to the fact that the change in anode voltage results in a change in orbital velocity of electrons. This alters the rate at which the energy is transferred to anode resonators and results in change of oscillation of frequency.

Magnetron is also susceptible to frequency variation due to changes in load impedance. This takes place regardless of whether these load variations are purely resistive or reactive variations. However, magnetron frequency variations are more severe for reactive variations. These frequency variations are known as *frequency pulling* caused by load impedance variations reflected in cavity resonators. To prevent frequency pushing a stabilised power supply is employed. Frequency pushing is prevented by using a circulator which does not allow backward flow of electromagnetic energy. It is placed before the wave guide connection at the output of the magnetron.

## Performance Characteristics of Magnetron

These are best studied by means of Rieke diagram (Fig. 8.37). The operating conditions of magnetron for a given load can be obtained from these diagrams which is basically a plot of anode voltage current with power output, efficiency, flux density, frequency deviation as parameters. The frequency pushing and pulling effects can be easily determined from this diagram.

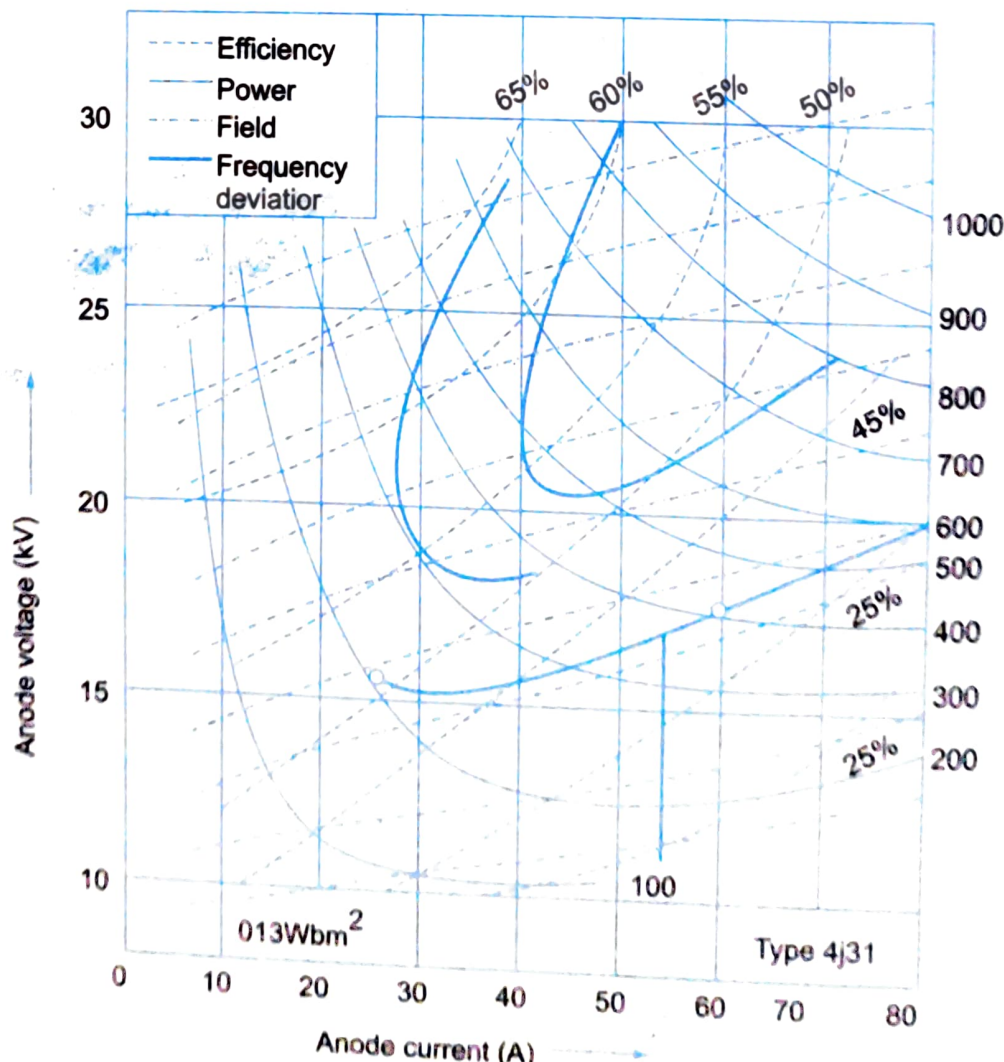


Fig. 8.37 Rieke diagram performance chart of magnetron

## Performance Characteristics

1. Power output : In excess of 250 kW (Pulsed mode)  
10 mW (UHF band) 2 mW (X band)  
8 kW (at 95 GHz)
2. Frequency : 500 MHz to 12 GHz.
3. Duty cycle : 0.1%
4. Efficiency : 40% to 70%

## Applications of Magnetron

1. Pulsed radar is the single most important application with large pulse powers.
2. Voltage Tunable magnetrons (VTM's) are used in sweep oscillators in telemetry and in missile applications. (200 MHz to X band with CW powers upto 500 W,  $\eta$  of 70%)
3. Fixed frequency, CW (continuous wave) magnetrons are used for industrial heating and microwave ovens (500 MHz–2.5 GHz frequency range, 300 W to 10 kW power outputs,  $\eta$  of 50%).

## Important Formulae

### Cavity Klystron Amplifier

$$\text{Electron velocity } v_0 = \sqrt{\frac{2eV_0}{m}} = 0.593 \times 10^6 \sqrt{V_0}$$

$$\text{Gap transit angle, } \theta_g = \omega \frac{d}{v_0}$$

$$\text{Beam-coupling coefficient, } \beta_i = \frac{\sin(\theta_g/2)}{(\theta_g/2)}$$

$$\text{d.c. transit angle between cavities, } \theta_0 = \frac{\omega L}{v_0}$$

$$\text{Bunching parameters, } X = \frac{\beta_i V_1}{2V_0} \theta_0$$

$$\text{Input voltage, } V = \frac{2V_0}{\beta_0 \theta_0} X$$

$$\text{Voltage gain, } A_v = \frac{|V_2|}{|V_1|} = \frac{\beta_0 I_2 V_2}{V_1} = \frac{\beta_0^2 \theta_0 J_1(X)}{R_0 X} R_{sh}$$

$$\text{Efficiency} = \frac{P_{out}}{P_{in}} = \frac{\beta_0 I_2 V_2}{2I_0 V_0} = \frac{0.58 V_2}{V_0}$$

Electron gain anode voltage for maximum power transfer

$$= \left( \frac{V_1}{V_0} \right)_{\max} = \frac{3.68}{2n\pi - \pi/2}$$

(as per Eq. 8)

## Multicavity Klystron Amplifier

Charge density,  $\rho = B \cos(\beta_c z) \cos(\omega_q t + \theta)$

Velocity perturbation,  $v = -C \sin(\beta_c z) \sin(\omega_q t + \theta)$

where  $B$  = constant of charge-density perturbation

$C$  = constant of velocity perturbation

$\beta_c = \frac{\omega}{V_0}$  is the d.c. phase constant of electron beam

$\omega_g = R\omega_p$  is the perturbation frequency of reduced plasma frequency

$R$  = the space charge reduction factor

$\omega_p = \sqrt{\frac{eP_0}{m_e}}$  is the plasma frequency

$\theta$  = phase angle of oscillation

Instantaneous convection beam-current density

$$J_{tot} = J_0 + J$$

$$J = \rho V_0 - \rho_0 V$$

$$J_0 = \rho_0 V_0$$

### Output Current and Power of Two-Cavity Klystron

$$I_2 = \frac{1}{2} \frac{I_0 \omega}{V_0 \omega_q} \beta_0^2 |V_1|$$

$$P_{out} = |I_2|^2 R_{shl} = \frac{1}{4} \left( \frac{I_0 \omega}{V_0 \omega_q} \right)^2 \beta_0^4 |V_1|^2 R_{shl}$$

$$\eta = \frac{P_{out}}{P_{in}} = \frac{P_{out}}{I_0 V_0} = \frac{1}{4} \left( \frac{I_0}{V_0} \right) \left( \frac{V_1 \omega}{V_0 \omega_q} \right)^2 \beta_0^4 R_{shl}$$

### Output Current and Power of Four-Cavity Klystron

$$|I_4| = \frac{1}{8} \left( \frac{I_0 \omega}{V_0 \omega_q} \right)^2 \beta_0^6 |V_1| R_{shl}^2$$

$$P_{out} = |I_4|^2 R_{shl} = \frac{1}{64} \left( \frac{I_0 \omega}{V_0 \omega_q} \right)^6 \beta_0^{12} |V_1|^2 R_{shl}^4 R_{load}^2$$

$R_{shl}$  = total short resistance of the output cavity including the external load.

# 9

# *Solid State Microwave Devices*

## 9.1 INTRODUCTION

As we have seen in the previous chapter of Microwave Tubes, the amplification, oscillation, switching, limiting or frequency multiplication basically employed velocity modulation theory. However in the recent past there has taken place a tremendous research activity for development of better, low noise, high frequency, greater bandwidth lesser switching time and other improvements in the performance characteristics for achieving the above functions. In this endeavor, several semiconductor microwave devices have been developed which include three terminal devices such as bipolar and field effect transistors and two terminal devices such as transferred electron devices (Gunn diodes, LSA diodes), avalanche transit time devices (IMPATT, TRAPATT, BARITT parametric devices), tunnel diodes, varactors, quantum electronic devices such as MASERS, semiconductor lasers and infrared devices.

All the above mentioned solid state devices employ negative resistance characteristics rather than velocity modulation for their operation. These devices have been commonly utilised for several applications that include modern communication systems, radars, navigation, medical and biological equipment and other industrial electronic products,

## 9.2 MICROWAVE TRANSISTORS

Similar to conventional tubes, transistors also suffer from high frequency limitations. The interelectrode capacitance, lead inductance and transit time again come into play at microwave frequencies. The high frequency response is limited by the interelectrode capacitance which makes  $\alpha$  and  $\beta$  of the transistor complex. Also the depletion layer width of the transistor junctions which is a function of the bias makes the problem much more complex than in tubes. Lead inductances have similar undesirable effect as in tubes but transistors being small in size have smaller leads.

Ideally, the effect of interelectrode capacitance and lead inductance must be kept minimum by proper choice of geometry and packaging of transistors. The transit time also has similar effects on transistors as in tubes but the effect seems a bit lesser on account of smaller distances electrons have to travel in a transistor. However this advantage is offset by smaller velocities of the current carriers (holes or electrons). The ion mobility, bias voltages, emitter delay time, base transit time, collector transit time are the parameters which have to be controlled for better performance.

### Construction

Silicon *n-p-n* transistors that can provide adequate powers at microwave frequencies have been developed, typically 5 watts at a frequency of 3 GHz with a gain of 5 dB. Normally these are made in planar form as a double diffused epitaxial device. A cross sectional view of such an *n-p-n* silicon transistor is shown in Fig. 9.1.

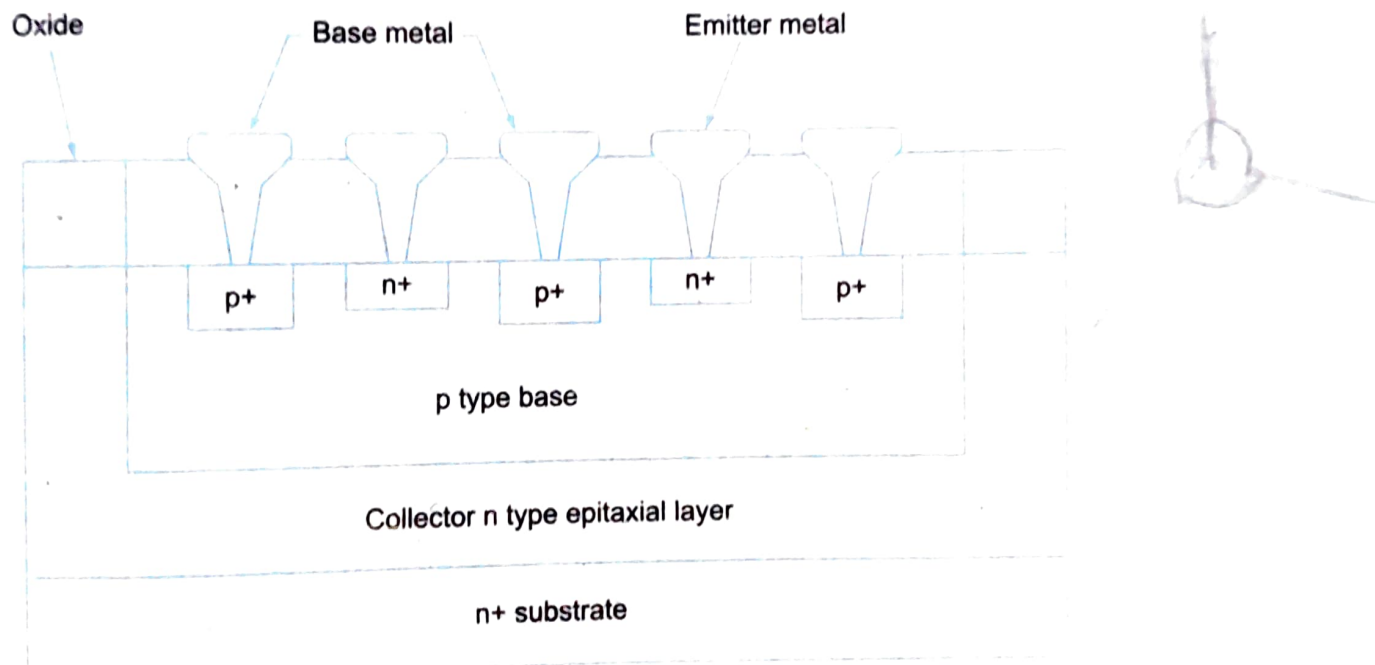
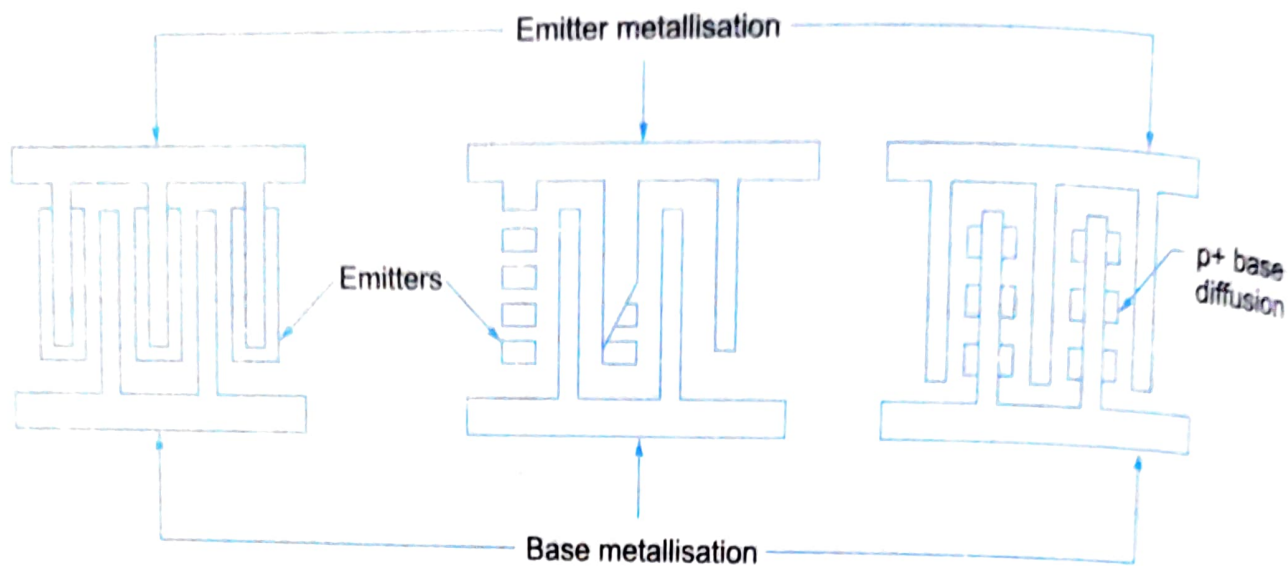


Fig. 9.1 *n-p-n* silicon double diffused epitaxial transistor

An *n* type epitaxial layer is grown on a *n+* substrate that constitutes the collector.  $\text{SiO}_2$  layer is then thermally grown over the *n* region in which a *p*-base and heavily doped *n*-emitters are diffused into the base. Contacts are provided by means of openings in the oxide and connections are made in parallel. The surface geometry of such transistors can have interdigitated, overlay or matrix forms as shown in Fig. 9.2.

Small signal transistors employ interdigitated surface geometry while power transistors employ all three surface geometries. The matrix geometry is sometimes called mesh or emitter grid.

The interdigitated geometry basically consists of a large number of emitter strips alternating with base strips. Both of these are metallised. The overlay geometry has a large number of segmented emitters overlaid through a number of wide metal strips. The matrix or mesh geometry has emitter that forms the grid, the base filling the meshes of this grid with a *p+* contact area in the middle of each mesh. Interdigitated structure is suitable for small signal applications in the L, S and C bands whereas overlay and matrix structures are useful as power devices in the VHF and UHF regions.



**Fig. 9.2** Surface geometry of *n-p-n* microwave transistor  
(a) interdigitated (b) overlay (c) matrix.

## Operation

In a microwave transistor, initially the emitter-base and collector-base junctions are reverse biased corresponding to class C condition. The microwave signal is applied between emitter and base and will forward bias this junction during the positive portion of the signal. If a *pnp* transistor is considered, the holes in the *p* region diffuse and drift through the thin base region to the collector and accelerate to the negative terminal of the bias voltage between collector and base terminals. A pulse of current flows through the load connected in the collector circuit.

## Performance Parameters #

The high frequency behaviour of microwave transistors is defined by  $f_T$ , the cut-off frequency and the maximum possible frequency of oscillation  $f_{\max}$  rather than  $\alpha$  (common base current gain), (common emitter current gain), cut-off frequencies  $f_{ab}$  and  $f_{ae}$

$$\beta = \frac{\alpha}{1 - \alpha} \text{ and } f_{ae} = \frac{f_{ab}}{\beta}$$

The cut-off frequency  $f_T$  is determined by the emitter-collector delay time  $\tau_{ec}$  and is given by

$$f_T = \frac{1}{2\pi\tau_{ec}} \quad \dots(9.1)$$

where,

and

$\tau_{ec} = \tau_e + \tau_b + \tau_d + \tau_c$

$\tau_e$  = the emitter base junction charging time,

$\tau_b$  = the base transit time,

$\tau_d$  = the collector depletion layer transit time and

$\tau_c$  = the collector depletion layer charging time.

Strictly speaking, for microwave transistors, the cut-off frequency is  $f'_T$  where,

$$f'_T = \frac{1}{\tau_{bec}} \quad \dots(9.2)$$

and

$$\tau_{bec} = \tau_{be} + \tau_{ec}$$

With  $\tau_{be} = rb'c_e$  and the base which is kept extremely narrow. Hence  $f'_T < f_T$ .

Alternately  $f_T$  can be defined as the current gain bandwidth frequency which is the frequency at which  $\beta$  falls to unity i.e., the highest frequency at which current gain may be obtained.

**Maximum Frequency of Oscillation ( $f_{max}$ )** is higher than  $f_T$  because although  $\beta$  has fallen to unity at this frequency and power gain has not. That is  $\beta = 1$ , output impedance is higher than input impedance, voltage gain exists and hence both generation and oscillation are possible. It is defined by the relation

$$f_{max} = \sqrt{\frac{f_T}{8\pi r'_B C_c}} \quad \dots(9.3)$$

where,  $f_T$  = cut-off frequency.

$r'_B$  = base resistance.

$C_c$  = collector capacitance.

Performance characteristics include high output power (particularly in the lower bands of the microwave region), high operating power efficiency (for class C operation), large operating bandwidth (for class A operation), lower signal distortion and noise levels. However structure of microwave transistors is quite complex than that of two terminal devices and also have problems of instability due to thermal runaway and breakdown.

### Power Frequency Limitations

As the frequency is increased, the output power drops mainly due to low impedance of the junction capacitance. This power frequency limitation was enunciated by Johnson and is due to

1. Maximum velocity of charge carriers in a semiconductor ( $6 \times 10^6$  cm/sec for electrons and holes in Si and Ge).
2. Maximum electric field that can be applied to a semiconductor ( $E_{max} = 2 \times 10^5$  V/cm for Si and  $10^5$  V/cm for Ge).
3. Width of the base that determines the maximum current.

### Voltage Frequency Limitations

If  $V_m$  is the maximum allowable applied voltage then

$$V_m = E_m L_m$$

where,  $E_m$  = maximum electric field

$L_m$  = maximum C-E distance

The charge carrier transit time cut-off frequency  $f_c$  is given by

$$f_c = \frac{1}{2\pi T_{av}}$$

where,  $T_{av} \approx$  base transit time ( $T_B$ ) + base collector depletion layer transit time ( $T_D$ )

$$f_c = \frac{V}{2\pi L_m}$$

$\therefore T_{av} = \frac{L_m}{V}$  (average charge carrier velocity)

$$V_m = E_m \times \frac{V}{2\pi f_c}$$

or  $V_m f_c = \frac{E_m V}{2\pi}$  (Voltage frequency limitation)

where,  $V$  is the drift velocity.

## Current Frequency Limitations

$$V_m = I_m X_c$$

where,  $I_m$  = maximum current limited by basewidth.

$$X_c = \frac{1}{\omega_c C_o}, \quad (C_o = \text{collector base capacitance})$$

Substituting for  $V_m$  in Eq. 9.4, we get

$$(I_m X_c) f_c = \frac{E_m V}{2\pi}$$

The power frequency limitation is given by the product of voltage frequency limitation and current frequency limitation. (Eqs. 9.4 and 9.5).

i.e.,  $f_c \cdot \sqrt{P_m X_c} = \frac{E_m V}{2\pi}$

As  $E_m \cdot V$  is a constant for a particular transistor as frequency is increased, maximum power capability decreases.

The power gain frequency limitation is given by

$$f \sqrt{G_m V_{th} V_m} = \frac{E_m V}{2\pi}$$

where,  $f$  = frequency of operation

$G_m$  = maximum available power gain

$V_{th}$  =  $KT/e$  (with usual notations)

## Performance Characteristics

1. Output power : 20 W to 150 mW for frequencies between 1 to 8 GHz.
2. Noise figure : 3.3 dB to 14 dB for frequencies between 4 GHz to 8 GHz.
3. Power gain :  $31 \pm 1.5$  dB over the frequency range 4 to 6 GHz with average power output of 15mW.
4. Voltage frequency limitation :  $2 \times 10^{11}$  V/s for Si and  $1 \times 10^{11}$  V/s for Ge.

## ~~9.4~~ CLASSIFICATION OF SOLID STATE MICROWAVE DEVICES

Solid state microwave devices can also be classified

1. Based on their electrical behaviour
2. Based on their construction.

Based on electrical behaviour we have,

- (a) Non-linear resistance type: *eg* varistors (variable resistances)
- (b) Non-linear reactance type : *eg* varactors (variable reactors)
- (c) Negative resistance type : *eg* Tunnel diode, Impatt diode, Gunn diode.
- (d) Controllable impedance type : *eg* PIN diode.

Based on construction we have,

- (a) Point contact diodes
- (b) Schottky barrier diodes
- (c) Metal oxide semiconductor devices (MOS).
- (d) Metal insulation devices.

The above solid state diodes have many applications, viz. amplification, detection down conversion, up conversion, modulation, switching, limiting, power generation, phase shifting etc. In this chapter we shall study principle of operation, constructional details, performance parameters, circuits and applications of some of the important semiconductor devices.

## 9.10 TRANSFERRED ELECTRON DEVICES (TED'S)

As we have seen before, the common characteristics of all active two terminal devices (solid-state) is their negative resistance. The real part of their impedance is negative over a range of frequencies. In a positive resistance the current through the resistance and the voltage across it are in phase. The voltage drops across positive resistance is positive and a power of  $I^2R$  is dissipated in the resistor. In a negative resistance the current and voltage are out of phase by  $180^\circ$ , the voltage drop across it is negative and a power of  $(-I^2R)$  is generated by the power supply associated with the negative resistance. In other words positive resistances absorb power (passive devices) and negative resistances generate power (active devices).

TED's are bulk devices having no junction, or gates as compared to microwave transistors which operate with either junction or gates. TED's are fabricated from compound semiconductors such as GaAs, InP (Indium phosphate) or CdTe (Cadmium telluride) as against Ge and Si transistors.

TED's operate with *hot* electrons whose energy is very much greater than the thermal energy. Transistors operate with *warm* electrons whose energy is not much greater than their thermal energy (0.026 eV at room temperature). Gunn diode is an example of this kind.

### **9.10.1 Gunn Effect Devices**

Gunn effect diodes are named after J.B. Gunn (1963), who discovered periodic fluctuations of current passing through the *n*-type GaAs specimen when the applied voltage exceeded a certain critical value. (2-4 kV/cms). Gunn effect can be explained on the basis of two valley theory of Ridley-Watkins-Hilsum (RWH) theory or the transferred electron mechanism.

Basic mechanism involved in the operation of bulk *n*-type GaAs devices is the transfer of electrons from lower conduction valley the *L*-valley, to upper subsidiary valley the *U*-valley.

As shown in Fig. 9.42, the curvature of the two valleys in the conduction band also called the sub bands are different so that an electron in *L*-valley has a smaller effective mass ( $m_1 = 0.072$  m<sub>0</sub>) than one in the *U*-valley ( $m_2 = 1.2$  m<sub>0</sub>). The different effective masses mean different mobilities for the *L*-valley ( $\mu_1 = 0.5$  m<sup>2</sup>/volt sec) and the *U*-valley ( $\mu_2 = 0.01$  m<sup>2</sup>/volt sec) respectively. The ratio of density of states in the *U*-valley to that in the *L*-valley is about 60. Thus the upper valley has a very high density of states compared with the  $k = 0$  location.

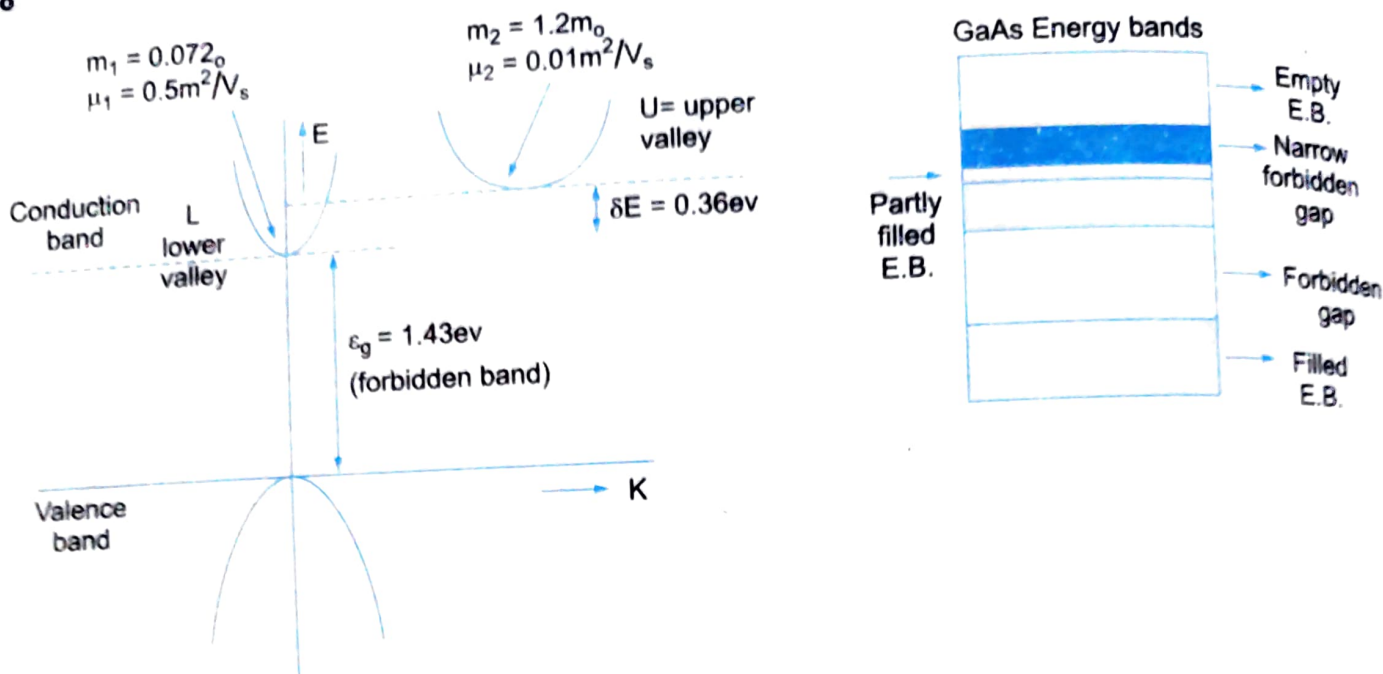


Fig. 9.42

At low (or zero) electric fields, conduction electrons are distributed in a manner determined by energy separation  $\delta E$ , the lattice temperature  $T_0$  and the density of states. With the typical values stated in the figure, most of the electrons at low electric fields and at low lattice temperatures will occupy states in the  $L$ -valley and carry ohmic current  $J = \sigma E$ .

With  $\sigma \approx p n_1 \mu_1 \approx e n_0 \mu_1$ , where,  $n_1$  is the carrier concentration in  $L$ -valley and is assumed to be equal to the total carrier concentration  $n_0$  and  $\mu_1$  is the mobility in the  $L$ -valley.

As the applied field is increased, the electrons gain energy from it and move upward in the  $U$ -valley. Actually the probability of this inter valley transfer of electrons is good as there are many available states in the  $U$ -valley. As the electrons transfer to this  $U$ -valley, their mobility decreases and the effective mass is increased thus decreasing the current density  $J$  and hence the negative differential conductivity. There is a certain threshold field, approximately 3.3 kV/cm above which this inter valley transfer (also known as the *population inversion*) of charges from lower  $L$ -valley to  $U$ -valley or the Transfer Electron effect takes place. As the transfer of electron is taking place, the current density should be given as

$$J = \sigma E = \rho (n_1 + n_2) \bar{\mu} E = e n_0 \bar{\mu} E \quad \dots(9.47)$$

where,  $\bar{\mu} = \frac{n_1 \mu_1 + n_2 \mu_2}{n_0}$  = the average mobility of electrons.

As the applied field is raised even higher almost all the electrons in the  $L$ -valley are transferred to  $U$ -valley and the current density will be given as

$$J = \sigma E \approx e n_2 \mu_2 E$$

where,  $n_2$  = carrier concentration

$\mu_2$  = mobility in  $U$ -valley

Thus a  $J$  vs.  $E$  curve is obtained similar to  $V$ - $I$  characteristic of  $pn$  junction diodes for the voltage controlled bulk negative conductance GaAs sample as in Fig. 9.43.

where,  $J_m$  = Maximum current density

$J_v$  = Valley current density

$E_m$  = Maximum electric field required before the onset of negative conductance region

$E_a$  = Maximum electric field for which  $J = \sigma E$  is valid

$E_b$  = Electric field for which  $J = en_2 \mu_2 E$  holds.

$E_v$  = Electric field corresponding to  $J_v$ .

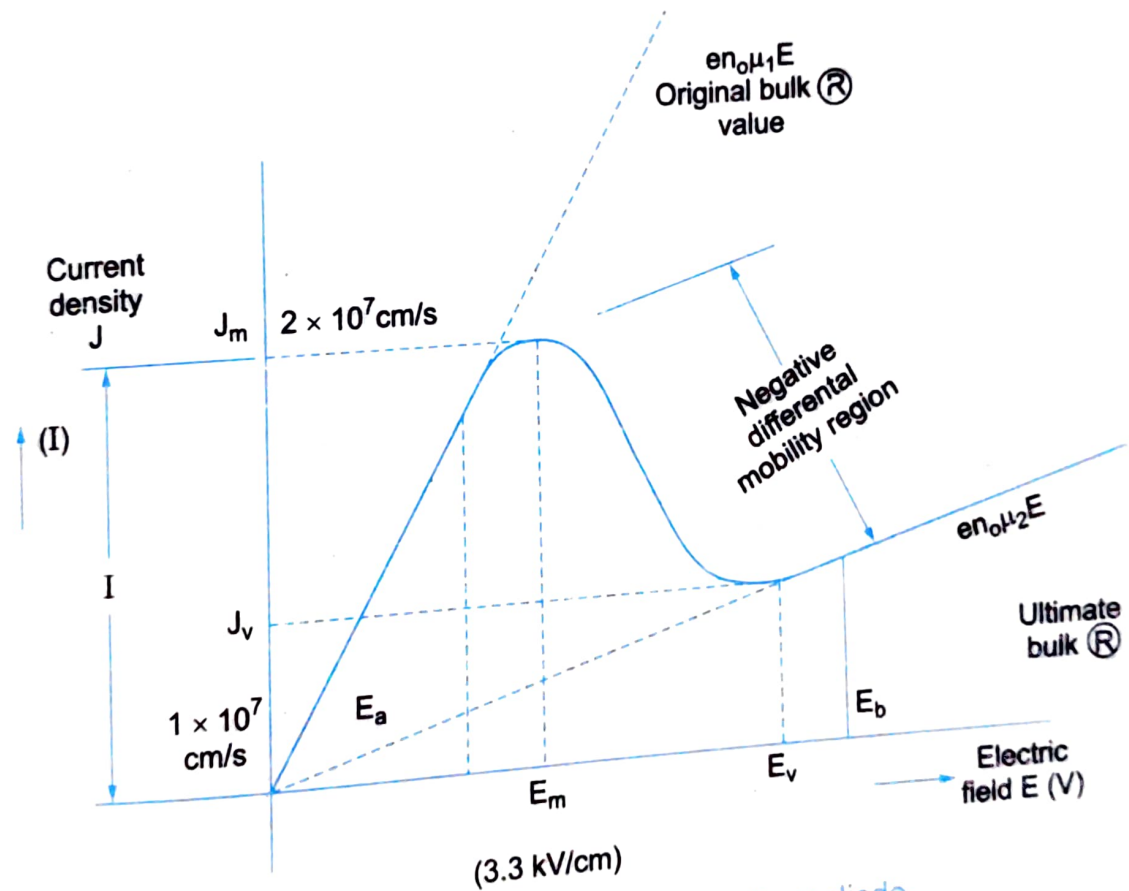


Fig. 9.43 JE characteristic of a Gunn diode.

$$\mu_l = \frac{V_d}{E}$$

$$\mu_n = \frac{dV_d}{dE}$$

$$\mu_u = \frac{V_d}{E}$$

$$V_d = fL$$

...(9.48)

where,  $V_d$  = electron drift velocity.

$f$  = frequency.

$L$  = device length.

$J \propto$  terminal current  $I$

Hence these  $J-E$  characteristics represent the  $V-I$  characteristic of Gunn diode.

The region of the characteristic between  $E_m$  and  $E_v$  where current density decreases with increasing electric field is one of negative differential resistivity (NDR).

Differentiating  $J = \sigma E = en_0 \bar{\mu} E$  w.r.t to  $E$  we get,

$$\frac{dJ}{dE} = \sigma \left[ 1 + \frac{E}{\sigma} \frac{d\sigma}{dE} \right]$$

The condition for negative conductance (or resistance) is

$$\frac{dJ}{dE} < 0 \text{ or } 1 + \frac{E}{\sigma} \frac{d\sigma}{dE} < 0$$

Hence if  $\partial E / \partial \sigma$  satisfies the above condition, i.e., if differential conductivity is negative then the slope of the  $V-I$  characteristic will be negative and the device will present a negative conductance (or resistance) to the external circuit. It is to be noted here that the inter valley transfer must take place at realistic field levels. The threshold field  $E_m$  should not raise the temperature so high as to cause significant generation of electrons from valence band by impact ionization. Thus  $\delta E$  should be less than  $E_G$  as in the case of  $n$ -type GaAs ( $\delta = 0.36$  eV,  $E_G = 1.43$  eV).

### 9.10.2 Domain Formation

When a dc bias of value equal to one more than corresponding to a threshold field of about 3.3 kV/cm is applied to an  $n$ -type GaAs sample, the charge densities and electric field within the sample become non-uniform creating domains i.e., electrons in some region of the sample would first to experience the inter valley transfer than the rest of the sample.

Dipole domain formation is as shown in Fig. 9.44. The electric field inside the dipole domain would be greater than the fields on either side of the dipole.

Applied field and the field due to accumulated charges are both present if applied field is threshold, the field at the anode side of the accumulation charge exceeds threshold and electrons in that region or domain move with less mobility  $\mu_2$  of the  $U$ -valley. This creates a slight excess of electrons in that region and a slight deficiency of electrons in the region immediately ahead. The region of excess and deficient electrons form a dipole layer.

As the dipole drifts along, more electrons in the vicinity will transfer to the  $U$ -valley until electric field outside the dipole region is depressed below threshold electric field. This continues towards the anode until it is collected. Upon collection, the field in the sample jumps immediately to its original value and the next domain formation begins as soon as the field value exceeds the threshold value and the process is then repeated cyclically.

The time taken by the dipole domain to travel from cathode to anode is the transit time of the device. The fundamental frequency in MHz is given by

## Direction of motion of electrons



Layer of excess electrons due to thermal fluctuation (noise) in carrier density

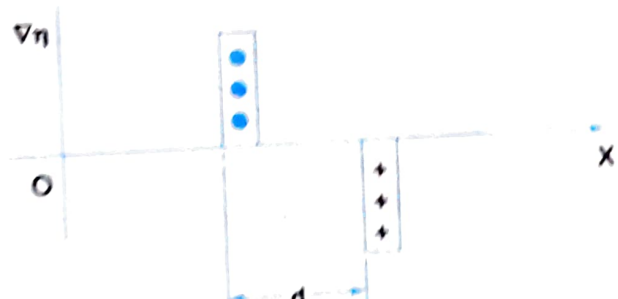


Fig. 9.44 Optically stimulated formation

$$f = \frac{V_d}{L}$$

...(9.49)

where,  $V_d$  = drift velocity ( $10^5$  m/s usually)

$L$  = Device length in  $\mu\text{m}$ .

The domain formation usually starts near the cathode and because of low field and high carriers charge carrier density in this region. The width of the domain is inversely proportional to the doping level in the sample.

The concentration-length product ( $n_0 L$ ) along with frequency of operation determines the mode of operation of the device. Efficiency is highest when  $n_0 L$  product is approximately  $\approx 10^{16}/\text{m}^2$ .

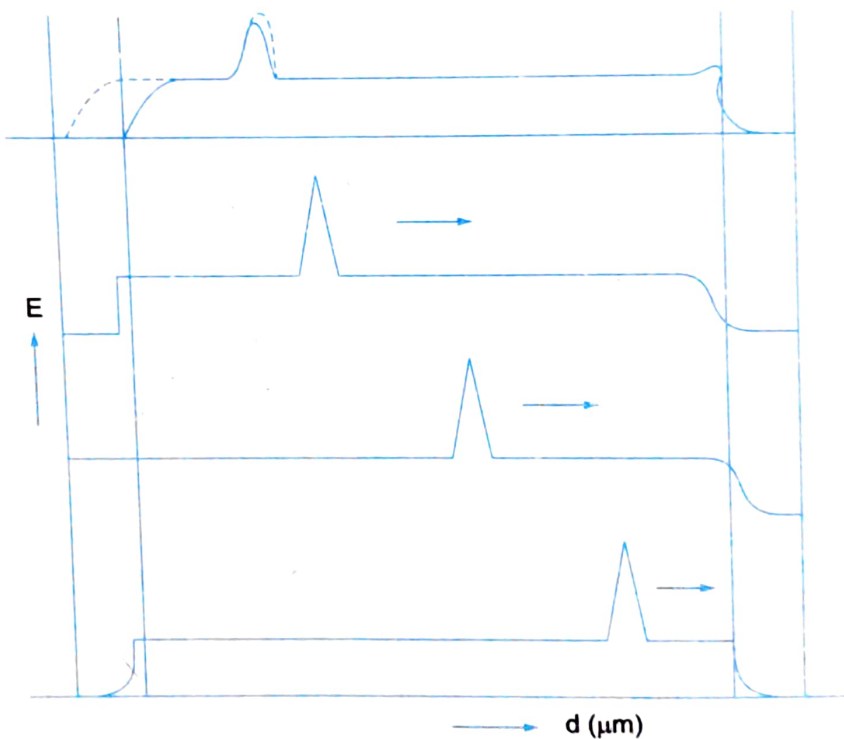


Fig. 9.45

Depending on the material parameters and operating conditions. A Gunn effect oscillator can be made to oscillate in any of the four frequency modes.

1. Domain mode (dipole transit time or travelling domain mode), discussed above.
2. Delayed or Inhibited domain mode.
3. Quenched domain mode.
4. Limited space charge Accumulator (LSA) mode.

### 9.10.3 Transit Time Domain Mode ( $fL = 10^7 \text{ cm/sec}$ )

This is also called the Gunn mode. Here  $fL = 10^7 \text{ cm/sec} = V_d$ , when  $V_d = V_s$  the sustaining velocity, the high field domain is stable. In that case the oscillation period = transit time i.e.,  $\tau_0 = \tau_t$ . This is shown in Fig. 9.47.

Efficiency is below 10% because the domain arrives at the anode at a lower current level. Refer to Fig. 9.46.

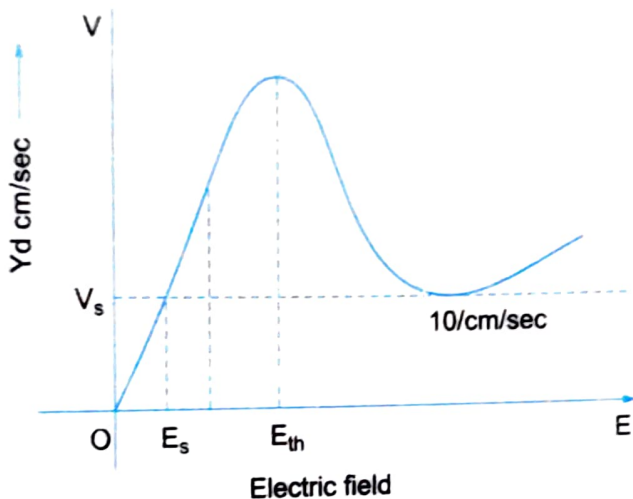


Fig. 9.46

The operating frequency ( $f = V_d/L$ ) in this mode is slightly sensitive to the applied voltage since the drift velocity  $V_d$  depends on the bias voltage. Bias voltage is normally maintained a little higher than  $E_{th}$  (Fig. 9.46). As bias voltage increases,  $V_d$  and hence the operating frequency decreases. This mode does not require any external circuit for its operation. It is a low power, low efficiency mode and requires that the operating frequency be lesser than 30 GHz. This limit on frequency is due to the fact that the device length otherwise will be ridiculously small.

### 9.10.4 Delayed domain mode ( $10^6 \text{ cm/sec} < fL < 10^7 \text{ cm/sec}$ )

When the transit time is chosen so that the domain is collected while  $E < E_{th}$ , a new domain cannot form until the field rises again above threshold. Here oscillation period is greater than transit time  $\tau_0 > \tau_t$ . This delay inhibited mode has an  $\eta$  of 20% approximately. Hence the operating frequency can be equal to or less than that in Gunn mode.

### 9.10.5 Quenched Domain Mode ( $fL > 2 \times 10^7 \text{ cm/sec}$ )

If the bias field drops below sustaining field  $E_s$  during the negative half cycle the domain collapses before it reaches the anode, i.e., The domain disappears somewhere in the sample itself. Hence the domain does not travel all the way to anode and thereby the operating frequency will be higher than that of Gunn mode or delayed domain mode. Certainly this depends on the external circuit. When the bias field swings back above threshold value  $V_{th}$ , a new domain will be formed and the process repeats. Hence in this mode, the domain is quenched before it reaches the anode.

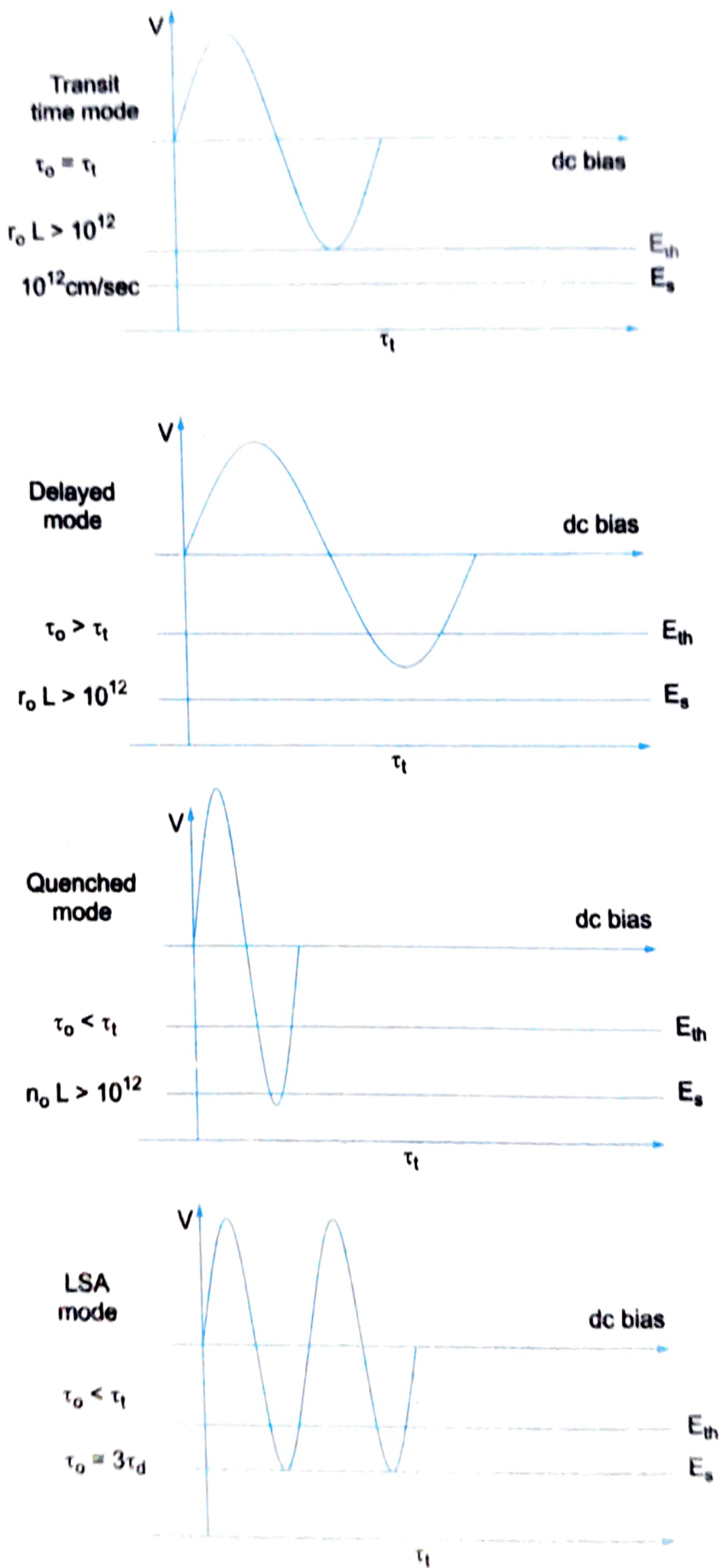


Fig. 9.47 Gunn diode modes

Therefore oscillation occurs at the frequency of resonant circuit rather than at transit time frequency  $\eta$  is 13%.

### 9.10.6 Limited Space Charge Accumulation Mode ( $fL > 2 \times 10^7$ cm/sec)

This is the most important mode of operation for Gunn oscillator as this mode gives high power upled with high efficiency. In this mode, the domain is not allowed to form at all. The frequency and RF voltage are so chosen that the domains do not have sufficient time form while the field is above threshold. As a result most of the domains are maintained in the negative conductance state during a large part of the voltage cycle.

The LSA mode yield high power and high  $\eta$  (20%). 16 to 23% compared to 5% for Gunn mode. The fields never approach the peak value, within a domain (as in Gunn mode) since the domain is not allowed to be formed. Hence high operating voltage is permitted without causing avalanche breakdown. This suggests high power operation. Operating frequency is 0.5-50 times more than that for Gunn mode. It can be used upto 100 GHz. Operation is heavily dependant on external circuit (High Q resonator needed for LSA mode). The device is easily destroyed if domain is formed.

### 9.10.7 Construction Gunn diode

The construction of a Gunn diode is shown in Fig. 9.48 (Encapsulation) and Fig. 9.49 (Construction details). The figure is self explanatory.

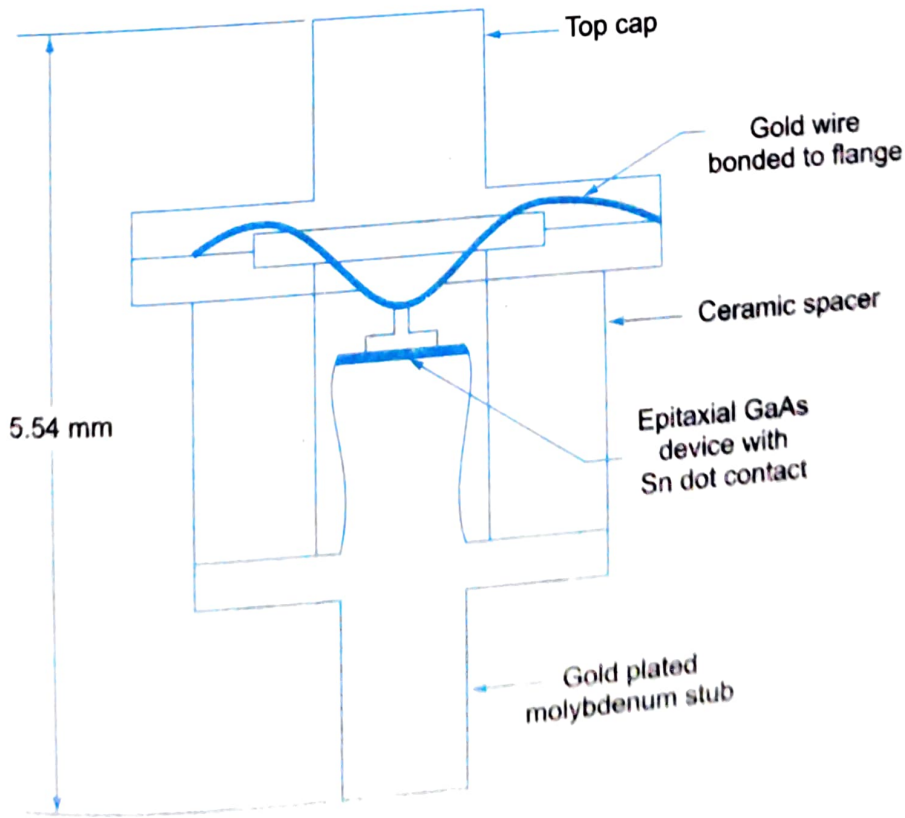


Fig. 9.48

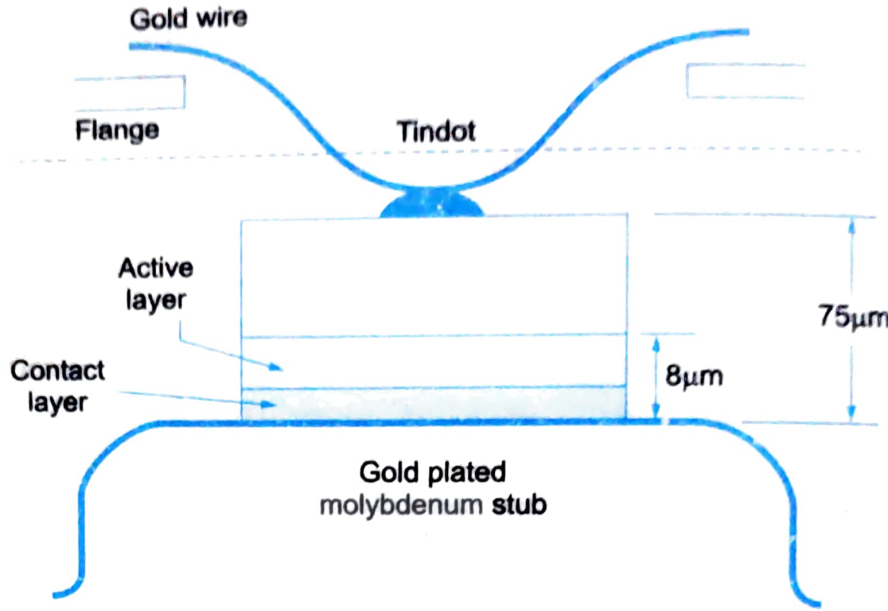


Fig. 9.49

### 9.10.8 Typical Characteristics

It typically uses a 10–12 V supply with typical bias current of 250 mA giving a continuous power of 25 mW in the X - band.

1. CW power : 25mW to 250 mW X band (5–15 GHz).  
100 mW at 18–26.5 GHz.  
40 mW at 26.5–40 GHz.
2. Pulsed power : 5W(5–12 GHz).
3. Efficiency 2% to 12% (at 1.5 W CW to 5 mW CW)

### 9.10.9 Gunn Diode Amplifier

Gunn diode with negative resistance characteristic can be used as an amplifier (similar to Tunn diode) but are not very popular. Gunn diode amplifiers available have been able to give the following performance characteristics.

1. Power : 1 W at frequencies between 4 and 16 GHz
2. Gain band width product : > 10 dB
3. Average gain : 1–12 dB
4. Noise Figure : 15 dB

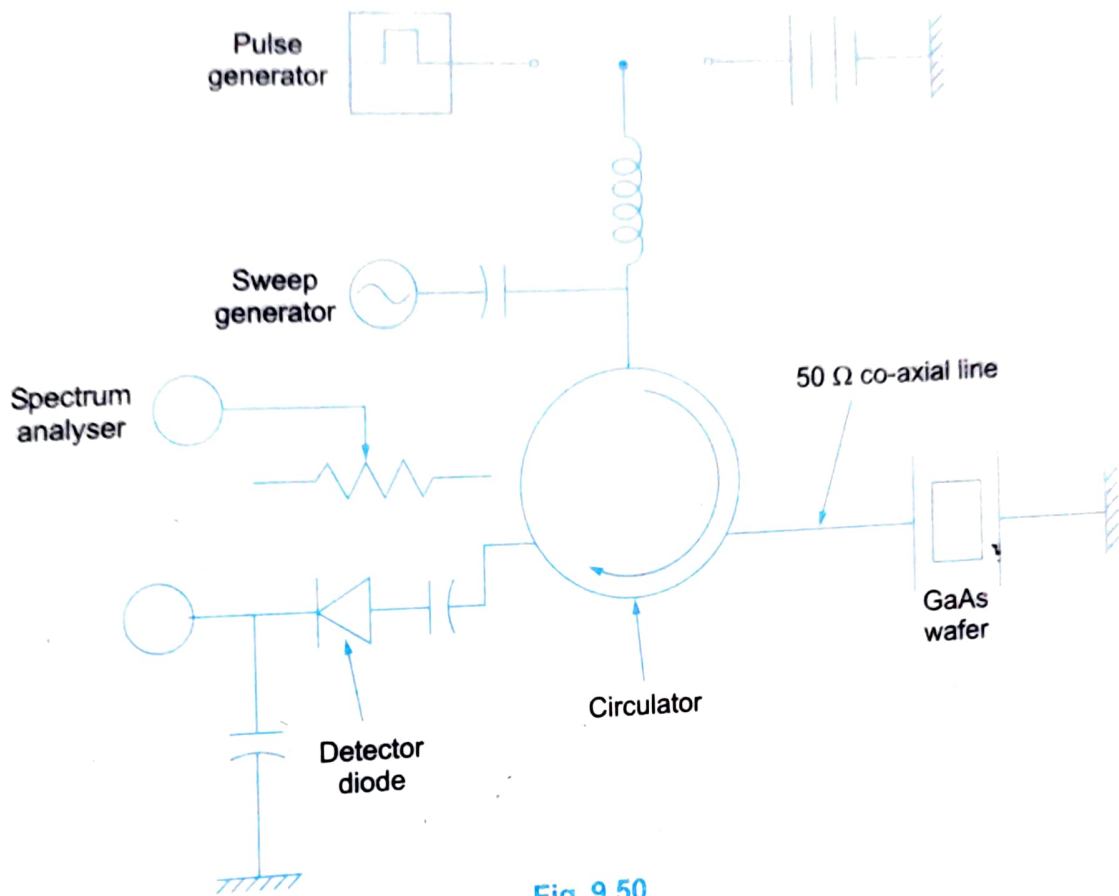


Fig. 9.50

### 9.10.10 Gunn Oscillator

Gunn diode oscillator circuits normally consist of a resonant cavity, an arrangement for coupling the diode to the cavity, a circuit for biasing the diode and a mechanism to couple the RF power from the cavity to the external circuit/load. A coaxial cavity or a rectangular waveguide cavity are commonly used and these are shown in Figs. 9.51 and 9.52.

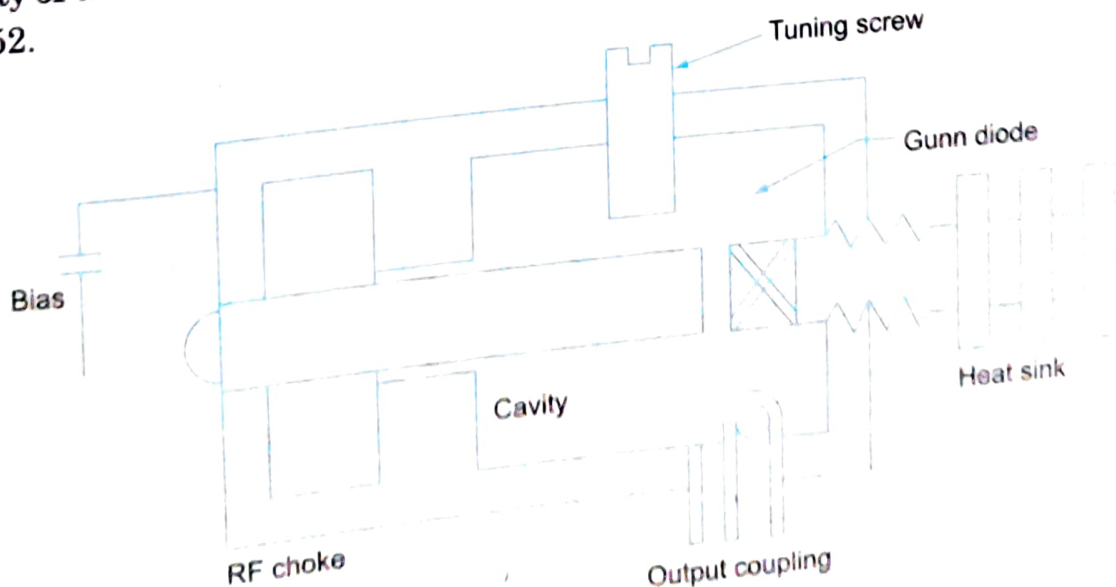


Fig. 9.51 Gunn oscillator using co-axial cavity

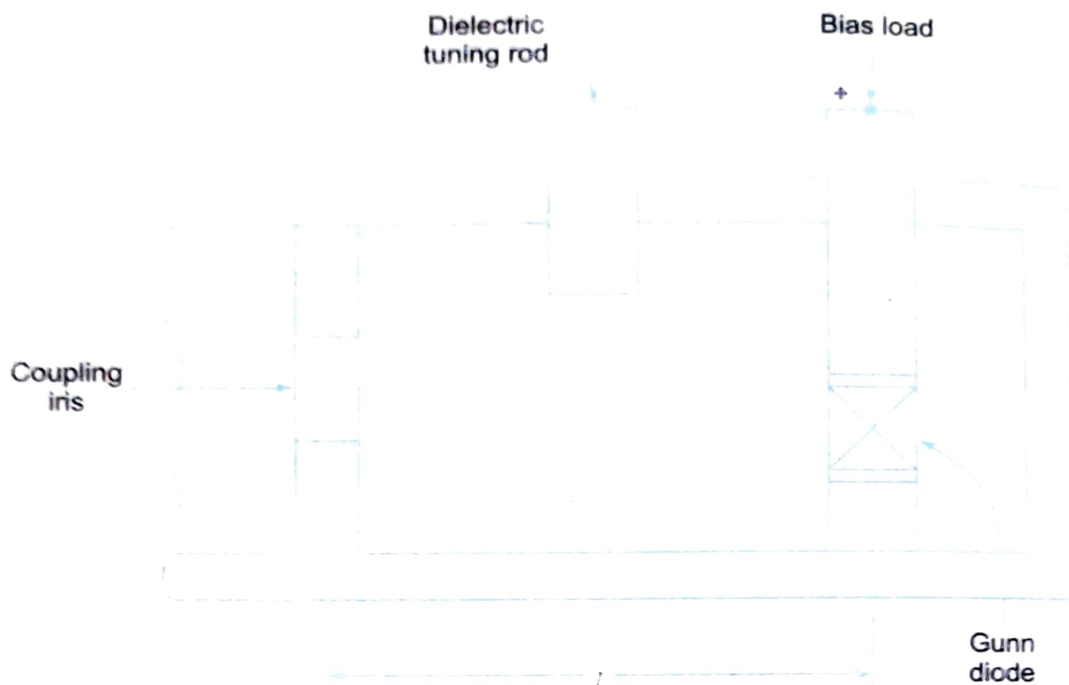


Fig. 9.52 Gunn oscillator circuit using waveguide

The circuit using coaxial cavity has the Gunn diode mounted at one end of the cavity and its continuation with the central conductor of the coaxial line. The output is taken using an inductive or capacitively coupled probe. The length of the cavity determines the frequency of oscillation. The location of the coupling loop or probe within the resonator determines the load impedance presented to the Gunn diode. Heat sink conducts away the heat due to power dissipation of the device. The circuit has an advantage that it can be easily fabricated but low  $Q$  of coaxial resonator and oscillation at harmonics of the desired frequency are the disadvantages.

The circuit using waveguide cavity is more popular, consisting of a simple waveguide section separated from the output waveguide by an iris. The Gunn diode is mounted in a post across the narrow dimension in the centre of the waveguide. The rectangular cavity operates in the  $TE_{101}$  mode. The diode post acts as a large inductive susceptance and the iris is also inductive. Hence the resonant frequency is lower than that for which the length  $l$  is  $\lambda_g/2$ . The dielectric tuning rod is used to adjust the frequency mechanically. Sapphire dielectric rod is commonly employed.

### ~~Applications of Gunn Diode~~

1. In Radar transmitters (Police Radar, CW Doppler Radar).
2. Pulsed Gunn diode oscillators used in transponders for air traffic (ATC) control and industry telemetry systems.
3. Broadband linear amplifier (replacing TWT's).
4. Fast combinational and sequential logic circuits.
5. Low and medium power oscillator in microwave receivers.
6. As pump sources in par amp.

Gunn diodes have an advantage over IMPATT diodes in that they have lesser noise. The disadvantage of Gunn diode is that it is very temperature dependent  $0.5\text{-}3 \text{ MHz}/^\circ\text{C}$  change. Well designed devices have  $50 \text{ kHz}/^\circ\text{C}$  for a range of  $-40^\circ\text{ C}$  to  $+70^\circ\text{C}$ .

### ~~9.11 AVALANCHE TRANSIT TIME DEVICES~~

It is possible to make a microwave diode exhibit negative resistance by having a delay between voltage and current in an avalanche together with transit time through the material. Such devices are called Avalanche transit time devices. They use carrier impact ionization and drift in the high field region of a semiconductor junction to produce negative resistance at microwave frequencies.

There are three distinct modes of avalanche oscillators.

1. IMPATT : Impact Ionization Avalanche Transit Time device.
2. TRAPATT : Trapped Plasma Avalanche Triggered Transit device.
3. BARITT : Barrier Injected Transit Time device.

#### ~~9.11.1 IMPATT Diode~~

Any device which exhibits negative resistance for dc will also exhibit it for ac i.e., If an ac voltage is applied current will rise when voltage falls at an ac rate. Hence negative resistance can also be defined as that property of a device which causes the current through it to be  $180^\circ$  out of phase with the voltage across it. Thus is the kind of negative resistance exhibited by IMPATT diode i.e., If we show voltage and current have a  $180^\circ$  phase difference, then negative resistance in IMPATT diode is proved.

A combination of delay involved in generating avalanche current multiplication together with delay due to transit time through a different space provides the necessary  $180^\circ$  phase difference between applied voltage and the resulting current in an IMPATT diode.

As shown in Fig. 9.53. IMPATT is a diode, the junction being between the  $p^+$  and  $n$  layers.

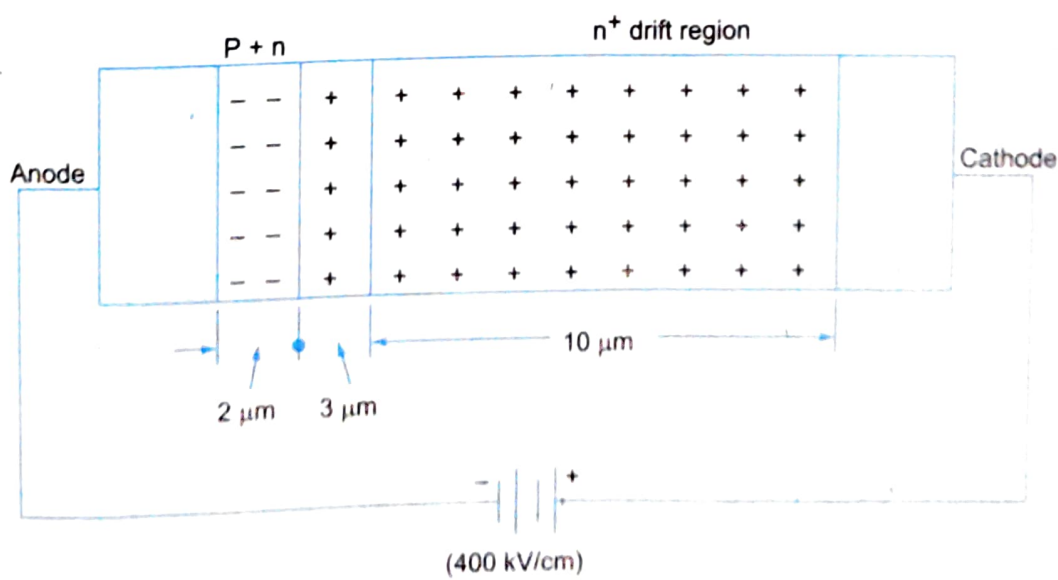


Fig. 9.53 IMPATT diode schematic

An extremely high voltage gradient (400 kV/cm) is applied to the IMPATT diode eventually resulting in a very high current. A normal diode would very quickly breakdown under these conditions but IMPATT is constructed such that it will withstand these conditions repeatedly. Such a high potential gradient back biasing the diode causes a flow of minority carriers across the junction. Let us consider application of a RF ac voltage superimposed on top of the high dc voltage. Increased velocity of electrons and holes result in additional electrons and holes by knocking them out of the crystal structure by so called Impact ionization. These additional carriers continue the process at the junction and it now snowballs into an avalanche. If the original dc field was just above the threshold of allowing this situation to develop, this voltage will be exceeded during the whole of the RF positive cycle and the avalanche current multiplication will be taking place during the entire time. Since it is a multiplication process avalanche is not instantaneous. This process in fact takes a time such that the current pulse maximum at the junction occurs at the instant when the RF voltage across the diode is zero and going negative. A 90° phase shift or phase difference between voltage and current has then been achieved.

The current pulse as shown in Fig. 9.54 (a) is situated at the junction. It does not stay there but moves towards the cathode due to applied reverse bias at a drift velocity dependant on the presence

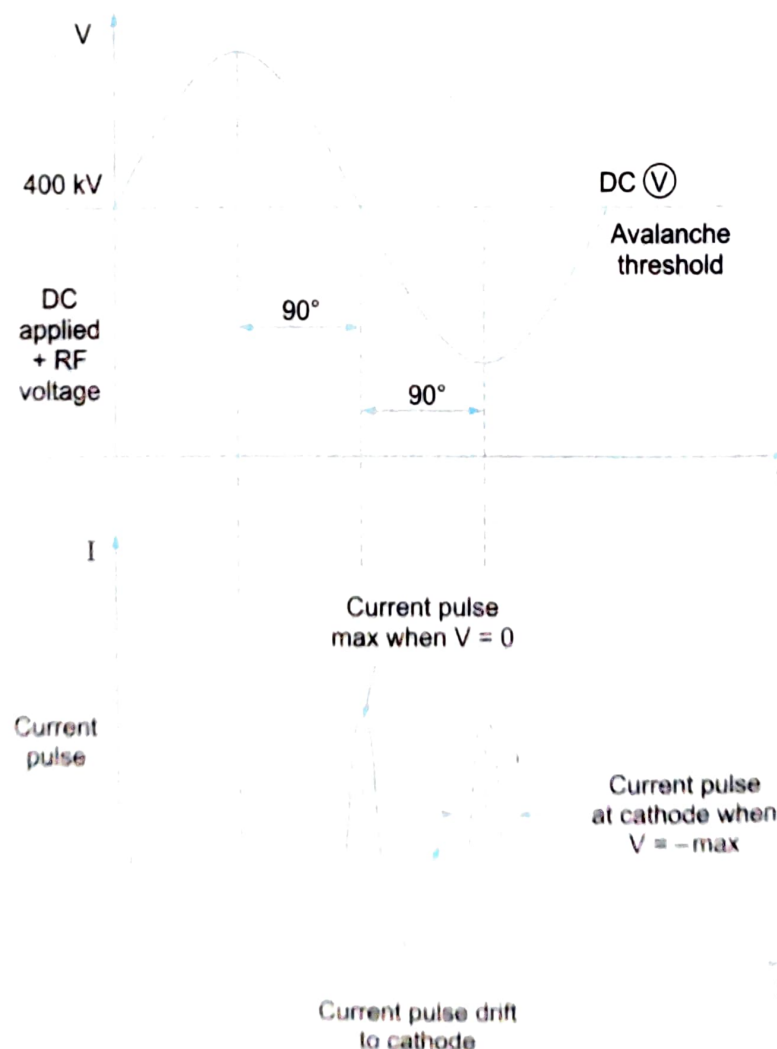


Fig. 9.54 Current-Voltage characteristics

of high dc field. The time taken by the pulse to reach the cathode depends on this velocity and on the thickness of the highly doped ' $n^+$ ' (charges) layer. The thickness is adjusted such that time taken for current pulse to move from  $V=0$  position to  $V=\text{negative maximum of RF cycle}$  is exactly  $90^\circ$ . Hence voltage and current are  $180^\circ$  out of phase and a dynamic RF negative resistance has been proved to exist. Hence IMPATT diode is useful both as an oscillator and as an amplifier. The Resonant frequency of IMPATT diode is given by

$$f = \frac{V_d}{2L} \quad \dots(9.50)$$

where,  $V_d$  = Carrier drift velocity.

$L$  = Length of the drift space charge region.

At a given frequency, the maximum output power of a simple diode is limited by semiconductor material and the attainable impedance level in microwave circuitry. The more widely used semiconductor materials are Si and GaAs invariably epitaxial and mostly MESA. GaAs is preferable since it gives lower noise, higher efficiency and higher maximum operating frequency, but is difficult to fabricate and expensive. The maximum power that can be given to the mobile carriers decreases as  $1/f^2$ .

The efficiency  $\eta$  of IMPATT diode is given by

$$\eta = \left( \frac{P_{ac}}{P_{dc}} \right) = \frac{V_a}{V_d} \left( \frac{I_a}{I_d} \right) \quad \dots(9.51)$$

where,  $P_{ac}$  = ac Power

$P_{dc}$  = dc Power

$V_a$  and  $I_a$  = ac voltage and current

$V_d$  and  $I_d$  = dc voltage and current

### Construction

Construction of a typical IMPATT diode is shown in Fig. 9.55a.

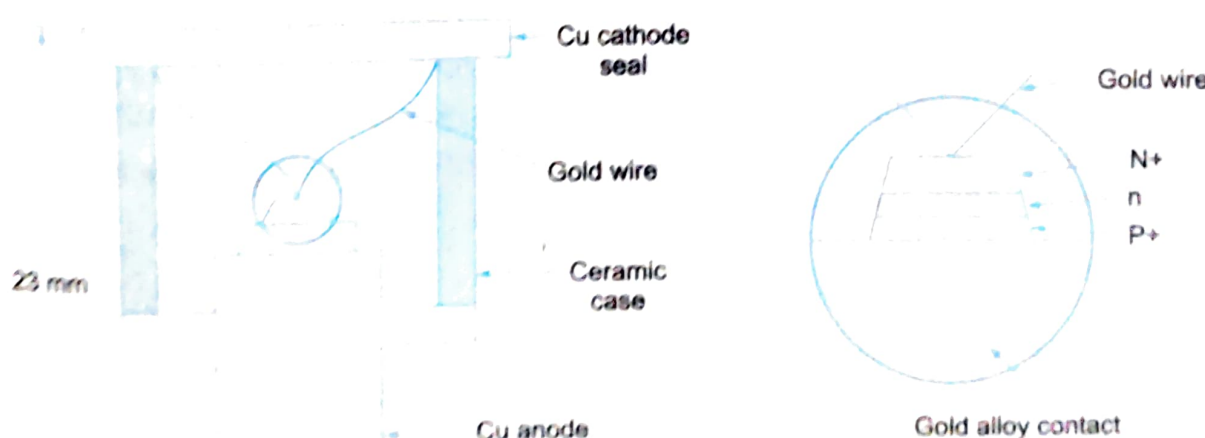


Fig. 9.55 (a) Constructional details of IMPATT

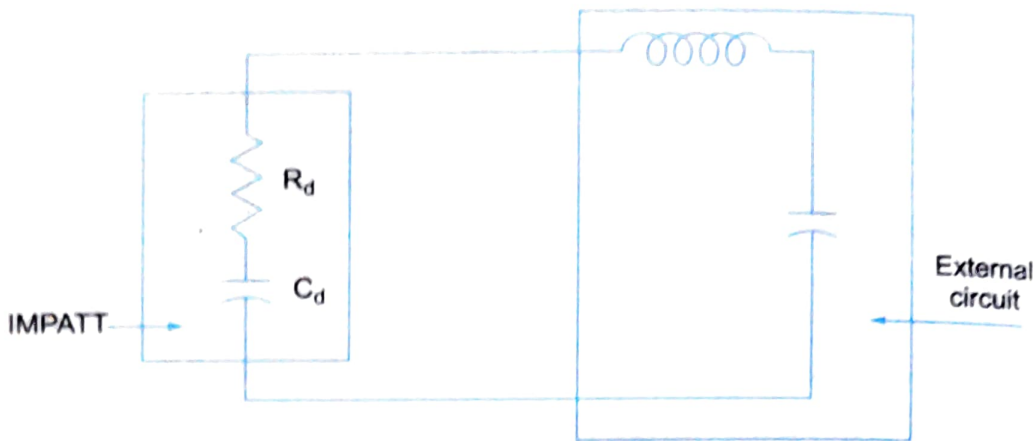


Fig. 9.55 (b)

Equivalent circuit of epitaxed IMPATT diode chip is as shown in Fig. 9.55b.

The magnitude of negative resistance  $R_d$  of IMPATT is less than the reactance  $X_d$ . Hence the IMPATT diode chip impedance is capacitive. For a typical 10 GHz IMPATT package diode chip, external epitaxed inductive wire has a value of 0.6 mH and a bulk capacitance of 0.3 pF.

## Performance Characteristics

Theoretical  $\eta = 30\%$  ( $< 30\%$  in practice) and,

15% for Si

23% for GaAs

Frequency : 1 to 300 GHz.

Maximum output power for single diode : 5 W in X band to 0.5 W at 30 GHz.

Several diodes combined : 40 W at X band

Pulsed powers = 4 kW.

## Disadvantage of IMPATT diode

The disadvantage of IMPATT diode is that it is very noisy because avalanche is a noisy process. Noise figures for IMPATT being 30 dB are not as good as klystron/Gunn diode/TWT amplifier.

Also, tuning range is not as good as Gunn diodes. Amplifiers are comparable to Gunn diode amplifier with higher power and frequency.

## Applications of IMPATT diode

IMPATT diodes are used as microwave oscillators such as (i) microwave generators (ii) modulated output oscillators (iii) receiver local oscillators and (iv) par amp pumps. IMPATT diodes are also suitable for negative resistance amplification. High Q IMPATTS are used in Intrusion alarm network, police radar and low power microwave transmitter whereas low Q IMPATTS are useful in FM (frequency modulated) telecommunication transmitters and CW (continuous wave) doppler radar transmitter.